SOLIDS MIXING IN SPOUTED BEDS

H. H. Cook

Balliol College

A thesis submitted for the
degree of Doctor of Philosophy
at the University of Oxford

Hilary Term 1981



To my parents

Abstract

Many industrial processes require contact between particles and a fluid or spray in order to effect drying, coating or granulation. One device capable of contacting fluid and particles efficiently is a spouted bed in which a jet of fluid is injected into solid particles. This forms an open channel or spout and induces material circulation in a downward moving annulus. For the continuous throughput of solids, knowledge is required of the mixing and particle motions within the bed.

When processing mixtures of particles differing in size or density, the components are often found to segregate into regions rich in larger or denser particles. In a spouted bed this tendency could affect the mixing of solids and residence times of different size fractions with which the process performance is associated.

Distributions of particle residence times were measured using a novel magnetic method of tagging. A thin coat of soft iron powder was applied to form tracer particles, a technique having potential for the investigation of mixing in many industrial processes. In this study, perfect mixing was observed for mono-size particle feeds and perfect self-mixing of each component in binary-size feeds. Generally, although not universally, the smaller particles in a mixture passed through the bed more quickly than larger particles. As the bed depth and gas flow rate were increased independently, the difference between the mean residence times of the components became greater and was also shown to be dependent on the position of the solids outlet.

The difference in residence times is attributed to segregation within the bed. Different residence times for each component will arise if the particles segregate in the spout, the fountain, the free surface, the annulus or as they are drawn off from the outlet. From the studies on

a 150 mm diameter bed, the key processes occur on the free surface and in the neighbourhood of the outlet. In larger diameter beds, segregation on the free surface is predicted to be of prime importance, especially when economy dictates the operation of the bed at low gas flow rates. The particles would then be deposited on the free surface near the spout and the cascading of solids towards the perimeter would lead to segregation.

Acknowledgements

For invaluable advice and guidance over many years, I would like to express sincere thanks to my supervisor, Professor J. Bridgwater.

Also, I would like to thank the many members of the Department of Engineering Science who have helped in a variety of ways, especially Messrs. R.A. Ducker and S.P. Walton for practical assistance in many aspects of the research work and motor car maintenance.

For research grants, I am indebted to the Separation Processes Service at the A.E.R.E., Harwell, and to the Science Research Council.

Finally, for help, patience, and much more during the preparation of this thesis, I would like to thank Linda.

CONTENTS

		Page
CHAPTER 1	INTRODUCTION	1
CHAPTER 2	BACKGROUND	5
2.1	Segregation	5
2.2	Tracing Methods and Mixing	8
CHAPTER 3	EQUIPMENT AND EXPERIMENTAL PROCEDURE	14
3.1	The Bed	14
3.2	Solids Supply	19
3.3	Gas Supply	24
3.4	Particles and Labelling	28
3.5	Experimental Procedure	32
CHAPTER 4	MIXING BEHAVIOUR AND MEAN RESIDENCE TIMES	38
4.1	Literature - One Species	38
4.2	Results - One Species	40
4.3	Literature - Two Species	44
4.4	Results - Two Species	50
4.5	Mean Residence Times	56
4.6	Small Half-Section Bed	74
4.7	Conclusions	80
CHAPTER 5	THE ANNULUS	82
5.1	Introduction	82
5.2	Wall Measurements	86
5.3	Equipment	95
5.4	Cycle Times	102
5.5	Short and Long Cycle Times	108
5.6	Summary	115
CHAPTER 6	FOUNTAIN, SPOUT, FREE SURFACE AND OUTLET	119
6.1	Introduction	119
6.2	Literature	122
6.3	Outlet Region	127
6.4	The Fountain	142
6.5	The Spout	159
6.6	Submerged Outlet	171
6.7	Summary	183
CHAPTER 7	CONCLUSION	187
APPENDIX A	Mixing in continuous flow systems	192
APPENDIX B	Particle properties	196
APPENDIX C	Details of 80 mm i.d. half-section bed	197
APPENDIX D	Calculation of the standard deviation of the ratio of two variable quantities	198
APPENDIX E	Estimation of void fraction in the spout	199
NOMENCLATURE		202
REFERENCES		208

CHAPTER 1

Introduction

The spouted bed is a device for contacting fluid and solids. For systems in which the solid particle size exceeds 0.5 mm and the fluid is a gas, spouting has industrial potential since it often holds the following advantages over fluidisation: (i) the pressure drop is only one half to two thirds that for fluidisation, (ii) the gas contacting is better because gas bypassing, which occurs when large particles are fluidised, is much reduced and (iii) the device is simpler in design having no distributor. The spouted bed may be used for drying, granulation, coating, adsorption/desorption, chemical reaction and many other processing operations [Mathur and Epstein (1974, I)].

The essential features of the spouted bed are shown in Figure 1.1. Gas is injected through the inlet nozzle and causes a spout to be formed which penetrates to the free surface. As the gas rises in the spout, it entrains particles from the inner surface of the annulus at every level. Some gas seeps from the spout into the annulus where it rises more slowly to the free surface. The gas and entrained particles disengage in the fountain and the particles then rain down on to the annular free surface, from where they move downwards and to some extent inwards, in the annulus.

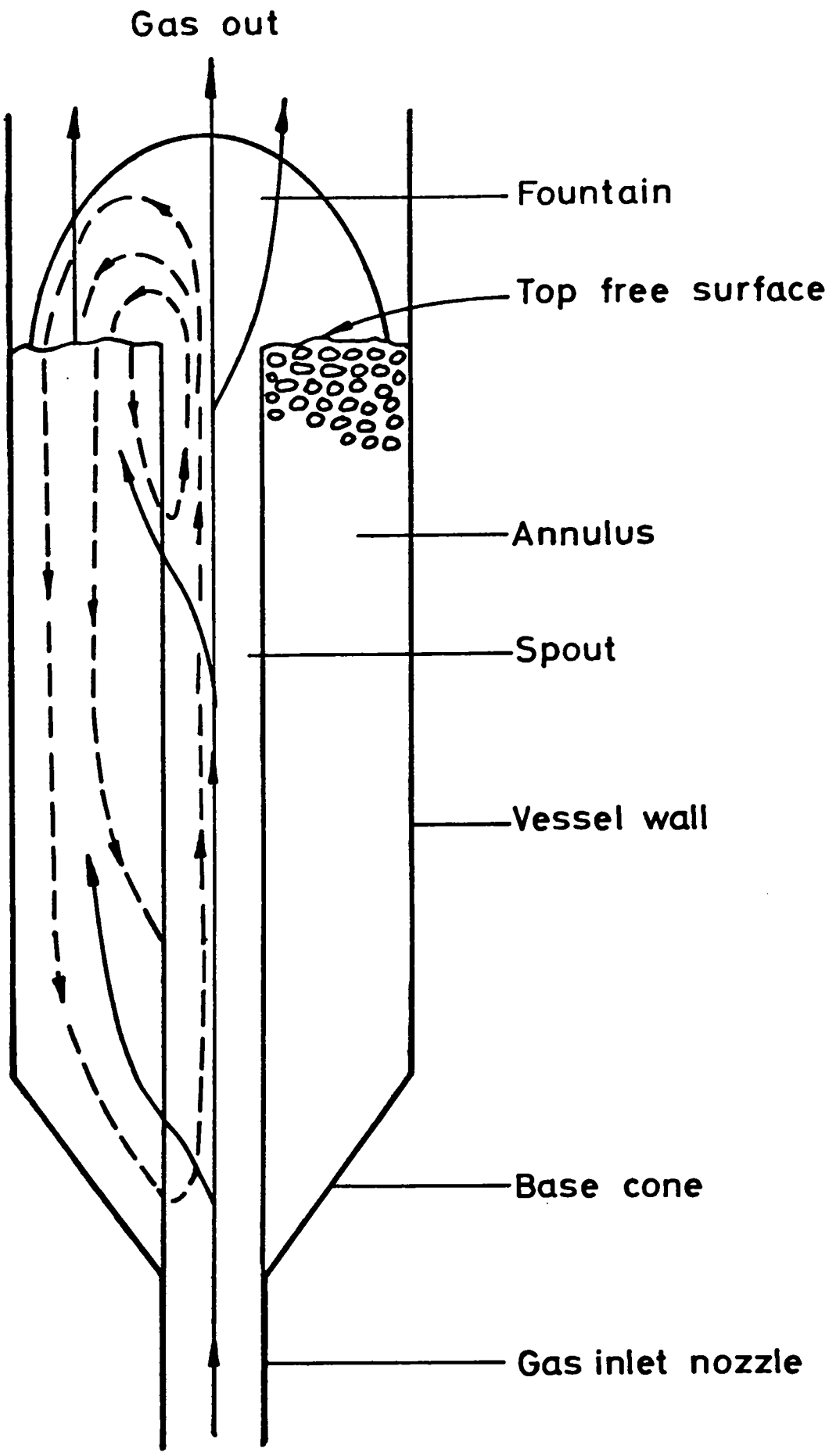


Figure 1.1 : The spouted bed

— → — — Particle streamlines
——→—— Gas streamlines

process performance of continuous beds, detailed knowledge is required of the particle flow pattern and residence times over all possible operating conditions. For beds up to about 500 mm diameter, previous workers have produced experimental data for a wide range of materials on important parameters such as the maximum bed depth at which spouting is possible, the minimum gas flow rate required to sustain spouting, the pressure drop across a spouted bed and the shape of the spout. Thus, knowledge of the spouting behaviour of closely-sized particles is extensive but for polydisperse material, knowledge is still limited. The mixing behaviour of spouted beds has been the subject of a few investigations, but most workers studied closely-sized material. Only recently has attention been directed at the mixing behaviour in beds of particles which are distributed in size or density.

The purpose of this thesis is to study thoroughly certain aspects of particle flow in spouted beds fed continuously with material distributed in size. The particular objectives pursued are:

(i) The development of a novel particle tagging technique enabling the mixing performance of spouted beds of closely sized particles to be studied simply and compared to the results obtained by previous workers.

(ii) To extend this tagging method to a binary sized particulate material, and thus isolate any effects of particle size on the mixing behaviour of continuous beds.

(iii) In continuous beds with a binary material feed, to study the dependence of the mean residence times of each component on the operating conditions.

(iv) To investigate the reasons for the dependences observed in (iii) and perform further experiments to isolate the mechanisms of key

importance.

(v) To suggest how mechanisms operating in these regions may affect the performance of continuous spouted beds when operated outside the range of parameters accessible with the present equipment.

CHAPTER 2

Background

The mixing behaviour of spouted beds has mainly been investigated using stimulus-response experiments where the residence time distribution (RTD) of particles charged to the bed at a steady rate was measured. If the material is distributed in size or density, deviations from good mixing can be expected due to particle segregation. In the differently structured regions of a spouted bed, segregation may be of several forms. Firstly, some types of segregation relevant to particle movement in a spouted bed will be discussed. Following this, the experimental approach of previous workers who have studied the overall mixing behaviour in spouted beds will be discussed. Such experiments require the use of special tracer particles. Many tracing methods have been used and those with possible applications in the present study are summarised below.

The papers which have direct bearing on specific topics are considered in more detail in the relevant chapters.

2.1 Segregation

Whenever a system contains cohesionless particles differing in size, density or surface character, segregation can occur. Four types of segregation are distinguished by Scott (1974) and his divisions will be followed here. In addition, segregation during the preparation of packed beds will be considered.

(i) Free-flight segregation

If particles are in free-flight, they are subject to drag forces [Jenike (1960)] which are dependent on their size. Hence,

if particles distributed in size or density undergo free-flight with a horizontal velocity component, they will land at different positions. In a spouted bed, this may be of importance in the fountain region.

(ii) Inter-particle percolation

When a powder or granular material undergoes shear strain, dilation may occur [Reynolds (1885)]. The dilation is concentrated in regions termed failure zones, 10 to 15 particle diameters wide [Roscoe (1967)]; between these zones, elastic deformation only occurs. Inter-particle percolation, hereafter referred to as percolation, is the drainage of one component, usually the smaller one, through another in these highly strained failure zones. Only if a component is very much smaller than all the others is percolation in the absence of any strain possible. Percolation induced by strain has been studied in a vertical cylinder fitted with a rotating shaft to which pins were attached [Willemse (1961)], in a vertical failure zone adjacent to a wall [Campbell and Bridgwater (1973)] but most extensively in a reciprocating shear cell [Bridgwater et al (1978), Cooke and Bridgwater (1979), Drahun (1979)] and in an annular shear cell [Foo (1978) and Stephens and Bridgwater (1978)]. Inter-particle percolation may occur in the annulus of spouted beds. However, all work on percolation has been performed in the absence of an upward gas flow; this is present in the spouted bed and would oppose the downward movement of percolating particles due to gravity.

(iii) Large particle segregation

Brown (1939) reported that if a granular mixture is vibrated, then large particles rise to the surface. Williams (1963) performed a similar experiment but with only one large particle in the mixture. He confirmed the results of Brown. Scott (1974) investigated large particle motion during inter-particle percolation in a reciprocating shear cell. He found that large particles initially in the middle of a failure zone did not move significantly whereas those at the top of the zone moved downwards. More recently, Foo (1978) performed experiments in an annular shear cell apparatus and found that large particles move towards the centre of a failure zone.

(iv) Free-surface segregation

If particles roll down an inclined free surface of material, then the large ones will roll further [Brown (1939)]. Recently Drahun (1979) has investigated this behaviour extensively. He found that in general large particles or less dense particles will roll further than small or dense particles when dropped on to an inclined slope of granular material. Segregation of this form may occur on the free surface of a spouted bed since this may, under certain conditions be sloping. The work of Drahun (1979) will be discussed in more detail in subsequent chapters.

(v) Packed bed segregation

The annulus of a spouted bed could be regarded as an aerated packed bed of granular material. Craven (1970) recognized that segregation could occur during the preparation of a packed bed and modelled the changes in performance of a chemical reactor due to irregular packing. Haughey and Beveridge (1969) show that the

local void fraction of material in a packed bed may increase considerably near the vessel wall. If the material used to prepare the bed is distributed in size then no matter how carefully the bed is filled in an attempt to obtain a uniform mixture, a higher proportion of small particles in the region adjacent to the vessel wall will result.

The extent to which these mechanisms control segregation of mixtures in spouted beds is unknown. However, knowledge of these mechanisms and their roles in the spouted bed is essential if the performance of chemical or separation processes is to be predicted. Studies of the overall mixing behaviour in a spouted bed when operated continuously are thus important.

2.2 Tracing Methods and Mixing

The mixing behaviour of spouted beds has been the subject of several investigations. Studies were made on beds operated continuously or in a batch manner and most were concerned with closely sized particles, usually seeds. Such work is considered in detail later. All experiments made use of specially labelled particles or tracers. The usual tracing technique adopted by previous workers has been the addition of tracing material to the solids feed, either in the form of a pulse or as a continuous stream. The solids at outlet are subsequently sampled at regular intervals to determine the concentration or proportion of the tagged material leaving the bed. If the solids are only available in limited quantities or if there are problems in handling large amounts of material, then the tracer must be completely removable at the end of an experiment, so that the bed material may be re-used. Also, the labelled material must be very similar, if not

identical, to the bulk material in the physical properties that affect the spouting and mixing characteristics of the solids. The most important of these are particle size, density and surface finish. A study has been made of labelling and tracing methods used by previous workers, whether for determining the RTD's of spouted beds or of other particle processing devices. These methods may be divided into four categories:

(i) Radioactivity

Radioactive isotopes are used to label tracer particles. Singer et al (1957) and Hull and Rosenberg (1960) used radioisotopes to study solids mixing in commercial-scale catalytic cracking plants. Sutherland (1961) irradiated one copper particle which was then dropped into a fluidized bed of copper shot fitted with a screw conveyor for removing solids from the bottom. The solids were returned to the top through an air conveyor and cyclone. Each passage of one radioactive particle through the conveyor was registered by a scintillation counter and chart recorder, thus enabling residence times to be calculated. This method can only be satisfactorily applied to devices where the mean particle residence time is relatively short, since a large number of measurements are required to give an accurate estimate of the RTD. Van Velzen et al (1974) used a scintillation counter to track the movement of an irradiated particle in a spouted bed. The use of irradiated particles as tracers requires safety precautions if, as in the present work, dust is formed.

(ii) Photometry

Sutherland (1961) also performed solids mixing studies in a fluidized bed of glass ballotini of diameter about 0.75 mm and used

coloured ballotini as a tracer. The material could be regenerated since the colouring agent was soluble in acetone. Analysis of material samples was by visual counting of the coloured ballotini under a reading lens. This was found to be very tedious and he abandoned the method. Image analysis equipment now available, though expensive, renders photometric tracing methods more conceivable.

Tailby and Cocquerel (1961) also studied fluidized beds of glass ballotini. A portion of the experimental material was coated with blue dye to act as a tracer. The dyeing solution used was made from blue dye and perspex granules dissolved in chloroform. The dissolved perspex gave the coating good adhesive properties. The proportion of tracer in each sample was determined by washing the sample with a known weight of chloroform and comparing the colour of the liquid with solutions of a known concentration in a spectrophotometer.

Kugo et al (1965) measured the RTD of wheat particles in a spouted bed. The feed was changed completely to coloured particles and the concentration of these in samples taken at the outlet was measured. Kugo does not describe the method of colouring the tracer particles, or the method, if any, of separation.

Shinohara et al (1973) measured the RTD of particles in a pneumatic escalator. The material used was glass beads between 315 and 401 μm in diameter. Some of the glass beads were coated with volatile blue ink to act as tracer material and the amount injected to the solids feed was about 3% of the solids hold-up within the escalator. Material leaving the escalator

was fed into a glass case (10 x 100 x 490 mm). When evenly illuminated, the intensity of reflected light varied along the length of the case, dependent upon the quantity of tracer present at each position. As a CdS photoelectric cell was passed over the case the output voltage of the cell was measured and recorded. A steady solids feed rate was maintained and the bulk density of material in the glass case assumed constant, hence the distance along the case was directly proportional to discharge time. A calibration curve of voltage vs. tracer concentration was prepared in advance and used to correct the recorded voltage curves, yielding curves of tracer concentration vs. discharge time.

The drawback with most photometric methods of labelling is that if the material is in limited supply and cannot be discarded, then large quantities of solvent are needed to regenerate the material.

(iii) Magnetism

Some workers have used as tracers, particles with different magnetic susceptibilities to the bulk, which in other physical properties are very similar.

Sutherland (1961) employed nickel as a tracer in a fluidized bed of copper shot. These metals are practically identical in the physical properties relevant to fluidization, but nickel is magnetic. Tracer particles could then be separated easily using magnets, for analysis of the samples and for removing all tracer material from the bed.

Bowling and Watts (1961) measured particle residence times in

beds of fluidized coal char. Some char was labelled by carbonizing coal particles in a fluidized bed at 500 °C. Firstly, the coal particles were impregnated with a concentrated solution of ferrous sulphate and then treated with concentrated ammonium hydroxide to form ferrous hydroxide. Particles were then dried in air, converting the ferrous hydroxide to a mixture of iron oxides and by heating in coal gas at 500 °C, the oxides were reduced to ferrous oxide and metallic iron. The particles were then passed through a magnetic separator to remove those which had been insufficiently treated. Tagged particles could then be removed magnetically from samples for analysis and for regeneration of the bed material.

Magnetic labelling allows easy separation of tracers from bulk material although if metal shot is used, a large capital outlay may be necessary.

(iv) Chemical Methods

Barton et al (1968) adopted a stimulus-response technique whereby the feed material was suddenly changed from coke to a highly volatile coal. The coal contained 39% volatile matter whereas the coke contained only 3%, so a measurement of the proportion of volatile matter in samples gave an estimate of the proportion of coal present. However, the coal and coke particles were of different densities and this would not be desirable for most applications of such a tracing method.

Of the methods of labelling reported here, a magnetic technique allows easiest separation of tracers from samples for analysis and from the whole bed material. For the present study a novel

form of the magnetic tracing technique was employed which was cheaper and simpler than those used by previous workers.

CHAPTER 3

Equipment and Experimental Procedure

3.1 The Bed

The bed (Figure 3.1a) is a 150 mm i.d. pyrex column (A) 2 m long and of 6 mm wall thickness. At heights of 845 mm and 790 mm from the lower end, two diametrically opposed holes of 50 mm diameter were drilled through the column wall to allow inflow and outflow of solids. Manifolds (B) were attached to the sides of the column at these points to permit the connection of solids feeding equipment and different outlets. Orifice plates as in Figure 3.1b could be placed in the outlet manifold to control the rate of solids outflow. The smaller hole in the orifice plate was only required for experiments described in Chapter 6 and was sealed for earlier experiments. The orifice plate in position is shown in Figure 3.1c.

A novel feature of the bed design was that for variation of bed heights, having fixed the positions of the solids inlet and outflow, the base cone (C) of 149 mm diameter and 60^{o} included angle could be raised or lowered within the column. Since the internal column diameter could vary by 2 mm along its length, pressurised rubber rings (D) around the cone were required to ensure an airtight seal. The effectiveness of this seal was checked by attaching a rubber sheet to the base of the column. The air lines passed through two holes in the sheet, and any air escaping between the column wall and the cone could be detected at a third hole as shown in Figure 3.1d. Pressurised to 2 bar, the ring seals were found to be completely airtight when spouting beds of wheat up to a depth of 600 mm.

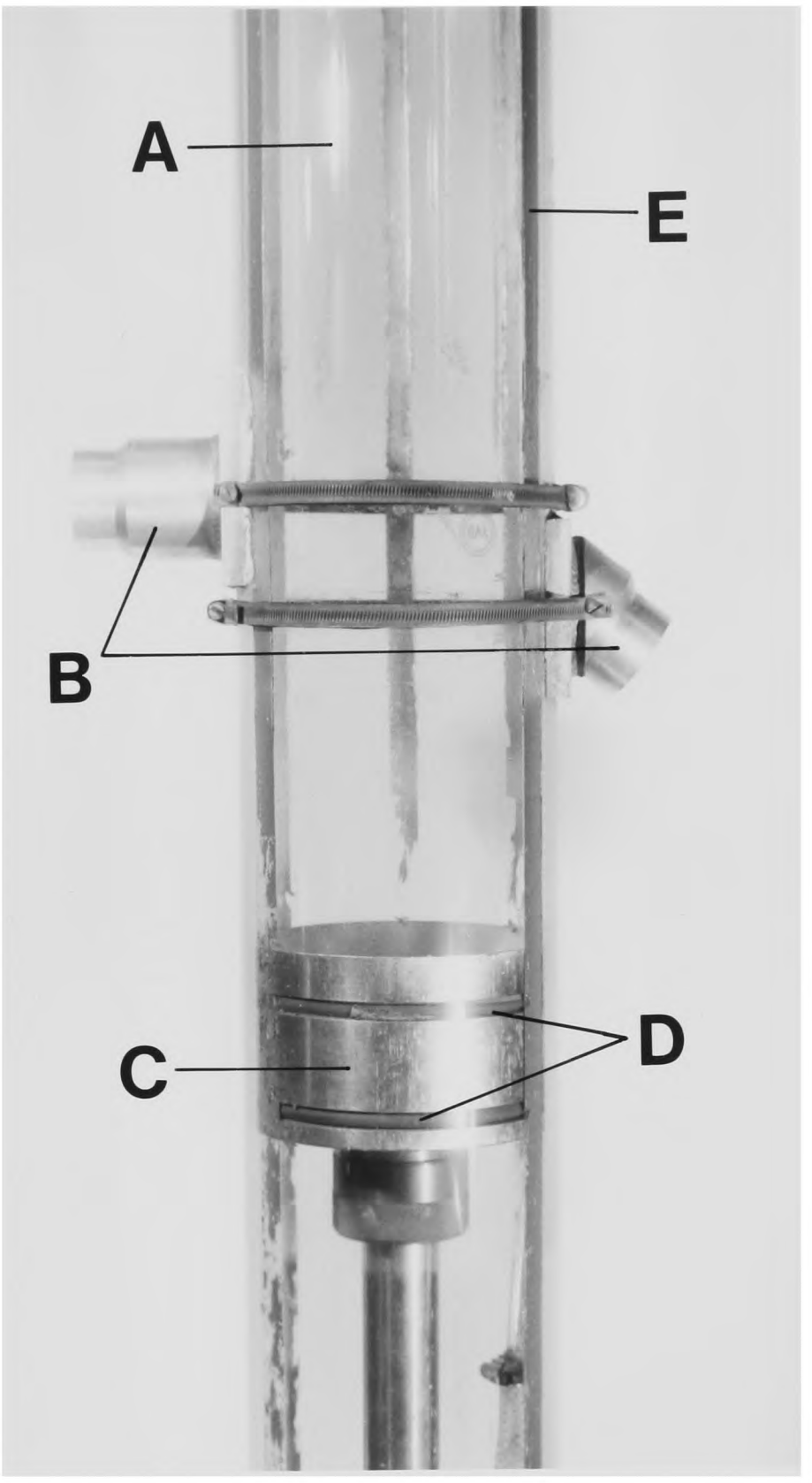


Figure 3.1a : The 150 mm i.d. bed

A : Pyrex column
B : Inlet and outlet manifolds
C : Base cone
D : Pressurised sealing rings
E : Earthed foil strips

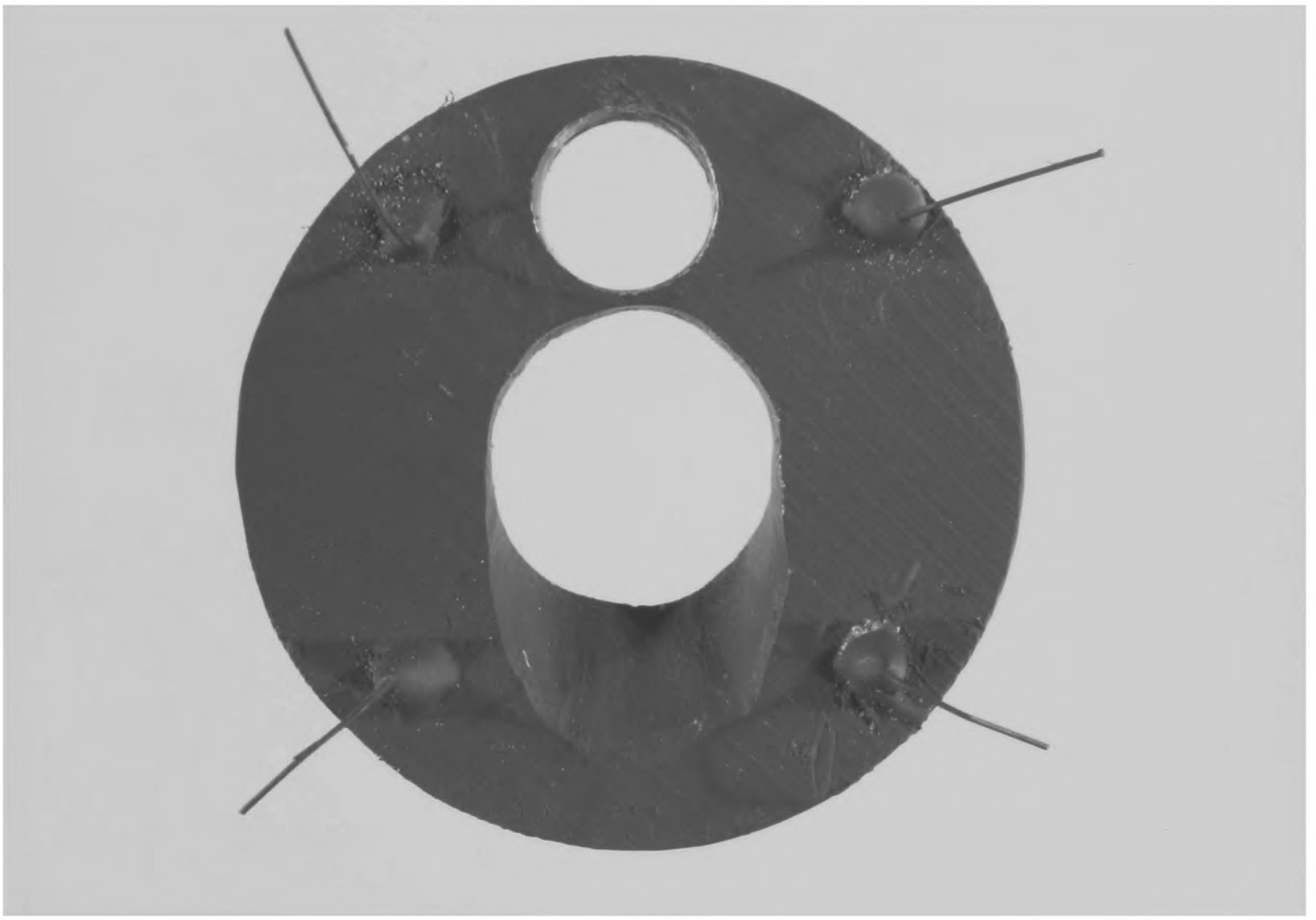


Figure 3.1b : The outlet orifice plate

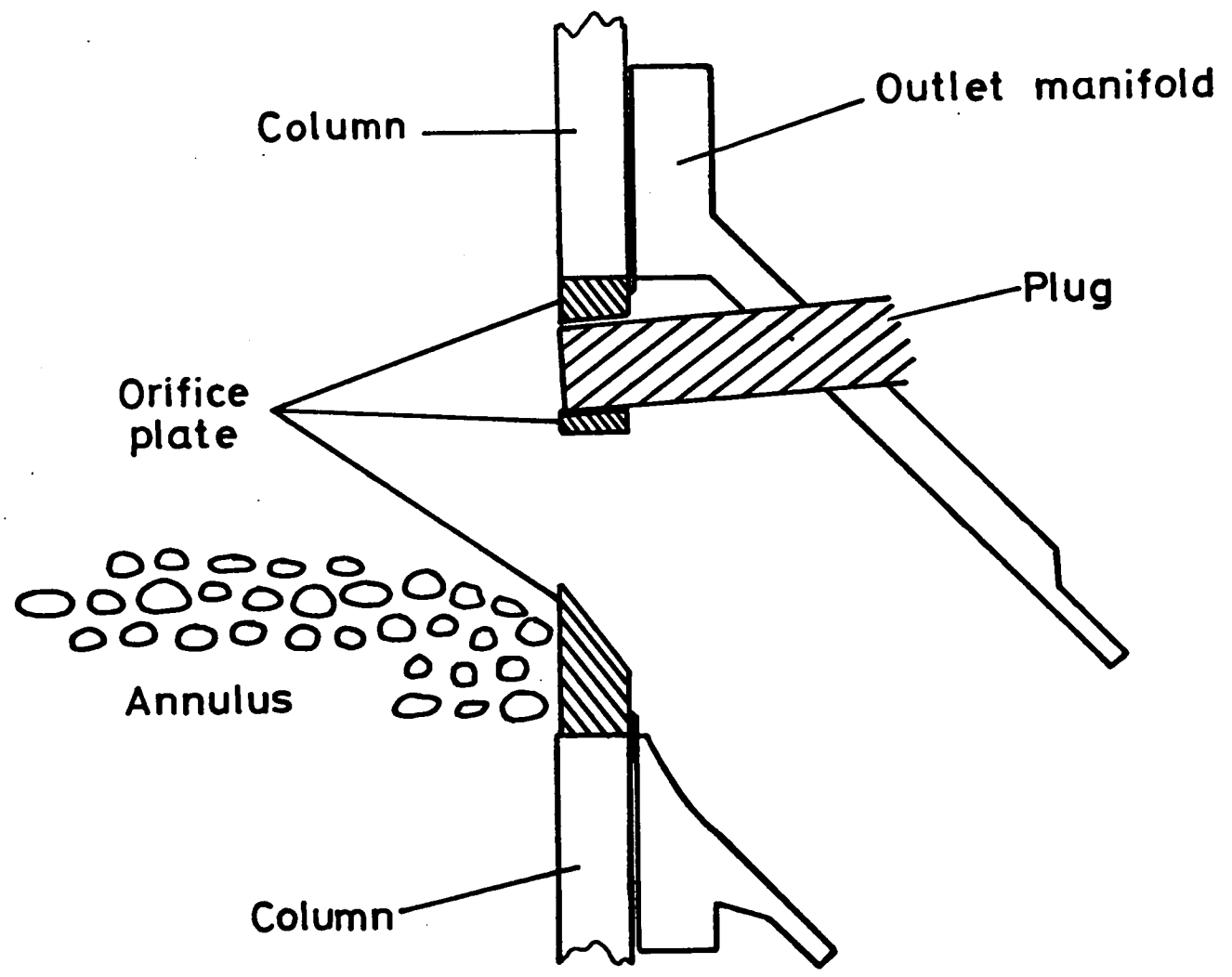


Figure 3.1 c : The solids outlet

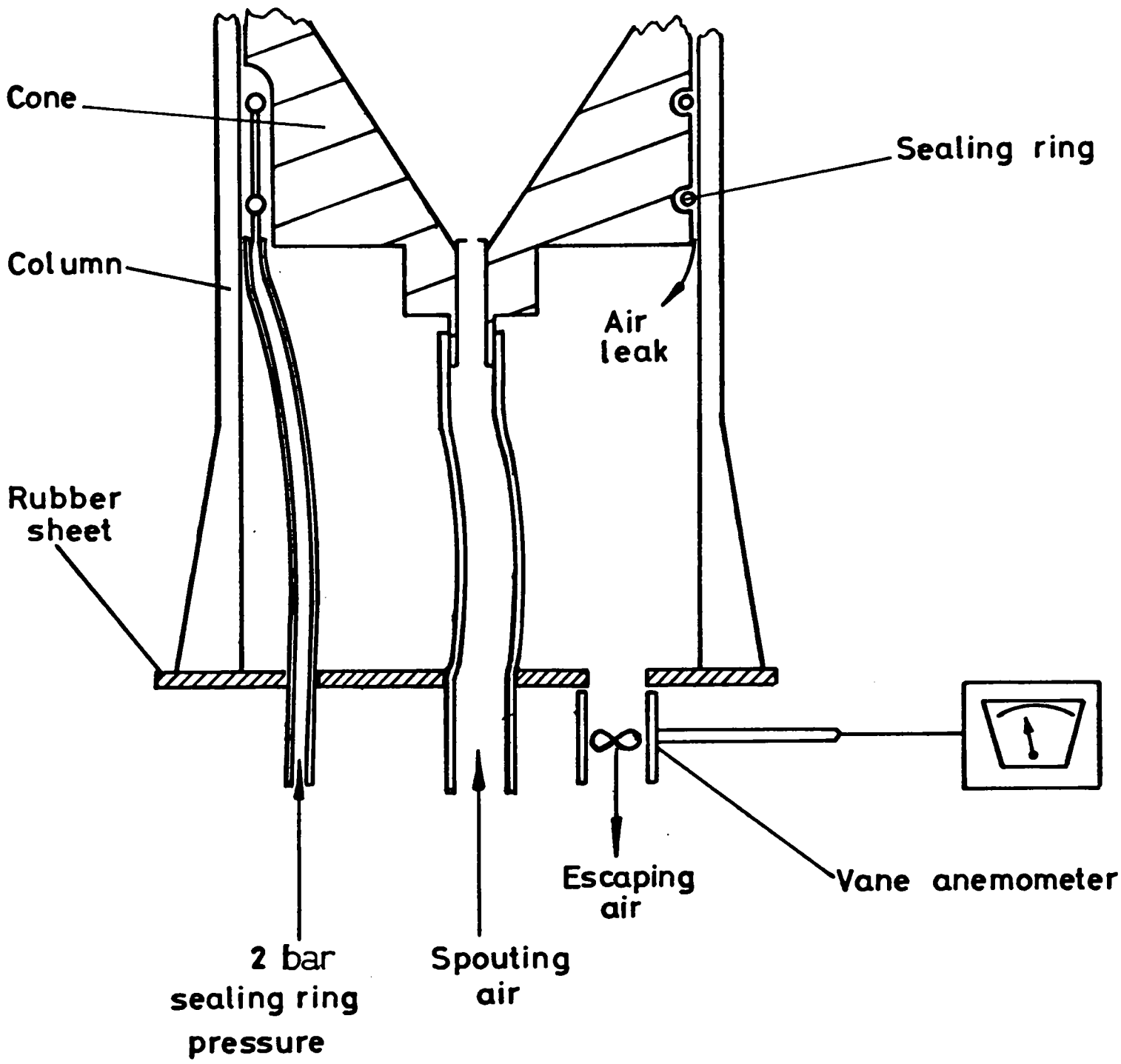


Figure 3.1 d : Procedure for testing for air leaks around the base cone

Although a gas inlet diameter of 10 mm was used for all experiments, the cone was designed to accept nozzles of different internal diameters. The nozzle and base cone used in this study are shown in Figures 3.1e and f. Details of the gas inlet are given in Figure 3.1g.

For certain runs, foil strips (E in Figure 3.1a) were attached to the inside of the column and electrically earthed to reduce the build-up of static electricity. All metal connections to the column were earthed for the same reason.

3.2 Solids Supply

The solids feed system was required to feed a homogenous mixture of particles at a steady, controlled rate into the spouted bed. Its components are shown in Figure 3.2a. Solids were charged to the bed surface from a perspex inlet hopper (A) of 94 mm i.d. by a screw feeder (B). The screw was of two turns and 60 mm diameter, driven through a 49.5:1 gearbox (C) by a "Motomatic" E650 motor (D) and E650M controller (E). The desired solids flow rate was achieved by adjustment of the motor controller. Small pulsations in solids flow rate occurred at every turn of the screw and for usual flow rates this was every ten seconds. These pulsations were considered to have a negligible effect since spouting performance was observed to be unaffected by reducing the solids feed rate to zero.

A mixture of two different size fractions was obtained by charging thin layers of each fraction to the hopper. The volume of material in each layer of a given size fraction was constant, achieved by filling many cups or small vessels of constant volume with material. Cups of material of each size fraction were then poured alternately into the hopper.



Figure 3.1e : The gas inlet nozzle

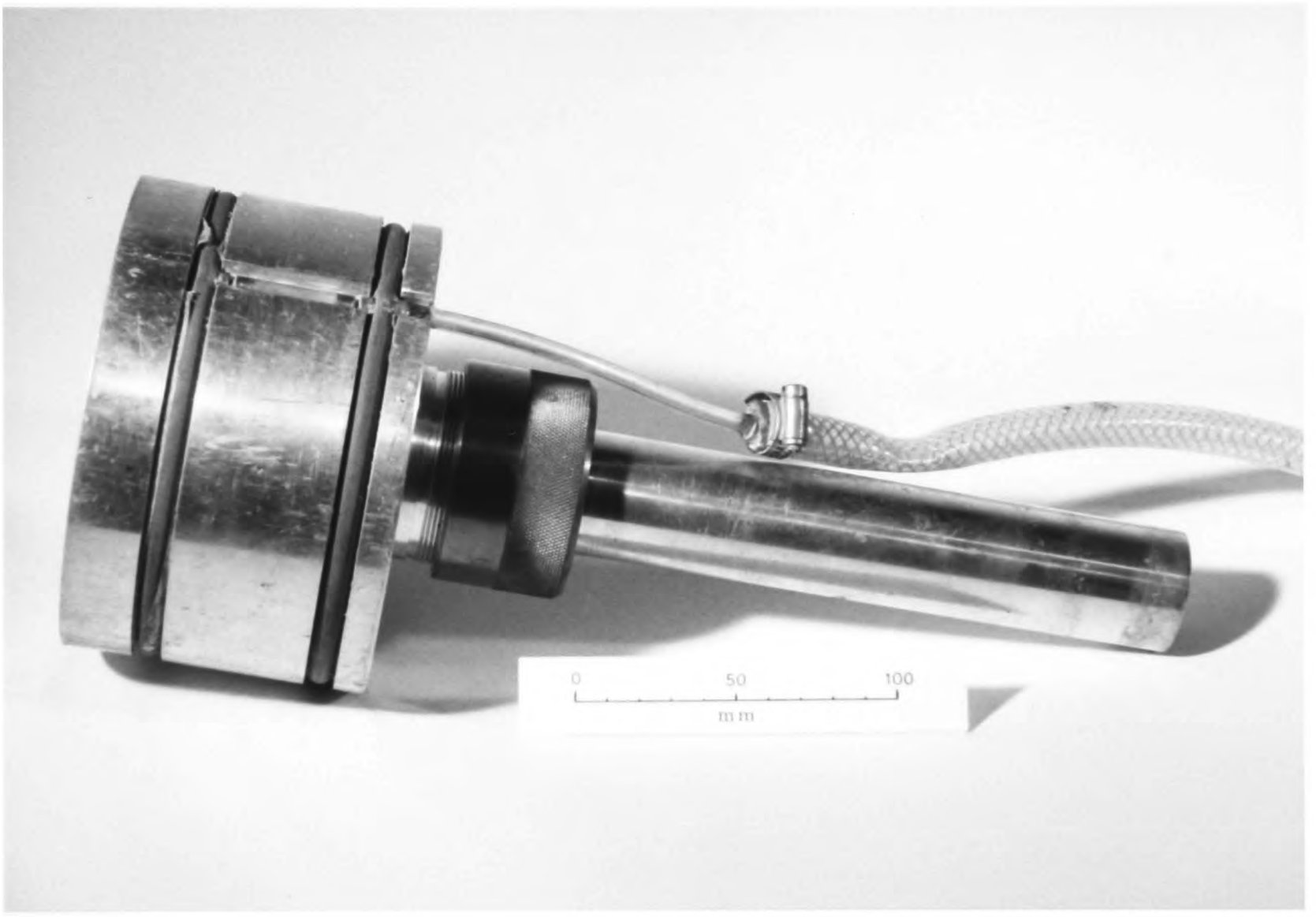


Figure 3.1f : The base cone and gas inlet nozzle

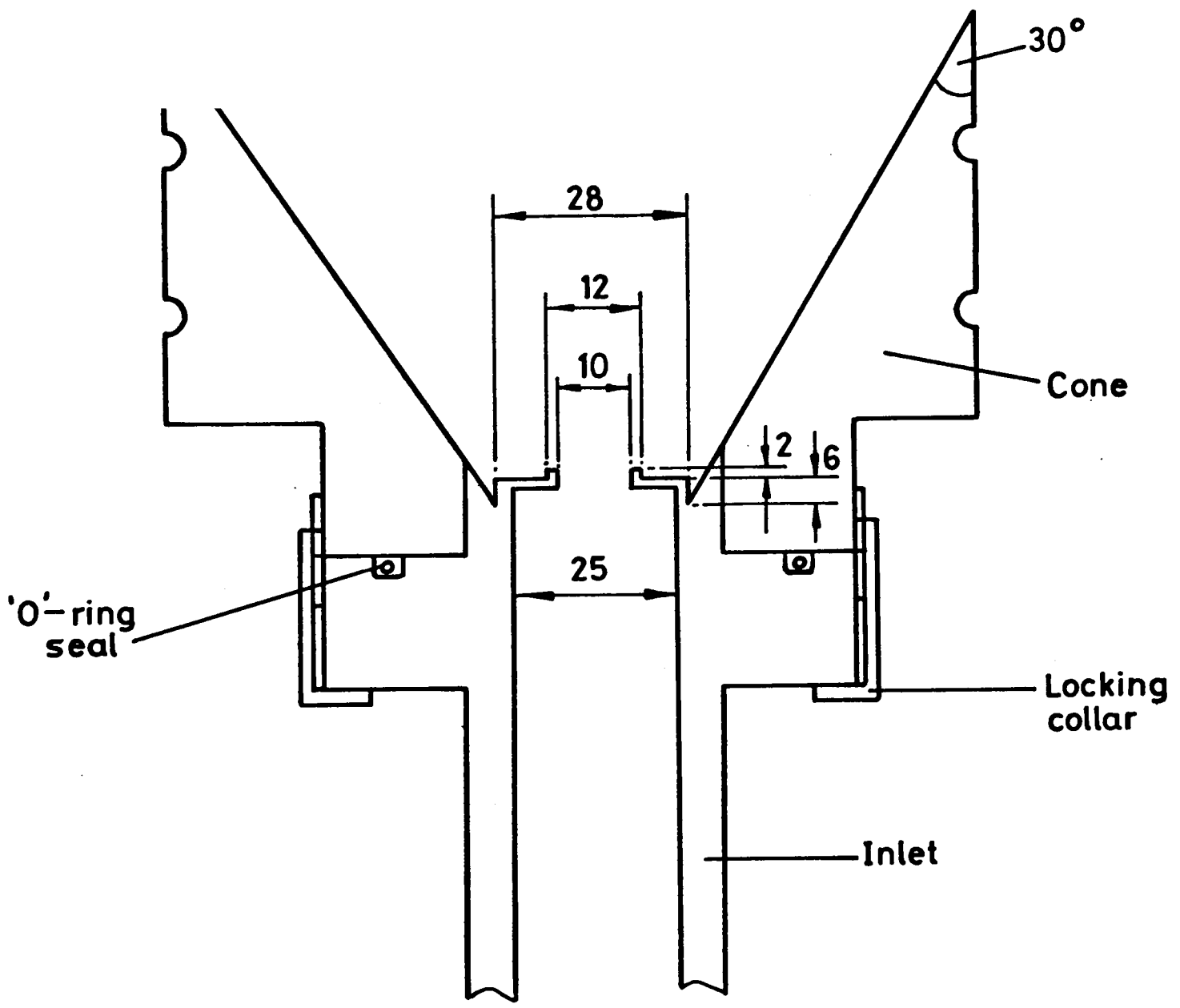


Figure 3.1 g : Details for the base cone and gas inlet

All dimensions in mm.

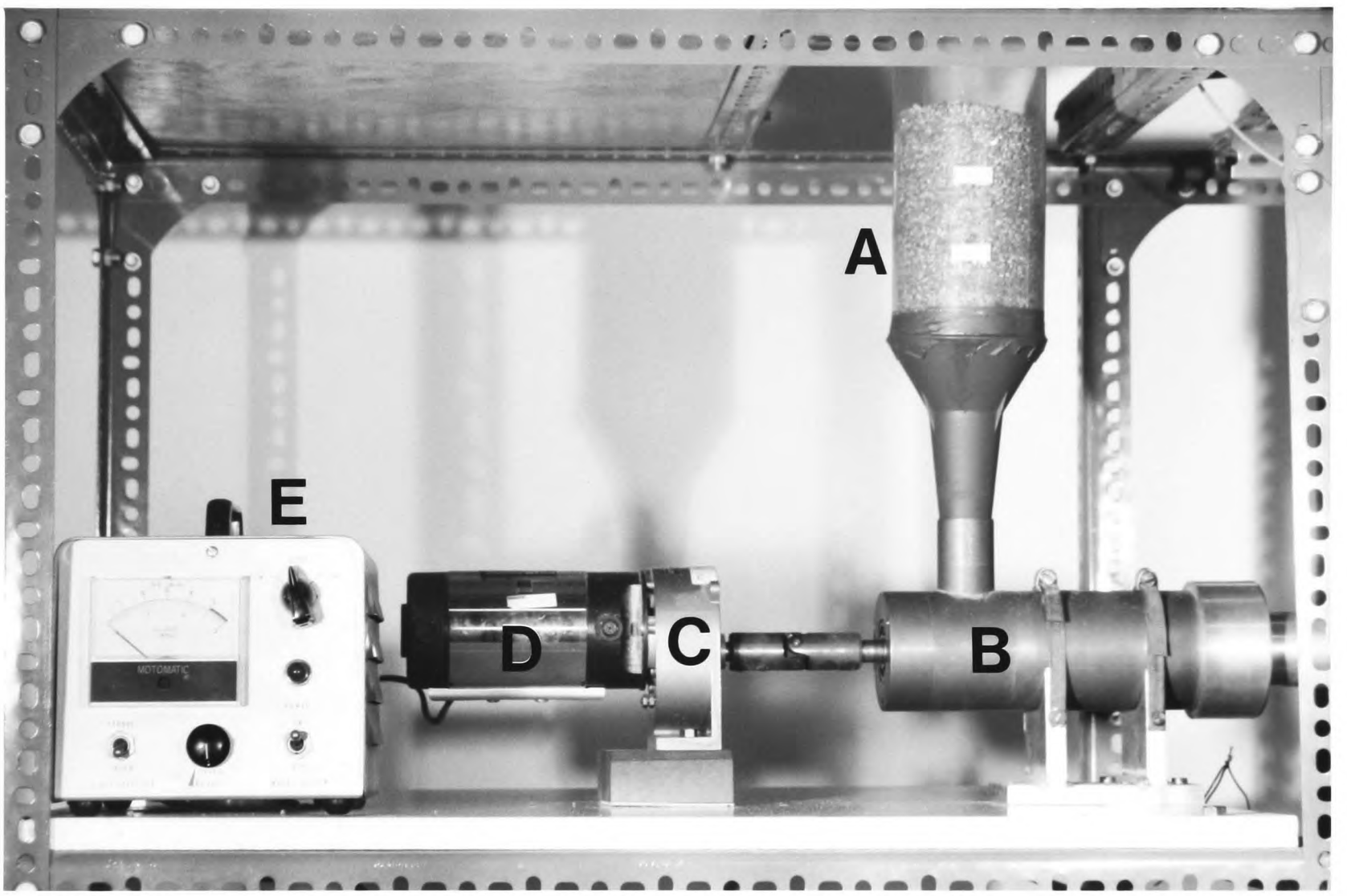


Figure 3.2a : The solids feed system

A : Perspex inlet hopper
B : Screw feeder
C : Gearbox
D : Motor
E : Motor controller

During an experiment the level in the hopper was allowed to fall, until refilled from the prepared cups of material. It was considered important that any segregation of the mixture in the hopper or feeder should be small. To assess this a series of experiments were performed, for which a full hopper was discharged through a screw feeder into a series of collection vessels. Three mixtures of wheat and brown mustard seed were fed at each of the three motor speeds. Any segregation occurring would initially result in a mixture richer or weaker in coarse particles to be discharged preferentially. The variation of the concentration of wheat in the mixture discharged z_a with height of material in the hopper h is shown in Figure 3.2b. The variation in mixture discharged is small enough to discount any segregation in the hopper or feeder and shows that reproducible mixture strengths can be achieved using the chosen filling method. Also, the solids flow rate is required to be independent of the height of material in the hopper and Figure 3.2c shows the relationship. For hopper depths between 0.1 and 0.9 m the variation in solids feed rate was less than 4%, except for a 50:50 mixture by volume at the highest flow rate. As only an occasional run was performed at flow rates higher than 8 gs^{-1}, the variation in m of the feed system was considered acceptable.

3.3 Gas Supply

Air was used as the spouting fluid for all runs. The air supply components are shown in Figure 3.3a. An ½" B.S.P. line was connected to the compressed air supply of the laboratory. The spouting air passed through an oil filter, a dust filter, a pressure regulating valve and a Saunder's flow control valve. Adjustment of the valves controlled the air flow rate to the spouted bed. The air flow rate was measured with a venturi meter. The gas flow rate W is given (B.S. 1042 : Part 1 : 64)

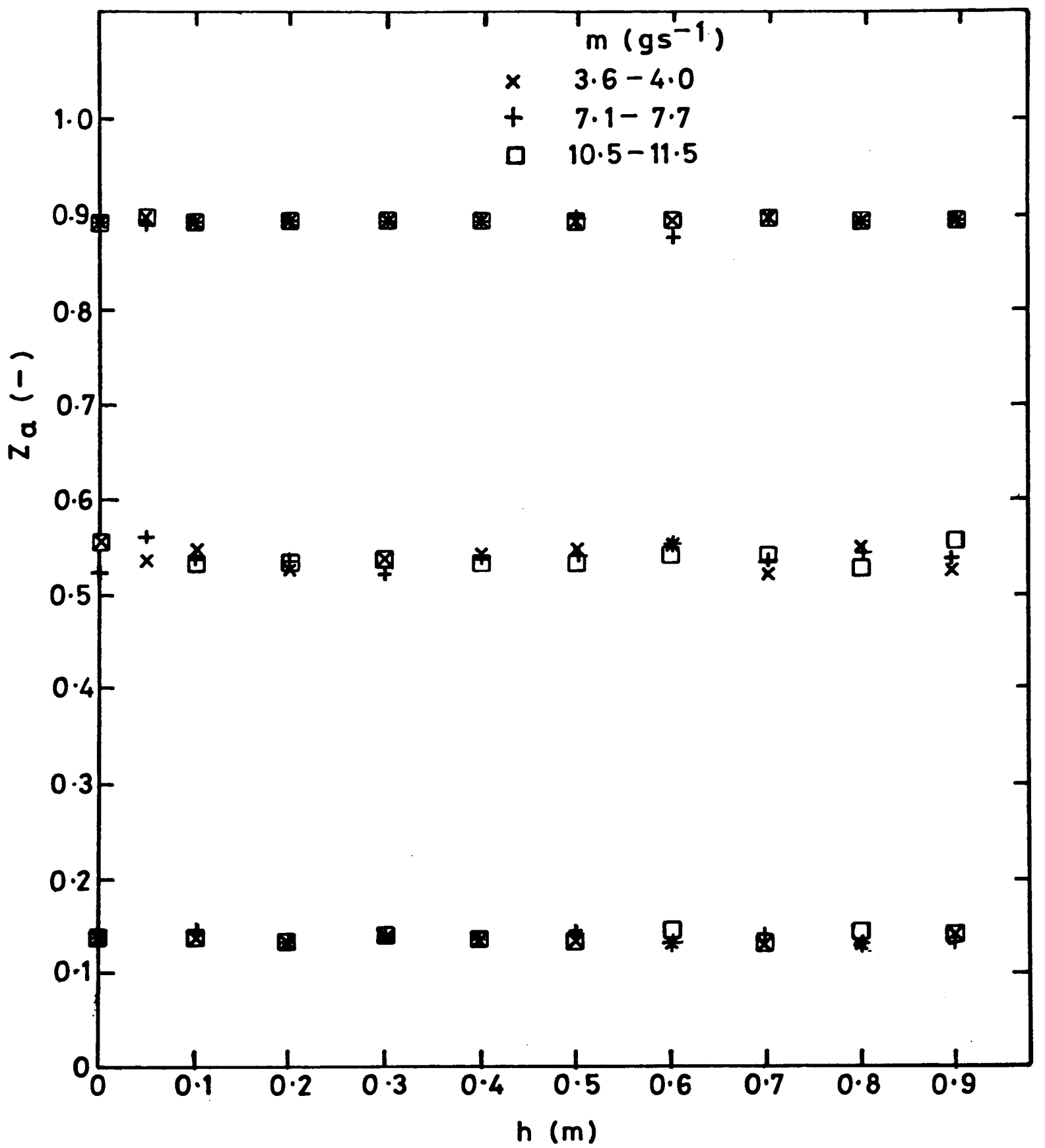


Figure 3.2 b : Mass proportion of wheat at the screw feeder outlet, z_a vs. Height of material in the hopper, h.

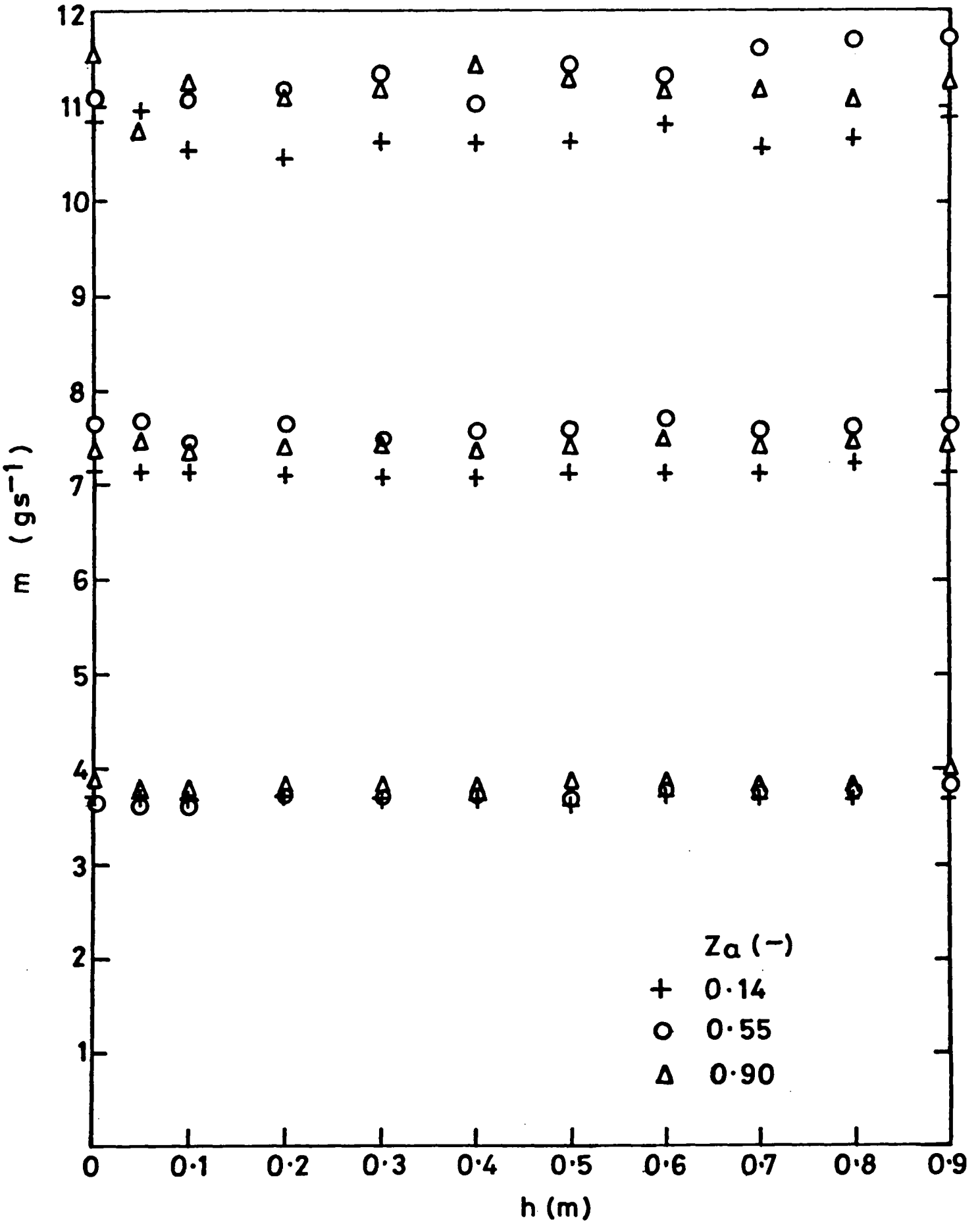


Figure 3.2 c : Mass flow rate of solids through the screw feeder, m vs. Height of material in the hopper, h.

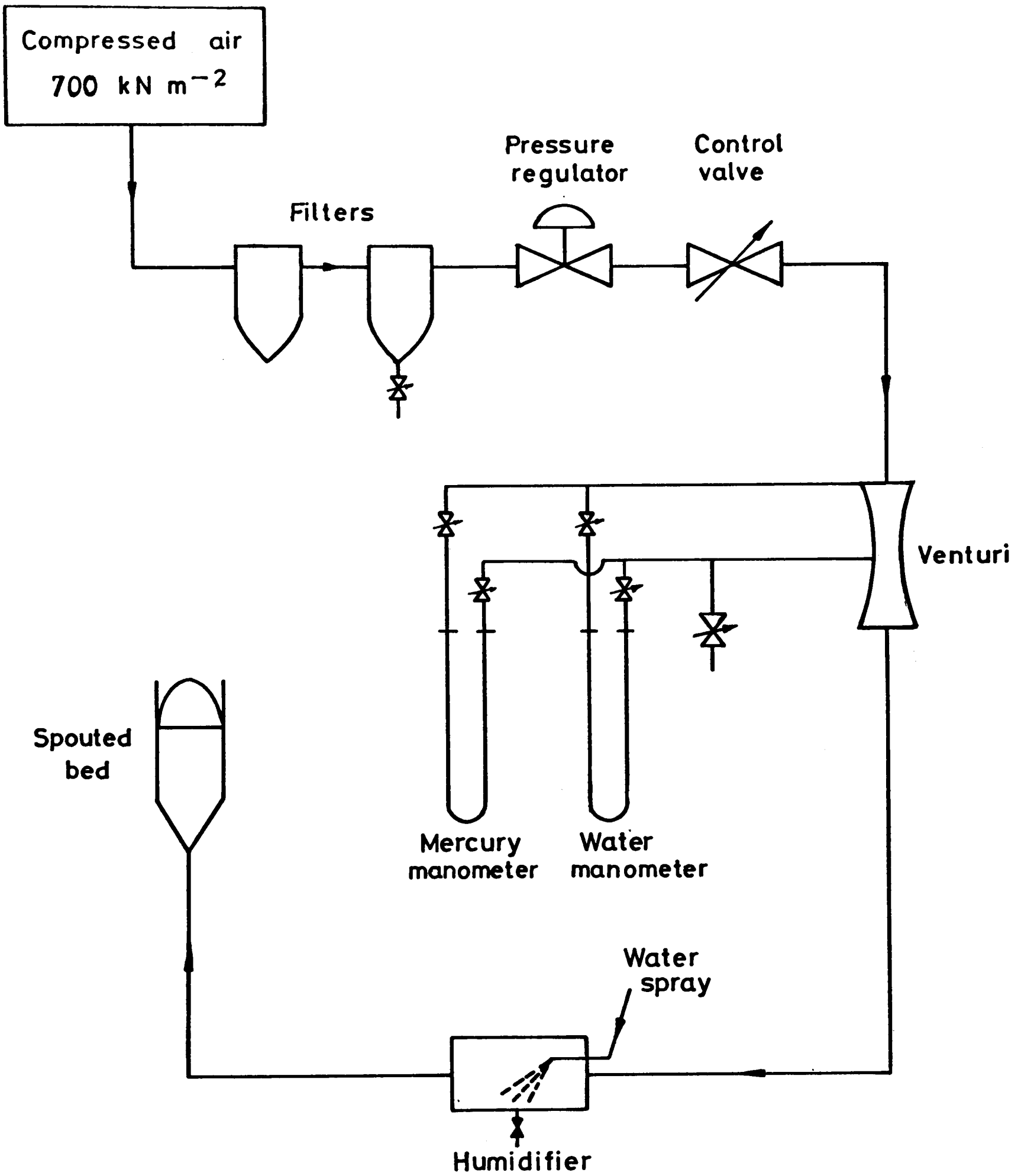


Figure 3.3 a : Details of the air supply

by:

$$W = 1.34 \times 10^{-3} \left(\frac{\Delta p \cdot p}{T_a} \right)^{\frac{1}{2}} \quad kg\ s^{-1} \qquad (3.1)$$

Where Δp is the pressure difference between the venturi tappings in mm of mercury, p is the absolute pressure at the upstream pressure tapping in mm of mercury and T_a is the absolute temperature at the upstream pressure tapping. The pressures were measured on manometers containing water or mercury and ambient temperature was found to be a good estimate of T_a. Equation 3.1 was used to calculate all air flow rates.

For certain runs a humidified air supply was required. This was achieved by injecting a fine water spray into a sealed container through which the air supply was passed. The humidifier was constructed of brass and is shown in Figure 3.3b. Excess water drained through the valve in the base of the container and the water level was kept sufficiently high to prevent any air leaks.

Some materials were found to attrite when spouted and the dust produced was carried out with the air. An air extractor was installed, its intake positioned 130 mm above the top of the column as shown in Figure 3.3c. This was sufficiently close to extract all air and dust from the bed but not close enough to lower the column pressure and affect spouting performance.

3.4 Particles and Labelling

Materials spouted in the bed were wheat seeds, white and brown mustard seeds and molecular sieve beads. These particles were chosen for the reasons of availability and low cost. The properties of all these particles used are given in Appendix B.

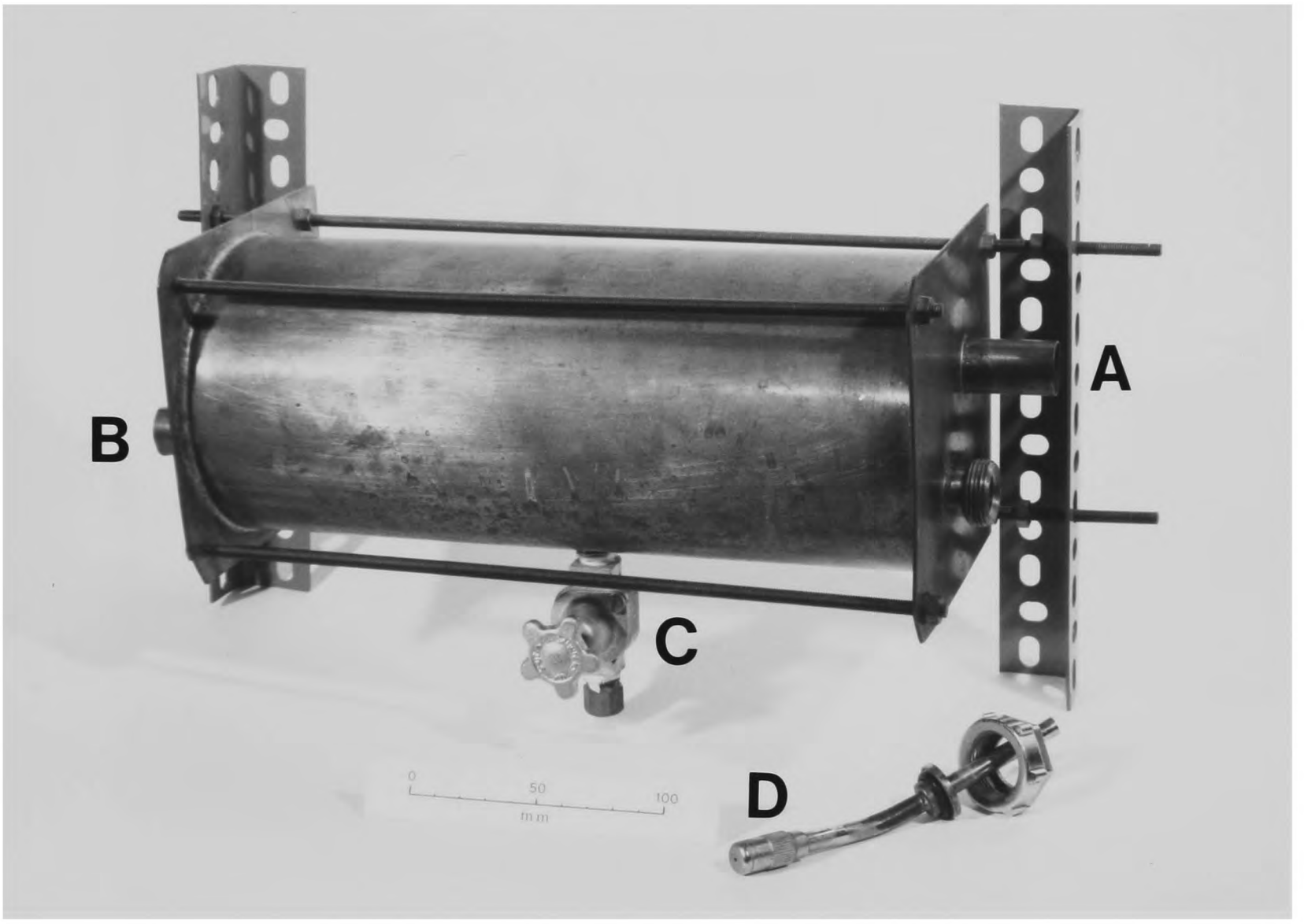


Figure 3.3b : The humidifyer

A : Gas in
B : Gas out
C : Drain valve
D : Water spray nozzle

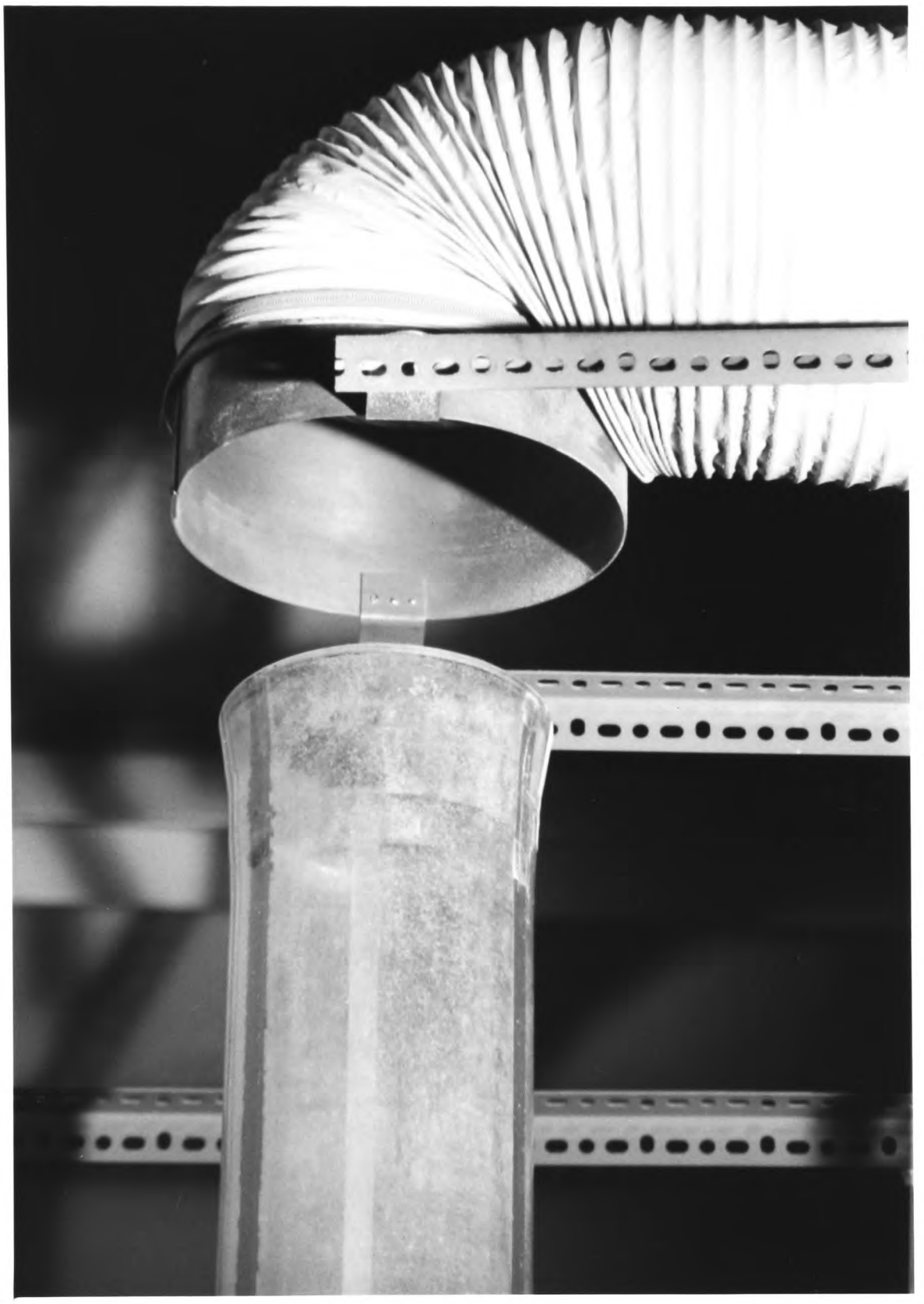


Figure 3.3c : The air extractor

To investigate the residence time distributions(RTD's) of particles in a vessel continuously fed with material, two methods are commonly used:

(i) a pulse of labelled material is injected into the inlet stream and subsequently samples from the outlet measured for the proportion of these labelled particles, and

(ii) a fraction of the inlet stream is changed from, say, red to white and then the fraction of white material in samples from outlet measured.

Each of (i) and (ii) lead to the evaluation of the RTD as described in Appendix A.

Method (i) was chosen for this study because of the limited quantities of labelled material available.

The requirements for the labelling are as follows:

a) it must cause no significant change in particle density, size or surface properties,

b) measurement of the proportion of tracer in each outlet sample should be quick and accurate, and

c) removal of labelled material from all outlet material to enable its re-use should be simple.

After a survey, described earlier, the method chosen was magnetic tagging. Particles to be labelled are mixed with a small quantity of soft iron powder and Tensol cement. A light coating of 2 or 3 mg of soft iron on a 50 mg particle results, and a finish of polyurethane spray prevents chipping of the surface. The labelling causes an increase in particle density of about 5% and an increase in surface roughness. The size increase is difficult to assess since the iron powder

rests in small specks and in surface hollows. Wheat and brown mustard seeds labelled in this way are shown with unlabelled particles in Figure 3.4a. Tagged particles are removed from the outlet material by passing all particles under a bank of seven "Alcomax" permanent magnets as shown in Figures 3.4b and c. The height of the magnets above the particle layer can be adjusted to give an optimum clearance. Particles lifted out in this way are weighed to give the proportion of tracer in each outlet sample. Recovery of 99% of the injected tracer is usual except in cases where the chosen bed depth and gas flow rates cause high rates of attrition of particles, where up to 25% of the labelled particles can be lost. The quantities of tracer used for each run varied, but were usually between 20 g and 50 g, equivalent to 0.1 to 1% of the total mass of bulk material used. This technique is a generally useful development in the field of particle mixing and could be used industrially.

3.5 Experimental Procedure

To prepare for a run, air is first supplied to the empty bed to prevent particles entering the air supply line at the base of the cone. The inlet hopper is then layered with particles of different sizes in the proportion of the desired mixture and material charged to the bed. The sealing rings on the base cone are then pressurised at 2 bar to prevent air leakage down the column. When the free surface of material approaches the solids overflow the air flow rate is increased to cause spouting. When a steady flow of material is leaving the bed a timer is started and the outlet material collected for set periods. To inject labelled particles the inlet hopper is allowed to almost empty, the tracer added to the inlet of the screw feeder and then the hopper re-

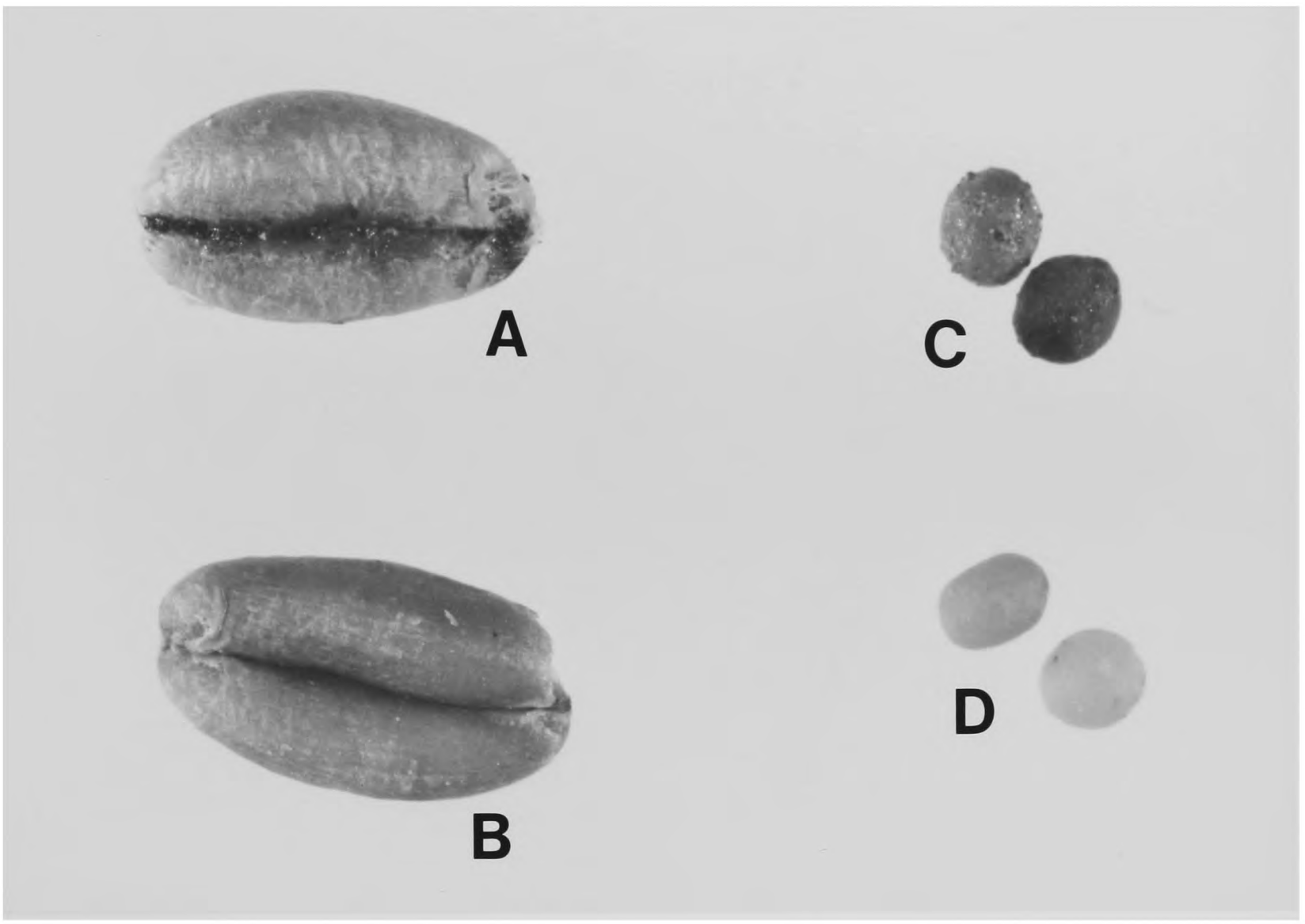


Figure 3.4a : The tracer particles used for measurement of RTD's.

A : Labelled wheat seed
B : Unlabelled wheat seed
C : Labelled brown mustard seed
D : Unlabelled brown mustard seed

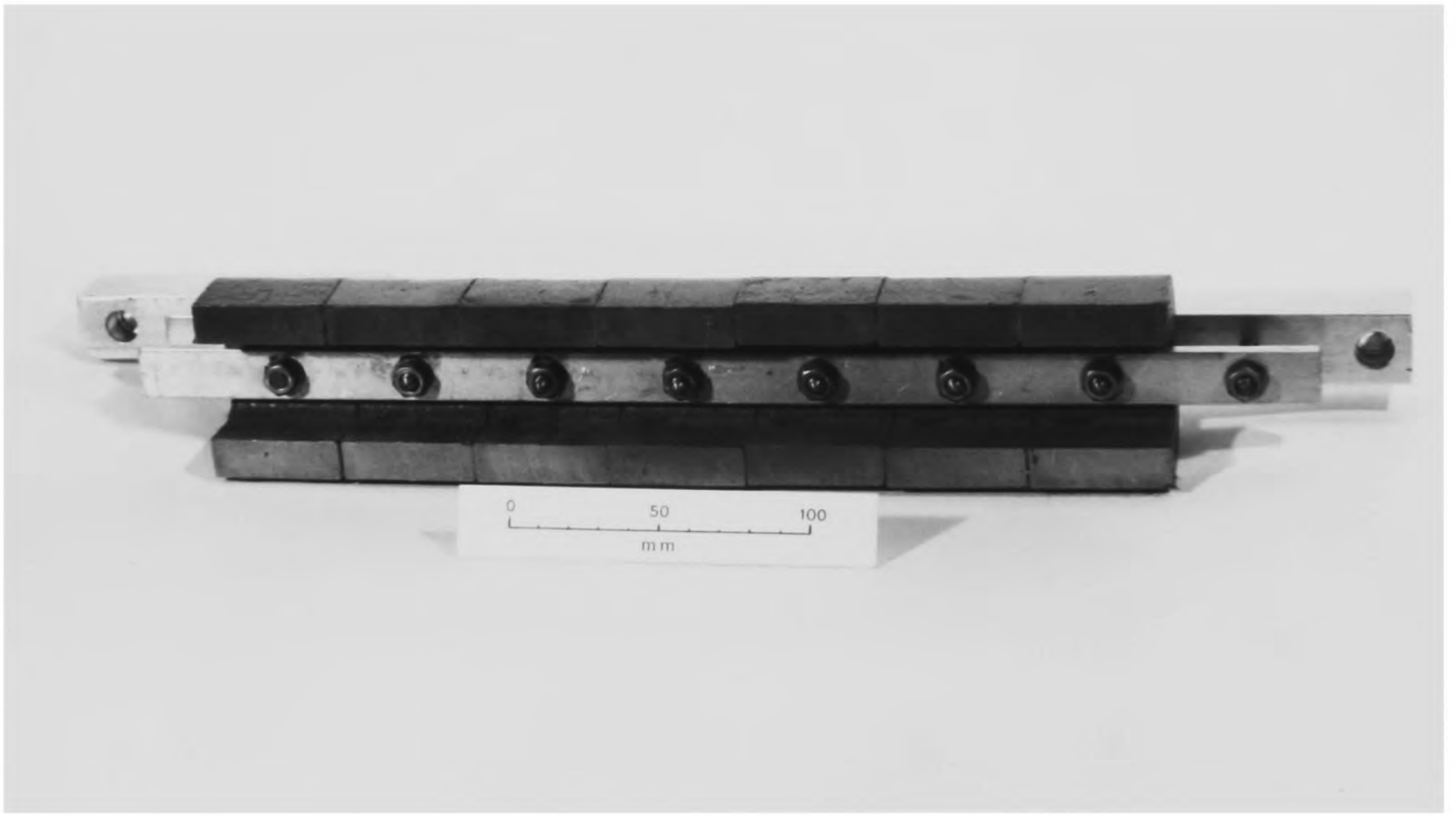


Figure 3.4b : The bank of permanent magnets used to retrieve tracer particles.

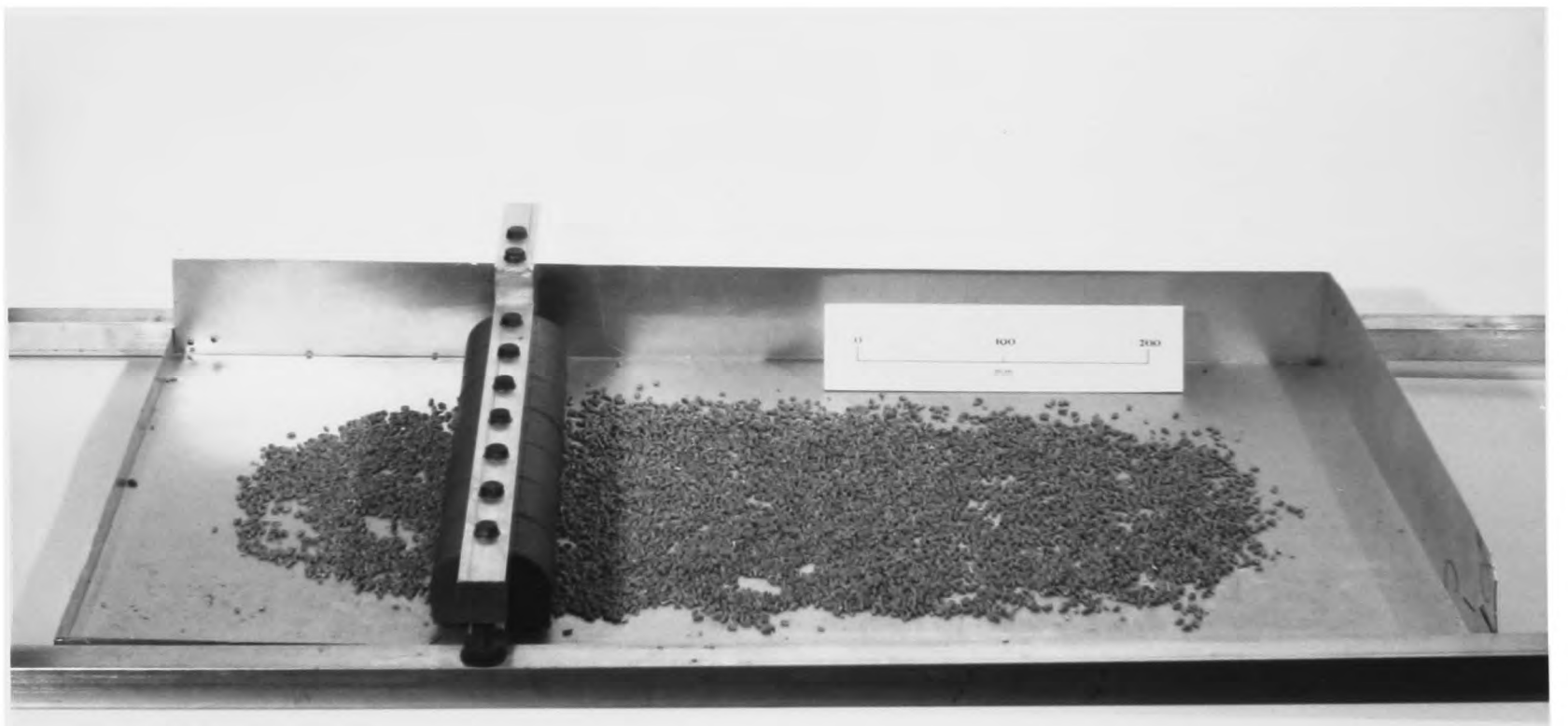


Figure 3.4c : Retrieval of tracer particles

filled immediately. After subsequent passage of up to four hold-up volumes of material the air flow is reduced to collapse the bed. The air supply to the sealing rings is turned off and the base cone and bed contents withdrawn from the lower end of the column. For experiments with a mono-size feed, tracer particles are then removed from each sample and the two components weighed. The accuracy of this measurement was ± 1 g for masses greater than 100 g and ± 1 mg for masses less than 100 g. For experiments with a binary feed the two different sized components are separated by hand sieving in a 0.46 m diameter sieve of an appropriate mesh size before removal of the tracers. The four components are then weighed.

The solids flow rate is calculated by dividing the total mass of solids passed through the bed by the duration time of the experiment. The mixture fed to the bed is calculated from the total masses of each component charged to the inlet hopper. The air flow rate is calculated as described in section 3.3. The bed depth H is the expanded bed depth and measured when the bed is spouting from a scale on the side of the column. H is the distance from the air inlet to the free surface as shown in Figure 3.5a.

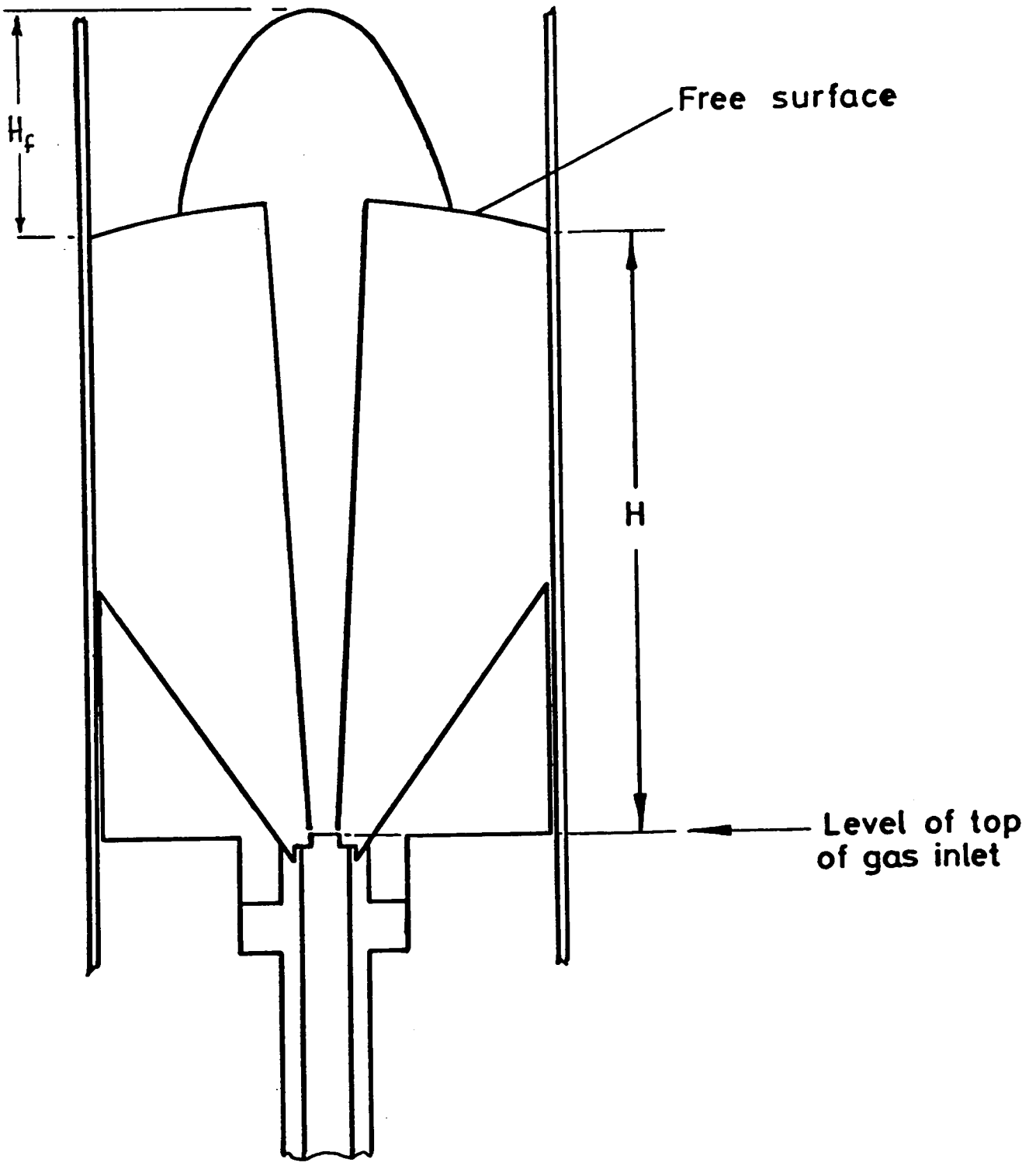


Figure 3.5 a : Definition of the bed depth, H.

CHAPTER 4

Mixing Behaviour and Mean Residence Times

4.1 Literature - One Species

The mixing of particles in continuous spouted beds has been the subject of a few investigations. Becker and Sallans (1960) injected slugs of dyed wheat particles at the feed point of a 229 mm i.d. bed and observed the decrease in concentration in the bed with time. It is not clear how this was done, but presumably spouting was discontinued and the bed was emptied for each measurement. For a range of feed rates, Becker and Sallans showed that an assumption of perfect mixing, where all material properties in the vessel are uniform and identical with those of the outgoing stream, was justified.

Kugo et al (1965) spouted wheat in beds of 98 mm and 150 mm i.d. The feed particles were suddenly changed to a continuous feed of dyed particles and the fraction of these in the outgoing stream (F(t) as described in Appendix A) was measured, although they do not say how this was achieved experimentally. The degree of mixing was assessed by calculation of the "hold-back", a term introduced by Danckwerts (1953), defined by

$$H_k = \frac{1}{\tau} \int_{t=0}^{\tau} F(t)\, dt \qquad (4.1)$$

where t is the time after the change of feed particles and τ is the mean residence time of feed material. Hold-back can be described physically as follows: if in a vessel of volume V the colour of inflowing material suddenly changes from white to red, hold-back is the fraction of V still occupied by white material after a volume V

of red material has been fed to the vessel. Kugo et al (1965) state that for plug flow, where the residence time of each particle is equal to the mean residence time, hold-back is zero and for perfect mixing is unity. For a range of gas velocities, bed depths and inlet nozzle diameters, the hold-back varied between 0.85 and 0.92. Mixing therefore, was nearly but not quite, perfect. As shown in Appendix A, for a perfectly mixed vessel

$$F(t) = 1 - e^{-t/\tau}$$

$$\text{whence } H_k = \frac{1}{\tau} \int_{t=0}^{\tau} (1-e^{-t/\tau})\, dt \qquad (4.2)$$

and on integration gives $H_k = 1/e$. For a vessel with plug flow of material,

$$F(t) = 0 \text{ for } 0<t<\tau$$
$$F(t) = 1 \text{ for } 0<t<\tau \qquad (4.3)$$

and on integration of equation 4.2 gives $H_k = 0$. Since the results of Kugo et al are otherwise consistent with those of other workers, it is clear that a correction factor of $\frac{1}{e}$ should be applied to their results, giving experimental values of hold-back between 0.30 and 0.34.

Barton et al (1968) used a 158 mm diameter bed and spouted a coke mixture screened to -6 +10 mesh and suddenly changed the feed to highly volatile coal, the volatility of which was constant at low temperatures. The fraction of volatile matter in the outflow was then measured using a gas chromatograph. A theoretical model was developed to describe the observed behaviour which assumed 92% of the bed volume to be perfectly mixed with 8% as deadwater, that part of the vessel which is by-passed by material flowing through. However, the coal and coke had a large density difference and thus segregation could give rise to different mean residence times for the coal and

coke. The theoretical model for a perfectly mixed vessel assumes a constant value of mean residence time, such a model would not then be expected to describe Barton's system. Barton et al observed no segregation in a perspex half-section model but did not investigate any possible selection mechanisms in the outlet region.

Epstein and Mathur (1971) correlated the solids mixing data from these three sources as shown in Figure 4.1, where the internal age distribution ($I(\theta)$ as described in Appendix A) is plotted against dimensionless time θ ($\doteq t/\tau$). From Barton's results, shown in this figure, it is apparent that if segregation was present it was not sufficient to cause a large deviation from perfect mixing.

Pallai and Németh (1971, 1972) using a 140 mm diameter glass column measured the residence time distribution (RTD) of plastic beads by injecting a pulse of coloured beads at the inlet. Again, the RTD was found to be very close to that for a perfect mixer.

4.2 Results - One Species

Preliminary experiments with a single component, in a system similar to those used by previous workers, were undertaken to prove the novel labelling technique suitable for the accurate measurement of RTD's.

All tracer concentrations, these being defined as the mass of labelled particles in a sample divided by the total mass of that sample, were calculated using a PDP11 computer. This concentration was then normalised by dividing by (Q/H_p) where Q is the mass of tracer injected at the solids inlet and H_p is the bed hold-up. Normalised tracer concentration in the outlet material was plotted

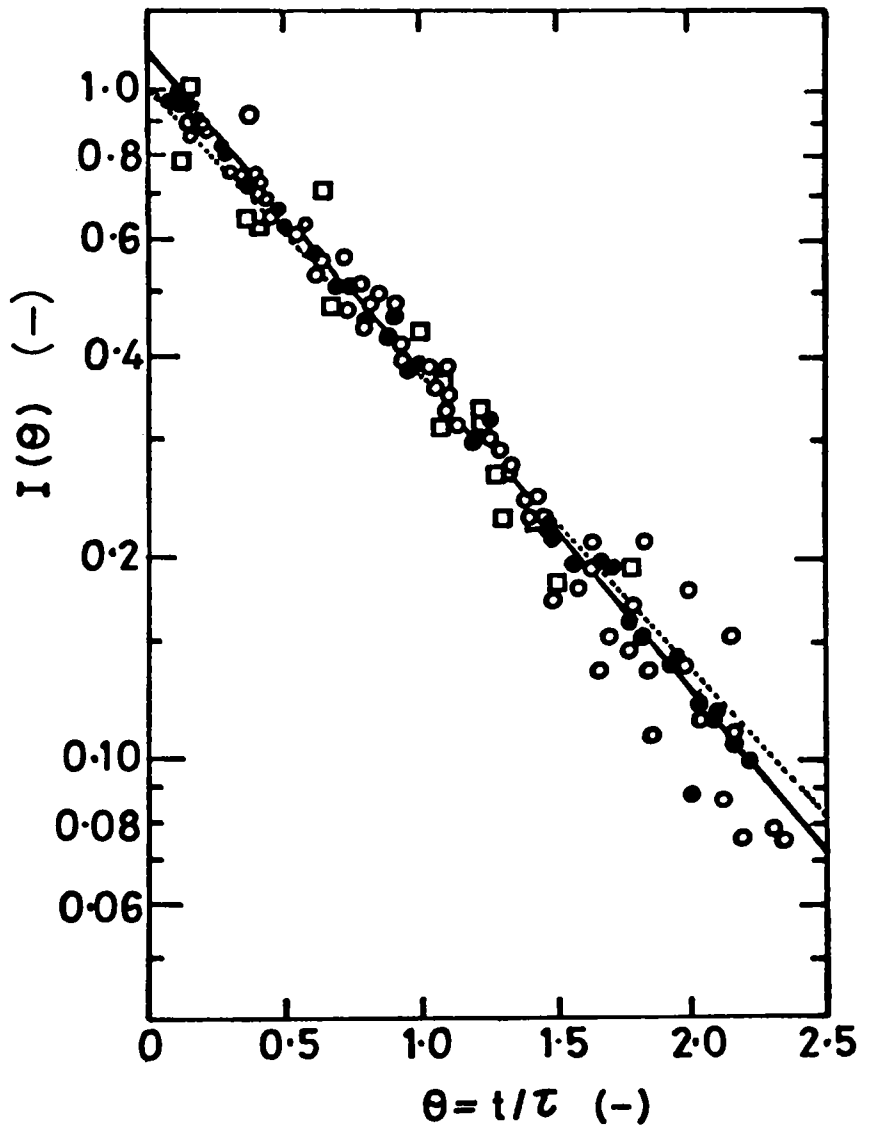


Figure 4.1 : Internal age distribution, I(θ) vs. Dimensionless time, θ .

Solids mixing data collated by Epstein and Mathur (1971)

- □ Becker and Sallans (1960)
- ● Kugo et al (1965)
- o Barton et al (1968)

——— Experimental straight line fit

····· Perfect mixing

against cumulative discharge from the bed. The RTD of wheat particles in the spouted bed is shown in Figure 4.2a. The program also draws the RTD for a perfectly mixed vessel with the same hold-up and material throughput as the spouted bed. This curve is of the form

$$E(\theta) = \exp(-D/H_p) = e^{-\theta} \qquad (4.4)$$

as shown in Appendix A. E is the normalised tracer concentration at outlet and D is the cumulative mass of discharged material. The shot of tracer can only be introduced to the bed over a discrete time interval, and because of its subsequent passage down the annulus before more rapid mixing in the spout all the tracer cannot become mixed immediately. The program thus permits the starting point of the theoretical perfect mixing curve (the value of D when E = 1) to be chosen to give the best fit to the experimental points which, for the example shown in Figure 4.2a, was a value of 0.3 kg.

RTD's have been obtained for a variety of feed materials and bed conditions. Materials used were wheat, brown mustard, white mustard and large and small molecular sieve beads; the physical properties are given in Appendix B. In all cases, the RTD's are very close to those for a single perfect mixer which is an exponential decay as shown in Appendix A. Experimental data were plotted and a computer library routine used to calculate by linear regression the best straight line fit of the form

$$\ln E(\theta) = a + b\theta \qquad (4.5)$$

where θ is dimensionless time ($\theta = \frac{t}{\tau} = \frac{D}{H_p}$) and a and b are constants. Results from beds of any depth and solids flow rate can be expected to be of this form. However, this straight line will not fit early measurements of tracer concentration since these are, or are very close

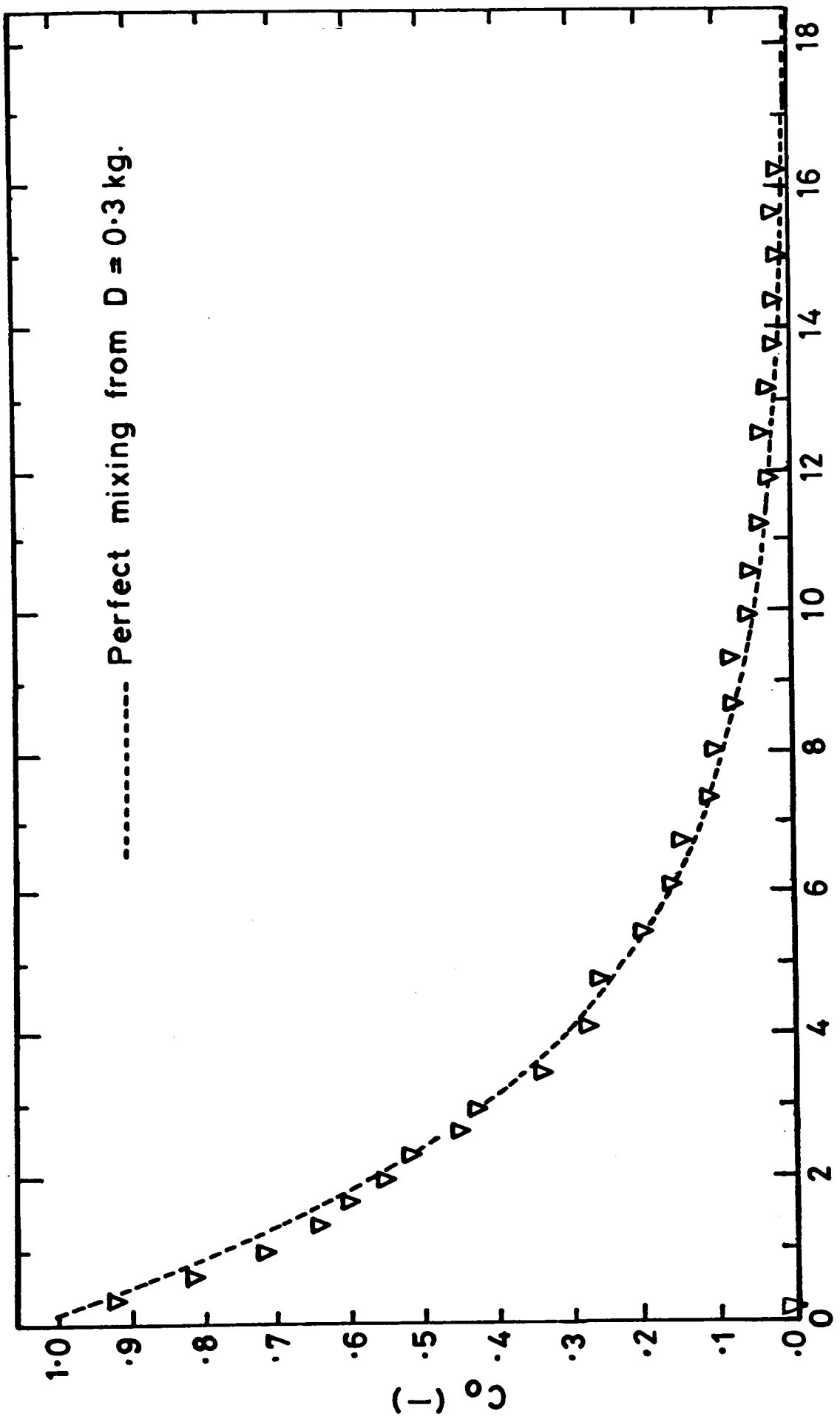


Figure 4.2a : Normalised tracer concentration, C_0 vs. Cumulative discharge, D. One species.

Experimental conditions : H = 280 mm, m = 0.38 kg min^{-1}
U_{ms} = 0.69 ms^{-1}; N_s = 1.05

Run : WHE 2; Material : Wheat.

to, zero (see Figure 4.2a). Therefore Equation 4.5 was only fitted to measurements taken after the maximum concentration was reached.

A typical set of results is shown in Figure 4.2b and a good set shown in Figure 4.2c. Values and standard errors of a and b for all runs are given in Table 4.2a. The experimental conditions of bed depth H, fountain height H_f, mass flow rate m and mean residence time τ of solids for these runs are given in Table 4.2b. As shown earlier, for perfect mixing a = 0 and b = -1.

The results show that for all materials and bed conditions used, mixing in the spouted bed is very nearly perfect.

4.3 Literature - Two Species

No work on the RTD of the components of a mixture in a spouted bed has been reported in the literature. However, previous work has noted the occurrence of segregation in spouted beds of mixtures with components varying in size or density.

Berquin (1964) studied granulation and observed that large granules segregated out in the upper part of the annulus near the column wall but the mechanism was not elucidated.

Piccinini et al (1977) used mixtures of glass ballotini in the size range 0.5 mm to 1.0 mm in an 80 mm i.d. plexiglass column. The bed was fed continuously with a mixture of two size fractions, the concentration of the coarse fraction at outlet was measured and the mass fraction in the bed calculated by mass balance. The fraction of coarse particles in the bed was up to twice that in the feed at low gas flow rates and independent of solids flow rate. The bed depth was varied to a small extent but no results from beds of depth greater

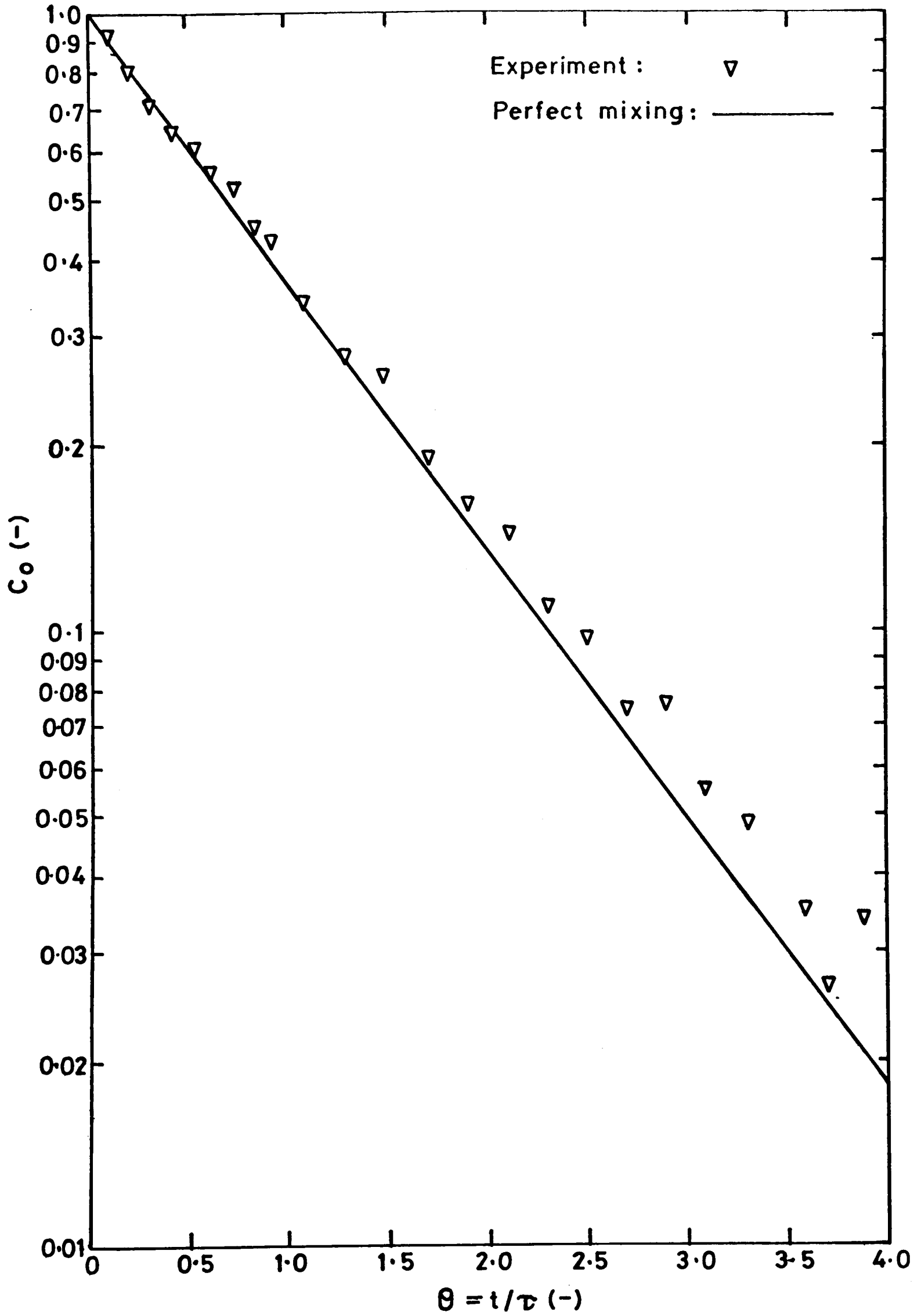


Figure 4.2b : Normalised tracer concentration, C_0 (= E) vs. Dimensionless time, θ. One species.

Experimental conditions : H = 415 mm, m = 0.41 kg min^{-1}
U_s =0.80 ms^{-1}, N_s= 1.01

Run : WHE 1; Material : Wheat.

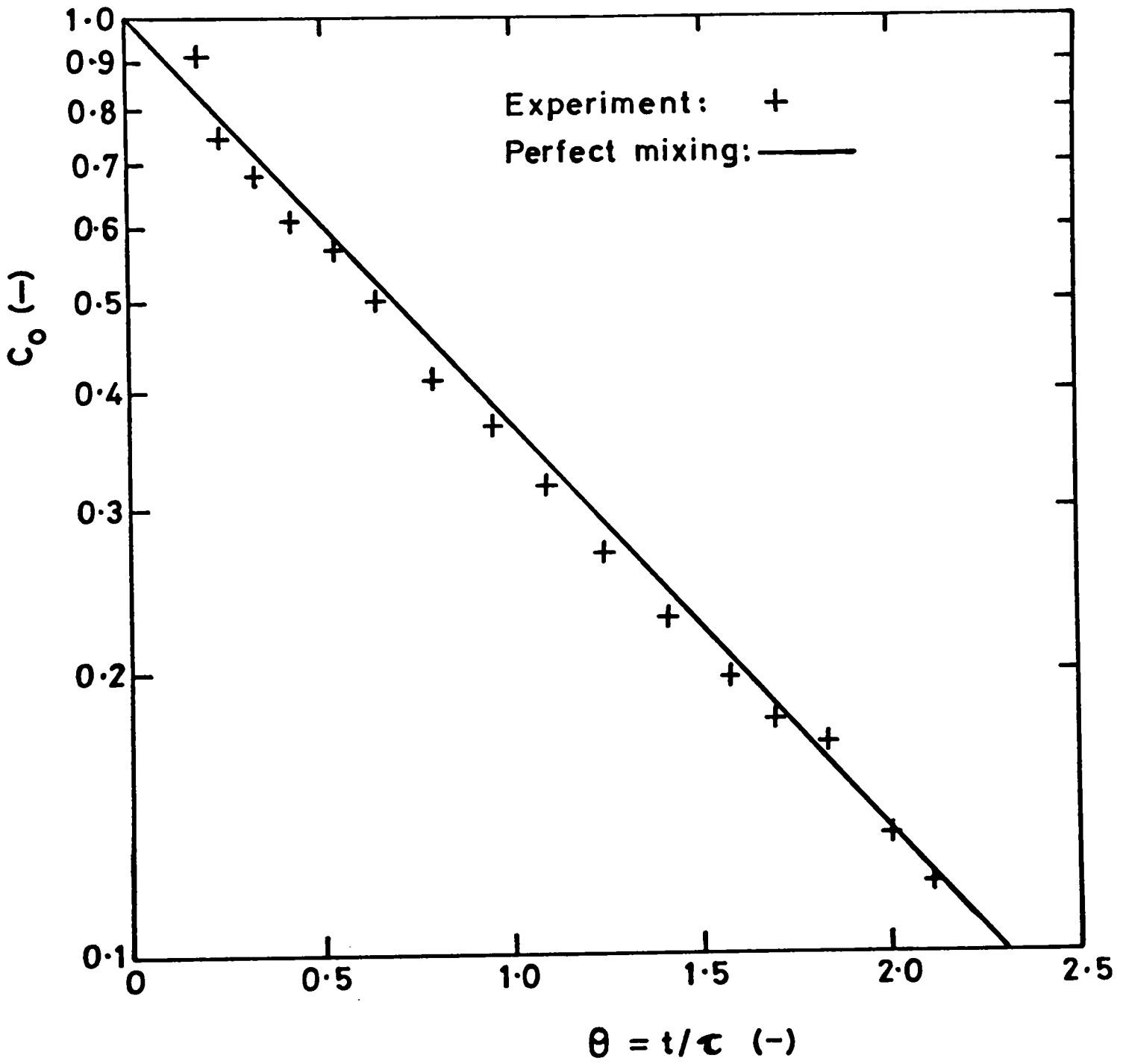


Figure 4.2c : Normalised tracer concentration, C_0 (= E) vs. Dimensionless time, θ. One species.

Experimental conditions : H = 292 mm, m = 0.15 kg min^{-1}
H_f = 270 mm, N_f = 1.9

Run : BRO 1; Material : Brown mustard.

Material	Run No.	b	s.e.(b)	a	s.e.(a)
BRO	1	-0.98	0.02	-0.04	0.02
BRO	2	-0.98	0.02	-0.05	0.02
WHE	1	-0.90	0.04	-0.09	0.05
WHE	2	-0.90	0.02	-0.05	0.06
WHE	3	-0.94	0.03	-0.03	0.07
WHE	4	-0.99	0.03	-0.03	0.06
WHI	1	-0.94	0.04	-0.07	0.08
WHI	2	-0.94	0.03	-0.06	0.07
MOL	1	-0.93	0.07	-0.15	0.11
MOL	2	-0.97	0.04	-0.16	0.06

Table 4.2a : Regression line parameters for RTD's.

Materials : BRO - Brown Mustard

WHE - Wheat

WHI - White Mustard

MOL - Large Molecular Sieves

Material	Run No.	H (mm)	H_f (mm)	U_{ms} (ms^{-1})	N_s (-)	m (kg min^{-1})	τ (min)
BRO	1	292	270	0.39	1.08	0.15	19.5
BRO	2	282	300	0.38	1.09	0.21	13.5
WHE	1	415	-	0.80	1.01	0.41	12.9
WHE	2	280	-	0.69	1.05	0.38	8.4
WHE	3	280	-	0.70	1.02	0.41	8.1
WHE	4	282	-	0.71	1.02	0.82	4.1
WHI	1	310	250	0.56	1.07	0.34	9.7
WHI	2	400	200	0.50	1.05	0.32	12.1
MOL	1*	380	-	Full fountain		3.63	1.8
MOL	2*	285	-	Partial fountain		2.79	2.2

Table 4.2b : Experimental conditions

Above parameters are defined on pages 37 and 49

Materials : BRO - Brown Mustard

WHE - Wheat

WHI - White Mustard

MOL - Large Molecular Sieves

* - Outlet diameter = 50 mm for these runs

than 1.2 times the cone depth were reported. The dependence of segregation on bed depth is not discussed. A half-section model and coloured ballotini were used to observe solids flow patterns within the bed. The following qualitative observations were made:

(i) At low gas velocities, the coarse particles preferentially moved to the upper inside part of the annulus.

(ii) With increasing difference in particle diameter of the two components, segregation became more pronounced.

(iii) Above a certain value of N_s (= U/U_{ms}) where U is the superficial gas velocity in the column and the subscript ms denotes the minimum velocity capable of spouting the material) good intermixing was observed except at the spout-annulus interface where, even at high gas velocities, there was a higher concentration of coarse particles.

(iv) For a mixture of 1 mm particles with a density ratio of 3, the behaviour of the denser fraction was similar to that of the coarse fraction mentioned in (i) and (ii) above.

Robinson and Waldie (1978) reported that segregation due to size difference occurred in the annulus. Their approach and results will be discussed in Chapter 5.

Cook and Bridgwater (1978) used a 193 mm diameter column and a mixture of mustard seed and glass beads to study radial and vertical segregation in a bed operated batchwise. The glass beads were larger in diameter and higher in density than the mustard seed. Using a dog-legged sampling pipe rising vertically through the base cone and annulus, material could be extracted at any radial or vertical position in the annulus. The radial concentration distribution was thus measured as a function of gas velocity and bed depth. Accumulation of

the dense, coarse fraction in the upper inner annulus, in accord with Piccinini et al (1977), was observed. However, for certain conditions, marked changes in concentration with depth were observed near the free surface and results suggested it was an oversimplification to assert that the more massive component always congregates in the upper inner annulus.

Piccinini (in press) used mixtures of glass beads, zirconium oxide and steel ball bearings in continuously operated 80 mm and 140 mm beds to study the effects of solids outlet position on particle segregation. Outlet positions used were 50 mm above the free surface, at the free surface (outlet 0), 10 mm below the free surface (S) or at two positions on the base cone (D high, B low). The fraction of coarse particles at outlet was measured until a steady state was reached, at which point the fraction in the discharge was different from that in the bed. Outlets O and S always initially discharged a mixture weaker in coarse particles than the feed. Outlet B always discharged a richer mixture in coarse particles. Outlet D discharged a richer mixture for high gas velocities and at low gas velocities, a weaker mixture. Reasons for these segregation trends such as different particle trajectories in the fountain were suggested but no detailed investigation was reported. Some studies of a mixture of materials differing in both size and density showed size difference to be the dominant cause of segregation although, as with other mixtures used, a comprehensive study of segregation for varying conditions was not reported.

4.4 Results - Two Species

The computer program used to analyse tracer concentrations for mono-size experiments was modified for use with a two component feed.

For each component, the tracer concentrations were normalised by dividing by (M_t/H_p), where M_t and H_p are the mass of tracer injected and the hold-up of that component at the moment of injection. RTD's were compared to those of perfectly mixed vessels with hold-ups and solids flow rates equal to those of each component. Each perfect mixing curve is again of the form

$$E(\theta) = \exp(-D/H_p) \qquad (4.6)$$

If the mean residence times of each component are different, the ratio of the hold-up masses, initially the same as the mass ratio in the feed (at the start of an experiment), will assume a new value in the steady state. During this transient period equation 4.4 would not describe the external age distribution of a perfectly mixed vessel since H_p is not constant. Therefore, if a comparison to perfect mixing is to be made, experiments to determine RTD's must be carried out once steady values of hold-up of each component are reached.

RTD's have been obtained for several bed conditions using wheat and brown mustard seeds as the large and small components. Physical properties of these materials are given in Appendix B. RTD's for wheat and brown mustard from a run using a mixture of 54% wheat fed to a bed of depth 595 mm are shown in Figure 4.4a which includes the theoretical curves for perfect self-mixing of each component. The same results plotted with a logarithmic ordinate, as described for a mono-size feed in section 4.2, are shown in Figure 4.4b. A computer library routine again calculated the best least squares fit of the form given in equation 4.5 and the values and standard errors of a and b are given in Table 4.4a. Experimental conditions for these runs are given in Table 4.4b.

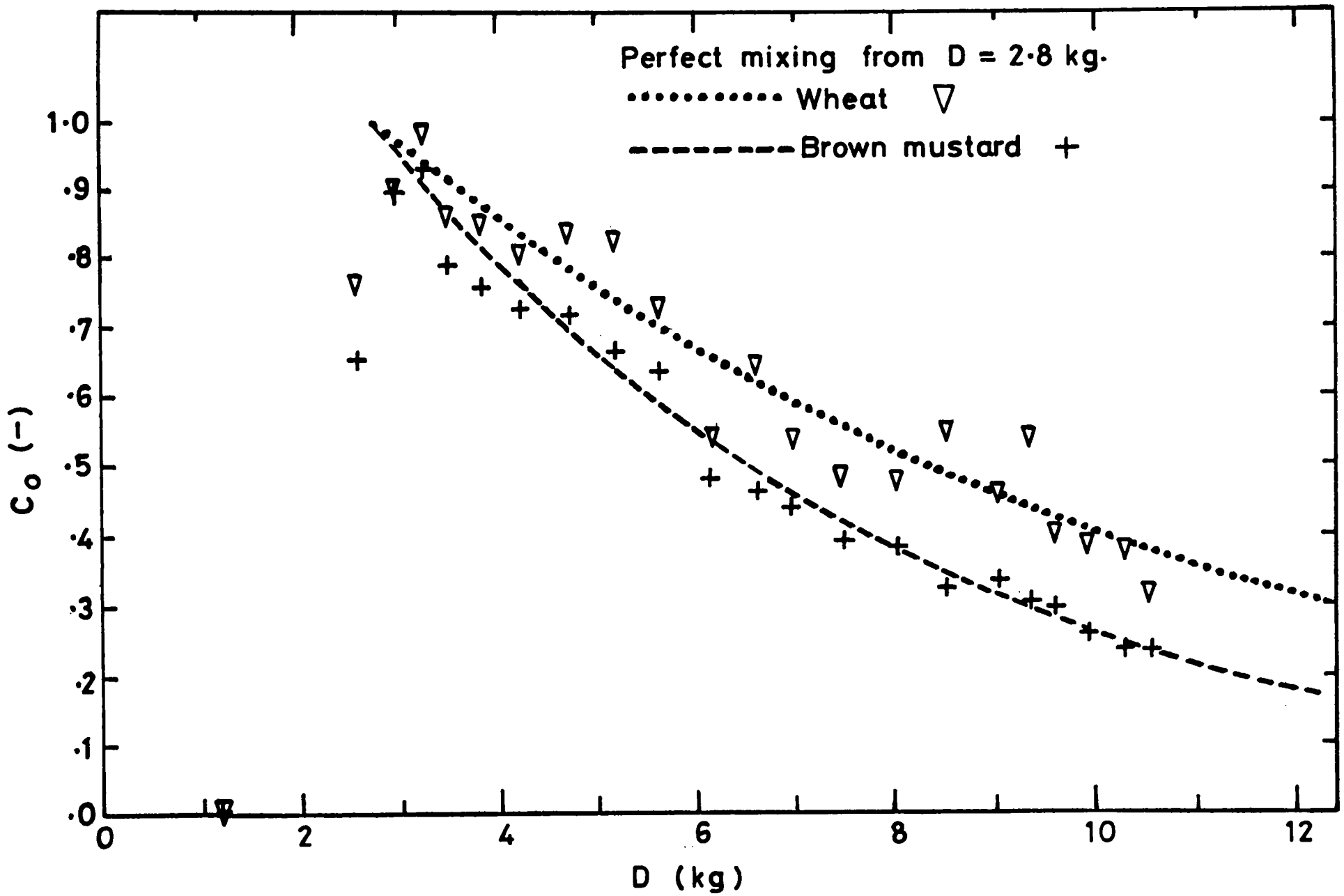


Figure 4.4a : Normalised tracer concentration, C_o (= E) vs. Cumulative discharge, D. Two species.

Run 26

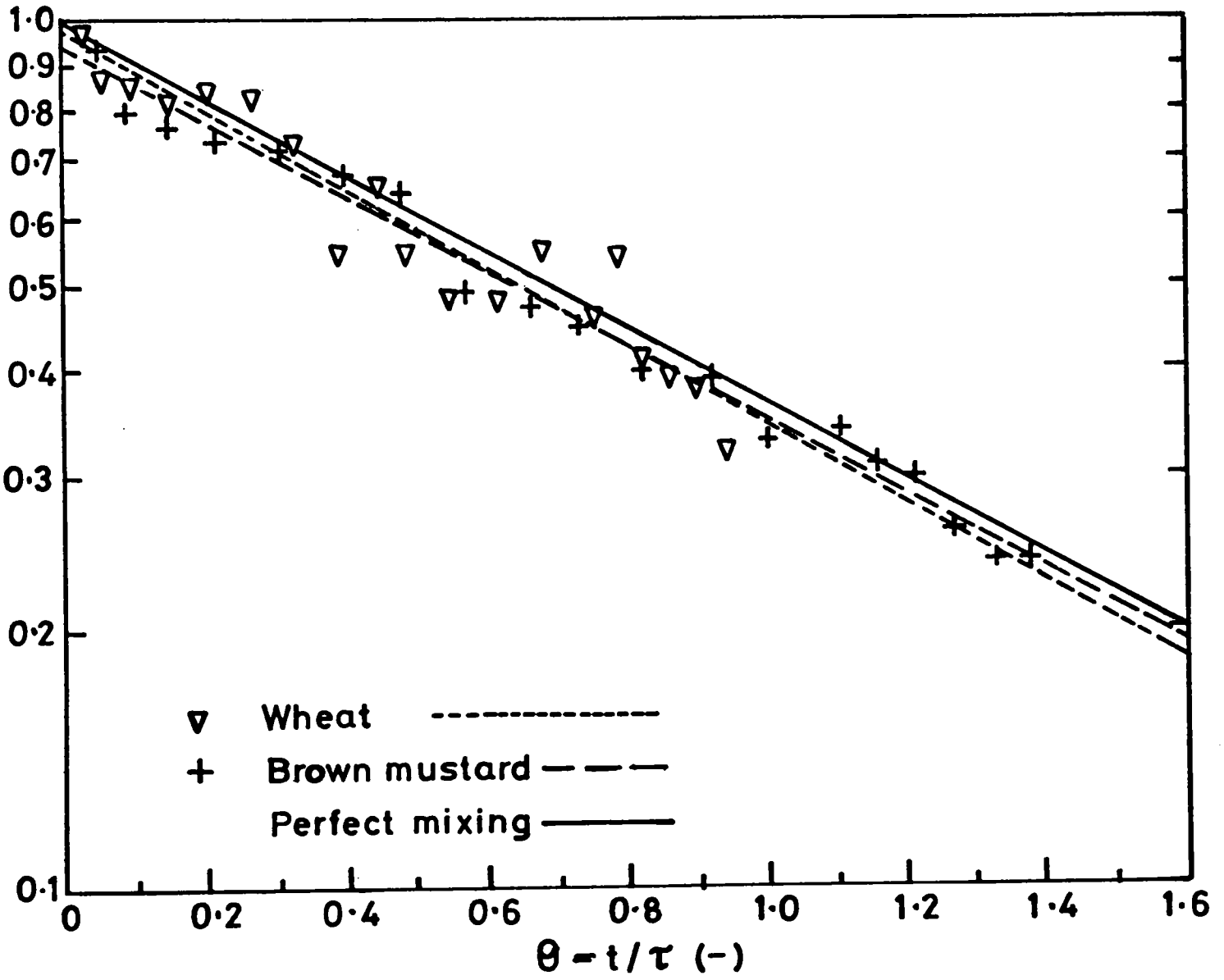


Figure 4.4b : Normalised tracer concentration, C_0 (= E) vs. Dimensionless time, θ.

Run 26

Run No.	Wheat				Brown Mustard			
	b	s.e.(b)	a	s.e.(a)	b	s.e.(b)	a	s.e.(a)
5	-0.97	0.02	2.55	0.12	-1.163	0.03	4.12	0.20
26	-1.04	0.08	0.34	0.07	-0.98	0.03	0.44	0.04
27	-1.08	0.08	0.39	0.07	-0.73	0.04	0.16	0.06
28	-0.98	0.05	-0.07	0.05	-1.07	0.02	0.06	0.02
41	-1.37	0.19	1.95	0.37	-1.14	0.06	1.98	0.15
76	-0.92	0.02	-0.13	0.06	-1.10	0.03	0.05	0.10
77	-1.10	0.09	-0.02	0.05	-1.03	0.03	-0.03	0.02
78	-1.04	0.07	0.02	0.05	-0.68	0.04	-0.25	0.04
81	-1.03	0.05	-0.01	0.05	-1.12	0.02	0.12	0.02
82	-0.94	0.02	-0.11	0.06	-1.12	0.03	0.08	0.10
83	-1.06	0.08	0.03	0.05	-0.71	0.04	-0.22	0.04
84	-0.99	0.05	-0.05	0.05	-1.08	0.02	-0.08	0.02

Table 4.4a : Regression line parameters for RTD's of binary mixtures

Run No.	z_a (-)	H (mm)	m (kg min^{-1})	N_f (-)
5	0.898	249	0.315	2.1
26	0.532	595	0.234	2.5
27	0.899	600	0.205	2.4
28	0.138	405	0.204	1.2
41	0.923	480	0.181	2.5
76	0.900	250	0.317	2.1
77	0.540	595	0.23	2.5
78	0.898	600	0.206	1.2
81	0.14	405	0.203	1.4
82	0.90	250	0.31	3.1
83	0.90	600	0.21	2.4
84	0.14	405	0.25	3.3

Table 4.4b : Experimental conditions. All parameters are defined in section 4.5

4.5 Mean Residence Times

As decribed in the previous section, any difference in the mean residence times of the two components fed to the bed causes a change in the bed hold-up of each until, in the steady state, the mass ratio of components in the feed and outflow are equal. The same computer program used to analyse tracer concentrations also calculated the changing mass fraction in the bed of either component and plotted this against cumulative discharge D. A typical plot of the mass fraction of wheat in a wheat-brown mustard system is shown in Figure 4.5a. The mean residence time of wheat was the longer for these conditions and the hold-up fraction of wheat increased accordingly.

The calculation of x_a and x_b, the mass fraction of the large and small components in the bed was by backstepping computation, starting with the hold-up mass of each component measured at the end of the run. This computation is accurate since all masses were measured to $\pm$ 1 g. Hereafter, the larger size fraction is referred to as component A and the smaller size fraction as component B. The mass fraction of A in the feed z_a is known and assumed constant. A mass balance on the bed over time Δt is performed assuming a constant volume of hold-up material.

For time Δt:

$$\text{Volume entering} = \frac{M_i z_a}{\rho_A} + \frac{M_i}{\rho_B}(1-z_a)$$

$$\text{Volume leaving} = \frac{M_{ao}}{\rho_A} + \frac{M_{bo}}{\rho_B}$$

where M_i is the total mass entering the bed in time Δt, ρ_A and ρ_B are the bulk densities of A and B, and M_{ao} and M_{bo} are the measured masses

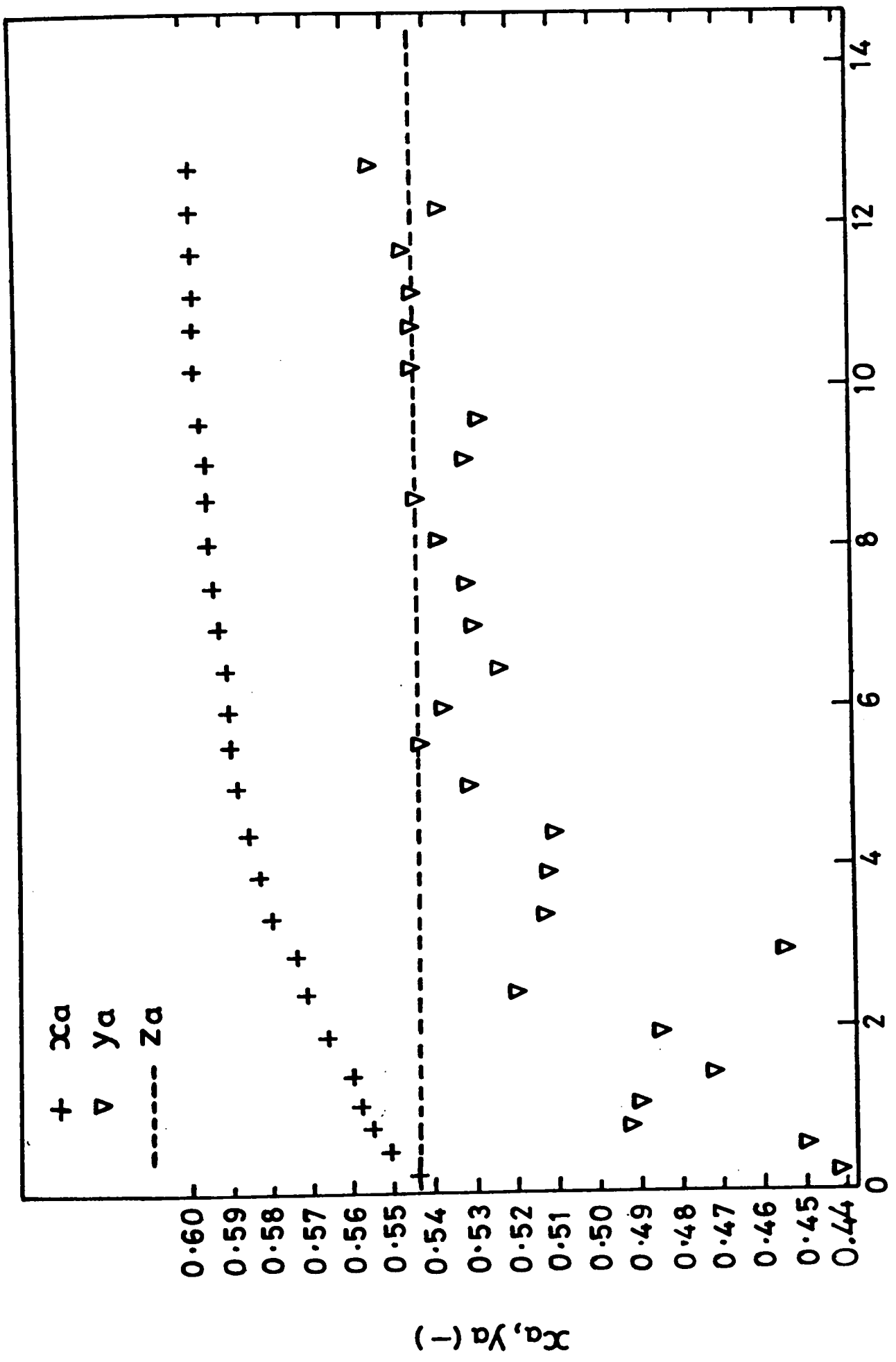


Figure 4.5a : Mass fraction of wheat in the bed X_a and mass fraction of wheat in the discharge y_a vs. Cumulative discharge, D.

Run B5

of A and B leaving the bed. These expressions are only accurate if the volume of the mixture is equal to the sum of the volumes of its components when separated. To assess the accuracy of this assumption, the "poured" [Haughey and Beveridge (1969)] and "packed" bulk densities of a range of mixtures of wheat and brown mustard were measured. Poured bulk density was measured by pouring simultaneously the two components of the mixture into a one litre narrow-necked measuring flask. Five readings were taken to obtain each bulk density. Packed bulk density was measured by compacting the material in the filled flask by agitation. This was achieved by placing the flask on a sieve-shaker and continually topping-up the flask with material of the same mixture; usually a constant volume was obtained after vibration for one minute. These measurements are given in Figure 4.5b; the broken lines show the expected bulk densities, given the above assumption. The maximum deviation of the measured bulk density from the expected is 6%. Poured, rather than packed bulk density is used in the following analysis since this is a better estimate of the bulk density of material in the bed, considered as a whole.

The hold-up volume is assumed constant, so equating the volumes of material entering and leaving gives:

$$M_i = (M_{ao}\rho_B + M_{bo}\rho_A) \; / \; (\rho_A + (\rho_B - \rho_A)\, z_a) \tag{4.7}$$

The mass fraction A in the bed at time t is defined thus:

$$x_a(t) = \frac{M_a(t)}{M_a(t) + M_b(t)} \tag{4.8}$$

Where M_a and M_b are the hold-up masses of A and B. In the

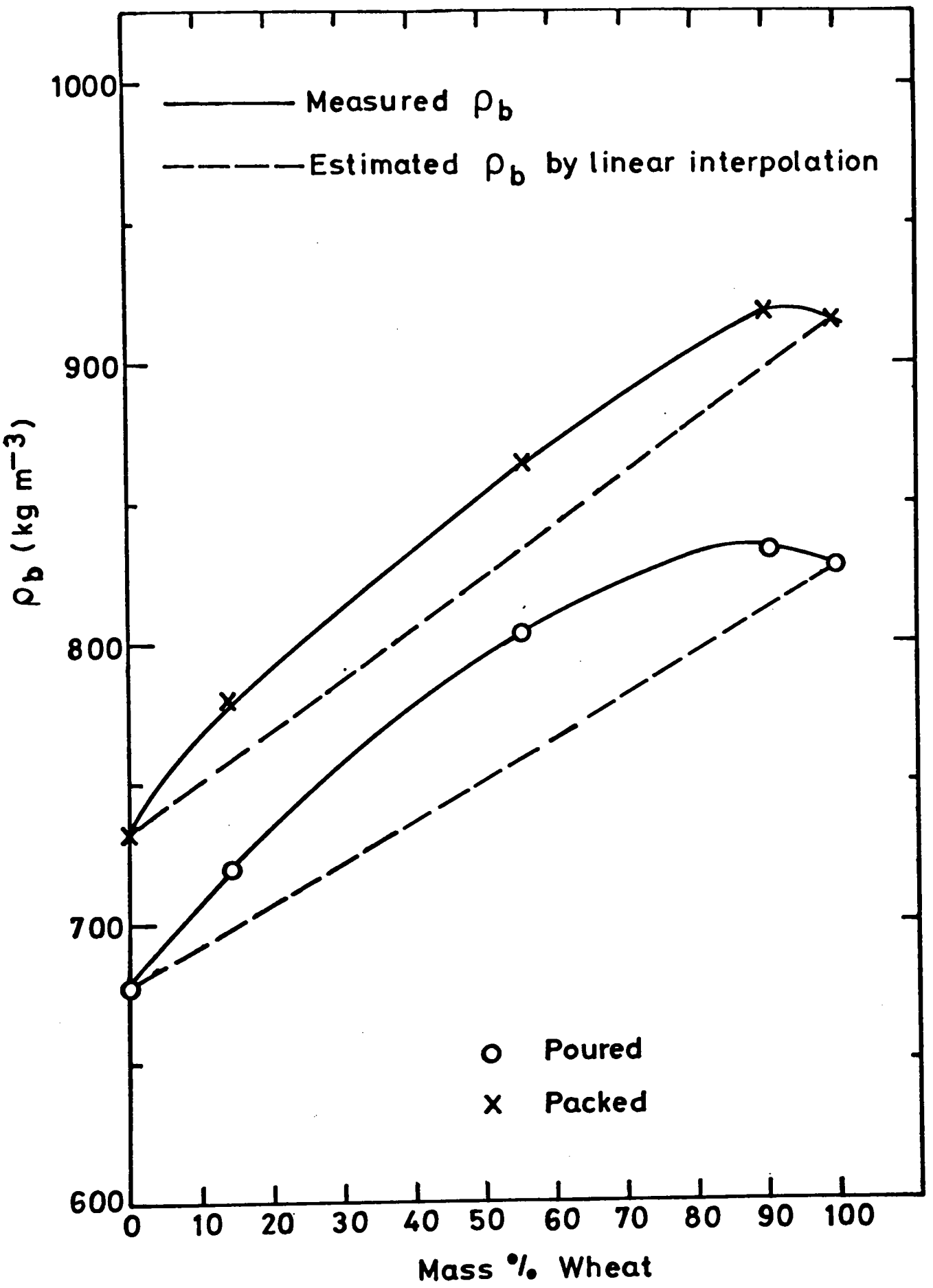


Figure 4.5 b : Variations of the poured and packed bulk densities of a wheat and brown mustard mixture

back-stepping calculation M_a and M_b are obtained from their known values at time $t + \Delta t$. A mass balance gives:

$$M_a(t) = M_a(t + \Delta t) + M_{ao}(t) - M_i z_a \tag{4.9}$$

and:

$$M_b(t) = M_b(t + \Delta t) + M_{bo}(t) - M_i (1-z_a) \tag{4.10}$$

Using equation (4.7) to determine M_i, $x_a(t)$ is calculated from equation (4.8).

The mean residence times for components A and B are given by:

$$\tau_a = \frac{M_a(\infty)}{m\ z_a} \tag{4.11}$$

and

$$\tau_b = \frac{M_b(\infty)}{m\ (1-z_a)} \tag{4.12}$$

where $M_a(\infty)$ and $M_b(\infty)$ are hold-up values in the steady state and m is the solids feed rate, calculated from the total mass of solids passing through the screw feeder during the course of the experiment. For each run τ_a and τ_b were calculated by dividing the steady-state hold-up masses of each component by their respective mass flow rates.

If the RTD's of each component in a bed fed continuously with a binary solids mixture can be regarded as equal to those expected in perfectly mixed vessels, as has been established, then the mean residence times alone of each component are sufficient to determine the RTD's (Appendix A, equation A.8). Mean residence times have been measured for widely varying bed conditions. The system investigated most extensively was for a wheat-brown mustard feed mixture. Three mixtures were used:

A : $z_a \simeq 0.14$

B : $z_a \simeq 0.55$

C : $z_a \simeq 0.90$

For each mixture the effects of varying bed depth when spouting H, solids feed rate m and gas flow rate on mean residence times was investigated. To assess the relative importance of each of these parameters, the ratio of mean residence times t_o was calculated for each run, where

$$t_o = \tau_a / \tau_b \qquad (4.13)$$

Piccinini et al (1977 and in press) studied the effect of gas flow rate on segregation by varying the spouting number N_s (U/U_{ms} as described in Section 4.3). However, since U_{ms} is dependent upon bed depth and the mixture ratio in the bed, N_s = 1.0 might describe a partial fountain in a deep bed but an overdeveloped fountain in a shallower bed (Figure 4.6c). Mean residence times could be more dependent upon the way in which the fountain distributes material on the free surface and the size of the fountain, than on N_s. Therefore to represent relative magnitudes of gas flow rates, a fountain shape number N_f is introduced. N_f is defined as H_f / H_{fo} where H_f is the measured fountain height and H_{fo} is the height of the fountain when "full", then

for a partial fountain $0 < N_f < 1$,

for a full fountain $N_f = 1$

and for an overdeveloped fountain $N_f > 1$

Using a scale on the side of the column, full fountain height H_{fo} was measured for mixtures A, B and C at various bed depths and the values, are plotted in Figure 4.5c. The dependence of t_o upon N_f and H is

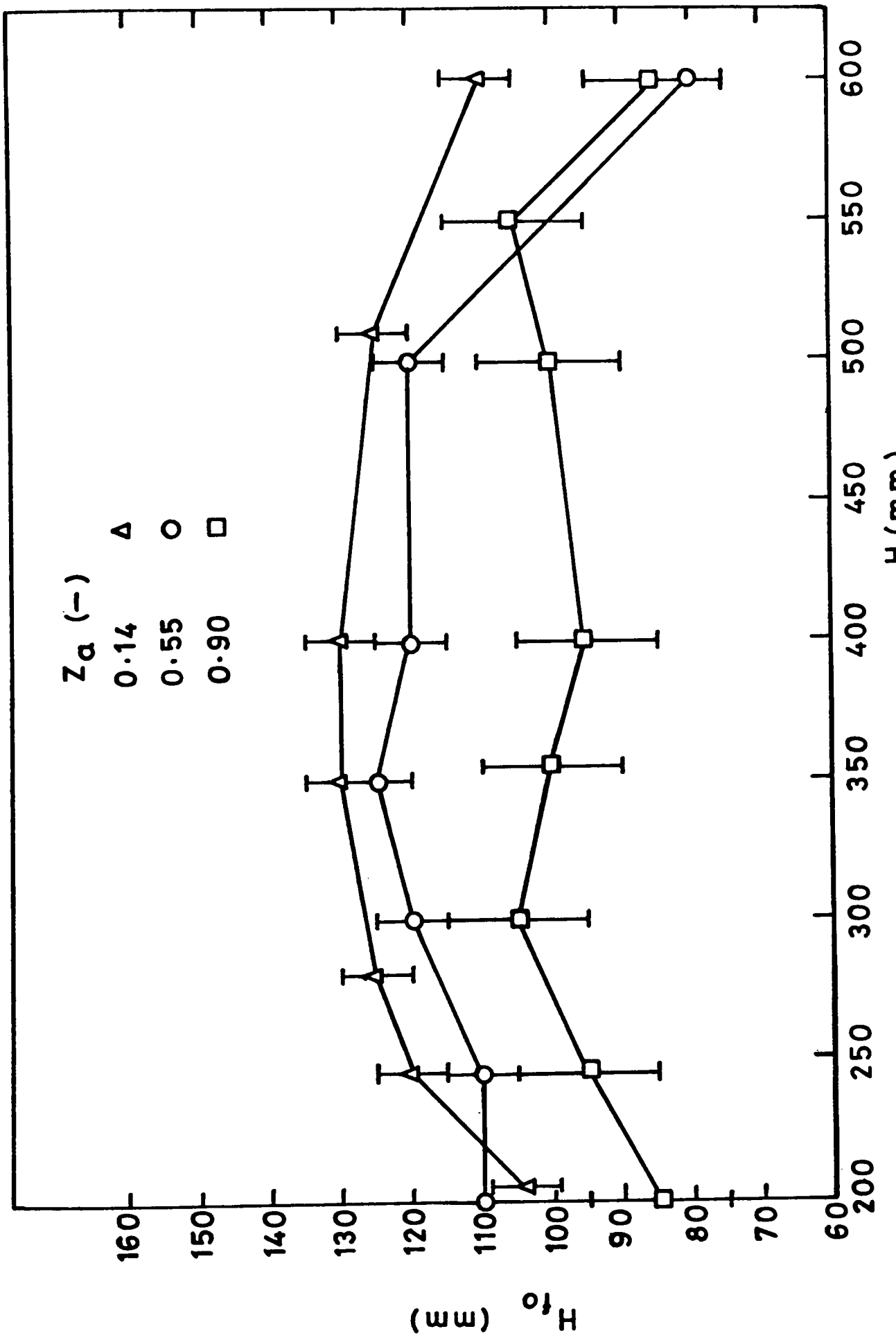


Figure 4.5 c : Height of the fountain when just covering the free surface, H_{fo} vs. Bed depth H when spouting a mixture of wheat and brown mustard.

discussed separately for the three mixtures and the effect of varying m for two cases with mixtures A and C is then discussed. Experimental conditions and results for all runs are given in Table 4.5a.

(i) Mixture A

Results are shown in Figure 4.5d. This is the only feed mixture for which values of t_o less than unity may be achieved. However, this is only the case in shallow beds (H = 245-250 mm) and for low values of N_f (< 1.4) in deeper beds. For bed depths greater than 400 mm, t_o increased to between 1.07 and 1.37 for values of N_f between 2.0 and 3.3.

In beds fed with mixture A, a free surface sloping down towards the spout was observed (Figure 4.5e). Wheat particles landing on this slope were seen to slide down towards the spout before sinking into the annulus. Drahun (1979) also observed large particles landing on a slope of small particles to "float" down the surface, however no upward gas flow was present in Drahun's work. In the spouted bed, a portion of the free surface will slope down towards the outlet for most solid flow rates, as shown in Figure 4.5e. Wheat particles floating down this slope would reach the overflow more readily than mustard seed and hence the wheat will have a shorter mean residence time (t_o < 1). On increasing the gas flow, the voidage in the upper annulus could increase sufficiently to allow larger particles to sink immediately on impact from the fountain. At higher gas flows t_o would then increase, as observed in bed depths greater than 400 mm.

If the findings of Drahun (1979) for large particles landing on a slope of small particles can be applied to a slope with an upward gas flow, then support can be found for the results with mixture A. This

Table 4.5a : Experimental conditions and mean residence time ratios.

Run No.	z_a	H	m	τ_a	τ_b	N_f	t_o	Comment
A1	0.139	245	0.283	7.2	8.5	1.67	0.85	
A2	0.142	250	0.188	8.5	13.0	1.65	0.66	
A3	0.142	250	0.188	8.1	13.0	2.5	0.62	
A4	0.142	250	0.188	9.2	12.9	3.33	0.72	
A5	0.141	245	0.615	2.6	3.8	1.67	0.67	
A6	0.141	245	0.396	4.0	5.9	1.67	0.67	
A7	0.139	245	0.098	20.8	22.5	1.67	0.67	
A8	0.139	245	0.039	65.6	54.9	1.67	1.20	
A9	0.138	240	0.968	2.3	3.0	1.67	0.76	H_s = 40 mm
A10	0.136	405	0.194	18.8	21.5	1.46	0.88	
A11	0.136	405	0.194	24.5	20.7	2.5	1.18	
A12	0.136	405	0.194	25.9	20.6	3.3	1.26	
A13	0.135	495	0.236	26.4	21.6	0.96	1.22	
A14	0.146	495	0.198	20.3	27.1	0.8-1.4	0.75	
A15	0.146	495	0.198	30.7	24.0	2.0	1.28	
A16	0.146	495	0.198	32.7	23.9	2.8	1.37	
A17	0.127	598	0.158	48.8	37.9	1.8	1.29	A,S,W
B1	0.543	246	0.322	8.9	7.2	1.82	1.24	
B2	0.544	250	0.218	12.4	10.8	1.82	1.15	
B3	0.544	250	0.218	13.8	9.5	2.91	1.45	
B4	0.544	250	0.218	14.4	8.9	3.64	1.62	
B5	0.544	485	0.262	24.1	19.3	1.0	1.25	
B6	0.549	490	0.220	27.2	21.0	1.0	1.30	
B7	0.549	490	0.220	28.1	20.2	1.8	1.39	
B8	0.549	490	0.220	29.1	19.1	2.5	1.53	
B9	0.549	490	0.220	30.1	18.1	3.33	1.66	
B10	0.541	598	0.274	29.0	23.7	0.69	1.22	
B11	0.558	595	0.116	70.3	45.9	2.5	1.53	W
B12	0.550	596	0.185	45.2	29.3	2.5	1.54	
B13	0.540	592	0.153	49.8	33.9	2.5	1.48	A,S,W
B14	0.532	595	0.234	34.3	23.2	2.5	1.48	A,S
B15	0.546	595	0.253	32.4	21.9	3.75	1.48	
B16	0.538	598	0.244	32.0	24.2	3.75	1.32	
B17	0.543	590	0.244	32.5	32.4	3.75	1.39	
C1	0.887	248	0.344	8.4	6.9	2.11	1.21	
C2	0.901	243	0.335	8.4	7.1	2.11	1.18	
C3	0.898	249	0.315	9.2	7.1	2.11	1.29	
C4	0.888	242	0.186	14.6	8.7	3.16	1.68	
C5	0.888	242	0.086	30.2	19.7	3.16	1.54	
C6	0.902	242	0.399	7.6	7.0	3.16	1.08	
C7	0.904	242	0.565	5.2	3.6	3.16	1.44	H_s = 40 mm
C8	0.904	242	0.043	70.0	32.7	3.16	2.14	
C9	0.902	240	0.471	5.6	5.3	3.16	1.06	
C10	0.902	240	0.294	9.0	8.1	3.16	1.12	
C11	0.902	240	0.061	44.9	28.0	3.16	1.60	
C12	0.899	242	0.215	12.9	10.2	3.16	1.26	
C13	0.890	245	0.585	6.0	3.6	3.16	1.64	H_s = 40 mm
C14	0.900	242	0.161	17.2	13.3	3.16	1.29	
C15	0.905	480	0.314	18.5	14.5	1.2	1.28	
C16	0.923	480	0.181	30.5	25.7	2.5	<1.19	
C17	0.920	480	0.214	26.4	20.8	2.55	1.27	
C18	0.903	590	0.171	41.9	30.9	1.15	1.36	A,S,W
C19	0.918	595	0.209	32.9	25.8	1.18	1.28	
C20	0.899	600	0.206	32.9	21.8	2.41	1.51	A,S

Comments : A - Humidified Air Supply W - Wetted Solids

S - Earthed Strips H_s - Depth of outlet centre below free surface.

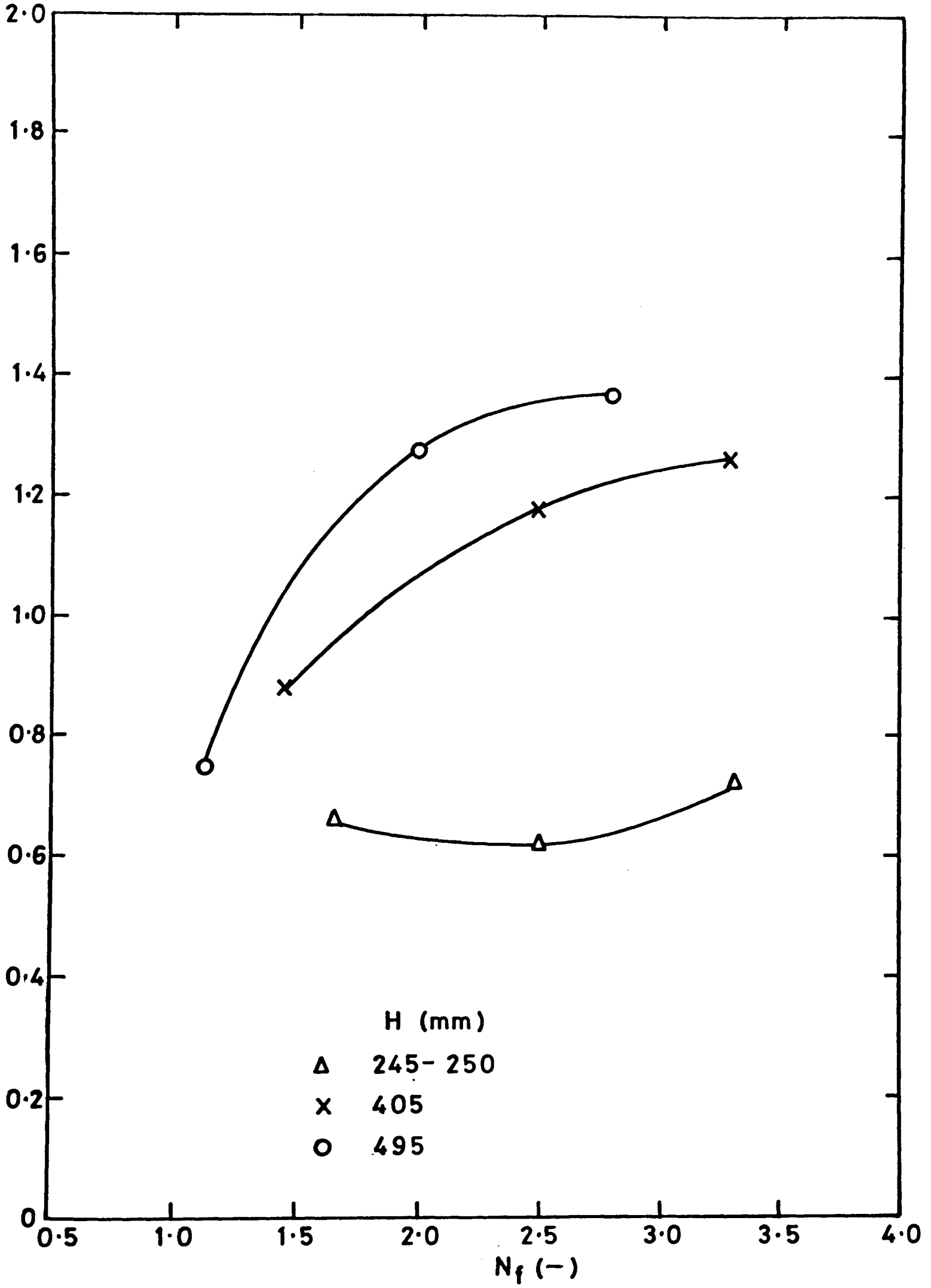


Figure 4.5 d : Mean residence time ratio, t_o vs. Fountain shape number, N_f.

Mixture A : z_a = 0.135 - 0.146
m^a = 0.188 - 0.197 kg min^{-1}

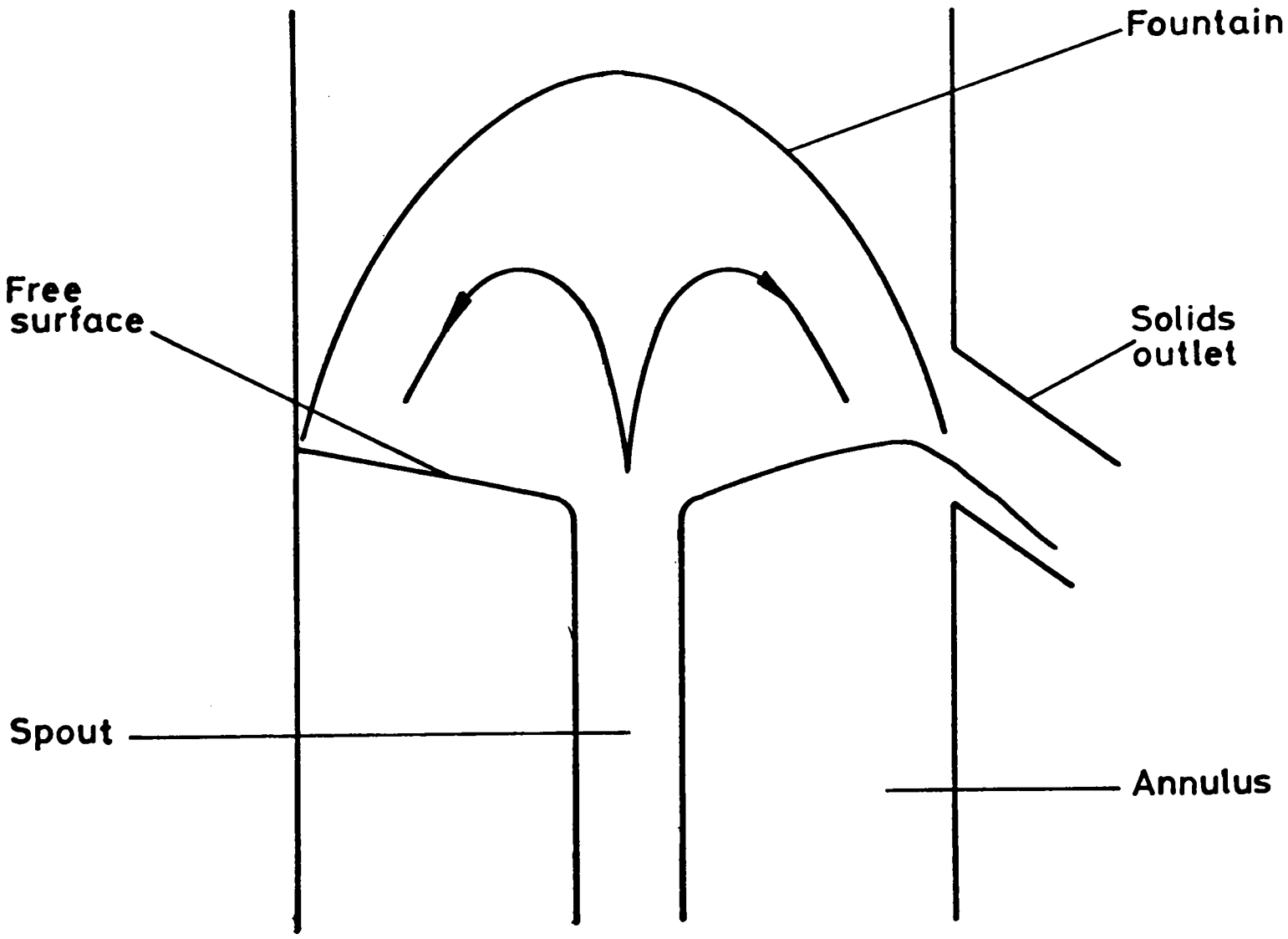


Figure 4.5 e : Profile of the free surface as observed when spouting
Mixture A : z_a = 0.13

is discussed in more detail in subsequent chapters.

(ii) Mixture B

For a feed with $z_a \simeq 0.55$, t_o is greater than unity for all values of N_f and bed depth. The results are shown in Figure 4.5f. t_o increases with increasing N_f for bed depths between 245 and 490 mm and values of t_o are higher for deeper beds at constant N_f. For the deepest beds (H = 590-598 mm), t_o increases from 1.22 to 1.5 as N_f increases from 0.69 to 2.5 but then falls to approximately 1.4 as N_f increases to 3.75.

The general trend, as with mixture A, is for t_o to increase with increasing N_f at constant bed depth and for t_o to be greater in deeper beds with the same value of N_f.

The mean residence time of a component in the bed is measured by dividing its hold-up mass in the bed at the end of the run by its mass flow rate through the bed. Each measurement of several kilogrammes of material is accurate to $\pm$ 1 g and therefore the quoted values of t_o are reliable estimates of the mean residence time ratios. The scatter in t_o of about 5% for some conditions in Figure 4.5f can be attributed to errors in measurement of fountain heights.

Since Drahun (1979) mainly studied slopes with only traces of minor components, for mixture B a physical mechanism in support of these results such as that proposed for mixture A is harder to draw. A more detailed discussion will be presented in subsequent chapters.

(iii) Mixture C

Results are shown in Figure 4.5g. All runs gave t_o greater than

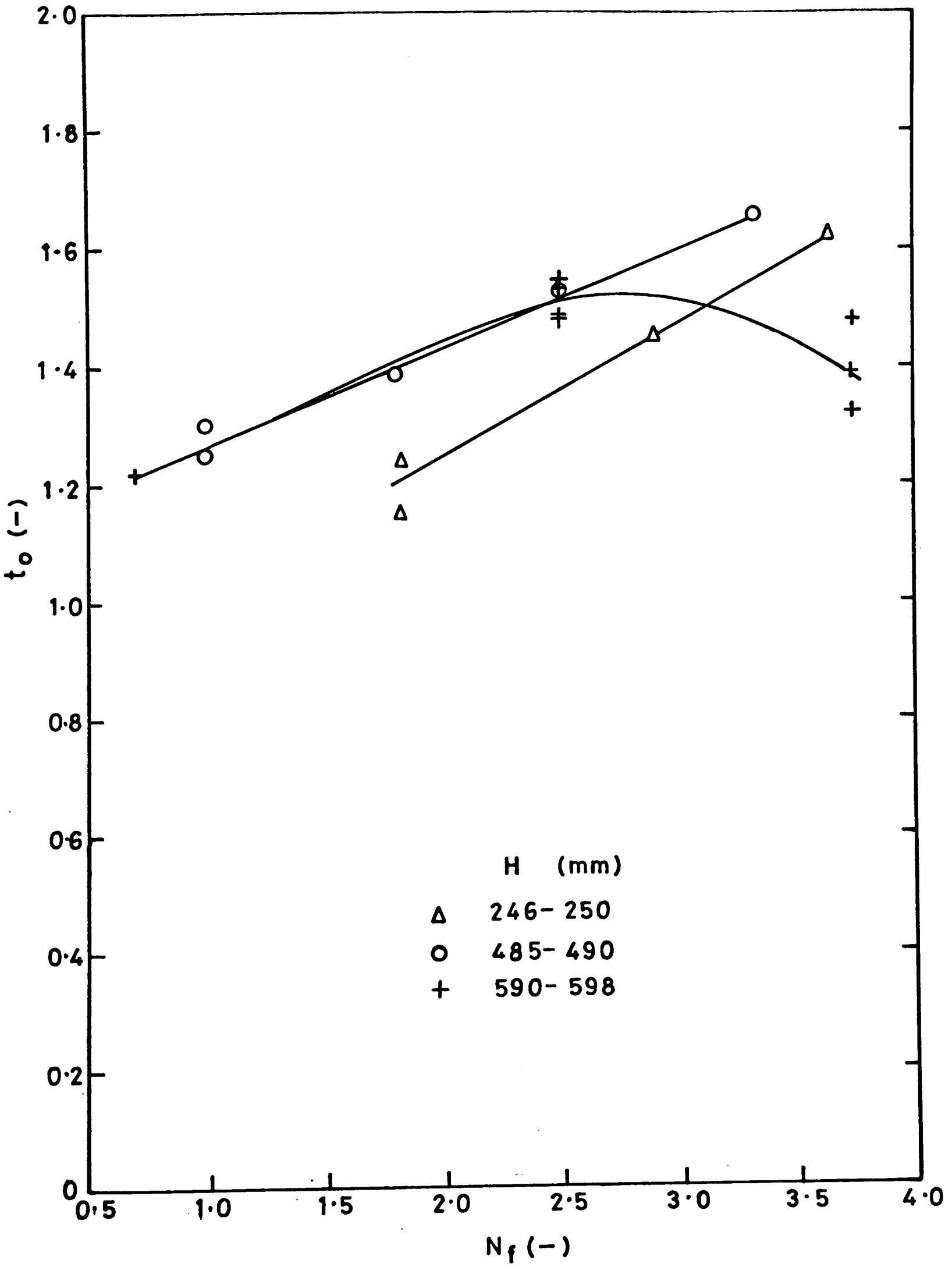


Figure 4.5 f : Mean residence time ratio, t_o vs. Fountain shape number, N_f.

Mixture B : z_a = 0.532 - 0.550
m^a = 0.151 - 0.273 kg min^{-1}

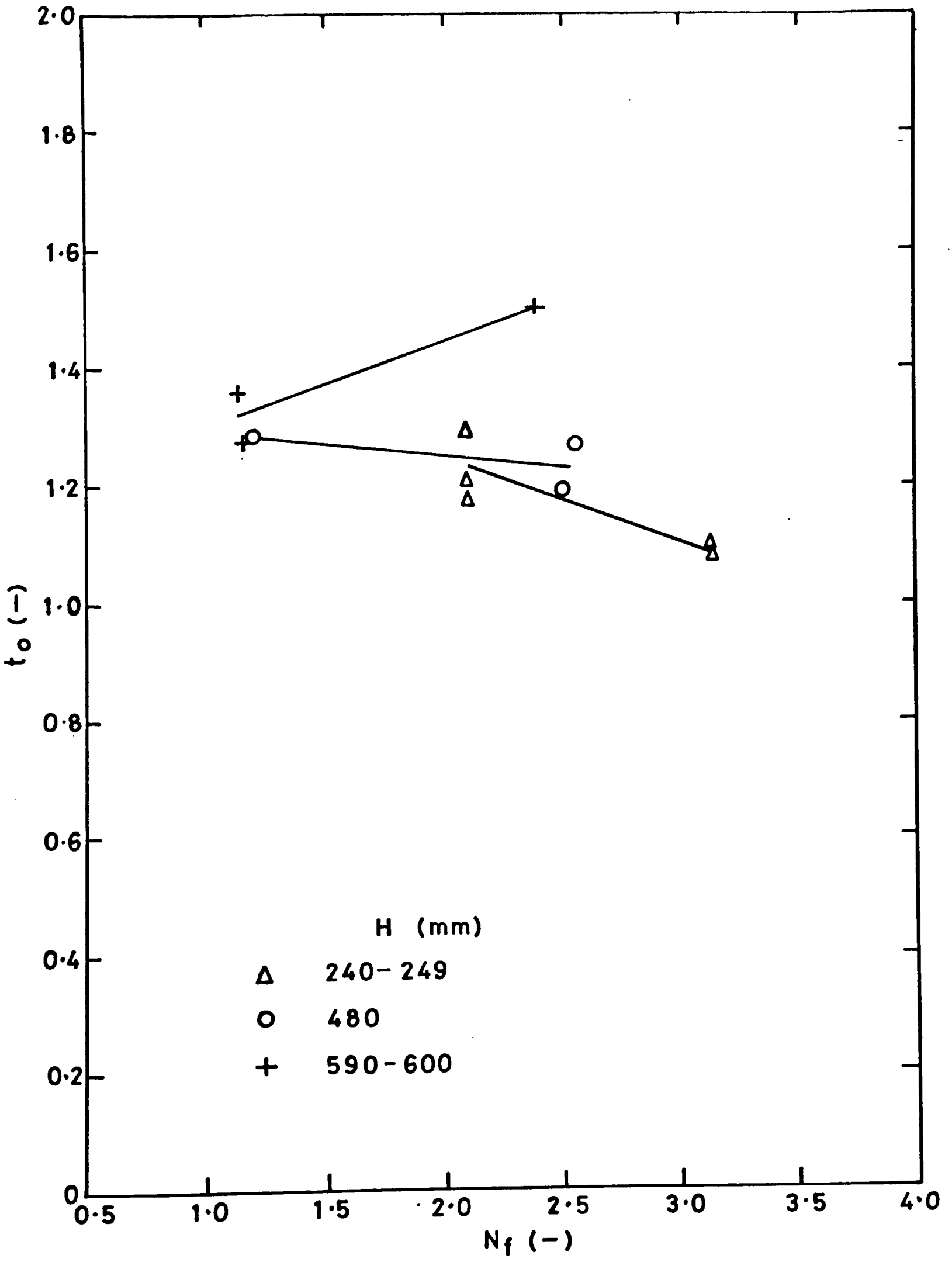


Figure 4.5 g : Mean residence time ratio, t_o vs. Fountain shape number, N_f.

Mixture C : z_a = 0.887 - 0.923
m^a = 0.161 - 0.344 kg min^{-1}

unity. With mixture C, the gas flow rate required to spout a given bed depth at a given N_f is greater than for mixtures A or B. Especially at high values of N_f, attrition of the smaller component was observed, a result of the high gas velocities at the air inlet, and runs in deep beds with high N_f were not performed. From the results available, there was a slight decrease in t_o with increasing N_f in bed depths below 500 mm. Results for the deepest bed (H = 590-600 mm) indicate that as before, t_o increases with increasing N_f.

For a mixture rich in the larger size component, results of Drahun (1979) show that small particles dropped onto a slope of larger particles, quickly sink into the interstices of the surface particles, and hence are termed "sinkers". If the results are applied to the sloping free surface around the overflow, we could expect landing mustard particles to have less chance of reaching the outlet than wheat particles. This would give t_o less than unity. Therefore, Drahun's observations do not support the results for mixture C, possibly because of the greater upward air flow than in mixtures A and B. Alternative mechanisms are discussed in subsequent chapters.

(iv) Variation of t_o with solids flow rate

The dependence of t_o on solids flow rate, m, was investigated in a bed of fixed depth and constant fountain shape number. Two cases were studied, both in beds of depth 240-250 mm. The first was of feed mixture A with N_f = 1.67 and the second of mixture C with N_f = 3.16. The results are shown in Figure 4.5h. For each case m was varied from 0.04 to 0.6 kg min^{-1}. At low values of m, most material reaching the outlet comes directly out of the fountain, the free surface being almost

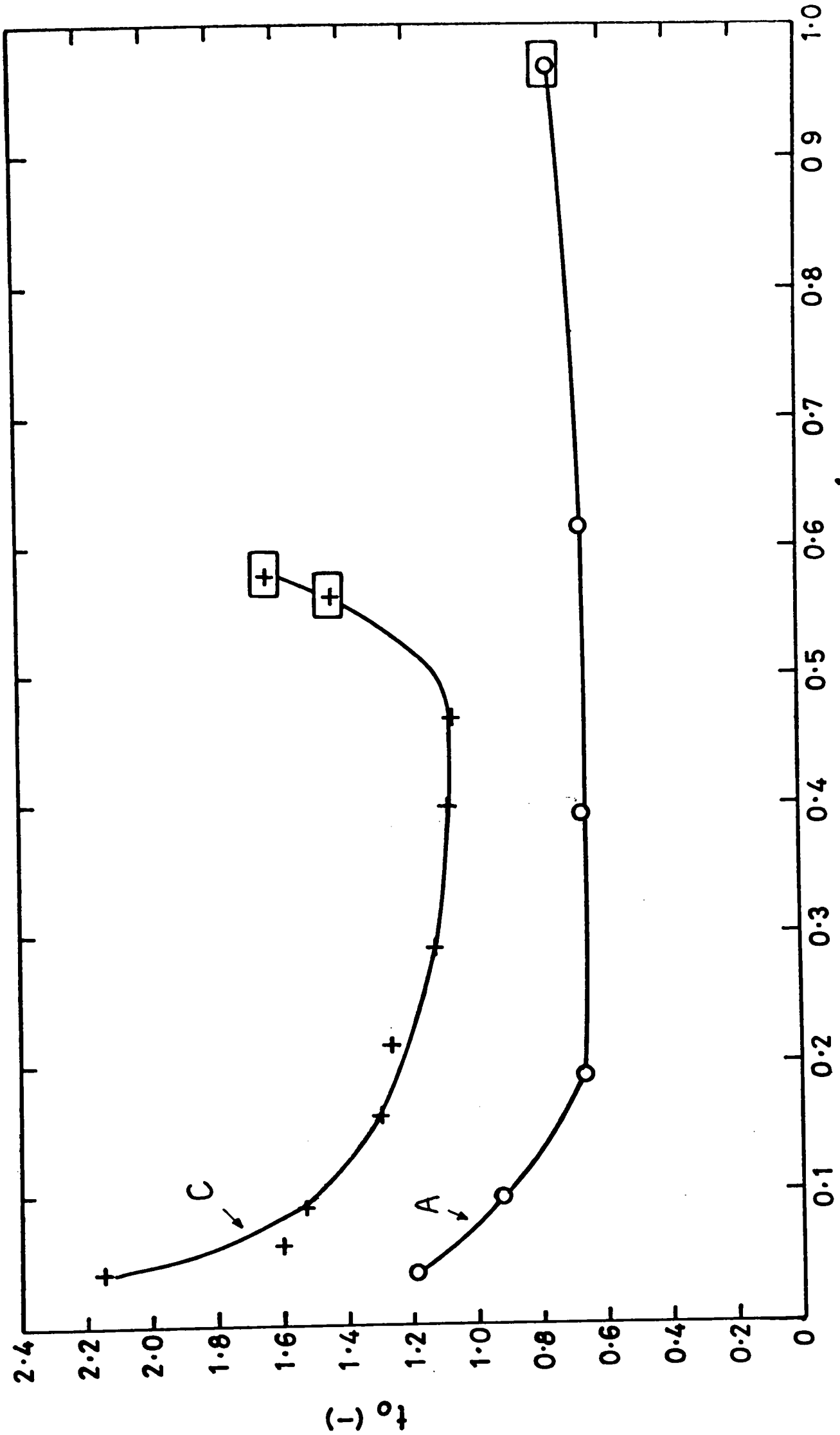


Figure 4.5 h : Mean residence time ratio, t_o vs. Solids mass flow rate, m.

H(mm)	N_f	z_a	Mixture
245	1.67	0.139 - 0.142	A
245	3.16	0.874 - 0.901	C

level with the lower edge of the outlet. At higher values of m the free surface level lies between the lower and upper edges of the overflow, some material in the outflow coming from the free surface and upper annulus, the rest from the fountain. At the highest values of m the outlet becomes submerged, all which leaves coming from the annulus. The height of the free surface above the centre of the submerged overflow H_s was 40 mm in runs C7, C13 and A9, those points boxed in Figure 4.5h.

In both cases studied, t_o is greater than unity for very low m and then reduces to a steady value as m increases. At high values of m, t_o remains at this value for mixture A even when the outlet is submerged. For mixture C t_o increases again as the outlet submerges. Higher values of m could not be investigated since the maximum solids flow rate is limited to that which will pass through an outlet of diameter 19 mm. The behaviour with mixture C could correspond to the three solids outflow mechanisms described, as shown in Figure 4.5i.

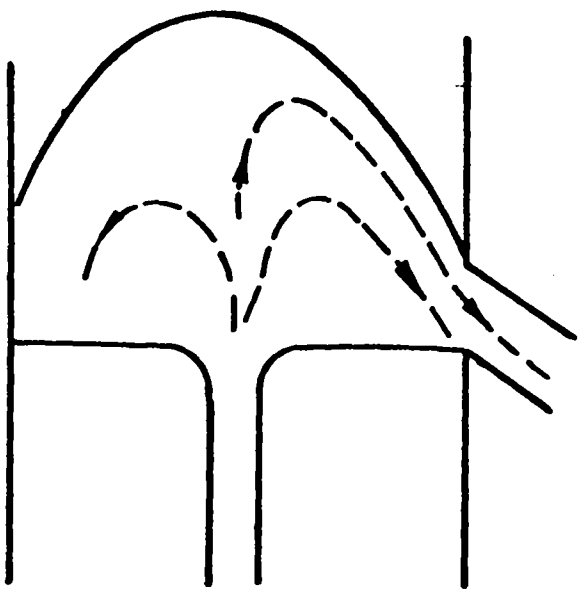
(v) Static Electricity

In some runs with high gas flow rates, static electricity was observed in outlet samples, it being especially noticeable on the brown mustard seeds. If like particles in the bed were similarly charged, it is possible that the mean residence times would be dependent upon the extent of charging. Three measures were taken to reduce static electricity:

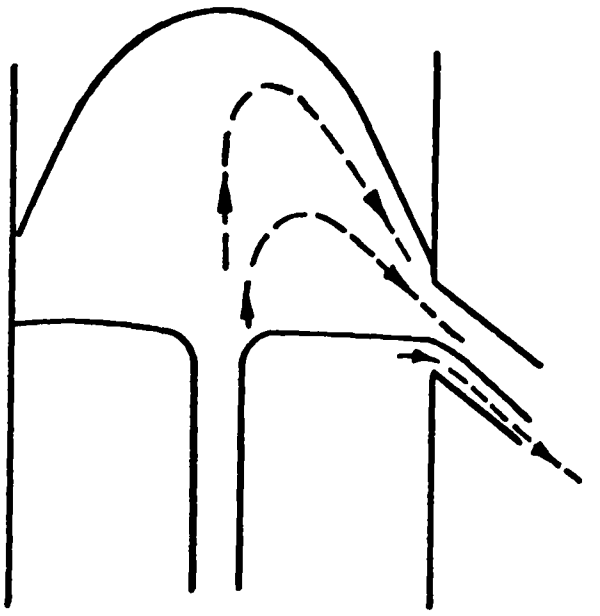
a) A water spray was introduced to the air supply line, increasing gas humidity.

b) Feed material was wetted to a moisture content (mass, dry basis) of 5% for wheat particles and 10% for brown mustard seed.

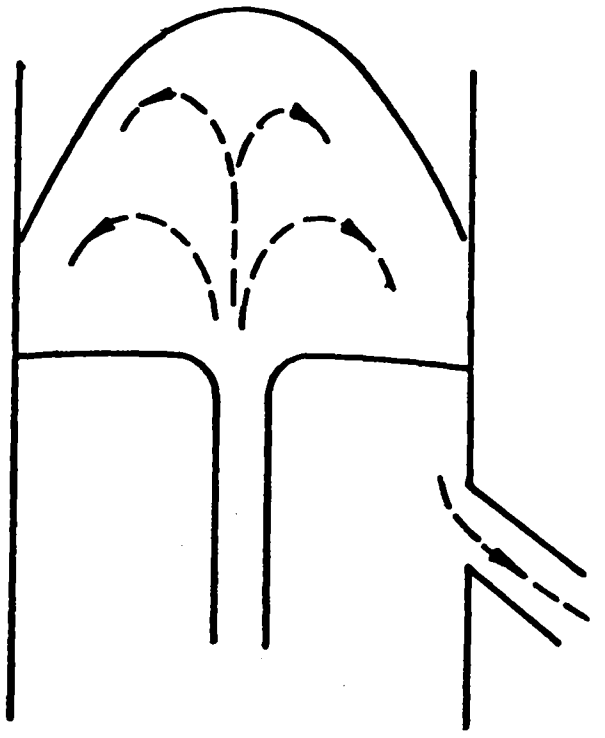
c) Six earthed foil strips, 20 mm wide, were fastened vertically



Low m



Medium m



High m

— ➤ — — Particle trajectories

Figure 4.5 i : Outflow mechanisms with varying solids mass flow rate, m.

to the inside of the column.

Combinations of these measures were used for two bed conditions where electrostatic effects had been particularly noticeable and the results are given in Table 4.5b. For both bed conditions studied, eliminating observable static effects caused a small change in t_o. For mixture B, t_o reduced slightly upon application of these measures; for mixture C, t_o increased. However the differences in t_o can be attributed to slight variations in solids flow rate between these runs. If similar variations in t_o with changing solids flow rate can be expected for mixture B as were observed for mixture C (Figure 4.5h), then a variation in t_o of about 15% would result. The maximum variation in t_o for the runs shown in Table 4.5b is 4%. This suggests that static electricity has little or no effect on t_o and that variation of t_o with m is less for mixture B than for mixture C over this range of solids flow rate.

4.6 Small Half-Section Bed

An 80 mm i.d. half-section perspex bed shown in Figure 4.6a and identical to that used by Piccinini et al (1977) was used to check the solids flow patterns they reported. Details of its construction are given in Appendix C. Material spouted was glass ballotini sieved into two size fractions, A (0.85-1.0 mm diameter) and C (0.5-0.59 mm).

A mixture of 190 g of C and 10 g of A, the latter dyed black to assist observation, was spouted and a long exposure photograph taken of the section is shown in Figure 4.6b. At this low gas velocity (N_s = 1.02) the paths of the coarse particles are concentrated in the upper inner annulus. At higher gas velocities intermixing improved. These observations are in accord with those of Piccinini et al and Figure 4.6b

Run	Water Spray	Wet Solids	Earthed Strips	t_o
B 12	No	No	No	1.54
B 14	Yes	No	Yes	1.48
B 13	Yes	Yes	Yes	1.48
B 11	No	Yes	No	1.53
C 19	No	No	No	1.28
C 18	Yes	Yes	Yes	1.36

Table 4.5b : Measures taken to reduce static electricity.

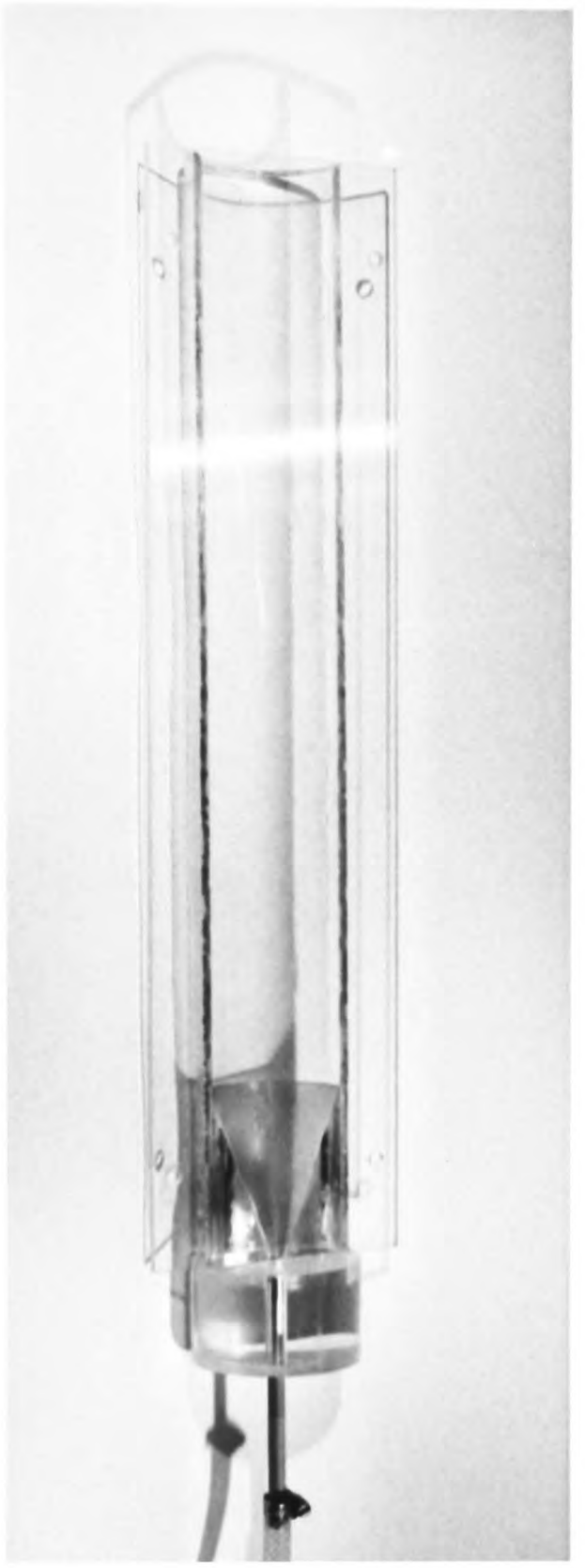


Figure 4.6a : The 80 mm i.d. half-section bed



Figure 4.6b : Glass ballotini spouted in the 80 mm i.d. half-section bed

Experimental conditions

Contents: 10 g Black ballotini, size A
190 g Clear ballotini, size C

H = 105 mm
N_s = 1.02
Exposure time = 10 s

is almost identical to that taken by Piccinini et al (1977 a).

However, some aspects of particle behaviour observed in this bed were not discussed in his first paper. An electrostatic charge built up on the ballotini, being more noticeable on the small size fraction where, with the higher surface area/volume ratio a surface charge could be expected to preferentially influence smaller ballotini. Charged particles became attached to the column and to the front face in the spout and above the free surface, disturbing the movement of ballotini in the fountain. At low air velocities (N_s < 1.05), a very slow moving region of particles formed at the outer upper part of the cone suggesting that the included angle in the base cone was too large to allow a smooth flow of solids. At higher air velocities this stagnant region disappeared. Sketches of particle paths at varying air velocities are shown in Figure 4.6c. The bed contained 10 g of size fraction A and 190 g of C.

The extension of Piccinini's results to predict behaviour in larger continuous beds could be inaccurate for the following reasons:

(i) Electrostatic forces affected particle movement in a batch operated half-section. These forces could influence the particle mean residence times in a continuous bed such as that used by Piccinini.

(ii) At low gas velocities, an almost stagnant region in the outer upper annulus could affect mean residence times.

(iii) The maximum bed depth used by Piccinini was 1.5 times the column diameter. With glass ballotini the maximum spoutable bed depth H_m, was approximately two times the column diameter. In a 150 mm diameter column H_m can be up to nine times the diameter depending on the material spouted.

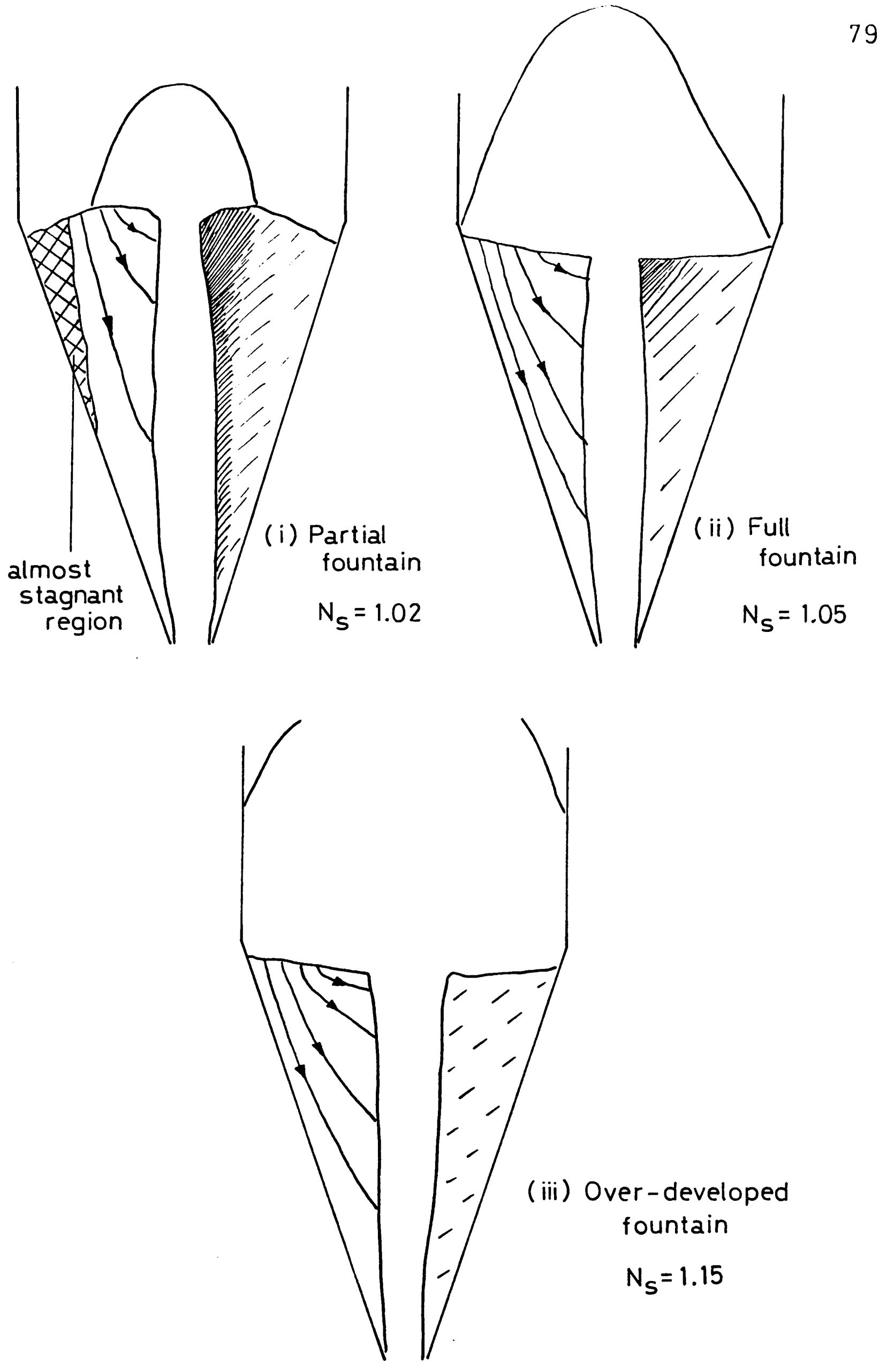


Figure 4.6c : Flow patterns and distribution of coarse fraction A in the 80 mm i.d. half-section bed.

Contents : Size fraction A = 10 g
Size fraction B = 190 g

——— Particle path of A

//// Distribution of A

Thus, flow patterns observed in the small bed may not necessarily apply to a larger bed.

4.7 Conclusions

The results for a mono-size feed show that mixing in the spouted bed is very nearly perfect. This agrees with the results of previous workers [Becker and Sallans (1960), Kugo et al (1965), Barton et al (1968) and Pallai and Németh (1971, 1972)] and justifies the assumption that the labelled particles can be regarded as identical to the bulk, any differences in particle density or surface properties being negligible. It is, though, subject to the approximation that the bulk density of a mixture can be estimated from the bulk densities of its components, when separated. These results prove the novel labelling technique suitable for the measurement of residence time distributions in particulate process systems.

Extending the technique to a binary size particle feed has shown the self-mixing of each component to be almost perfect. If this can be assumed, then the RTD is prescribed, given values of mean residence time for each component. Although the RTD's are close to those for perfect self mixing, the mean residence times of each component are not equal and their ratio depends upon feed mixture, bed depth, fountain shape and solids flow rate. For mixtures A and B, the mean residence time ratio t_o generally increased with increasing N_f and H. Values of t_o less than unity only occurred using mixture A in shallow beds and in deeper beds with low fountain shape number. For mixture C, t_o again increased with increasing H, but the dependence on N_f was not as clear.

Dependence of t_o on solids feed rate was also marked in the two cases

studied. For mixtures A and C, t_o was greater than unity for very low m, when outflowing material comes mainly from the fountain. At higher m, t_o decreased to a lower limit which, for mixture A, was below unity. At high m when the outflow is submerged, t_o increased again for mixture C, but remained less than unity for mixture A.

CHAPTER 5

The Annulus

5.1 Introduction

The particles in a spouted bed spend most of their time in the annulus. The flow pattern of solids in the annulus is thus important in determining its performance for applications such as drying, granulation and coating. Particle circulation can be described quantitatively by several parameters, such as mass circulation rate, particle velocities in the spout and annulus and the particle cycle time distribution. For mono-disperse systems, these parameters have been studied extensively and the experimental findings and theoretical predictions of this work are summarised by Mathur and Epstein (1974)

The studies of polydisperse systems are fewer in number. Piccinini et al (1977) described qualitatively particle flow patterns in an 80 mm i.d. bed, work discussed in Chapter 4. Robinson and Waldie (1978) used a 145 mm i.d. half-section perspex column with a conical base. Sodium chloride particles with a size distribution from 1.4 mm to 4.8 mm were spouted, with 200 particles from each of five intermediate size fractions dyed five different colours. Observations of particle movement were made at the transparent front face. Cycle times were estimated by timing particles from their landing position on the free surface to entry into the spout using a stopwatch. From cine film, particle trajectories were plotted and further cycle times measured. Both particle trajectories and cycle times were found to be dependent on particle size. Smaller particles tended to take long

cycles more frequently, having an arithmetic mean cycle time longer than large particles in the same bed. Two factors responsible for the shorter cycle times of larger particles were proposed:

(i) The greater the radial distance from the spout on landing, the longer the subsequent path through the annulus, as seen in the trajectories [Thorley et al (1959)] for wheat particles. Robinson and Waldie observed that large particles landed more frequently on the free surface near the centre of the column. They would then undergo short cycles more frequently. This observation is attributed to particle velocities and radial positions in the spout being dependent on particle size, but no quantitative data are available.

(ii) From the same radial position on the free surface, smaller particles tended to take a longer path back into the spout. Especially within a radial distance of about six particle diameters of the spout wall, the medium to small size fractions were observed to travel nearly vertically downwards for some distance as shown in Figure 5.1a.

Two possible mechanisms can explain the observed trajectories. Firstly, the smaller particles may percolate through the larger ones assisted by the straining of material in the annulus [Scott and Bridgwater (1975)]. Secondly, the radial component of gas flow in the annulus will have a greater effect on the smaller particles.

Segregation in the annulus can affect the practical performance of a spouted bed in two ways:

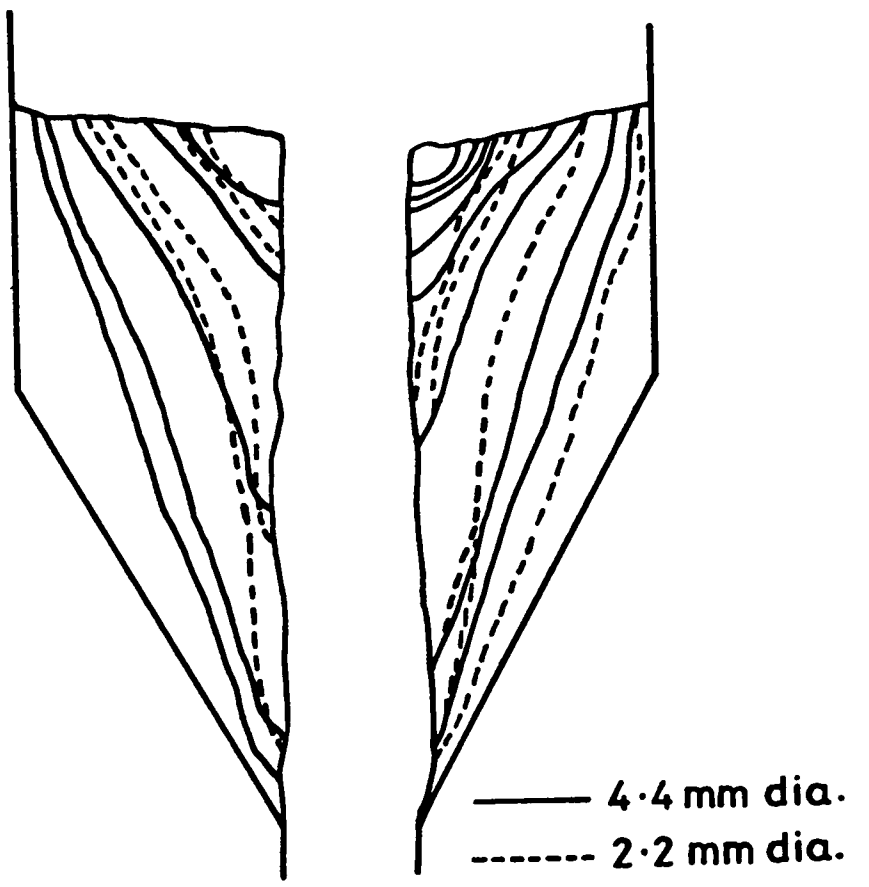


Figure 5.1 a : Particle trajectories in the annulus as reported by Robinson and Waldie (1978)

Material : sodium chloride particles

(i) Since drying or granulation will occur at different rates in the spout and annulus, particles spending a greater fraction of their cycle time in the annulus (those with longer cycle times) will be subject to different drying or granulation rates than those with shorter cycle times.

(ii) For continuous beds, any segregation in the annulus causing an accumulation of a particular size fraction near the outlet may result in a shorter mean residence time for that fraction.

In the present work, two separate studies of segregation in the annulus have been made, both using a mixture of wheat and brown mustard seeds. Firstly, segregation at the vessel wall was investigated by measuring particle velocities at the column wall. Observed behaviour at the wall may not be representative of behaviour in the rest of the annulus because of the variation in voidage near the wall of packed beds [Haughey and Beveridge (1969)] but is nevertheless important since material from this region is selected by outlets placed at the wall. Secondly, to investigate segregation in the annulus as a whole, the distributions of cycle times for different sized particles in the same bed were measured. From the work of Robinson and Waldie (1978) these could be expected to differ.

To measure cycle times, previous workers have timed a single labelled particle as it passed a detector in the bed. Van Velzen et al (1974) used a scintillation counter to monitor the vertical position of a radioactive particle within the bed. From the trajectory measurements, the elapsed time between two upward passages in the bed was measured. Advantages of this method are the ability to mount the

detector above the disengagement zone such that it does not interfere with particle flow and the use of a tracer particle identical in size and density to the bulk. The disadvantage is that special safety procedures are necessary for handling radioactive material, especially if dust is present. Mann and Crosby (1975) used a magnetic particle and a detecting coil located around the spout in an air-suspension coating unit. The magnetic particle, weighing 0.926 g was a 9.52 mm diameter polystyrene sphere in which a 6.35 mm hole was drilled to house a small magnet. Bulk particles were polystyrene spheres with diameter and weight 6.35 mm and 0.15 g respectively. The advantage of this method is that no special safety procedures are required. The disadvantages are that to ensure a large enough signal for detection, a tracer particle larger in size and density than the bulk must be used to represent the bulk behaviour. The presence of the detecting coil also disturbs the flow of material in the fountain, and may consequently affect the distribution of cycle times.

The method adopted for the present study was the second, but a more sensitive detection system was developed which allowed tracer particles with properties closer to those of the bulk to be used.

5.2 Wall Measurements

Particle velocities at the column wall were measured using two methods. Firstly particles were timed by stopwatch over a 100 mm distance marked on the column. Secondly, for certain conditions, cine film was taken of a 100 mm wide by 80 mm deep section of the annulus and then projected onto a screen at reduced speed allowing particles to be timed more accurately. All measured velocities are given in Table 5.2. The velocity of each particle is given by the

Run	z_a (-)	H (mm)	N_f (-)	H_t (mm)	D_t (mm)	v_a (mm/s)	v_b (mm/s)	v (-)	σ_v (-)	t_o (-)	Group
AT 1	0.139	245	1.67	190	100	13.1	12.4	1.06	0.02	0.85	1
" 2	0.135	495	0.96	410	"	20.9	18.6	1.12	0.04	1.22	1
" 3	"	"	"	145	"	19.5	19.4	1.01	0.02	"	
" 4	0.146	500	1.1	410	"	26.6	23.1	1.15	0.08	0.75	1
" 5	"	"	2.0	"	"	24.0	22.7	1.06	0.04	1.28	1
" 6	"	"	2.8	"	"	26.7	24.0	1.11	0.05	1.37	1
BT 1	0.543	246	1.82	190	100	20.0	19.8	1.01	0.02	1.24	1
" 2	0.544	485	1.0	410	"	28.4	24.5	1.11	0.08	1.25	1
" 3	"	"	"	145	"	26.4	25.6	1.03	0.02	"	
" 4	0.541	598	0.69	520	"	36.4	23.9	1.53	0.22	1.22	2
" 5	"	"	"	145	"	28.8	27.3	1.06	0.05	"	
" 6	0.550	596	2.5	520	"	61.9	41.9	1.48	0.20	1.48	2
" 7	0.546	595	3.75	520	"	53.7	32.6	1.63	0.27	1.48	2
" 8	"	"	"	145	"	37.0	37.1	1.00	0.07	"	
" 9	0.538	598	"	520	"	49.6	34.9	1.43	0.16	1.32	2
" 10	"	"	"	145	"	34.1	34.1	1.00	0.04	"	
" 11*	0.550	605	"	525	50	55.7	40.2	1.38	0.22	—	2
CT 1	0.887	248	2.11	190	100	29.0	28.5	1.02	0.05	1.21	1
" 2	0.901	243	"	"	"	29.9	28.5	1.05	0.04	1.18	1
" 3	0.890	245	3.16	"	"	32.3	30.9	1.04	0.05	—	1
" 4	0.905	480	1.2	410	"	50.0	39.3	1.27	0.28	1.28	
" 5	0.900	595	1.18	520	"	57.9	45.0	1.29	0.35	1.28	2
" 6	"	"	"	145	"	53.4	52.6	1.01	0.03	"	
" 7*	0.9	"	1.76	525	50	60.9	43.8	1.39	0.17	—	2
" 8*	0.9	"	"	255	"	62.5	62.0	1.01	0.03	—	
" 9	0.900	"	2.35	520	100	66.8	43.5	1.53	0.23	1.49	2
" 10	0.900	"	3.53	"	"	75.4	50.6	1.49	0.31	—	2

Table 5.2: Particle velocities at the column wall

* indicates measurements from cine film

distance travelled D_t divided by the time taken to cover that distance. At least twelve measured velocities were used to obtain average values. For each run, the mean velocities of wheat particles v_a and of mustard particles v_b are shown in Table 5.2. Also listed are the experimental conditions: mass fraction of wheat fed to the bed z_a, bed depth H, fountain shape number N_f, depth over which the particles were timed D_t, height at which D_t was centred H_t, ratio of mean measured velocities v ($=v_a/v_b$) and its standard deviation σ_v, and the mean residence time ratio t_o when the bed had been operated continuously. The standard deviation of the velocity ratio is calculated as detailed in Appendix D. Many of the velocity ratios have large standard deviations. This may be attributable in part to the small number of particles timed but the main reason is the large variation in measured times for brown mustard seeds. In moving down the annulus, mustard seeds were sometimes observed to be trapped by wheat particles and thus travelled at the same speed as the wheat. Often they would become free due to the settling of wheat particles and then be slowed by upward moving interstitial gas. Times for mustard seeds to travel 100 mm therefore varied greatly, especially in the upper part of the bed where voidage at the wall appeared to be greatest.

Velocity ratios have been divided into two categories, those measured in the upper half of the annulus, $H_t/H > 0.5$ and those measured in the lower part, $H_t/H < 0.5$. These are plotted in Figures 5.2 a and b against N_f, with H and z_a as parameters. Confidence limits of 95% on the distribution of velocities at each point are shown. The results can be summarised as follows:

(i) All mean velocity ratios are greater than unity,

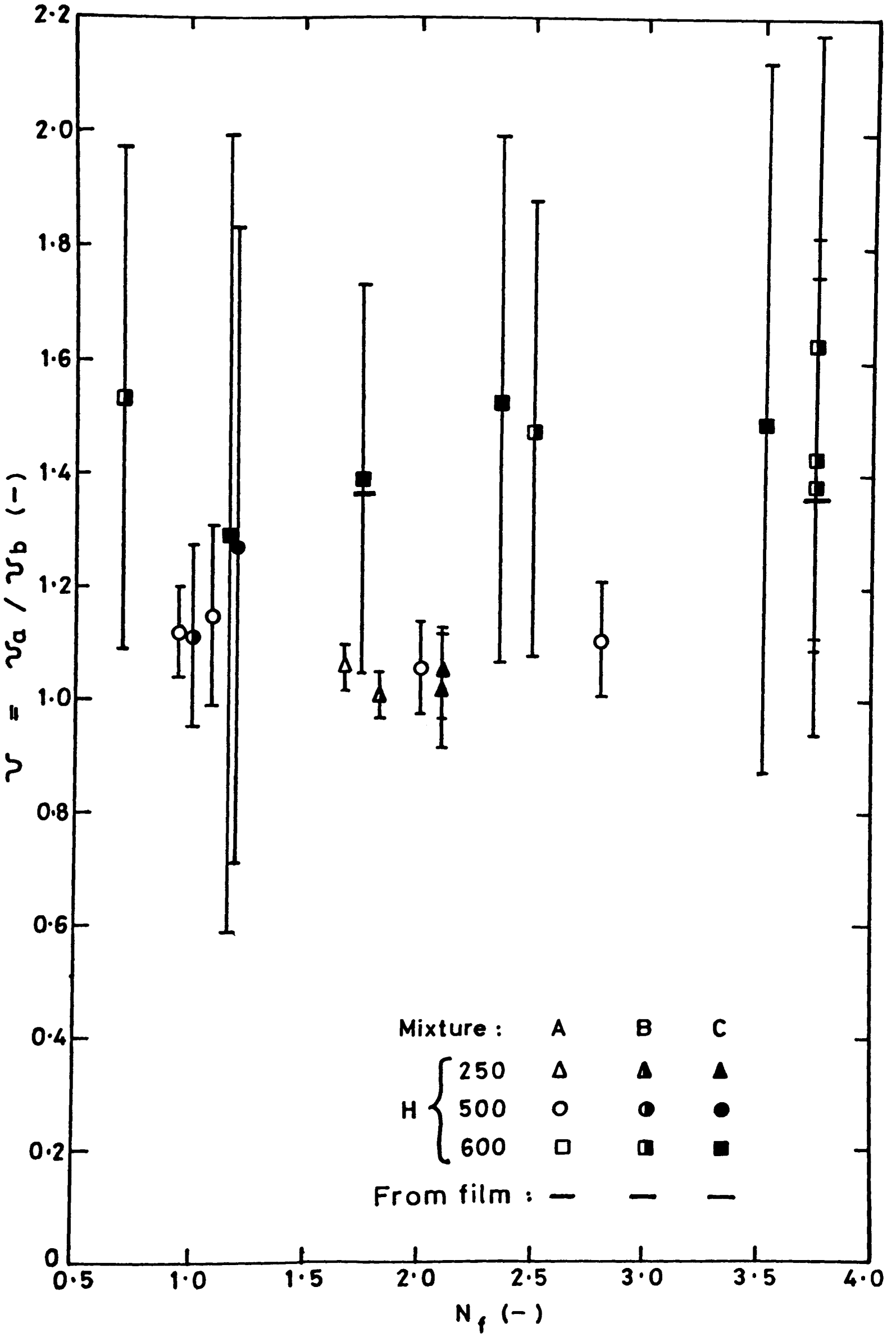


Figure 5.2 a : Velocity ratio, v vs. Fountain shape number N_f, with H and z_a as parameters

$\frac{H_t}{H} < 0.5$ for all points

Mixture : A B C
z_a : 0.13 0.55 0.90

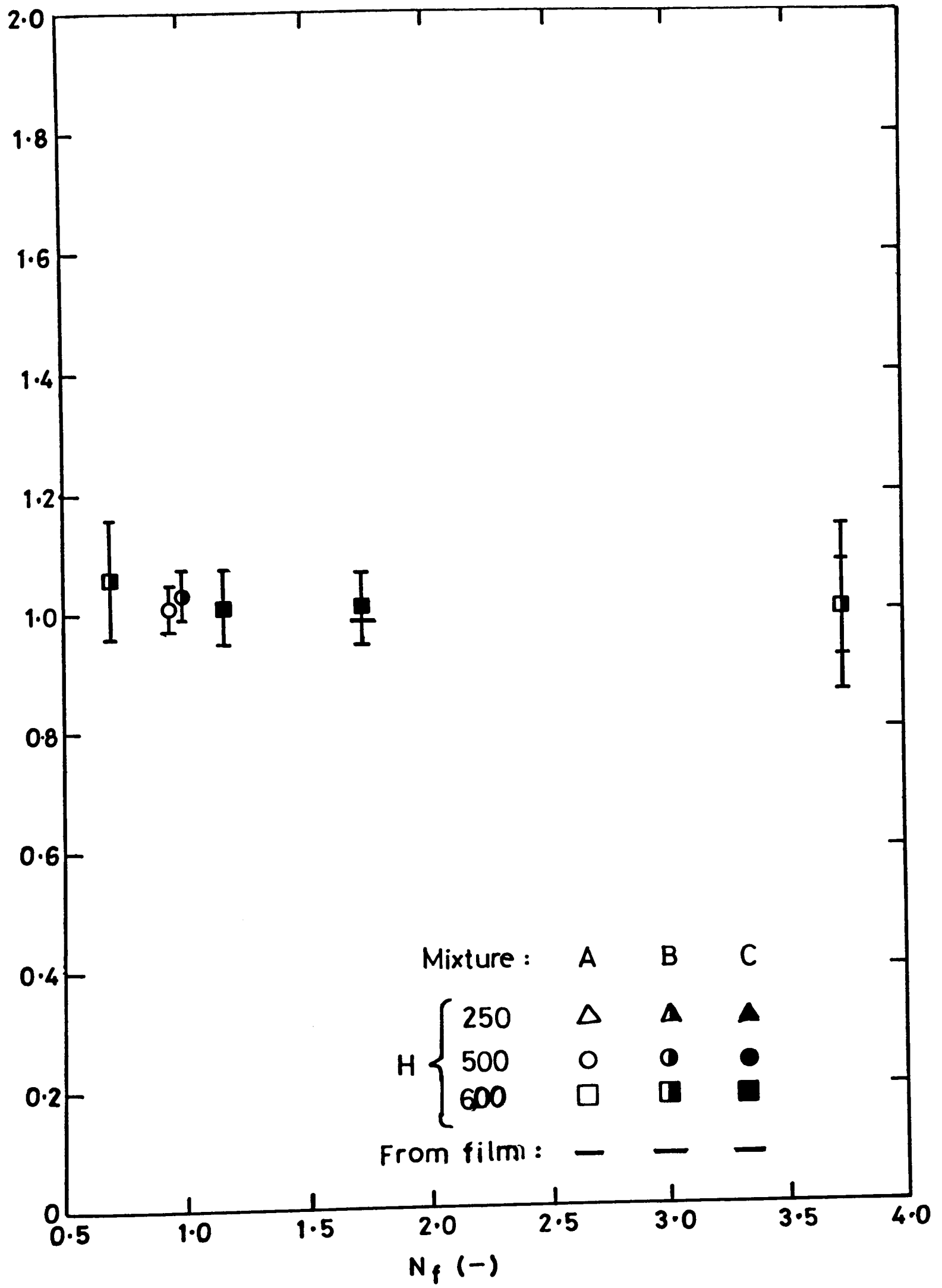


Figure 5.2 b : Velocity ratio, v vs. Fountain shape number N_f, with H and z_a as parameters

$\frac{H_t}{H} < 0.5$ for all points

Mixture :	A	B	C
z_a :	0.13	0.55	0.90

(ii) Mean velocity ratios greater than 1.15 were only observed for mixtures B and C in beds deeper than 500 mm, measured in the upper annulus,

(iii) Velocity ratios measured in the lower annulus, $H_t/H < 0.5$, were approximately unity irrespective of the values of H, z_a and N_f,

(iv) Measurements taken from cine film support those made visually.

Despite the large standard deviations of velocity ratios in 600 mm deep beds of mixtures B and C, the mean velocity ratios for these conditions appear quite different to the mean velocity ratios measured in 250 mm deep beds and for mixtures A and B in 500 mm beds. To assess the significance of this difference, a t-test was performed on the two groups. Group 1 in Table 5.2 contains mean velocity ratios in 600 mm deep beds of all mixtures; group 2 contains those in 250 mm beds and of mixtures A and B in 500 mm beds.

For group 1: $\bar{v}_1 = 1.073$

$s_1 = 0.0569$

$n_1 = 10$

For group 1: $\bar{v}_2 = 1.46$

$s_2 = 0.259$

$n_2 = 9$

$$\text{where } \bar{v}_1 = \frac{\sum_{k=1}^{n_1} \left(\sum_{j=1}^{\ell} v_{j,k} \right)}{\left(\sum_{k=1}^{n_1} \ell \right)}$$

and $$s_1 = \left[\sum_{k=1}^{n_1} \left(\frac{\sigma_{v1}^2}{\ell} \right) \right]^{\frac{1}{2}}$$

and similarly from group 2. $\bar{v}_1$ is the average of the mean particle velocity ratios in group 1, s_1 the standard deviation of $\bar{v}_1$, n_1 the number of points in group 1, ℓ the number of ratios used to calculate the k^{th} point and σ_{v1} the standard deviation of the k^{th} point in group 1. The t value is given by

$$t = \frac{\bar{v}_1 - \bar{v}_2}{s\sqrt{\frac{1}{n_1} + \frac{1}{n_2}}} \qquad (5.1)$$

where

$$s = \left[\frac{(n_1 - i)\ s_1^{\ 2} + (n_2 - 1)\ s_2^{\ 2}}{n_1 + n_2 - 2} \right]^{\frac{1}{2}} \qquad (5.2)$$

and here yields t = 4.63. For the hypothesis that $\bar{v}_1 = \bar{v}_2$ to be significant as the 99% probability level with 17 degrees of freedom, |t| would have to be less than 2.57. Since the calculated value of t is much larger, there is no statistical evidence to support this hypothesis. Hence, mean velocity ratios calculated for the upper annulus at the wall of 600 mm deep beds are significantly larger than those measured in shallow beds.

As described in Chapter 4, for continuously operated beds the mean residence time ratio t_o was greatest for deep beds of a given mixture. Since the velocity ratio in the upper annulus is also maximum in deep beds for mixtures B and C, a correlation between t_o and v seems possible. A plot of $\frac{v_a}{v_b}$ vs. t_o is shown in Figure 5.2c.

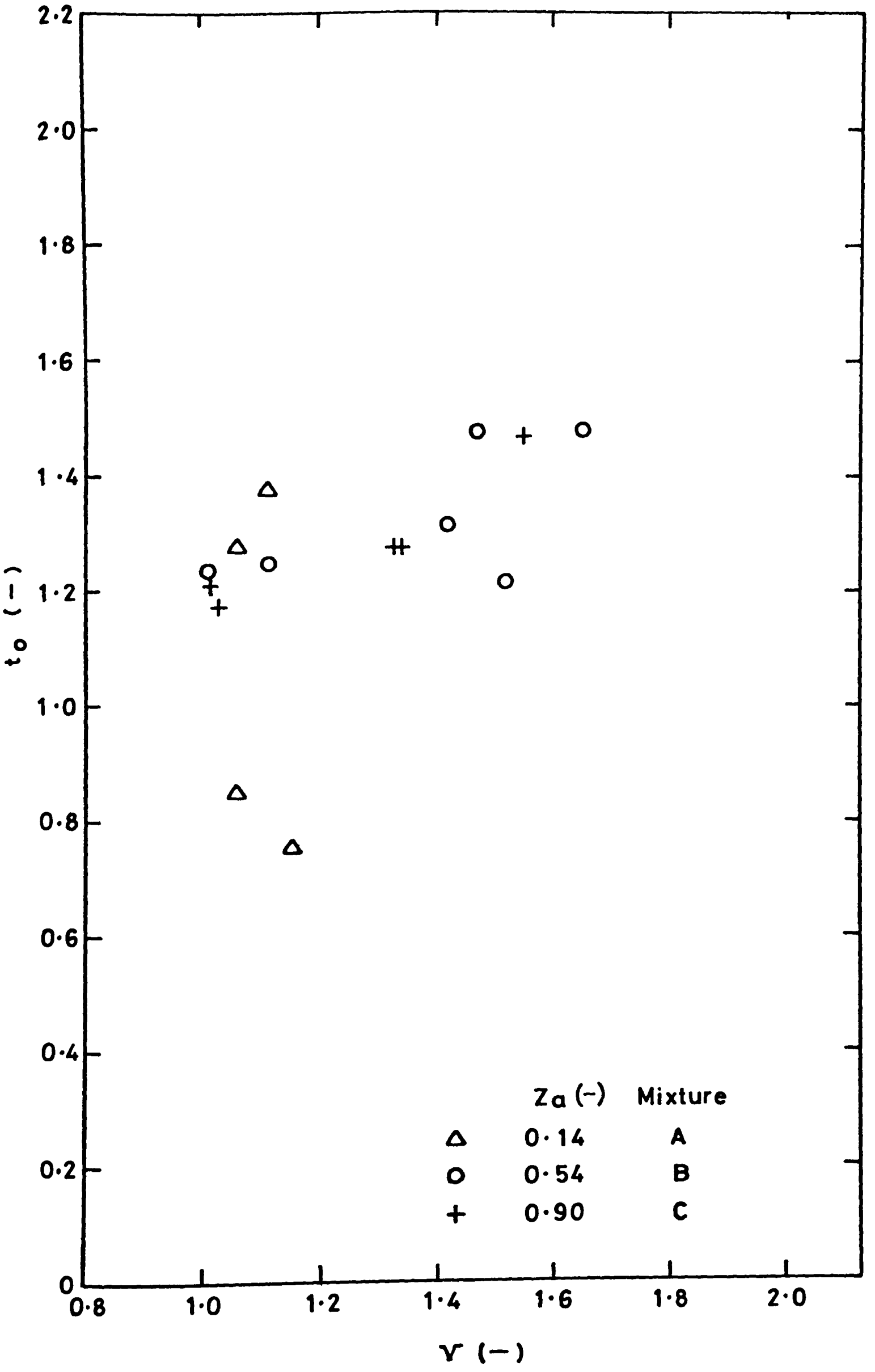


Figure 5.2 c : Correlation between mean residence time ratio t_o, and velocity ratio at wall v.

Points taken are for a wide variation of H, z_a and N_f. However, in Chapter 4 t_o was shown to be dependent under certain conditions on the solids flow rate m. The velocity ratio v is determined by the structure of the bed and gas flow rate at the outer edge of the annulus and little, if any, dependence of v on m can be expected. Since t_o is dependent on m, all points shown in Figure 5.2c use values of t_o measured at similar solids mass flow rates.

The results in Figure 5.2c can be summarised as follows:

(i) For mixture A, no correlation between v and t_o is apparent

(ii) For mixtures B and C, with one exception, higher values of t_o are generally associated with increasing values of v in the upper annulus.

Since the overflow is positioned at the top of the annulus, any difference in mixture concentration in this region could directly affect mean residence times of the mixture components. High values of v in the top of the annulus are caused by low values of mustard velocity v_b. Lower values of v_b in the upper annulus will result in higher concentrations of mustard in the outlet region, supporting the observed t_o values for mixtures B and C.

In addition to the vertical variation in mustard concentration, a radial variation within a few particle diameters, of the wall may also be present. Haughey and Beveridge (1969) report a sharp increase in voidage within one bulk particle diameter of a cylindrical surface. These voids may only be filled by smaller particles : mustard seeds in mixtures B and C. This increase in mustard concentration at the wall could also be a factor in determining t_o.

For mixture A, wall effects do not support the large variations in t_o reported in Chapter 4; for this mixture free surface segregation as mentioned earlier may be a more dominant mechanism.

5.3 Equipment

The cycle times of circulating particles were measured using a single tracer particle, a sensing coil and an electronic phase-sensitive detection system. A detection ring was positioned centrally in the bed, level with the free surface as shown in Figure 5.3a. Most circulating material passes through the centre before falling back into the annulus from the fountain, although a small amount of material might short-circuit, passing under the coil and into the annulus directly. During experiments the labelled particle was detected at regular intervals, so the proportion of material possibly short-circuiting the coil can be assumed to be very small.

The wheat tracer particle was a wheat seed,drilled out, with a small ferrite chip glued inside. This was identical in size and weight to the original seed. To obtain a signal large enough for detection, a small particle was made from ferrite powder and epoxy resin to represent a brown mustard seed. This was 1.4 mm in diameter and weighed approximately 3 mg, 1.5 times the density and 0.9 times the diameter of an average seed. These particles are shown in Figure 5.3b.

The detection ring was 28.3 mm deep, 36.7 mm i.d. and 68 mm o.d. with a 9.5 mm high sloping perspex ring fastened to the top surface to allow landing particles to slide off into the annulus. As shown in Figure 5.3c, the ring (A) was supported by three 3.1 mm diameter steel rods (B) hanging vertically from the top of the column and three

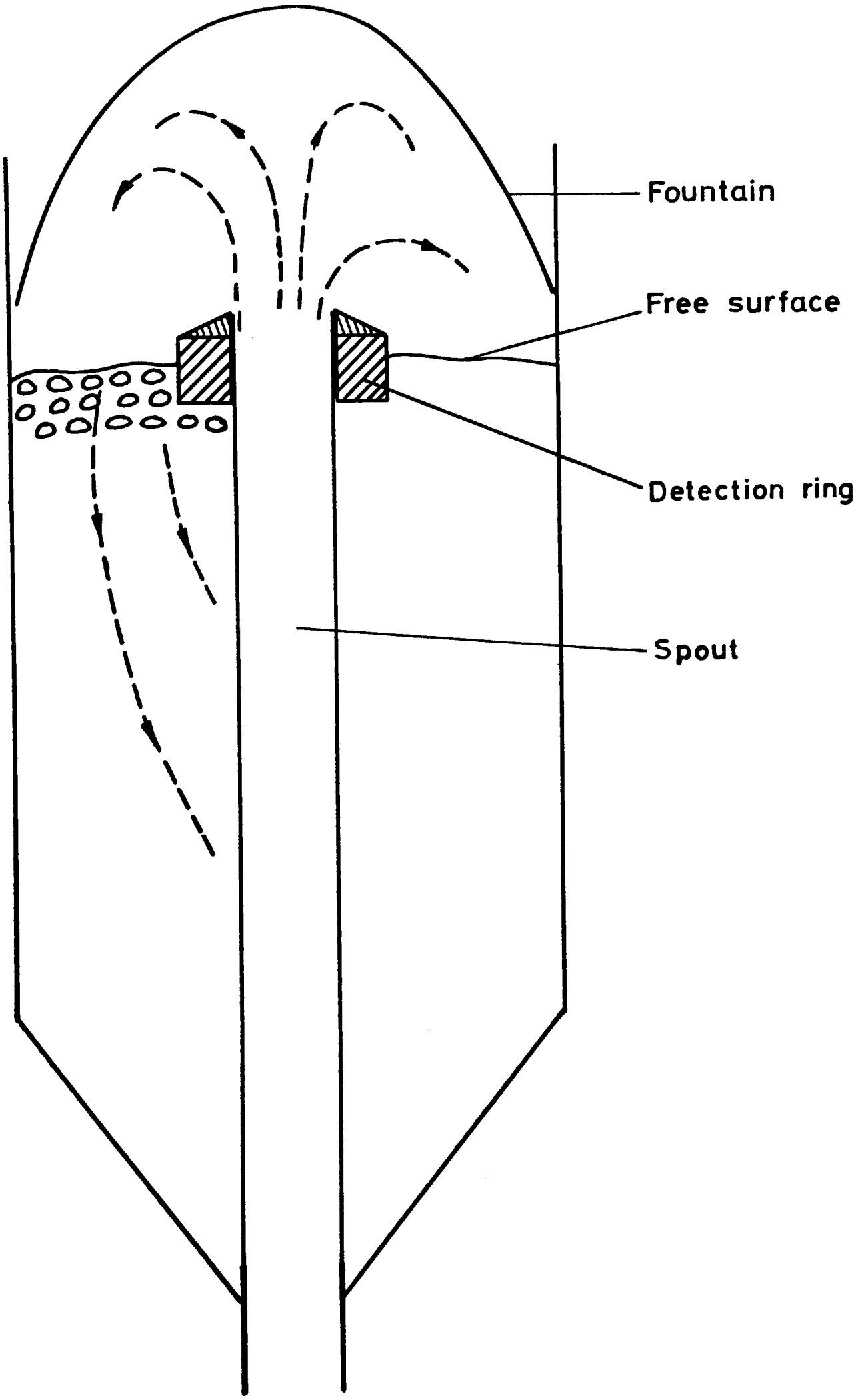


Figure 5.3 a : Position of detection ring

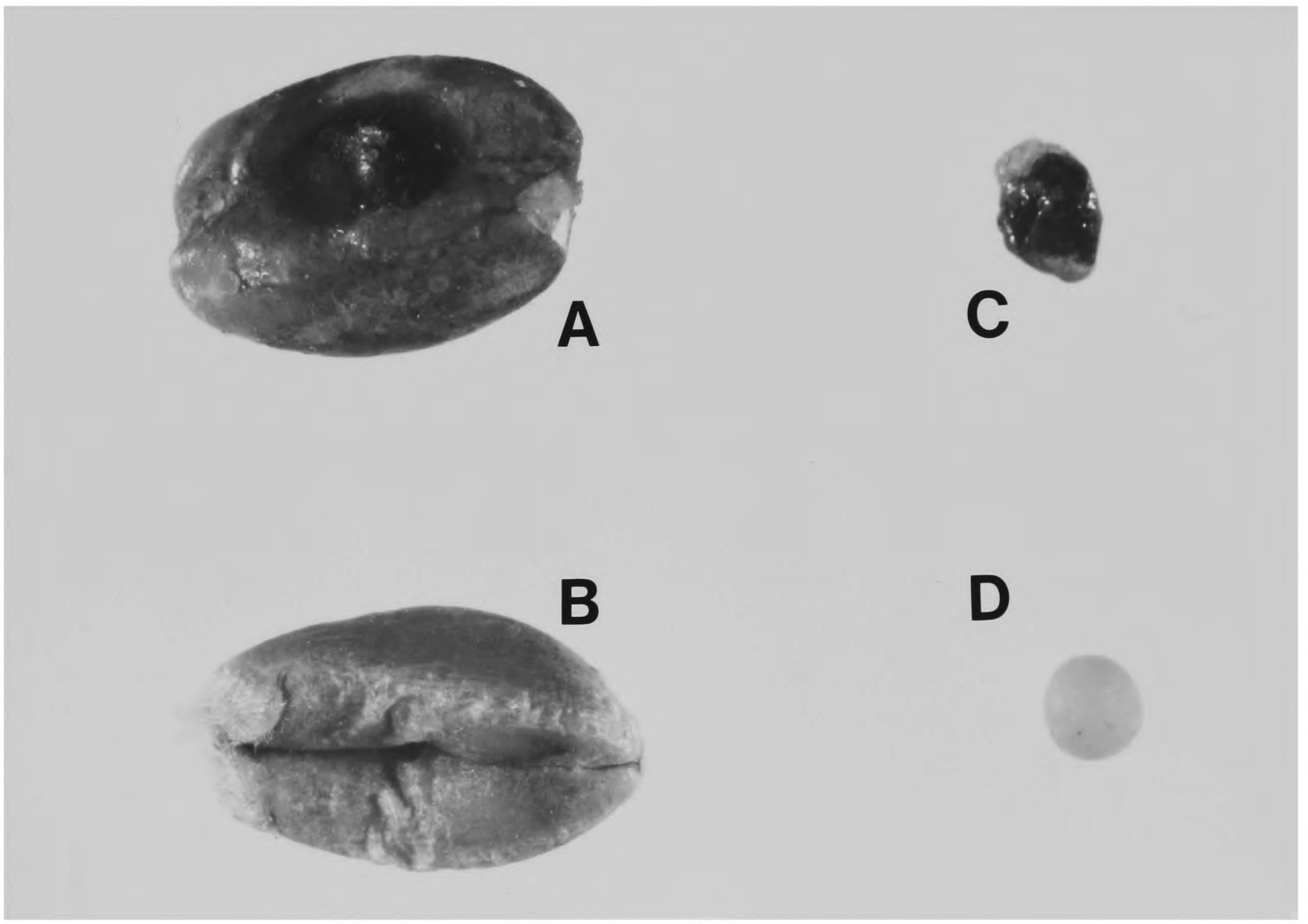


Figure 5.3b : Tracer particles used for cycle time measurements

A : Labelled wheat seed
B : Unlabelled wheat seed
C : Surrogate brown mustard seed
D : Brown mustard seed

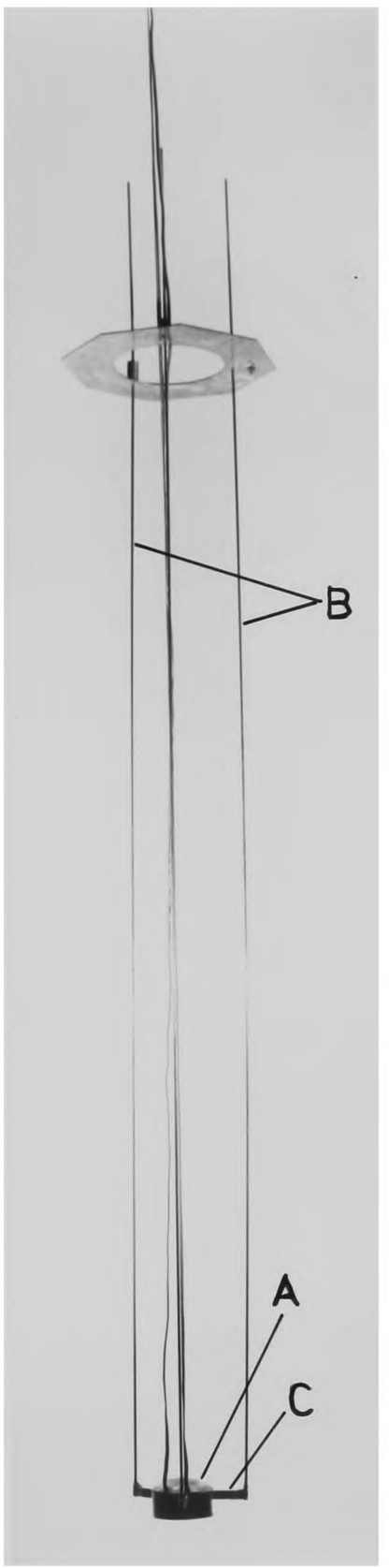


Figure 5.3c : Supporting structure for detection ring

A : Detection ring
B : Steel rods, 3.1 mm diameter
C : Aluminium strip

radial aluminium strips (C) 1 mm thick and 9.7 mm deep. The detection ring and supports were wired to earth. The ring contained a Tufnol former onto which three coils had been wound: two primary coils in series and opposing, each 500 turns of 36 s.w.g. copper wire and one secondary coil, 2000 turns of 40 s.w.g. copper wire, between the primaries. The primary coils were driven with a 3 V r.m.s., 5 kHz supply from an R.D.P. Electronics' D12/7 transducer amplifier. Since the magnetic flux from the primary coils cuts the turns on the secondary, as a ferrite particle passes through the coil disturbing the field an electromotive force (emf) is induced in the secondary coil. As the phase of the induced emf changes with respect to driving supply, the d.c. output voltage of the transducer amplifier varies.

Further equipment registered this change in output voltage and recorded cycle times. The transducer amplifier output voltage was amplified with a Hewlett Packard 463A Precision Amplifier, and a small a.c. ripple removed with a RC filter. The signal produced by passage of a labelled particle through the ring is shown in Figure 5.3d, as seen on an oscilloscope. For the given detection coil, the magnitude of this signal is governed by three factors: the mass of ferrite in the particle, the permittivity of the ferrite and the velocity of the particle. Typical signals measured were 0.2 V peak to peak for a wheat tracer particle and 0.05 V for a mustard tracer particle. The output from the H.P. 463A was fed into a signal conditioning unit where it was compared to a chosen reference voltage. Should the signal level become higher than the reference, the system input control unit records the time from the timer counter and the time is recorded on paper punch tape. Times recorded in this way were read into a PDP 11 computer for analysis. The detection system is shown in Figure 5.3e.

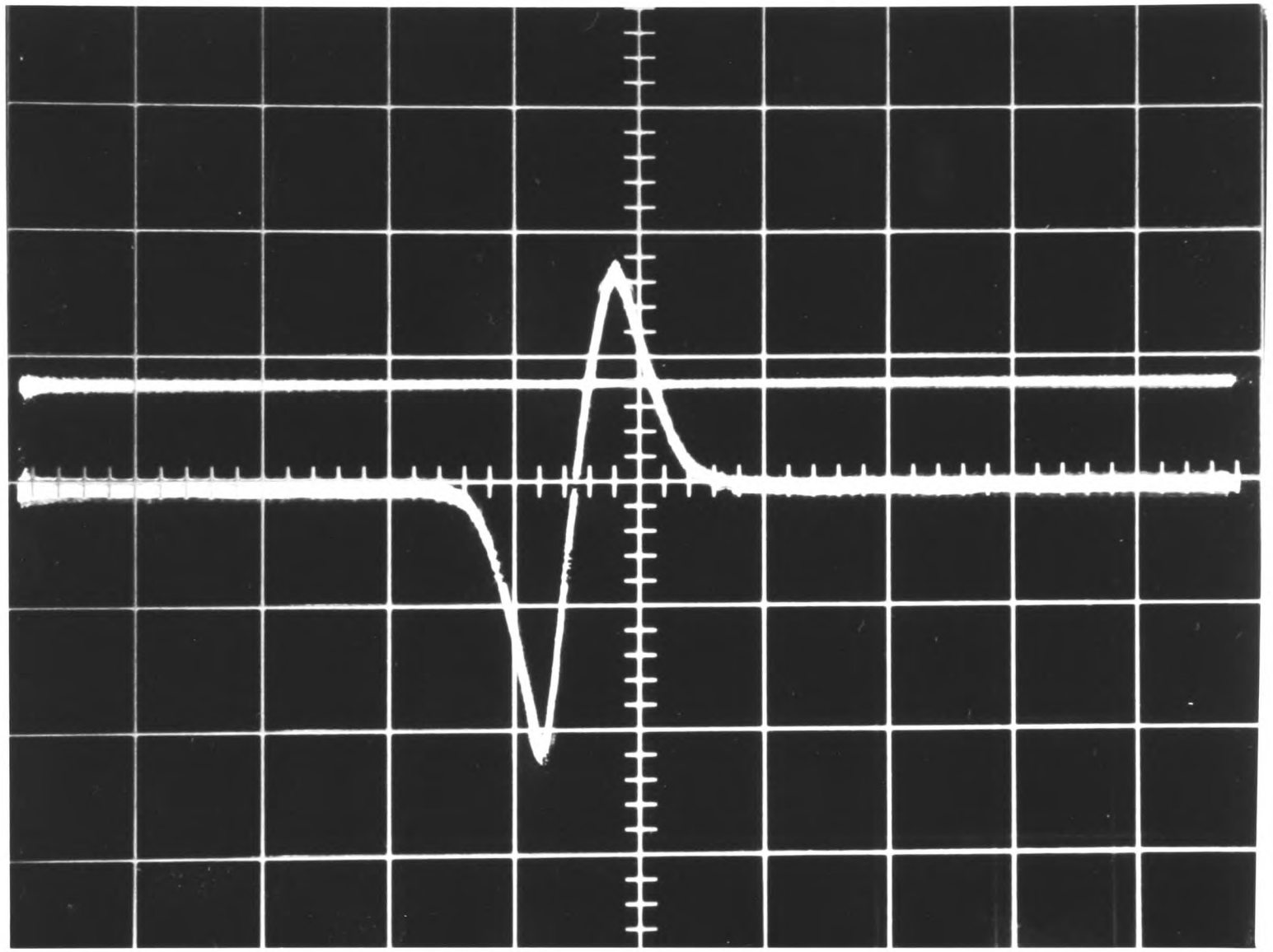


Figure 5.3d : Detection of wheat tracer particle : photograph from the oscilloscope

Abiscissa : Time (20 ms per large division)

Ordinate : Voltage (50 mV per large division)

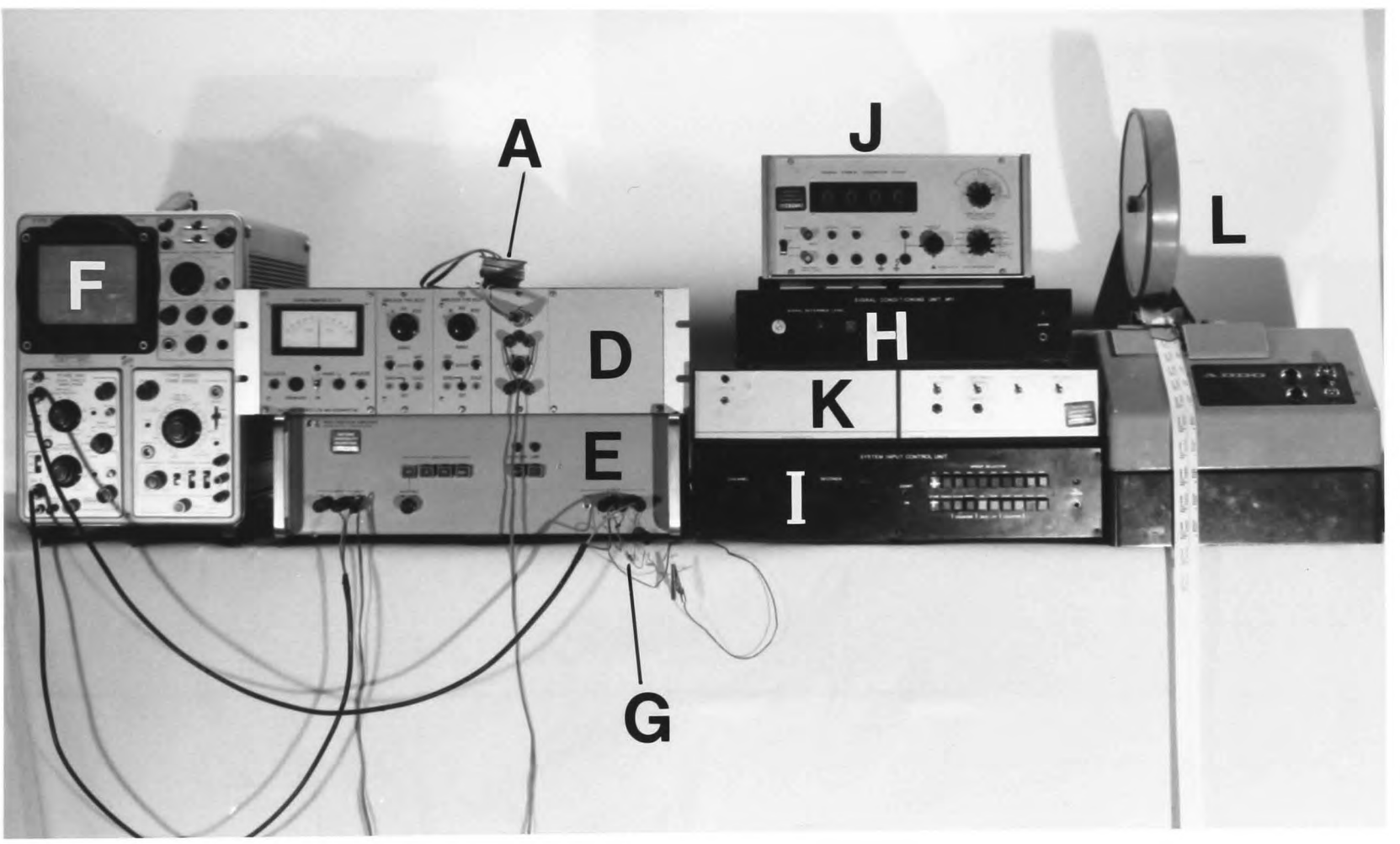


Figure 5.3e : Equipment for measurement of particle cycle times

A : Detection coil
D : Transducer amplifier
E : Precision amplifier
F : Oscilloscope
G : RC filter
H : Signal conditioning unit
I : System input control unit
J : Timer counter
K : Punch interface
L : Paper punch

5.4 Cycle Times

For a circulating system, define N(t) as the number of cycles of length between t and t + Δt undergone by a particle or fluid element during an operating time T. Then the distribution of N(t) over all possible t is as shown in Figure 5.4a when determined experimentally by a detection method such as that used in this study. For $t > t_{max} + \Delta t$, N(t) is necessarily zero since t_{max} is the cycle time of a particle taking the longest possible path around the vessel. This distibution of N(t) is hereafter referred to as the number of cycles distribution (NCD) of the system.

Number of cycles distributions have been obtained in beds of varying depth and fountain height. Each NCD was produced from several hundred cycle times. Punched tape recordings of cycle times were analysed on the Department's PDP 11 computer and NCD's were plotted out as histograms such as that in Figure 5.4a. The time increment Δt in the histogram can be chosen independently but must be greater than 0.1 seconds, the resolution of the recording equipment. A computer library routine was used to calculate mean cycle time $\bar{t}$, standard deviation σ and coefficient of skewness K_s for each distribution. Also calculated was the median cycle time t_m (50% of the circulating solids have cycle times greater than the median cycle time). Occasionally a passage of the tracer particle would not be detected and upon its next passage a cycle time approximately doubled would be recorded. Therefore the upper cycle time t_{max}, above which recorded cycle times would be disregarded, was chosen for each run. The

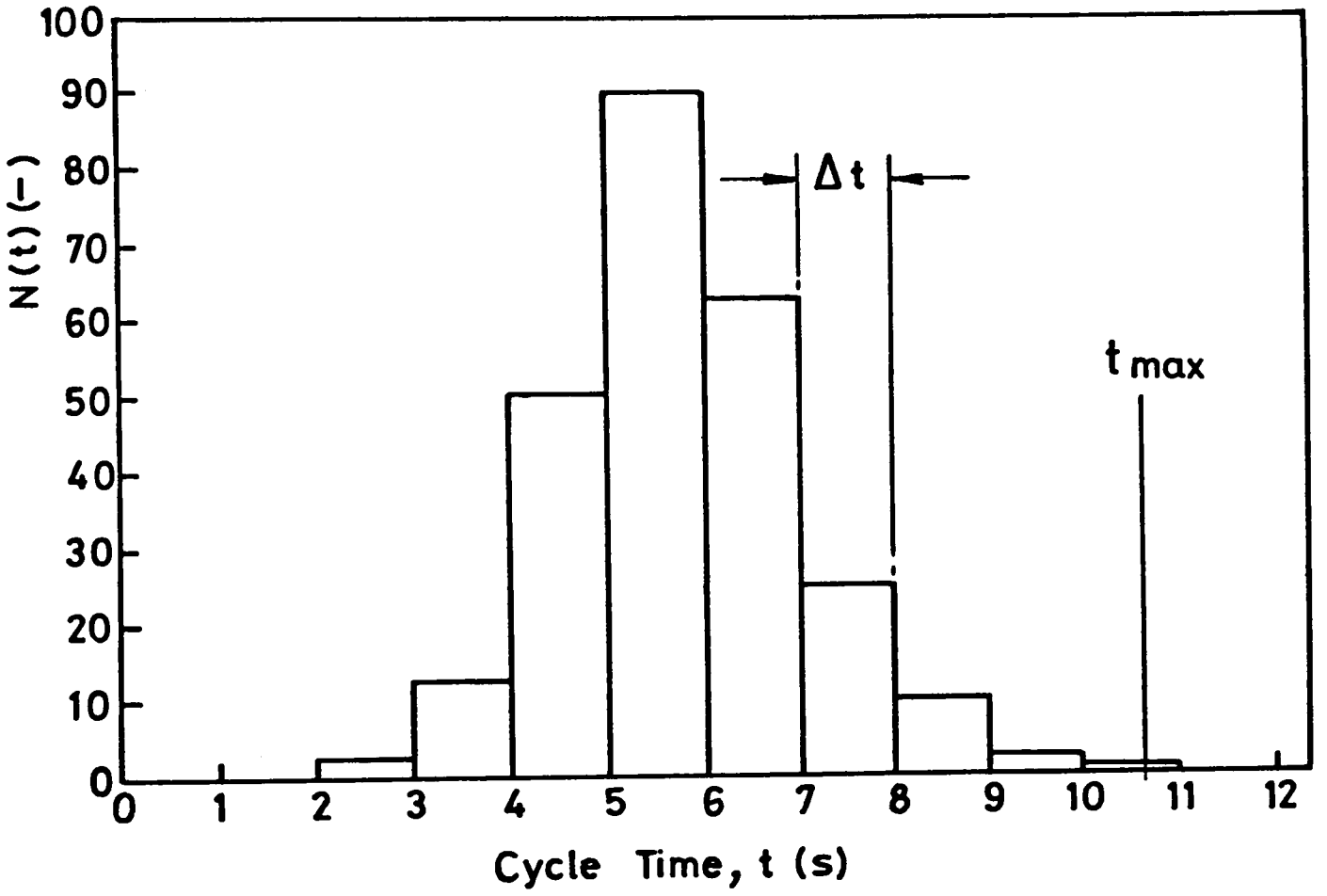


Figure 5.4 a : A number of cycles distribution (NCD).

largest cycle time for a bulk particle is that taken on a path next to the column wall. As shown in Figure 5.4b, for a particle taking this path, its time in the annulus can be estimated from a measurement of the time t_v taken in the vertical part of the column, a depth of (H - 100) mm. The time in the annulus would therefore be

$$t_v \times \frac{H + 15}{H - 100}$$

15 mm being the increased path length due to the slope on the base cone. The time spent in the annulus has been approximated as 90% to 95% of the actual cycle time [Robinson and Waldie (1978)], so an estimate of t_{max} for a bulk particle is given by

$$t_{max} = t_v \times \frac{H + 15}{H - 100} \times \frac{1}{0.90} \qquad (5.3)$$

For runs with a bed of 100% wheat and a "mustard" tracer, the NCD's usually had large σ. The value of t_{max} was then estimated directly from the NCD.

Any mechanisms causing NCD's to be dependent on particle size, such as interparticle percolation [Robinson and Waldie (1978)] should be enhanced at extremes of the mixture range. Thus bed contents chosen for study were 100% wheat and 100% brown mustard, in each case the NCD's being measured for a single wheat tracer particle (A runs) and for a single "mustard seed" tracer (B runs).

Calculated parameters and experimental conditions for all runs are shown in Table 5.4a. The detection system was sensitive to electrostatic discharges. These sometimes produced spurious signals

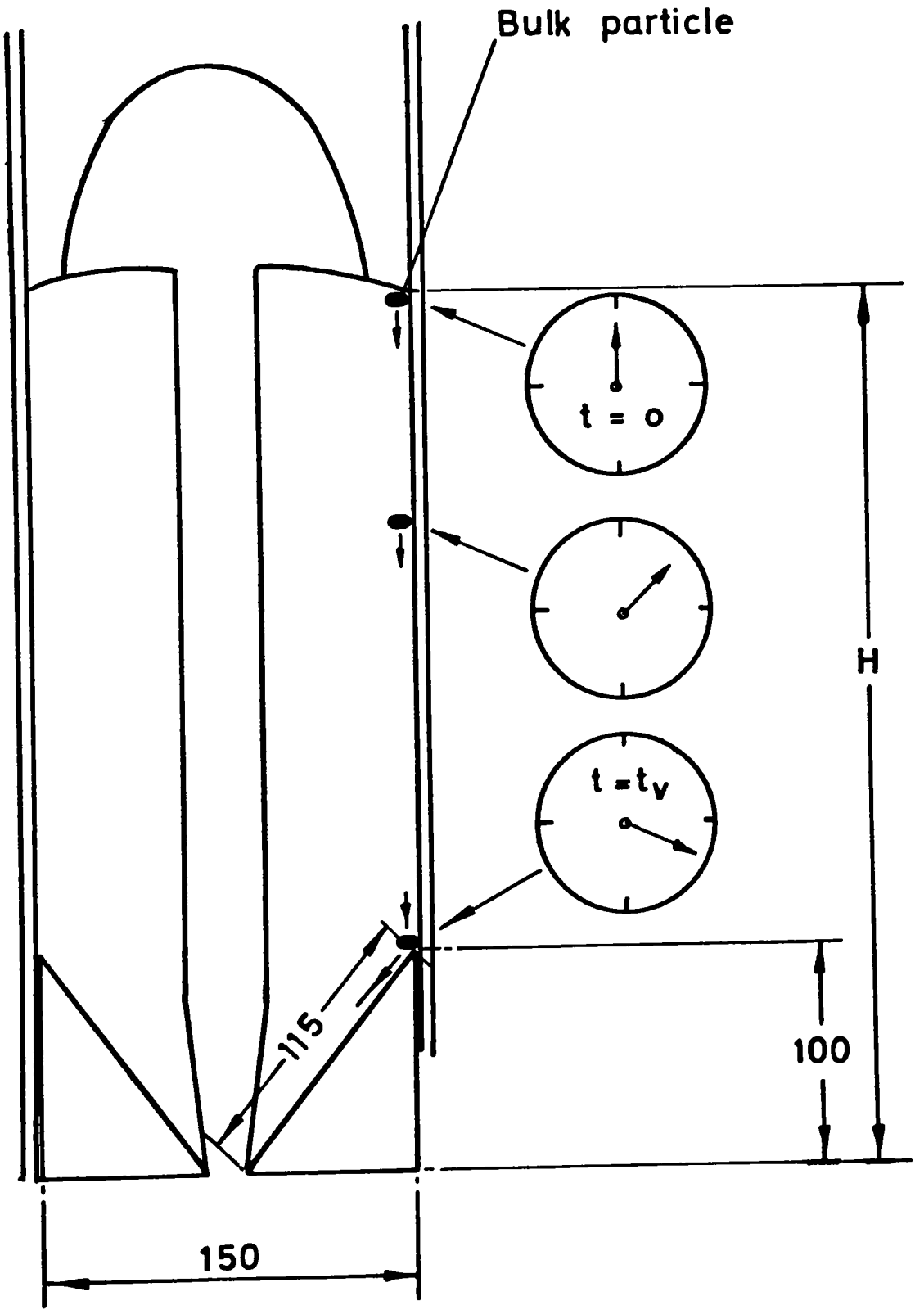


Figure 5.4 b : Measurement of the maximum possible cycle time

All dimensions in mm

Run No.	x_a (-)	H (mm)	H_f (mm)	$\bar{t}$ (s)	σ (s)	K_s ( )	t_{max} (s)	t_m (s)
1A	1.0	250	250	5.17	0.55	-2.8	7	5.2
1B	"	"	"	5.14	0.75	-0.9	7	5.1
2A	"	"	160	5.38	0.91	-2.8	7.6	5.5
2B	"	"	"	5.55	0.70	-0.1	8.0	5.5
3A	"	405	200	7.05	0.79	-4.8	8.6	7.2
3B	"	"	"	7.28	0.75	-0.4	9.0	7.3
4A	"	515	200	6.95	2.06	-1.8	9.6	7.7
4B	"	"	"	7.61	1.23	-1.5	10.0	7.8
5A	"	595	250	8.07	0.54	-4.4	9.6	8.1
5B	"	"	"	8.38	0.63	-0.2	10.0	8.3
6A	0.0	270	235	14.32	2.23	-3.3	18.0	14.9
6B	"	"	"	13.94	2.63	-2.1	20.0	14.5
7A	"	400	180	15.1	2.8	-2.7	21.0	15.7
7B	"	"	"	14.17	4.56	-1.56	21.0	16.0
8A	"	585	200	10.5	6.02	0.0	21.0	9.9
8B	"	"	"	12.26	6.19	-0.4	22.0	16.1

A runs - wheat tracer
B runs - "mustard" tracer

Table 5.4a: Experimental conditions and parameters of the parent NCD's

Notation:

x_a mass fraction of wheat charged to the bed

H bed depth

H_f fountain height

$\bar{t}$ mean cycle time

σ standard deviation of distribution

K_s coefficient of kurtosis of the distribution

t_{max} maximum possible cycle time of bulk particle

t_m median cycle time

which caused extra readings of short cycle times, especially for B runs, where a high sensitivity was required to detect the relatively small signal produced by the passage of a "mustard" tracer. A small number of these readings at low cycle times is sufficient to reduce the mean cycle time significantly. For this reason, the median cycle time time t_m, not $\bar{t}$, will be used to compare NCD's.

For all runs in a bed of 100% wheat, t_m for a wheat tracer was almost equal to t_m of a "mustard" tracer. The largest difference was 3% for runs 5A/B. This is in sharp contrast to the results of Robinson and Waldie (1978), who found differences greater than 100% between particles of mean diameter 2.2 and 4.4 mm. However their data, although obtained using a bed of the same diameter, was only for a single bed depth of 170 mm, lower than any used in the present study. At low bed depths, a large proportion of material is held within the base cone. Here, particle paths are not approximately vertical as in the annulus of deeper beds. Hence the results of Robinson and Waldie are not easily applied to deeper beds, as used in this investigation. Also, Robinson and Waldie measured the particle velocities at the flat front face of the bed. It is possible that wall effects were responsible, at least in part, for the large difference in cycle times, since these were calculated from velocity measurements at the wall.

For runs with $x_a = 0$, the NCD of bulk mustard particles is similar to that of a single wheat tracer particle. Only for runs 8A and 8B is the difference between median cycle times marked. The low median cycle time for the wheat tracer in run 8A is a result of its atypical NCD, which is two-peaked as shown in Figure 5.5b. This particular NCD will be discussed in more detail in the next section.

5.5 Short and Long Cycle Times

Thorley et al (1959) showed that the length of the path taken by a particle in the annulus is determined by the radial position on the free surface at which it impacts from the fountain. Robinson and Waldie (1978) suggested that a particle which lands at a small radial distance from the centre of the bed will consequently enter the spout at a high level and have less time to accelerate in the spout. Hence it would enter the fountain with a low velocity and then be more likely to land again at a small radial distance. This self-sustaining mechanism would be counteracted by dispersion processes such as particle collisions and movement of the spout. No quantitative evidence supporting this possible segregation mechanism has been reported previously and the cycle time data already obtained can be used for an assessment.

A large number of successive cycle times were measured to calculate the NCD's of each tracer particle. Using a computer program it was possible to search through the list of cycle times for values greater or less than a specified cycle time. If the cycle time was less than say, the median cycle time, the cycle time following this was noted. These cycle times form a NCD for cycles following a shorter than the median cycle time. Similarly a NCD is obtained for cycle times longer than the median cycle time. The discussion will be conducted in terms of these NCD's,hereafter referred to as subsequent number of cycles distributions (SNCD). The time dividing low and high cycle times was arbitrarily chosen to be the median cycle time of the parent NCD. The distribution parameters and experimental conditions are given in Table 5.5a. The median time of

Run No.	SNCD	x_a (-)	H (mm)	H_f (mm)	$\bar{t}$ (s)	σ (s)	K_s ( )	t_{max} (s)	t_m^* (s)	t_m (s)
1A	Low	1.0	250	250	5.16	0.45	-2.6	7.0	5.2	5.2
	High	"	"	"	5.20	0.53	-2.2	"	5.2	"
1B	Low	"	"	"	5.37	0.56	0.0	"	5.1	5.1
	High	"	"	"	5.05	0.68	-0.1	"	5.0	"
2A	Low	"	"	160	5.35	0.88	-2.6	7.6	5.5	5.5
	High	"	"	"	5.51	0.67	-3.6	"	5.6	"
2B	Low	"	"	"	5.71	0.55	+0.6	8.0	5.5	5.5
	High	"	"	"	5.60	0.60	+0.4	"	5.5	"
3A	Low	"	405	200	6.84	1.07	-4.1	8.6	7.0	7.2
	High	"	"	"	7.29	0.48	-3.9	"	7.3	"
3B	Low	"	"	"	7.05	0.70	0.0	9.0	6.9	7.3
	High	"	"	"	7.24	0.61	-1.6	"	7.3	"
4A	Low	"	515	"	7.53	0.83	-2.0	9.6	7.7	7.7
	High	"	"	"	7.90	0.64	-0.3	"	7.9	"
4B	Low	"	"	"	7.80	1.13	-1.3	10.0	8.0	7.8
	High	"	"	"	7.75	0.63	+0.1	"	7.8	"
5A	Low	"	595	250	8.05	0.51	-4.7	9.6	8.1	8.1
	High	"	"	"	8.10	0.47	-2.2	"	8.2	"
5B	Low	"	"	"	8.24	0.48	+0.7	10.0	8.1	8.3
	High	"	"	"	8.52	0.58	+0.1	"	8.6	"
6A	Low	0.0	270	235	13.94	2.31	-3.0	18.0	14.5	14.9
	High	"	"	"	14.61	2.23	-3.8	"	15.1	"
6B	Low	"	"	"	14.30	1.78	-0.2	20.0	14.3	14.5
	High	"	"	"	14.15	2.24	-2.2	"	14.5	"
7A	Low	"	400	180	14.71	2.73	-2.7	21.0	15.7	15.7
	High	"	"	"	15.72	2.40	-3.0	"	16.2	"
7B	Low	"	"	"	13.89	4.53	-1.4	"	15.6	16.0
	High	"	"	"	15.25	3.58	-2.0	"	16.5	"
8A	Low	"	585	200	7.65	4.84	+0.9	"	5.8	9.9
	High	"	"	"	13.84	5.24	-1.0	"	16.1	"
8B	Low	"	"	"	10.00	5.69	+0.1	22.0	10.1	16.1
	High	"	"	"	14.75	5.63	-1.1	"	17.3	"

Table 5.5a: Experimental conditions and parameters for NCD's of cycle times following low and high cycle times (SNCD's)

a SNCD is denoted by an asterisk as t_m^*. Examples of the NCD's obtained are shown in Figure 5.5a. The first histogram is the parent NCD and the two SNCD's are shown overleaf. For low cycle times the SNCD is shown as a continuous line and for high cycle times as a broken line. For this case, run 7A, the median time of the SNCD for high cycle times is 0.5 s greater than the median time of 15.7 s in the parent NCD. Thus if a wheat particle undergoes a long cycle, there is a greater chance that the subsequent cycle is also long, although for this case the tendency is not marked.

For all runs with x_a = 1.0, the difference between the two SNCD's is small. A slightly greater difference is found for runs with x_a = 0 and H greater than 400 mm, in particular for runs 8A and 8B. For these runs the bulk material was mustard. For run 8A the parent NCD, using a wheat tracer particle was two-peaked as shown in Figure 5.5b. This suggests that the circulating wheat particle was likely to take one of two distinct particle paths of quite different lengths. Each SNCD from this distribution has a single peak. The SNCD for low cycle times peaks at low times, with a median of 5.8 s and the SNCD for high cycle times has a median of 16.1 s. This confirms the existence of two preferred particle paths. The median time of the SNCD for high cycle times is close to that median time predicted for a bed of depth 585 mm by extrapolation of those median times measured in runs 6A and 7A; hence this SNCD is not a result of unusual particle paths. However, the median time of the SNCD for low cycle times is three times smaller. This indicates that a wheat particle in a deep bed of 100% mustard seed has a strong tendency to undertake further short cycles, once one has occurred. Short cycle times will occur if (i) the particle leaves the spout with a low velocity, or

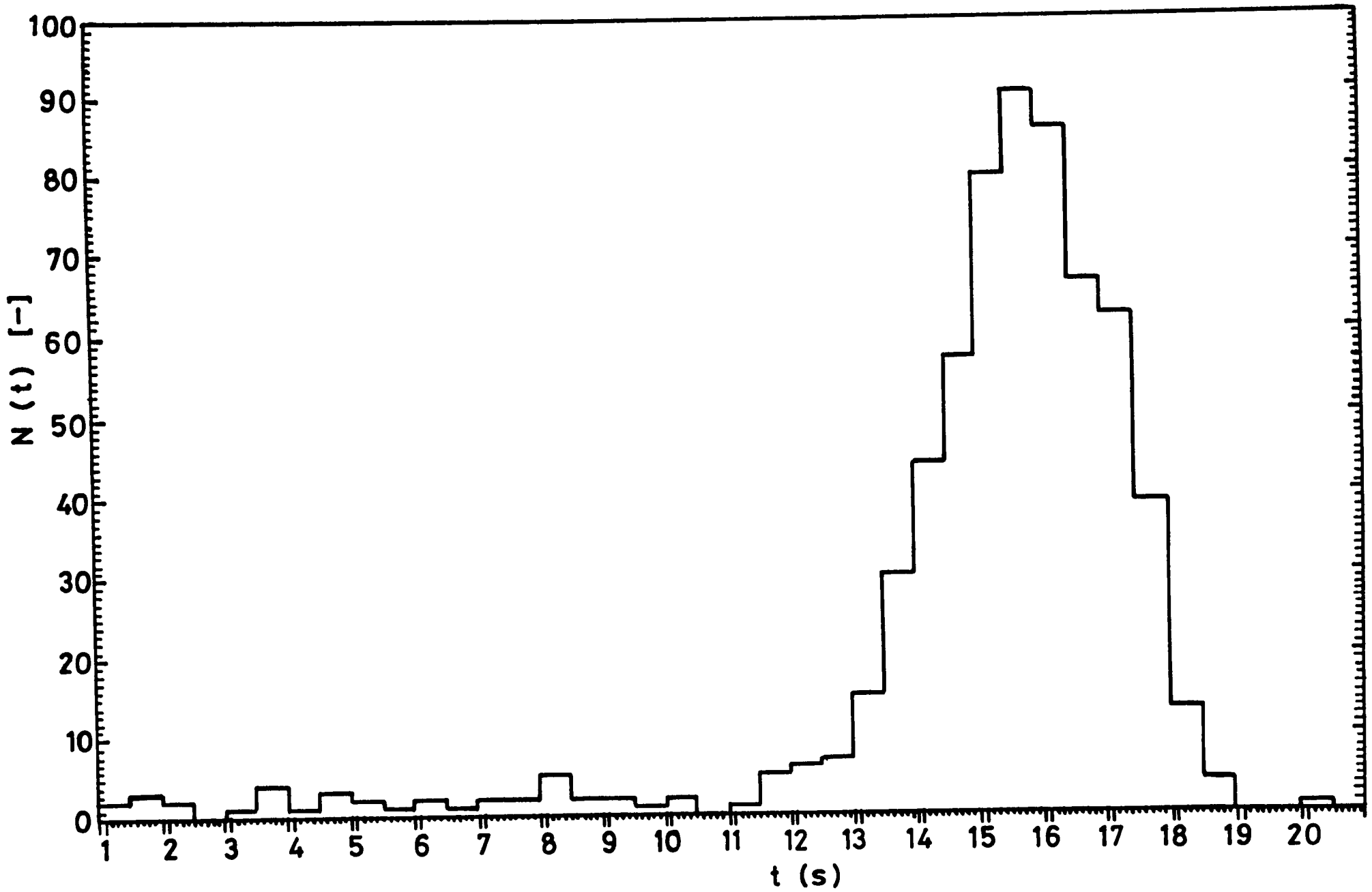


Figure 5.5 a (i) : Parent NCD for run 7A.

Wheat tracer particle in a bed of brown mustard.
Mean cycle time = 15.1 s, Median cycle time = 15.7 s

SNCD's for this run are shown overleaf.

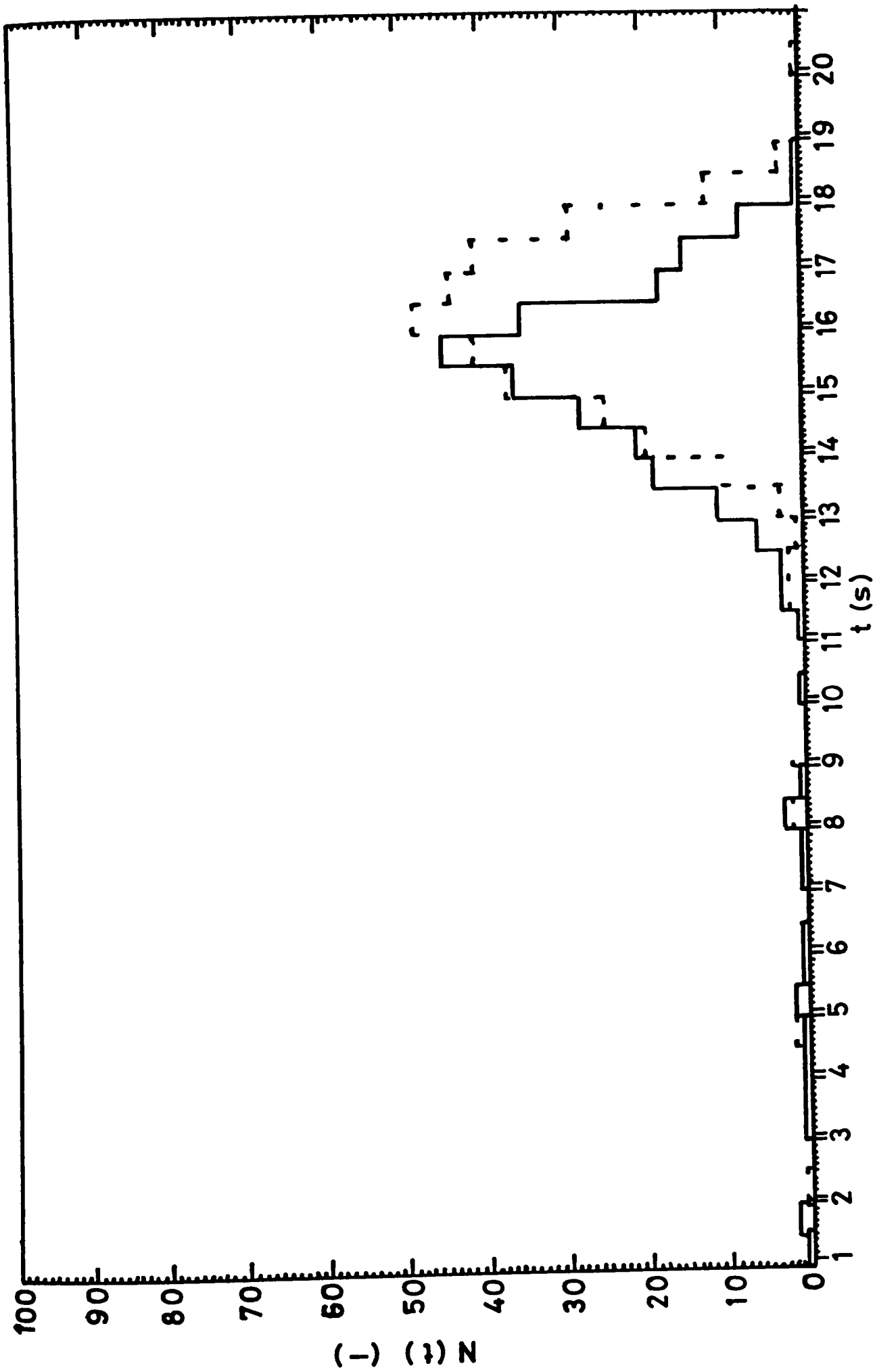


Figure 5.5a (ii) : Subsequent number of cycles distribution (SNCD) for run 7A.

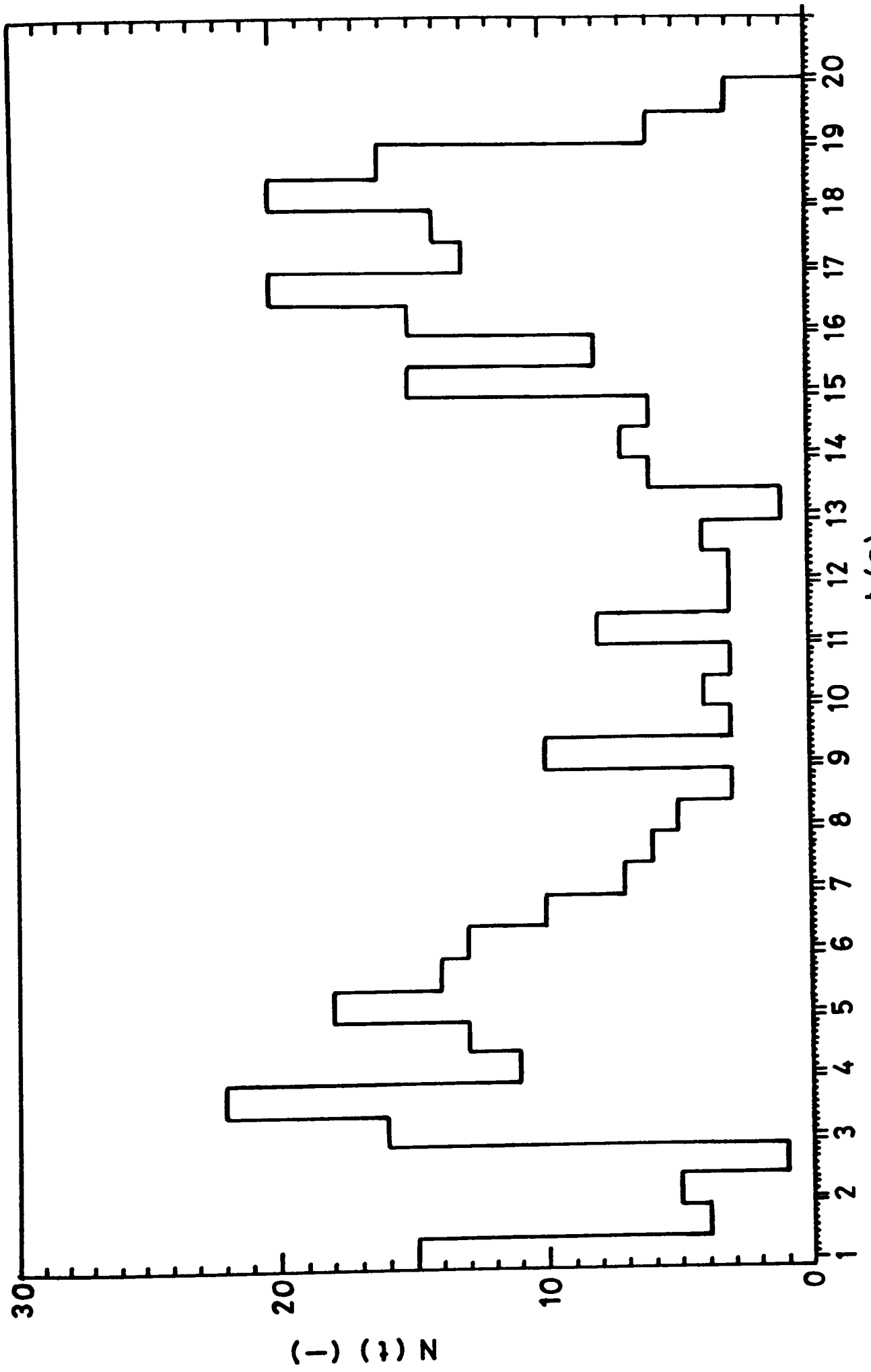


Figure 5.5 b (i) : Parent NCD for run 8A.

Wheat tracer particle in a bed of brown mustard
Mean cycle time = 10.5 s, Median cycle time = 9.9 s

SNCD's for this run are shown overleaf.

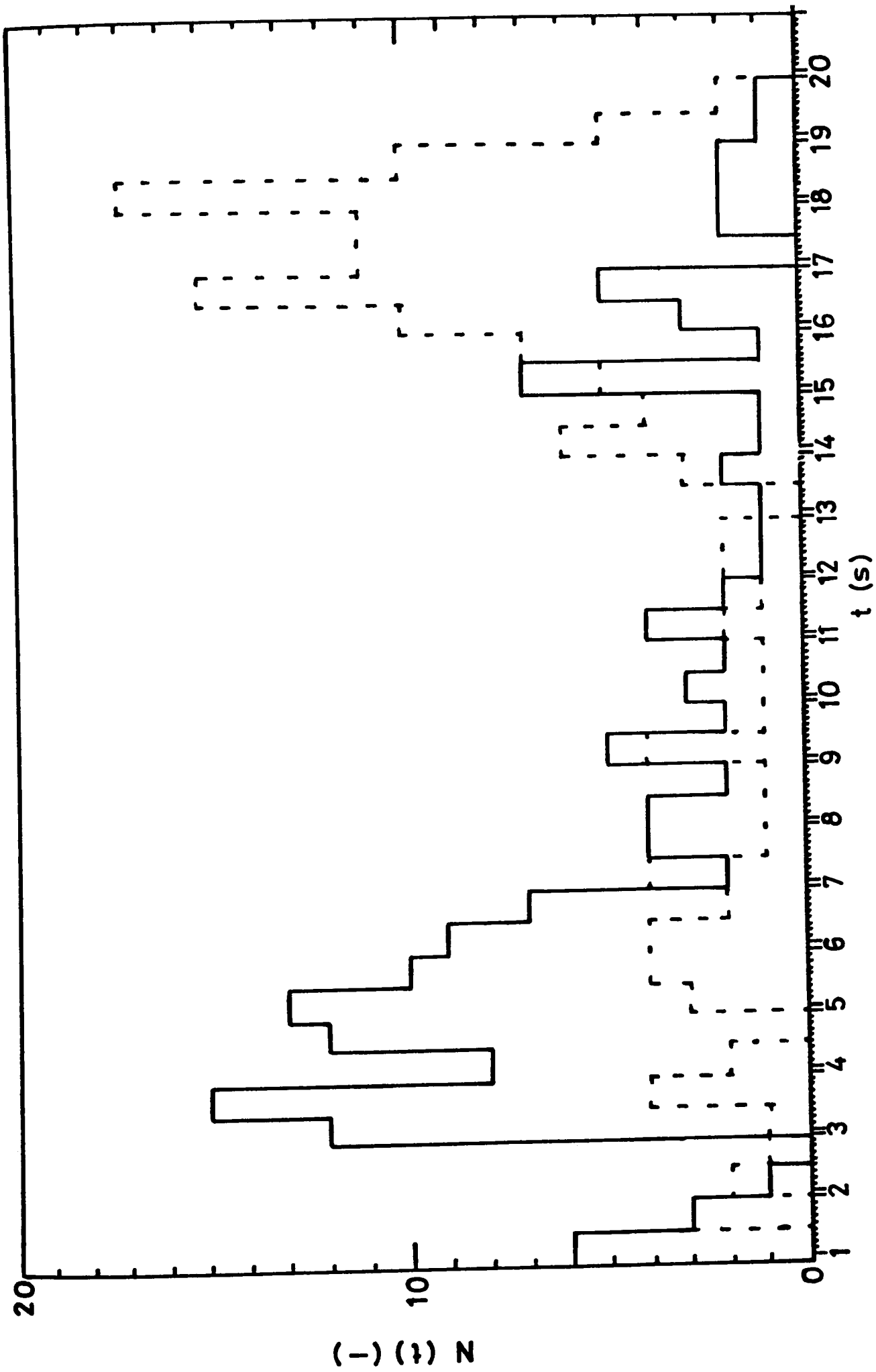


Figure 5.5b (ii) : SNCD's for run 8A.

Wheat tracer particle in a bed of brown mustard.

SNCD less than median time

Mean cycle time = 7.7 s,
Median cycle time = 5.8 s.

SNCD greater than median time

Mean cycle time ; 13.8 s,
Median cycle time = 16.1 s.

if (ii) upon landing it moves on the free surface towards the centre of the bed. The first mechanism requires the velocity profile of particles in the spout to be dependent on particle size. Previous workers have not studied this, although some data obtained from further experiments is reported in Chapter 6. This indicates that particle velocities in the spout may be size dependent, but for the bed conditions studied the difference was not marked. The second mechanism was observed and is reported in section 4.5 (i). It is that mechanism described by Drahun (1979): when large and small particles land on a slope of smaller particles, large particles become "floaters" and move down the slope more easily than small particles.

These mechanisms explain the two-peaked NCD of run 8A and the self-sustaining processes required to produce the very different SNDC's found for this run.

5.6 Summary

a) Wall measurements

In beds containing mixtures of wheat and brown mustard seed, particle velocities have been measured at the column wall and the ratio of these velocities v (wheat/mustard) calculated. All mean velocity ratios were greater than unity, but were only greater than 1.15 in the upper annulus of beds filled with mixtures B and C to depths greater than 500 mm. In the lower annulus, velocity ratios for all conditions studied were approximately unity.

Values of v greater than unity will give rise to concentrations of mustard above average in the outer edge of the upper annulus. This will allow preferential selection of mustard by an outlet or overflow in this region resulting in values of mean of residence time ratio t_o greater than unity. A correlation of t_o and v, does not support this selection mechanism for beds of mixture A but does for mixtures B and C. For these mixtures, a higher value of t_o was generally associated with an increase in v.

b) Number of cycles distribution (NCD)

Bulk segregation in the annulus as reported by Robinson and Waldie (1978) has been studied by measurement of NCD's. A more sensitive detection system than has been used by previous workers [Mann and Crosby (1975) and Van Velzen et al (1974)] was developed to measure accurately NCD's. Using this system, the NCD of a labelled particle representing the behaviour of the bulk particles was compared to the NCD of another labelled particle of a different size and density.

For large bulk particles, wheat seeds, the NCD of a particle 3 times smaller in mean diameter and 1.5 times more dense was found to be very close to the NCD for the bulk, indicating that any segregation which might occur in the annulus, spout, fountain or free-surface (of a reduced area) was not sufficient to cause a marked difference in median cycle times.

For small bulk particles, brown mustard seeds, the median cycle time of a bulk particle was found to be within 3% of that of a single wheat tracer particle, except for one case.

For a bed of depth 585 mm the NCD of the wheat particle became two-peaked as a result of a tendency to take very short cycles regularly. Segregation of particles on the free surface is a likely cause and a two-peaked NCD may be produced whenever the bed conditions give rise to a sloping free surface as observed here for deep beds of Mixture A.

All experiments were conducted with a detection ring centred in the bed at the top of the annulus and because of the resulting disturbance to particle movements in both the spout and fountain, the measured NCD's cannot represent exactly the NCD's occurring in normal beds. However, any segregation occurring in the annulus, spout or fountain of a normal bed could also be expected to occur in this case and would then be apparent from measured NCD's.

c) Subsequent Number of Cycles Distribution (SNCD)

After making one short cycle, the possible tendency of particles to make a second short cycle, as suggested by Robinson and Waldie (1978) was investigated by measurement of subsequent NCD's (SNCD's). For beds of coarse particles, no evidence was found to support this. For beds of smaller particles, this tendency is slight, but only became pronounced in the deepest bed using a large tracer particle. The large particle, having executed a long cycle was then much more likely to take another long cycle, and similarly for short cycles.

In continuously operated beds coarse particles present in bulk of small particles could be expected to accumulate in the upper inner annulus. The accumulation would be greatest in

deep beds and coarse particles would then be less likely to reach an overflow positioned at the upper outer annulus. A higher value of mean residence time ratio t_o would result. This mechanism supports the observed results for mixtures A and B described in Chapter 4, where t_o was found to increase as bed depth increases.

CHAPTER 6

Fountain, Spout, Free Surface and Outlet

6.1 Introduction

In a spouted bed, continuously fed with a mixture of different sized particles, any segregation which causes a particular size fraction to preferentially reach the outlet will result in a lower mean residence time for that size fraction. In the spouted bed used for this study, the outlet is positioned near the free surface and material leaves the bed directly through the outlet orifice, from the fountain or by overflowing from the upper few particle layers of the annulus.

Consider the wall of the spouted bed around the solids outlet to be vertical and flat, with the origin of a coordinate system at the centre of the outlet, as shown in Figure 6.1a. For a particle of a given size fraction landing at the point (x,y), let the probability of it leaving the bed soon after landing be $P(x,y)$. Since particles may impact at different angles and velocities, $P(x,y)$ is the probability of exit averaged over all possible impact angles and velocities. Those particles which do not leave the bed immediately after impact will travel downwards in the annulus. If $n_i(x,y)$ is the number flux of particles of a given size fraction impacting (number per unit area per second), then the rate at which particles of that size fraction leave the bed n_e is given by

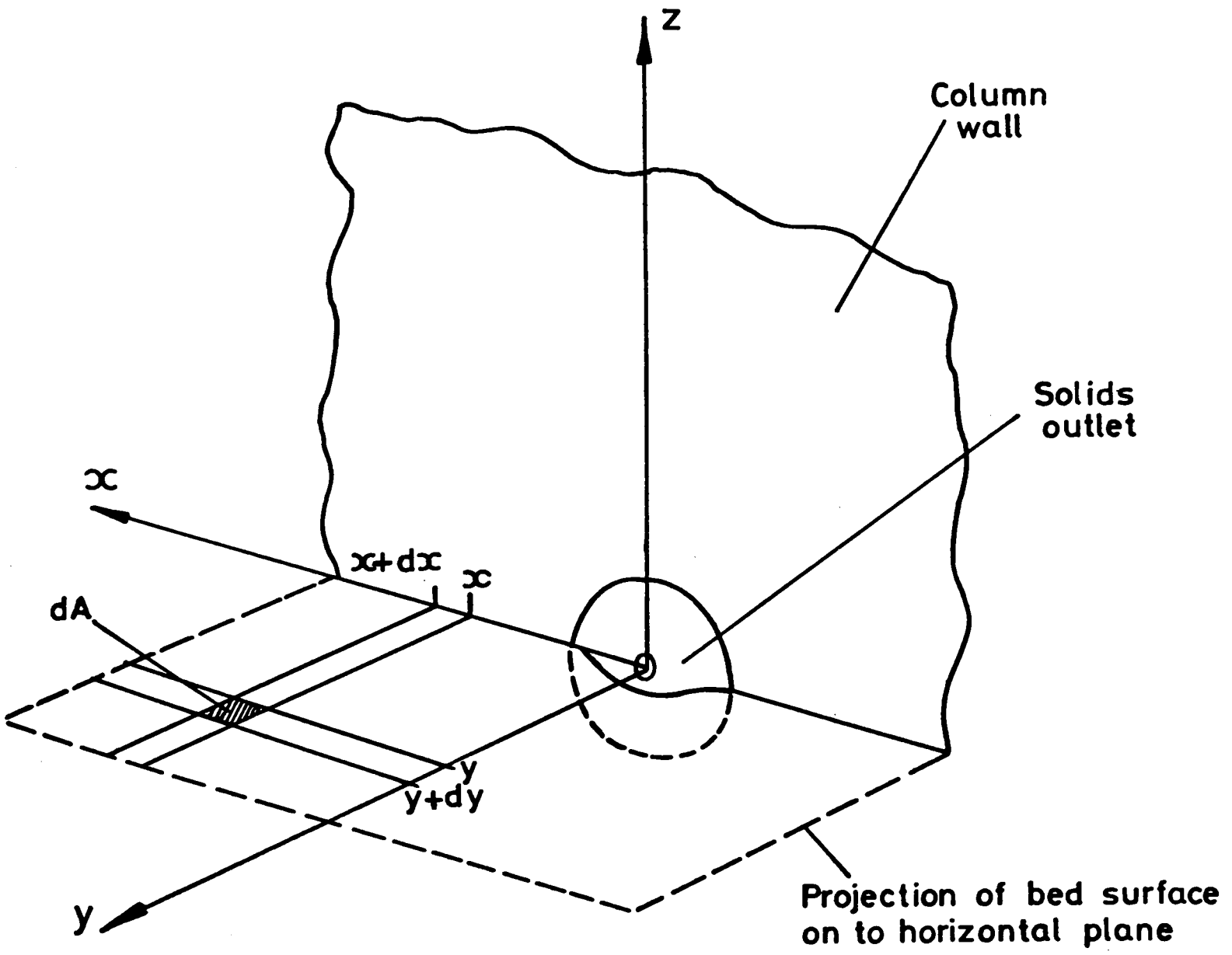


Figure 6.1 a : Coordinate system in the outlet region

$$n_e = \int_{x=-\infty}^{\infty} \int_{y=-\infty}^{\infty} P(x,y)\, n_i(x,y)\, dx dy \qquad (6.1)$$

For the binary size material feed used in the present study, the mean residence time of each size fraction is controlled by n_e and hence, by P and n_i for that fraction.

P is governed by segregation which may occur on the free surface or in the upper few particle layers of the annulus after the impact of a particle. For each size fraction, n_i is a function of the velocity and concentration of those particles at (x,y) in the fountain and is controlled by two factors. Firstly, even if the velocities and positions of particles at entry to the fountain are the same for all size fractions, particles of each size fraction may subsequently take different trajectories in the fountain. This could be due to different free fall velocities of the size fractions or be a result of greater disturbance to the trajectories of smaller particles when in collision with other particles. Secondly, the initial velocity and position of particles entering the fountain influence the subsequent trajectories. The flux of a particle size fraction into the fountain is related to its radial concentration profile and its velocity profile at the top of the spout. If these profiles are different for each of the size fractions in the bed, an uneven distribution of material both in the fountain and on the free surface will result.

In this chapter, literature relevant to particle behaviour in the spout, fountain and free surface will be examined and particular attention paid to results which, although obtained for a closely sized material, are relevant to a size-distributed material. Then, experimental work using wheat and brown mustard seeds in batch and

continuous beds is described. This is concentrated in three main areas: (i) the extent to which free surface segregation controls the mean residence time ratio, by measurement of P under different conditions in a continuously fed bed, (ii) a study of particle velocities and trajectories in the fountain and (iii) a study of particle velocities and trajectories in the spout using high speed cine-photography.

As reported in Chapter 4, for certain bed conditions, submergence of the solids outlet could influence the mean residence time ratio. Results of an investigation into this behaviour are given.

Finally, the consequences of these results for the processing of mixtures by spouted beds is assessed.

6.2 Literature

Previous workers have indicated that the fountain plays an important part in segregation, but no work is reported on spouting particle mixtures. McNab and Bridgwater (1979) summarize earlier work by McNab (1977). A batch operated half-column was used for the investigation and the particles spouted were closely-sized seeds of wheat, mustard and linseed. Cine film of the fountain and surface region of the bed was examined using a stereophotogrammetric method. Using a stereoscope two frames of film were observed simultaneously and contours of the average radial and vertical particle velocities were drawn. The stereoscope was small, and the accuracy of the absolute velocity measurements was uncertain. However, the relative velocities were considered reliable. Three types of fountain were observed: partial, full and overdeveloped, as defined in Figure 4.6c. For the last type, a quantitative study was not possible since particle motion was too chaotic for streamlines or velocity contours to be drawn. For the first two types, the radial

position of a particle at the top of the spout was plotted against the position at which it landed. For a full fountain, these results are shown in Figure 6.2a. All measurements were for beds filled with closely sized particles of one material and it is not possible to infer from this work the different trajectories which may occur if a size-distributed mixture is spouted.

Grace and Mathur (1978) developed a theoretical model to describe the characteristics of the fountain region of spouted beds. The following assumptions were made: (i) the void fraction of particles in the core of the fountain decreases to a minimum near the top of the fountain, (ii) this minimum is equal to the void fraction of the material when loosely packed, (iii) no radial spreading of the fountain core occurs until this minimum is reached, (iv) the gas attains a uniform superficial velocity above the bed surface and (v) the empirical relationship between particle velocity in the spout at bed surface level v_o and the void fraction in the spout at this point ϵ_s, as given by

$$v_o = \epsilon_s^m \, v_{o\,max} \tag{6.2}$$

holds where $v_{o\,max}$ is the particle velocity at the centre line of the spout at surface level and m is a fitted constant. The model can be used to predict the fountain height and vertical profiles of particle velocity in the upward moving central part of the fountain from particle velocity and spout voidage data at the bed surface level. Columns of diameter 0.152, 0.241 and 0.292 m were used and the fountain region was studied using beds of wheat seeds, polystyrene, millet, glass beads and ammonium nitrate; the resulting equation to predict fountain height was

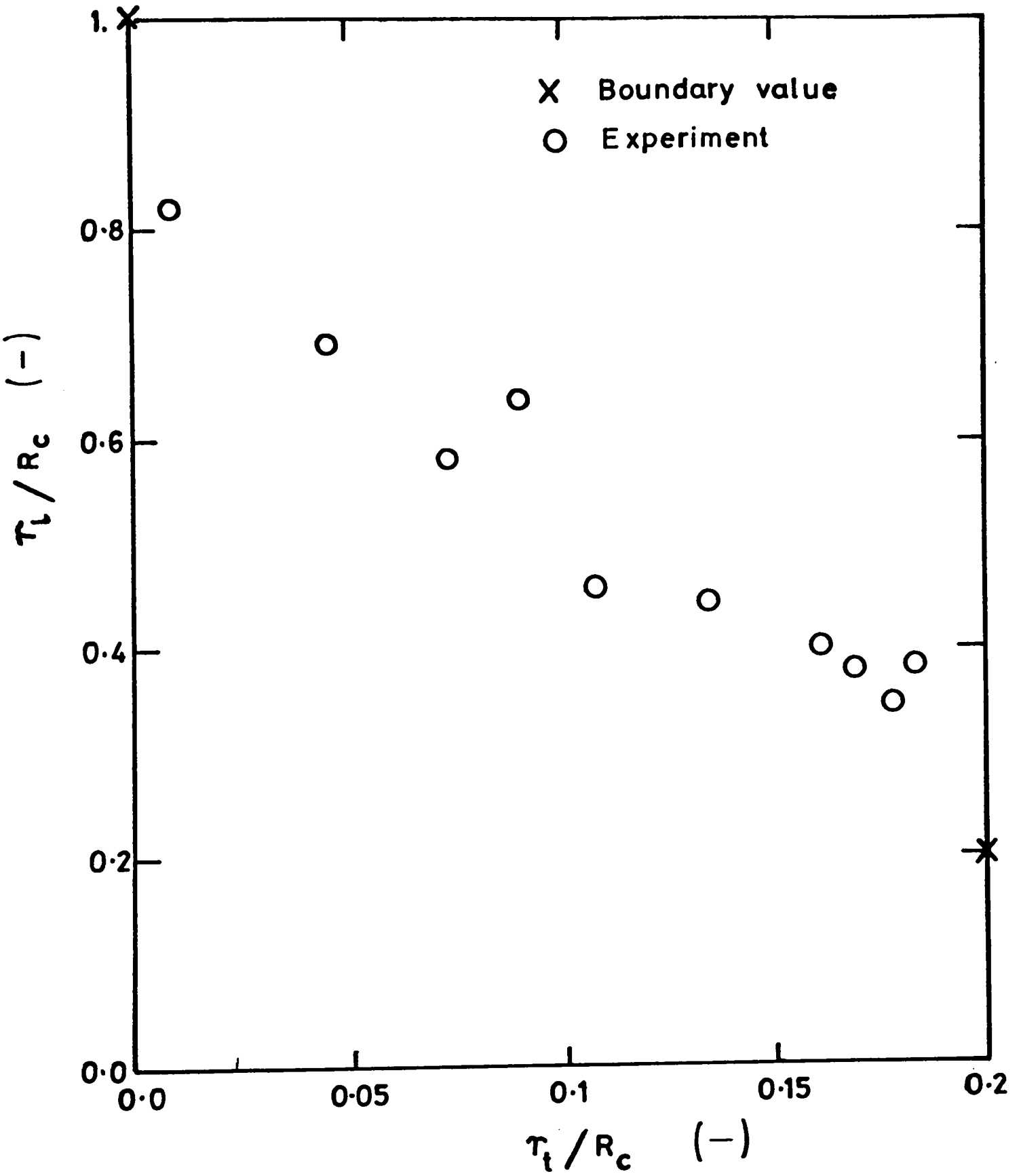


Figure 6.2a : Radial position of particle on landing r_1/R_c vs. Radial position at top of spout r_t/R_c.

Data of McNab (1977b)

Fountain : full; Material : Mustard seed.

$$H_f = \epsilon_s^m \frac{v_o^2}{2g} \left(\frac{\rho_s}{\rho s - \rho g} \right) \qquad (6.3)$$

where H_f is fountain height and ρ_s and ρ_g are the solid particle and gas densities respectively. The empirical constant m was found to give the best fit to experimental data when equal to 1.46. If a mixture of particles is present in the bed, equation (6.3) could be applied to each component separately if v_o is measured for each size fraction and ϵ_s estimated for the mixture. Since v_o and ρ_s may differ for each component, trajectories and fountain heights may also be different.

No investigation of particle velocities in the spout of a bed of size-distributed material has been reported in the literature to date. Lim and Mathur (1978) studied particle motion of mono-sized materials in three half-section beds of i.d. 0.152 m, 0.241 m and 0.292 m. Materials used were the same as those of Grace and Mathur (1979). Vertical particle velocities were measured from the film at three locations across the spout radius and average values calculated by integrating the velocity profile. Spout voidage was calculated from continuity considerations at different levels in the bed, using the above particle velocity data. Most data was found to obey the equation

$$\frac{v_s}{v_{s_{max}}} = 1 - \left(\frac{r}{r_s} \right)^n \qquad (6.4)$$

where v_s is the vertical particle velocity at a radius r, $v_{s\,max}$ is the vertical particle velocity at r=0, r_s is the spout radius and the parameter n varies between 1.3 and 2.2. However, a model was not developed to predict the radial velocity profile or spout voidage if a mixture of particle sizes was present.

Drahun (1979) developed a novel piece of equipment to study free surface segregation in a system representative of a poured heap. Essentially, bulk material and small quantities of tracer were fed onto an inclined slope. Two principal types of behaviour were observed. Some tracers, termed sinkers, disappeared beneath the free surface within a few centimetres of the start of the inclined slope. Others, termed floaters, were transported to the far end of the slope. The distribution of bulk tracers was approximately even. The particle properties studied in detail were size and density. Sinkers were smaller or denser than the bulk and floaters were larger or lighter. Three processes were believed to be causes of segregation:

(i) convection of tracers down the slope in avalanches,

(ii) inter-particle percolation [Bridgwater, Cooke and Scott (1978)] removing particles from the active zone of a few surface layers, and

(iii) particle migration causing particles to remain in avalanches and rise to the free surface.

It was not possible to isolate the effects of particle shape or surface roughness, but results suggested that except in extreme cases, these factors did not contribute to segregation. The effect of free fall height on segregation was studied and as the free fall height was increased from 8 bulk particle diameters, for floaters and sinkers by virtue of size, segregation became less marked. In the extreme case of a large free fall height (125 particle diameters), a sinker due to its size could behave like a floater. Transport down the slope was then by bouncing. The distribution of tracers was unaffected by varying the proportion of tracer from less than 1% to 75% of the bulk. In a spouted bed, if the effects of upward flowing gas in the annulus were neglected, the above results could be applied to particles landing on the sloping part of the free

surface near the outlet. The gradient of this slope is dependent on the solids mass flow rate and upon the upward gas flow rate. Bridgwater (1975) predicts a decrease in surface gradient with increasing gas flow rate. Also an increase in the gradient of the free surface near the outlet can be expected to accompany an increase in the rate of solids throughput, especially when the outlet is nearly submerged, due to a very high solids feed rate.

6.3 Outlet Region

To determine the probability function $P(x,y)$ experimentally, tracer particles for each size fraction present were dropped to the bed surface and the number which immediately left the bed was counted.

a) Preliminary experiments

Mixtures of wheat and brown mustard seeds were used for all experiments. In preliminary experiments, the tracers were dropped from a pipe of 11 mm i.d. for wheat and 7 mm i.d. for mustard, positioned 150 mm above the centre of the outlet orifice to represent particles impacting from the fountain. This feed system is shown in Figure 6.3a. Tracers falling down the feed pipe will collide with the walls of the pipe and bed and leave the pipe with a distribution of speeds and directions. The landing positions of tracers on the free surface will then be distributed over a certain area. Difficulties then arise in the analysis of results, since if Equation (6.1) is to be used, values of P at specific values of x and y are required. A further disadvantage with this method is that for overdeveloped fountains, collisions between particles in the fountain and falling tracer particles will alter the distribution of landing positions of tracers; the resulting distribution can not be easily predicted. Any

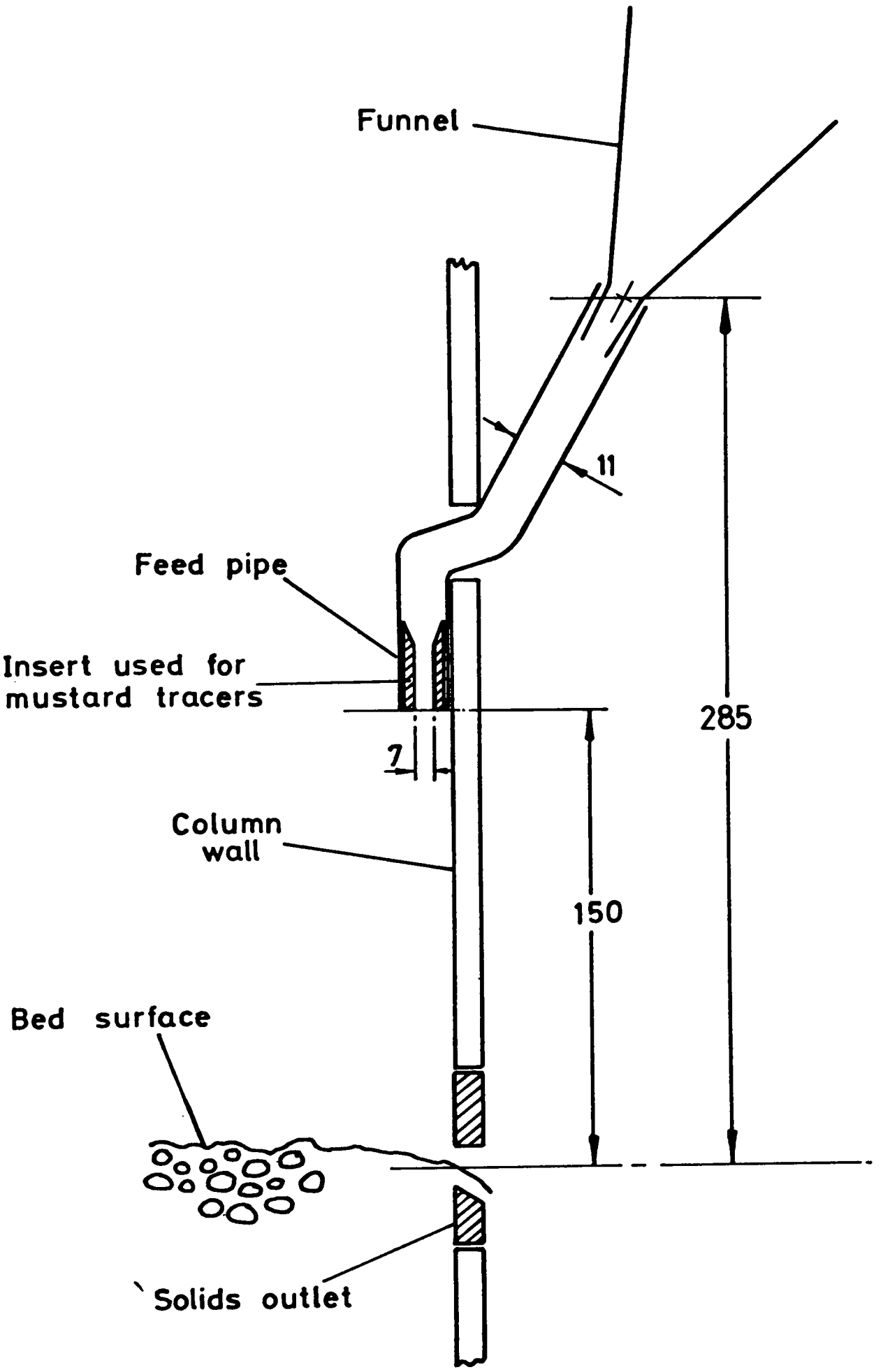


Figure 6.3 a : Tracer feed system used in preliminary experiments

Not to scale
All dimensions in mm.

evaluation of P without this information would be suspect, hence a different method of dropping tracer particles to the bed surface was adopted.

b) Main investigation

In subsequent experiments, tracer particles were dropped onto the bed surface from a glass pipe of 11 mm o.d. and 9 mm i.d. The location of the feed pipe is shown in Figure 6.3b. It extends into the bed through an upper hole in the outlet orifice plate (see Figure 3.1b) and when rotated manually, tracer particles slide out into the bed. This method worked well for wheat tracer particles, but the mustard tracer particles are more spherical and were found to roll out of the pipe in an uncontrolled manner. Therefore, half of one end of the feed pipe was blanked off as shown in Figure 6.3b, which enabled a controlled release of the mustard tracers from this end of the pipe as it was rotated. This technique allows all tracer particles to be dropped to the same point on the bed surface and permits an exact evaluation of $P(x,y)$ in the outlet region. Since a general study would be time consuming, a single point was chosen on which to drop the tracers. P, measured at this point, should show any segregation trends and help to clarify the mechanisms involved. Disadvantages with this method are (i) the feed pipe projects into the bed above the outlet and disturbs material in the fountain in this region, and (ii) tracer particles do not exactly represent material falling from the fountain since they fall from a much lower height.

Tracer particles were required to have properties the same as the bulk material. Fifty magnetic tracers for wheat particles were made in the same way as the single tracer particle used for NCD

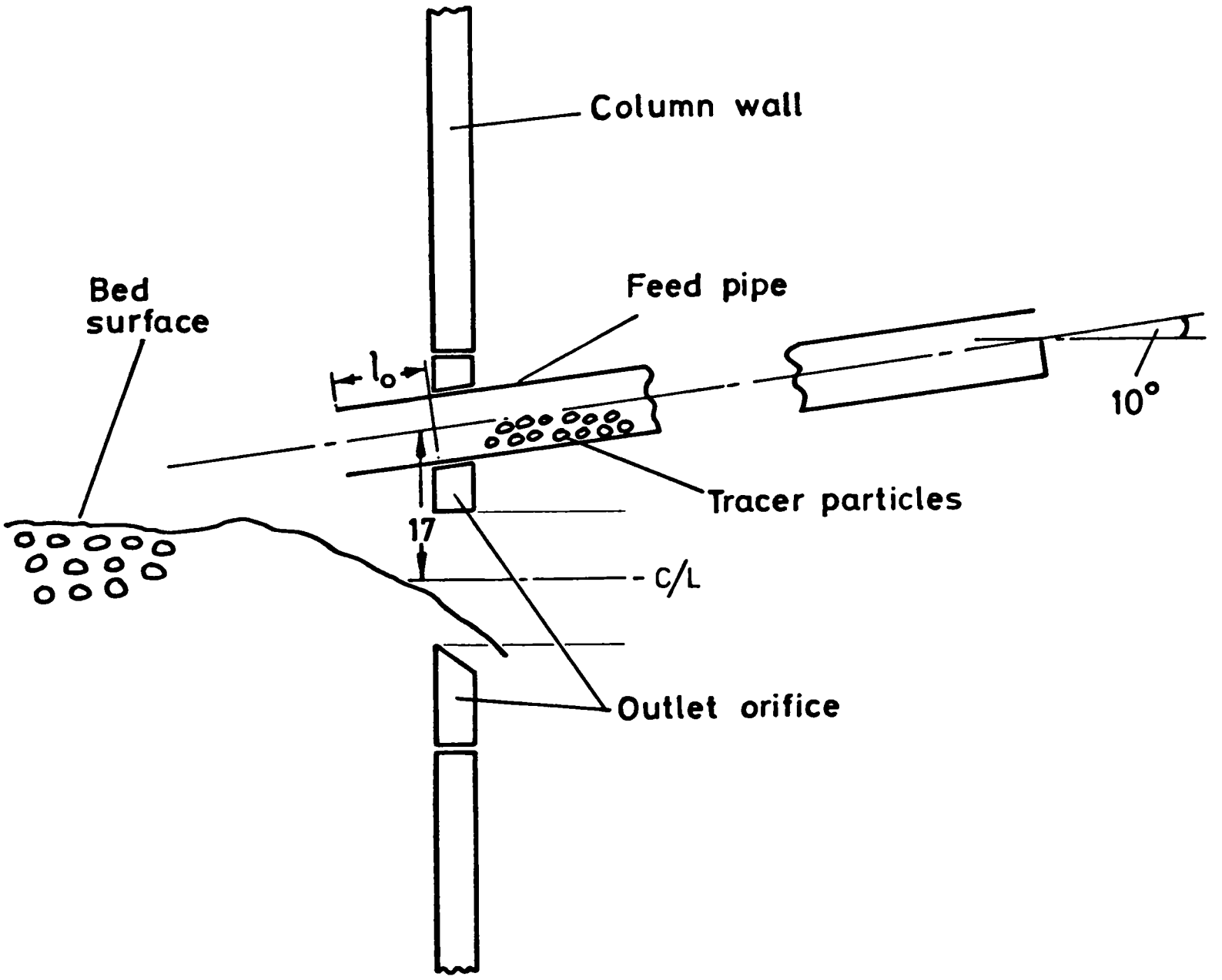


Figure 6.3b : Tracer particle feed system

Dimensions in mm.
Overhang distance l_o = 10 mm for all runs.

measurements, described in section 5.3. After these tracer particles had been released from the feed pipe, they were subsequently recovered using a single permanent magnet. This was lowered into the fountain to collect those particles remaining in the bed and lowered into the outflowing material to recover those particles leaving immediately after impact. Mustard tracer particles were seeds which had been spray-painted. Different coloured tracers were used for each run, so recovery of tracers which remained in the bed was unnecessary. Mustard seed tracers were recovered manually from the outflowing material. Wheat tracers were not significantly different in weight or surface finish from wheat seeds. Mustard tracers were 5% greater in weight with either a matt or shiny surface finish. These properties are given in Appendix B.

If tracer particles dropped to the point (x,y) on the bed surface have a probability P of leaving the bed, the probability of exit measured by experiment P_m from a finite number of drops N will not be exactly equal to P. P can reasonably be expected to lie within the 95% limits of confidence on P_m, which can be found in tables of the binomial distribution. For this study, the upper and lower limits of confidence were obtained from Geigy (1970). With a mixture present in the bed, a probability of exit for each component, P_1 and P_2 can be calculated. For the particles used in this study, P_1 is the probability of exit for wheat particles and P_2 is that for brown mustard seeds.

The exit probability ratio P_1/P_2, hereafter P_o, is plotted against the fountain shape number N_f in Figures 6.3c, d and e. Limits of 95% confidence for P_o were calculated in the same manner as those for the particle velocity ratio v, as described in Appendix D. Results and experimental conditions for all runs are given in Table 6.3a. The extent to which free surface segregation

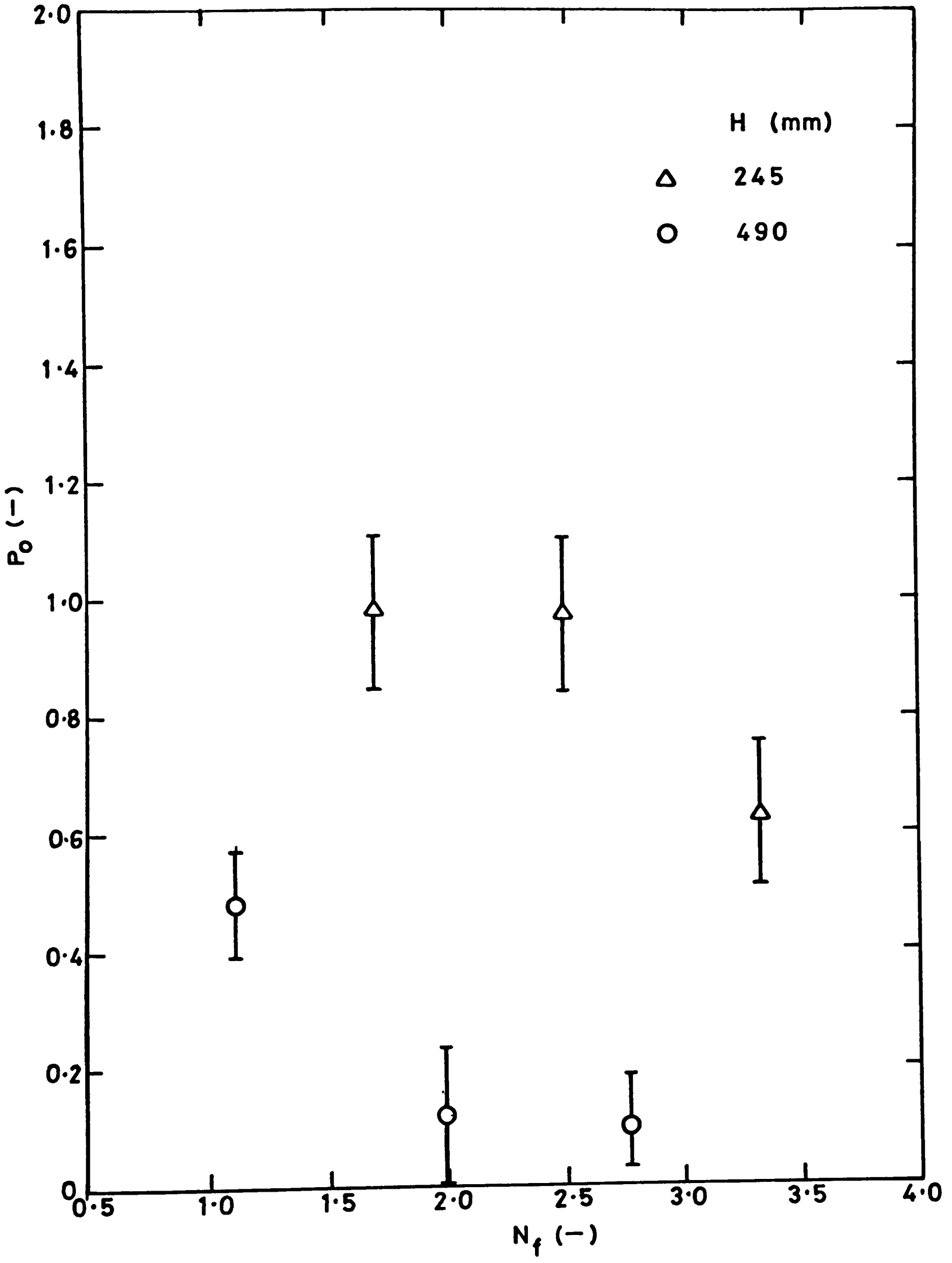


Figure 6.3 c : Variation of exit probability ratio P_o with fountain shape number N_f.

Mixture A : $z_a = 0.13$

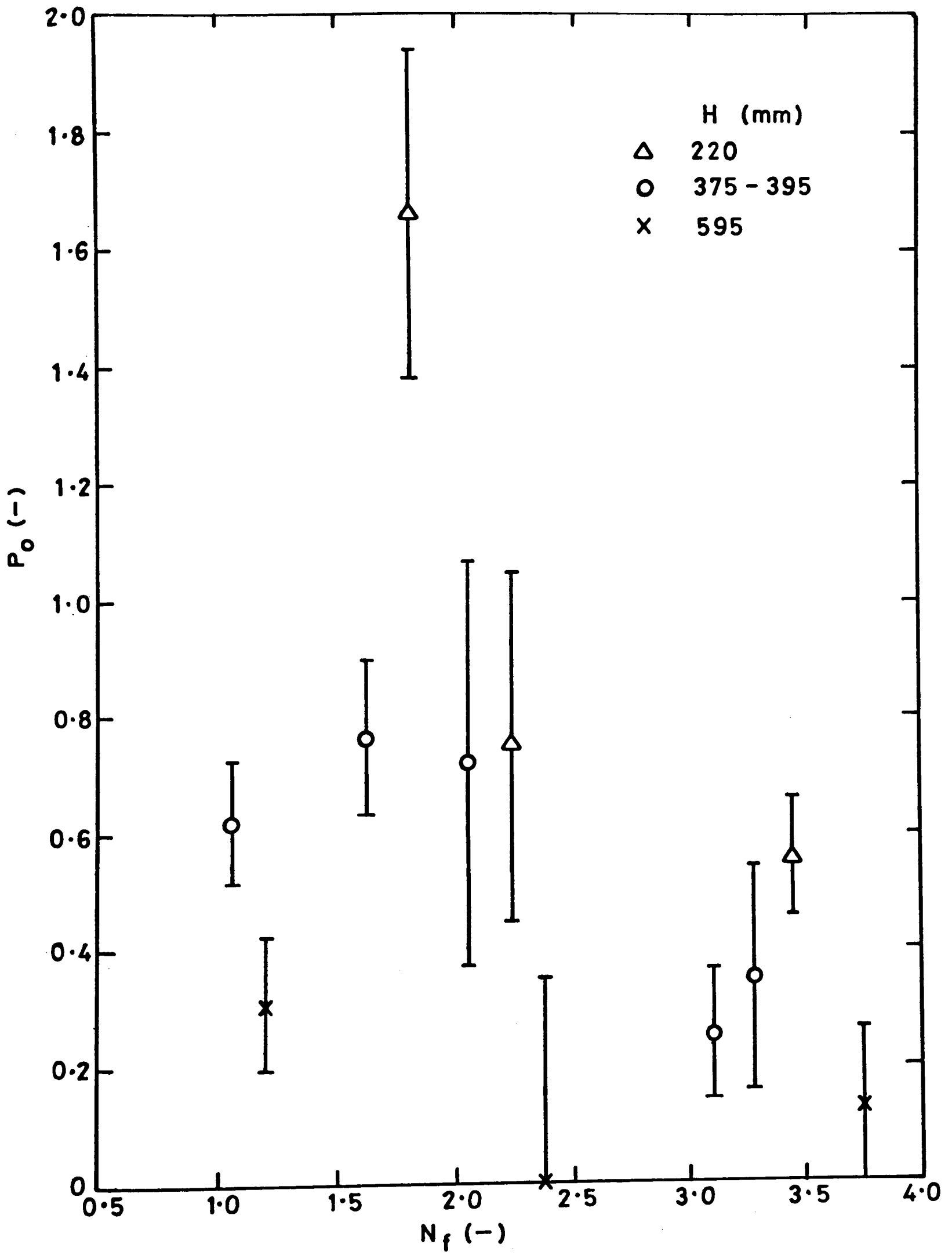


Figure 6.3 d : Variation of exit probability ratio P_o with fountain shape number N_f.

Mixture B : $z_a = 0.55$

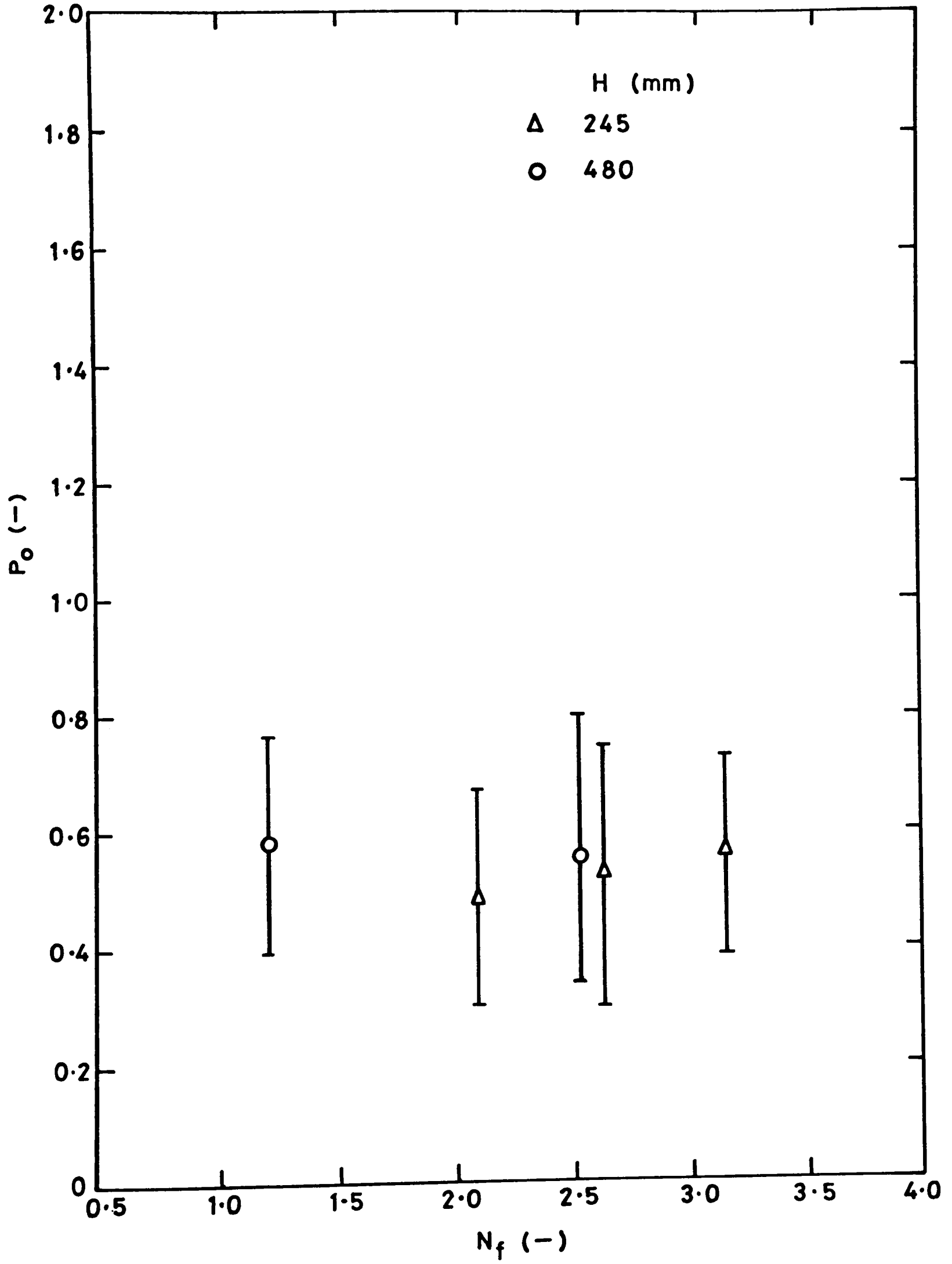


Figure 6.3 e : Variation of exit probability ratio P_o with fountain shape number N_f.

Mixture C : $z_a = 0.90$

Run No	z_a (-)	H (mm)	m (kg min^{-1})	N_f (-)	N_1 (-)	N_2 (-)	P_1 (-)	P_2 (-)	P_o (-)	95% Confidence Limits on P_o (-)	t_o (-)
P18	0.13	240	0.20	1.69	131	300	0.70	0.71	0.98	± 0.13	0.66
P19	0.13	245	0.20	2.5	132	300	0.69	0.71	0.98	± 0.13	0.62
P20	0.13	245	0.20	3.33	135	285	0.46	0.72	0.64	± 0.12	0.72
P22	0.13	490	0.20	1.11	160	327	0.42	0.87	0.48	± 0.09	0.75
P23	0.13	490	0.20	1.98	180	317	0.03	0.23	0.12	± 0.12	1.28
P21	0.13	490	0.20	2.77	180	298	0.04	0.42	0.11	± 0.08	1.37
P 7	0.55	220	0.22	1.82	234	231	0.65	0.39	1.66	± 0.28	1.20
P14	0.55	220	0.22	2.27	89	300	0.26	0.35	0.75	± 0.30	1.31
P 8	0.55	220	0.22	3.45	231	107	0.39	0.70	0.56	± 0.10	1.58
P13	0.55	376	0.22	1.06	275	300	0.40	0.64	0.62	± 0.10	1.15
P 9	0.55	376	0.22	1.63	278	300	0.42	0.55	0.76	± 0.13	1.28
P12	0.55	380	0.22	2.05	175	300	0.12	0.17	0.72	± 0.35	1.35
P11	0.55	395	0.22	3.28	186	287	0.08	0.23	0.35	± 0.19	1.43
P10	0.55	376	0.22	3.10	180	600	0.11	0.44	0.26	± 0.11	1.56
P15	0.55	595	0.22	1.20	131	299	0.19	0.62	0.31	± 0.11	1.31
P17	0.55	590	0.22	2.38	86	300	0.00	0.12	0.00	+ 0.35	1.50
P16	0.55	600	0.22	3.75	128	298	0.03	0.24	0.13	± 0.13	1.39
P24	0.90	245	0.23	2.10	131	332	0.20	0.41	0.49	± 0.18	1.23
P26	0.90	245	0.23	2.63	131	303	0.16	0.31	0.52	± 0.23	1.16
P25	0.90	245	0.23	3.16	131	302	0.27	0.48	0.56	± 0.17	1.09
P27	0.90	480	0.23	1.21	131	314	0.26	0.45	0.58	± 0.19	1.28
P28	0.90	480	0.23	2.53	88	309	0.08	0.14	0.56	± 0.47	1.24

Table 6.3a : Exit probability values and experimental conditions.

influences the mean residence time ratio t_o can not be assessed directly from these Figures. Hence, in Figures 6.3f , g and h, P_o is plotted against t_o for beds of mixtures A, B and C respectively.

(i) Mixture A (z_a = 0.13)

For two bed depths and a range of fountain shape numbers, t_o increases from 0.62 to 1.37 as P_o decreases from 0.98 to 0.11.

Let us assume for the moment that the wheat and mustard particles in the spouted bed do not segregate, except in the region of the free surface and annulus close to the overflow and segregation of particles in this region causes the difference in mean residence times of the two components. The extent of this segregation can be assessed using the parameter P_o and a correlation between t_o and P_o should yield:

(a) values of P_o greater than unity for the experimental conditions which give values of t_o less than unity and vice versa, and

(b) decreasing values of P_o for those conditions which give rise to increasing values of t_o.

Consider again the results for mixture A (z_a = 0.13) in Figure 6.3f. The trend of these results is consistent with (b) and this evidence alone suggests that free surface segregation in the outlet region is a factor controlling the mean residence time ratio. However, for conditions giving t_o less than unity, P_o is also less than unity and this does not fulfil condition (a). Failure to satisfy this condition can

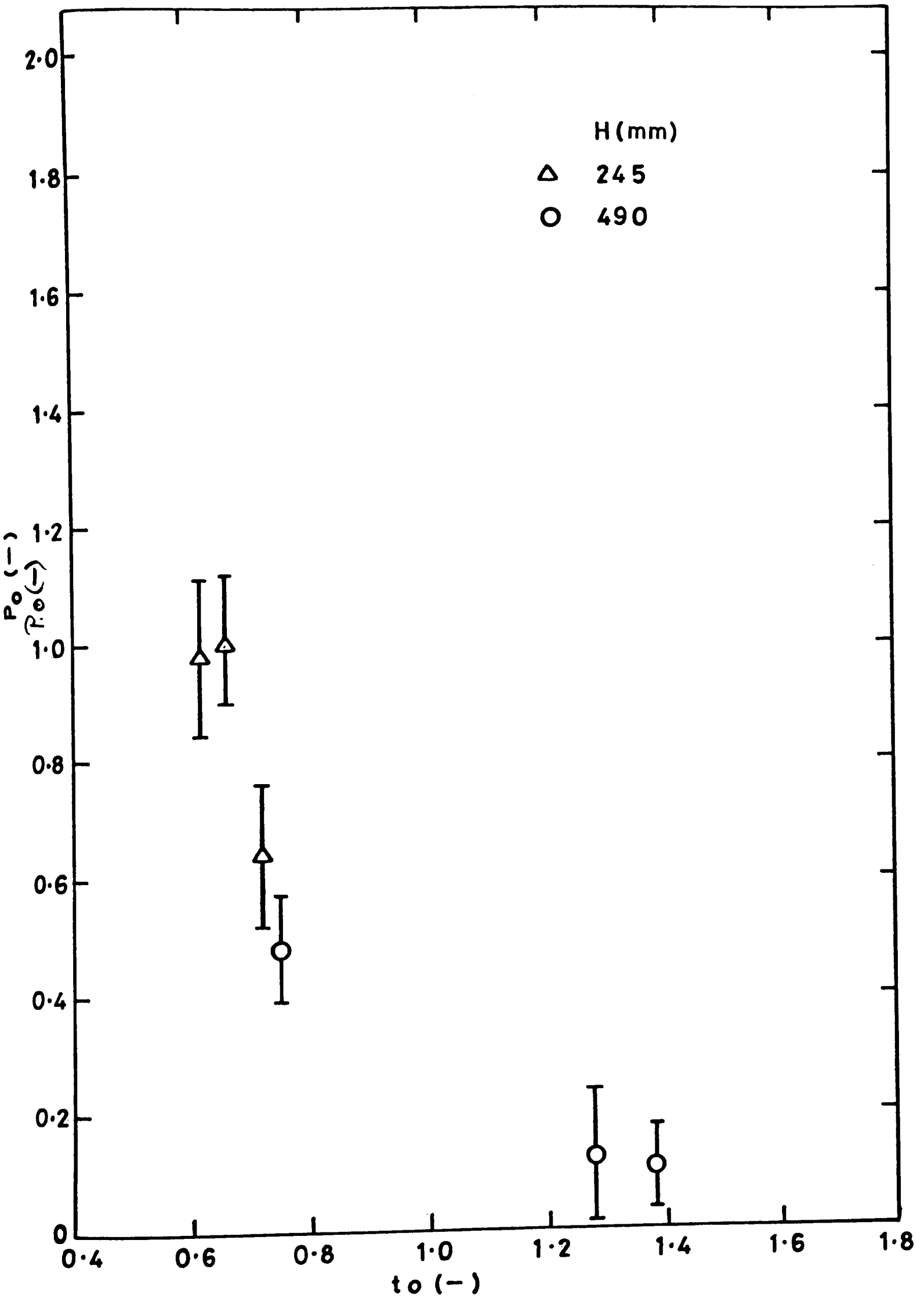


Figure 6.3 f : Correlation between exit probability ratio P_o and mean residence time ratio t_o.

Mixture A : $z_a = 0.13$

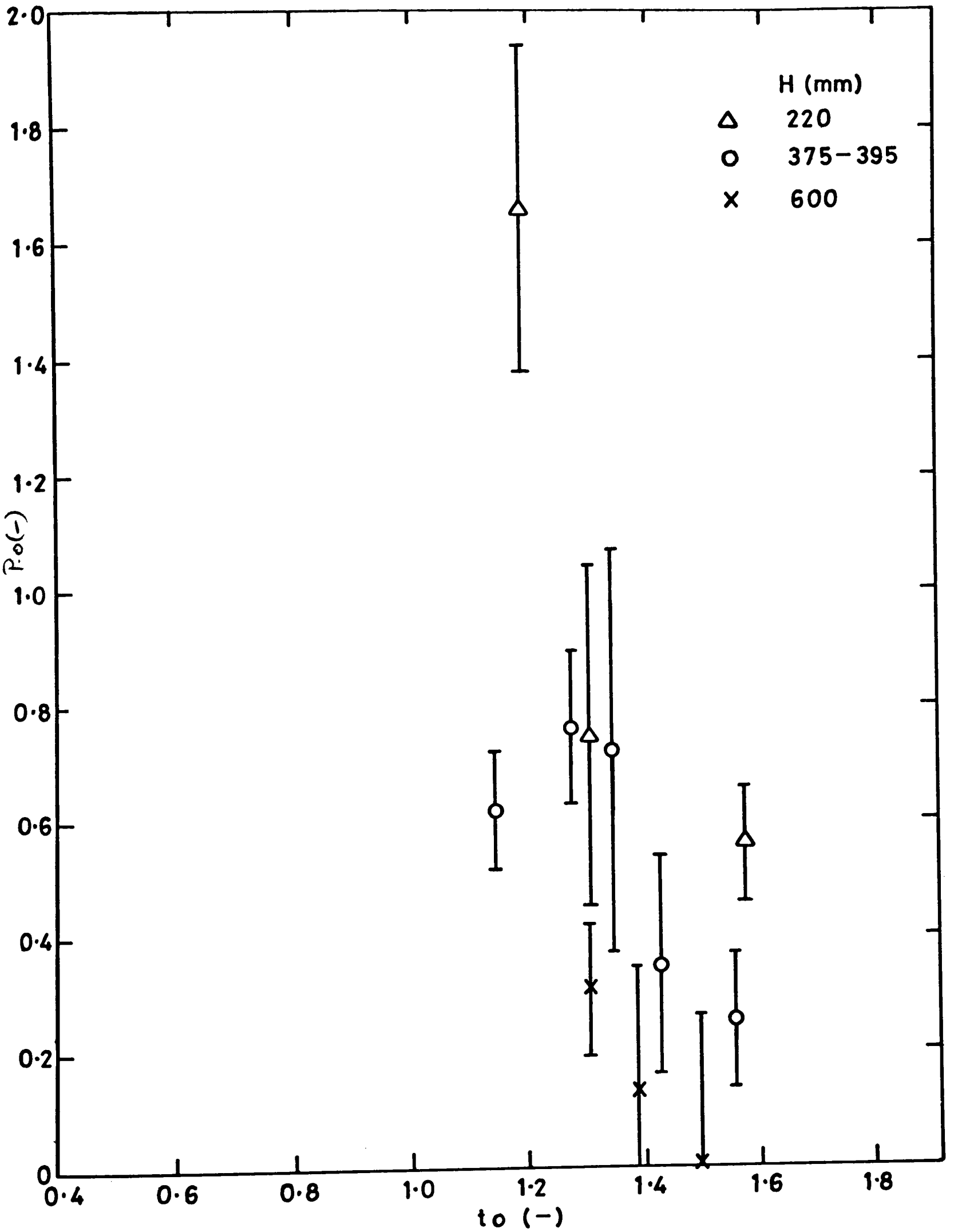


Figure 6.3 g : Correlation between exit probability ratio P_o and mean residence time ratio t_o.

Mixture B : $z_a = 0.55$

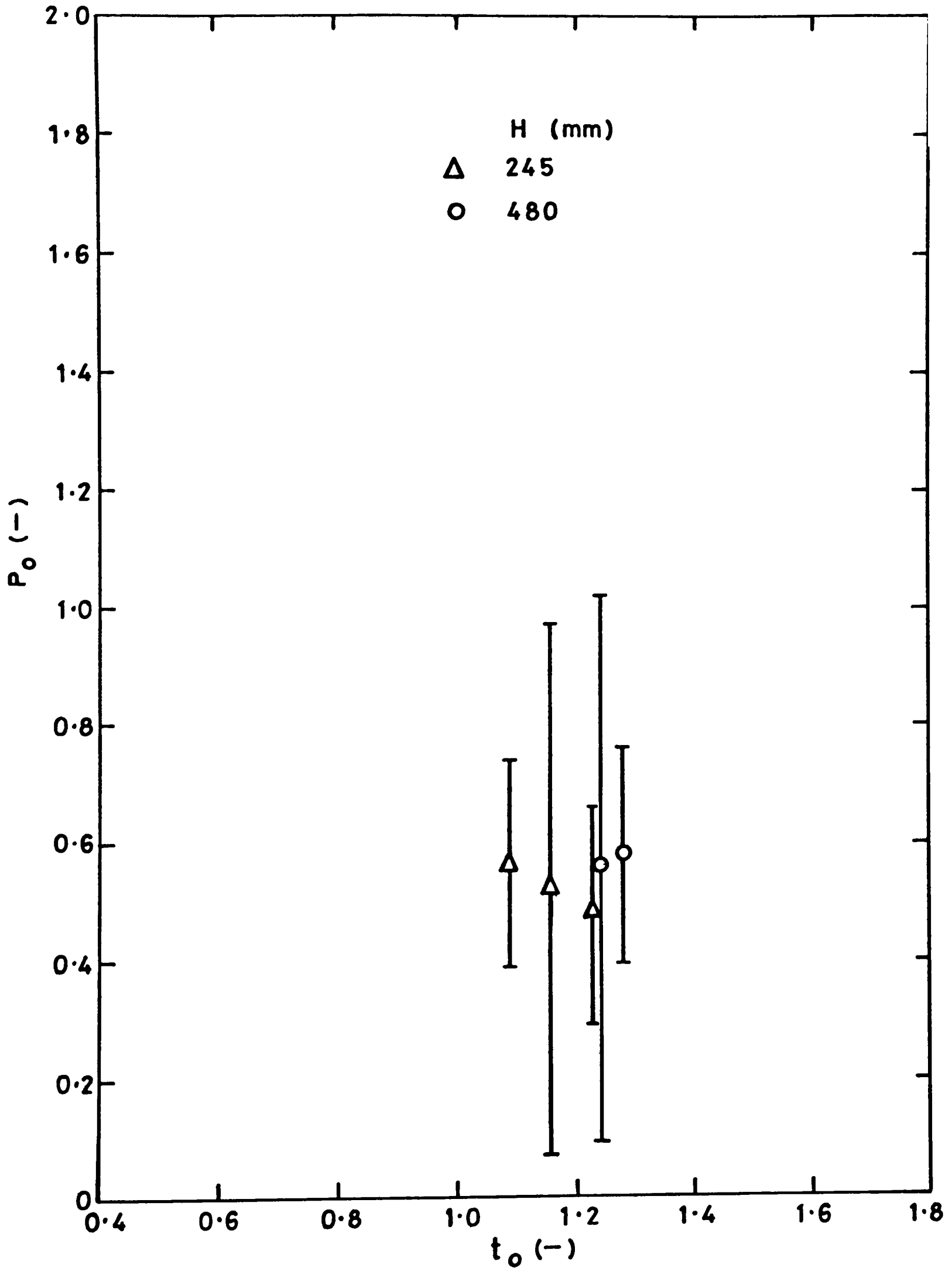


Figure 6.3 h : Correlation between exit probability ratio P_o and mean residence time ratio t_o.

Mixture C : z_a = 0.90

arise for two reasons. Firstly, segregation which gives rise to a difference in mean residence times does not occur in the outlet region alone and secondly, that a measurement of the exit probability ratio P_o does not give an accurate guide to free surface segregation in the outlet region. Each of these is likely to be true in part. The first can be substantiated by evidence for segregation in the fountain and spout, presented in following sections; the second is a result of the inflexibility of the experimental technique whereby the exit probability ratio can be measured only for particles dropped from a low height (about 10 mm) to the free surface, and dropped only to one position on the free surface. If the exit probability ratio was measured over a wide range of dropping points and heights, a better understanding of the relationship between P_o and t_o could be expected.

(ii) Mixture B ($z_a = 0.55$)

Figure 6.3g shows the correlation between P_o and t_o for this mixture. Three bed depths were studied for a range of values of N_f. At each bed depth H, decreasing values of P_o are associated with increasing values of t_o with the exception of one point at H = 380 mm. Excepting one point again, at H = 220 mm, all values of P_o are less than unity when the associated values of t_o are greater than unity.

Each observation supports the hypothesis that, as with mixture A, free surface segregation in the outlet region is a major factor controlling t_o.

(iii) Mixture C (z_a = 0.90)

It is seen from Figure 6.3h that over a wide range of bed conditions the variation in t_o is small. Therefore a correlation between P_o and t_o is not easy to assess. However, values of P_o are all less than unity for conditions where t_o is greater than unity. This again suggests that free surface segregation is a factor controlling t_o for mixture C.

Except for shallow beds of mixture A and for low values of N_f in deeper beds of that mixture, the smaller sized component is always found to have the shorter mean residence time ($t_o > 1$). Since the correlations between P_o and t_o suggest that free surface segregation plays an important part in determining t_o, the work of Drahun (1979) on surface segregation will be considered again.

For mixtures weak in the larger sized component Drahun states that large particles impacting on a slope of the mixture will become "floaters". In a spouted bed with a free surface sloping towards the outlet the large particles will then reach the outlet more easily than smaller particles and values of t_o less than unity will result. This is observed experimentally.

For mixtures richer in the larger sized component, small particles landing on the slope at outlet should become "sinkers" and have less chance of reaching the outlet than the larger floaters. This mechanism also promotes values of t_o less than unity, but this is not supported experimentally. However Drahun suggests an alternative segregation mechanism which may operate when particles impact the sloping surface from a height of more than 100 particle diameters, as do many particles in beds spouted at high values of N_f. Particles

which are normally sinkers by virtue of size (mustard seeds) may become floaters; convection down the slope is then by bouncing. If this alternative mechanism is dominant, then values of t_o greater than unity will result. For beds of mixtures B and C this is observed and hence lends further support to the importance of free surface segregation as a mechanism controlling mean residence times.

6.4 The Fountain

Usually the spout is near the centre-line of a fully cylindrical spouted bed and thus direct observation of radial and vertical variations in behaviour is not possible. However, information can be obtained by building a half-bed with semicircular cross-section containing a half-cone and semicircular gas inlet. Particle motion then becomes visible if a transparent flat face is fitted to the column. Although exact numbers should be treated with caution, there is good reason to believe that behaviour is little affected. For example, Lefroy and Davidson (1969) showed the relationship between pressure drop and fluid flow rate to be very similar in full and half beds.

To observe particle motion in the fountain, a perspex half-bed of 140 mm i.d. and 1100 mm height was constructed and is shown in Figure 6.4a. The base cone was made of wood with a 60^{o} included angle and the gas inlet of copper pipe. The diameter of the gas inlet orifice was 10 mm and identical in section to that in the cylindrical bed used for the earlier experiments. Details are given in Figure 3.1g.

Cine film was taken of a region 140 mm wide and 230 mm high at the top of the bed which included the fountain and upper 50 mm of



Figure 6.4a : The 140 mm i.d. half-section bed

annulus. To enable individual particles to be traced from one frame to the next a film speed of at least 800 frames per second (fr s^{-1}) was necessary. The material spouted was a mixture of wheat and brown mustard seeds, but it was not possible to study all of the mixtures used in earlier work. A mixture with a high proportion of wheat seeds was chosen to permit easier viewing of the coarse particles against the flat face of the annulus. A small proportion of mustard and wheat seeds were sprayed with white paint to aid observation. The increase in particle weight was 5% for the brown mustard seeds and 2% for wheat seeds and was considered small enough to assume the observed behaviour of painted particles to be representative of bulk behaviour. A bed depth of 665 mm was chosen and partial, full and overdeveloped fountains were filmed. Film was also taken in a bed of depth 245 mm.

The film was examined using a Lafayette film analyzer and particle trajectories traced out for each run. These are given in Figures 6.4b, c and d; all trajectories which were traced out are shown in these Figures. However, of all the particles visible in the fountain only a small proportion have flight paths adjacent to the front face and it is these paths which must be traced if genuine particle trajectories are to be recorded. This was achieved by projecting the film in reversed slow motion and then only tracing the paths of those particles seen adjacent to the wall in the upward-moving annulus. For the bed conditions chosen, the fountain and upper part of the spout were found to wave across the front face with a period of about one and a half seconds. This is an effect reported by Madonna (1968) and McNab (1977 a) and was most pronounced for the overdeveloped fountain. For this fountain the flight time of a particle on the highest possible trajectory in the fountain was 0.35 s; this is less than a quarter of the time for one oscillation of the

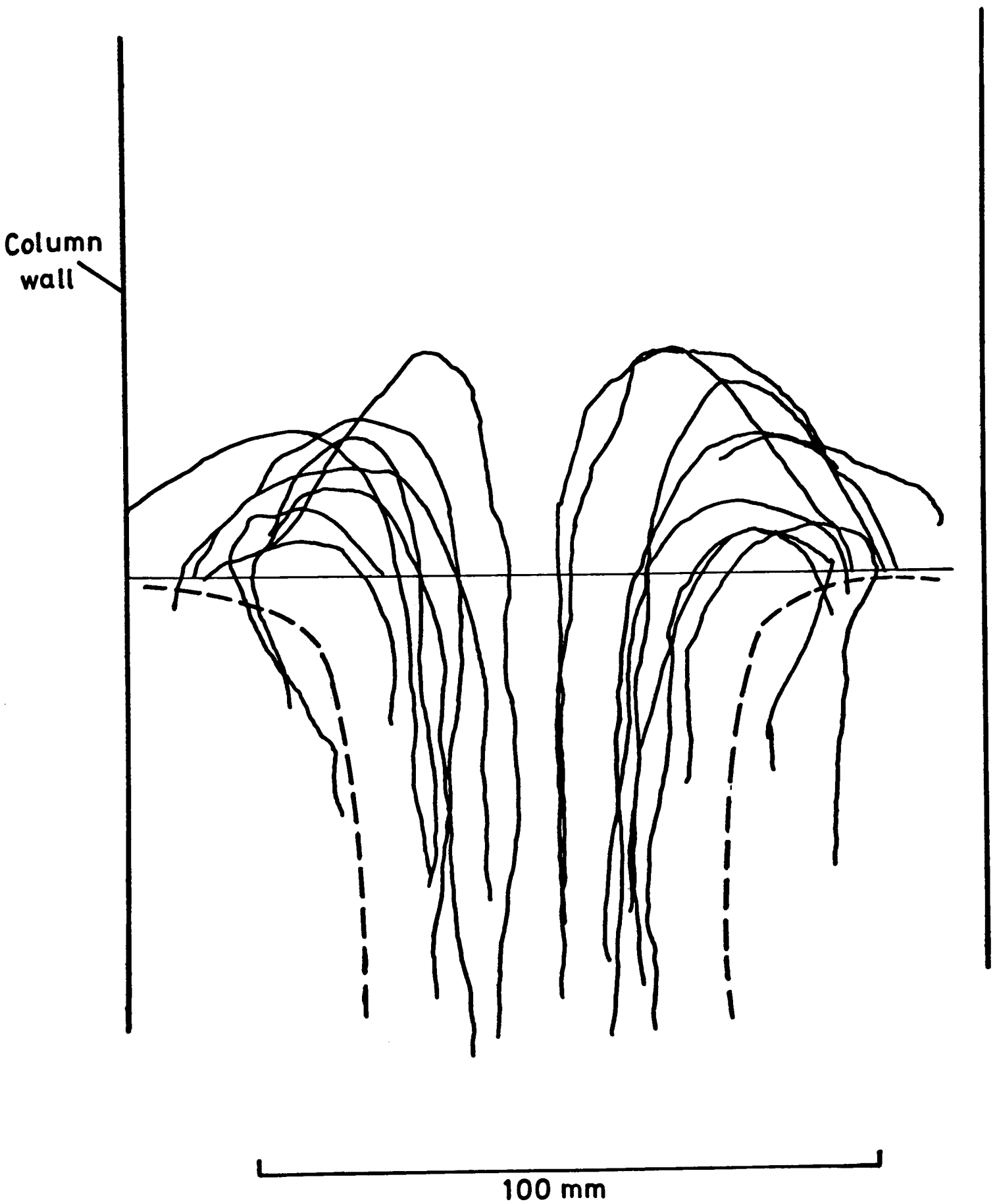


Figure 6.4 b (i) : Wheat trajectories in a partial fountain.

Wheat and brown mustard seed mixture (z_a = 0.9).

Experimental conditions in Table 6.4a : Run A.

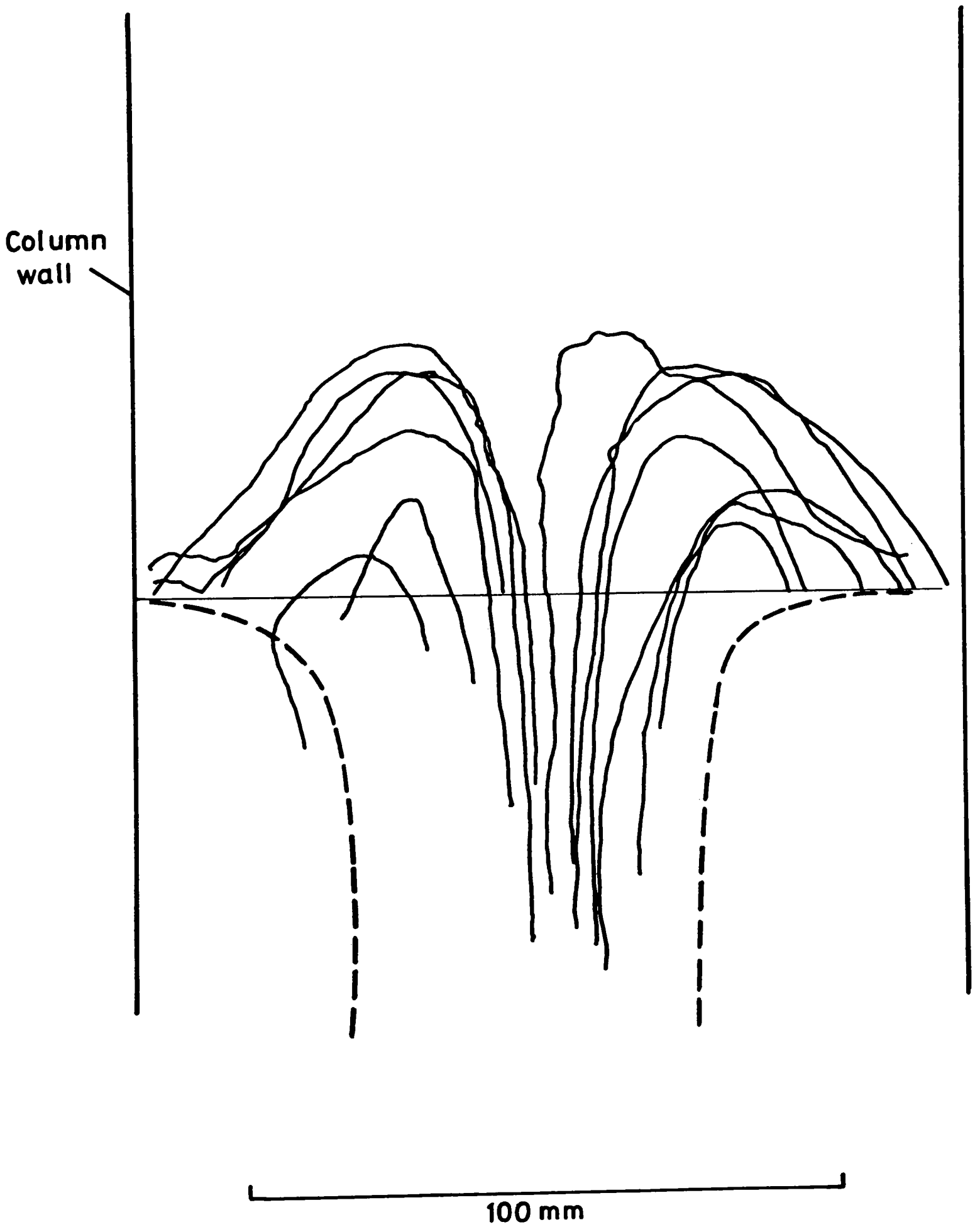


Figure 6.4 b (ii) : Brown mustard trajectories in a partial fountain

Wheat and brown mustard seed mixture (z_a = 0.9).
Experimental conditions in Table 6.4 a : Run A.

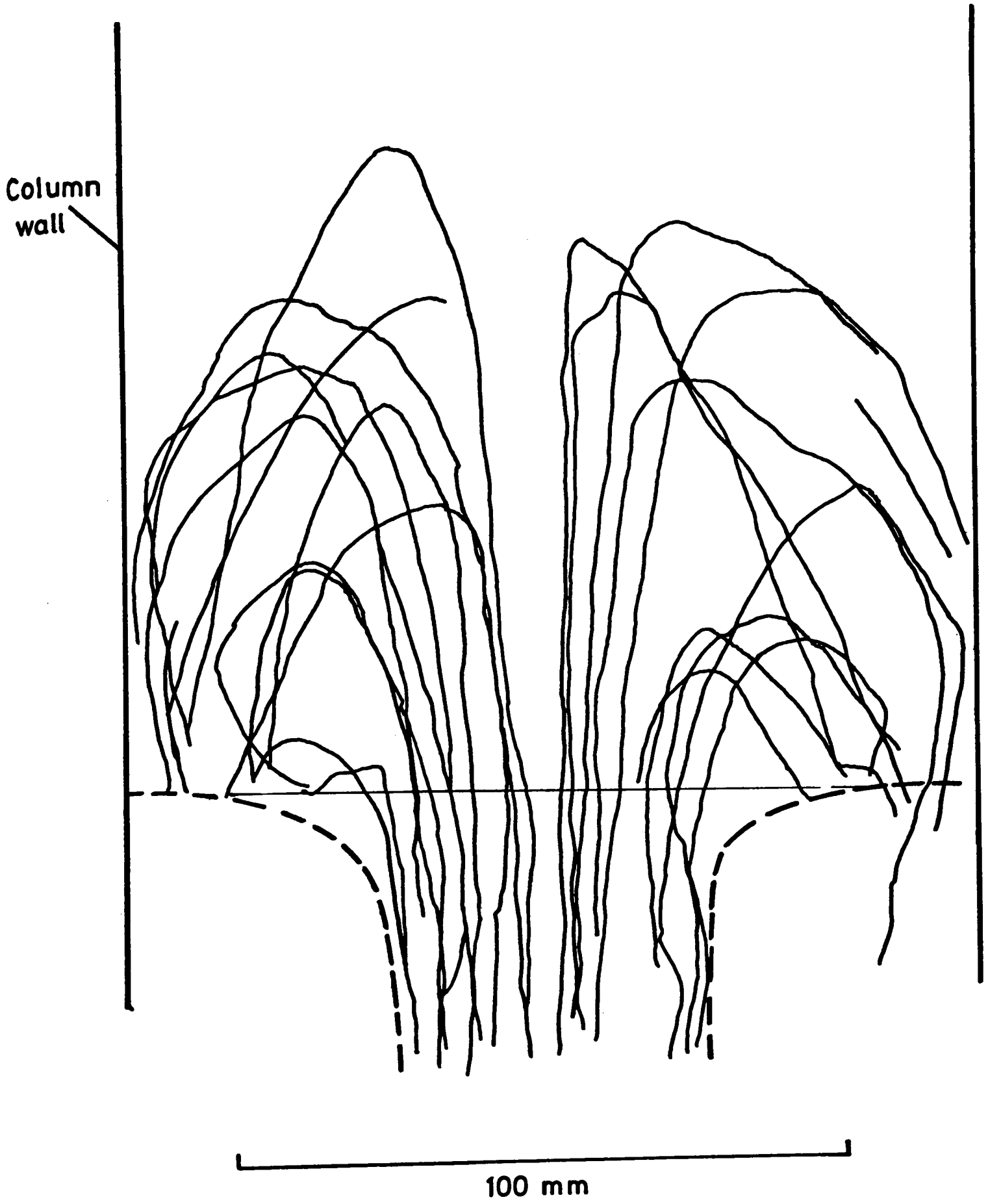


Figure 6.4 c (i) : Wheat trajectories in a full fountain

Wheat and brown mustard seed mixture (z_a = 0.9).

Experimental conditions in Table 6.4 a : Run B.

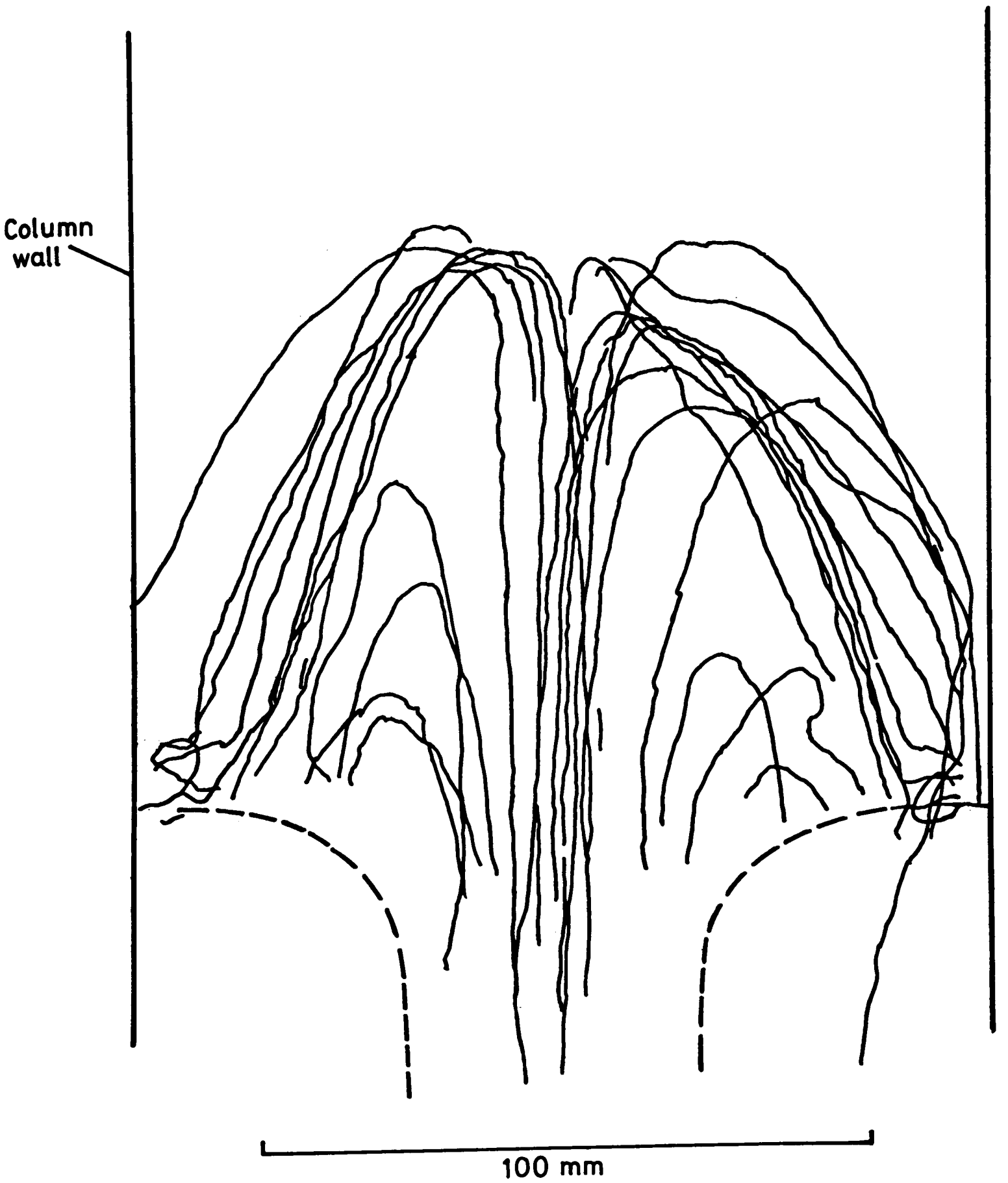


Figure 6.4 c (ii) : Brown mustard trajectories in a full fountain

Wheat and brown mustard seed mixture (z_a = 0.9).

Experimental conditions in Table 6.4 a : Run B.

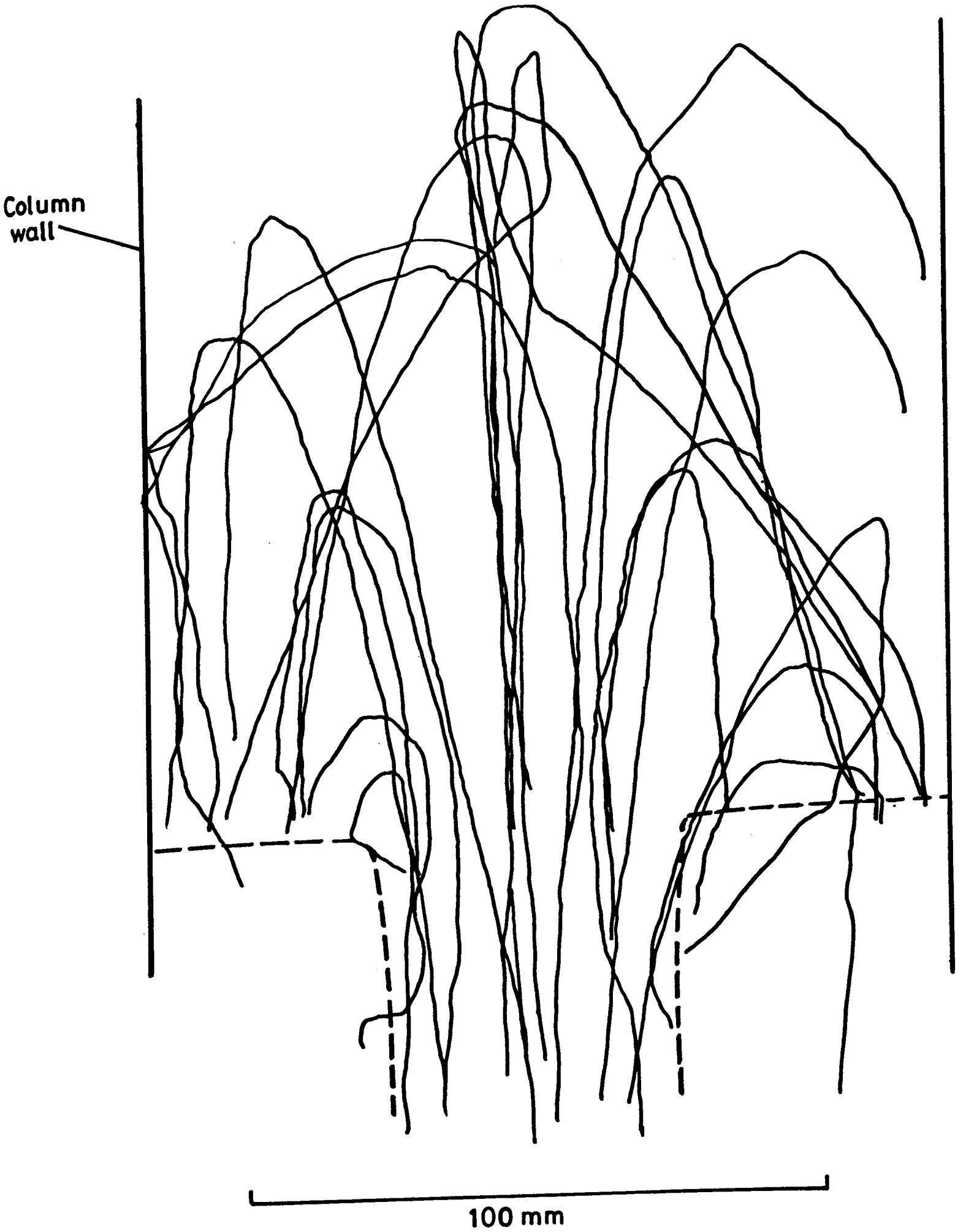


Figure 6.4d (i) : Wheat trajectories in an over-developed fountain.

Wheat and brown mustard seed mixture (z_a = 0.9).

Experimental conditions in Table 6.4a : Run C.

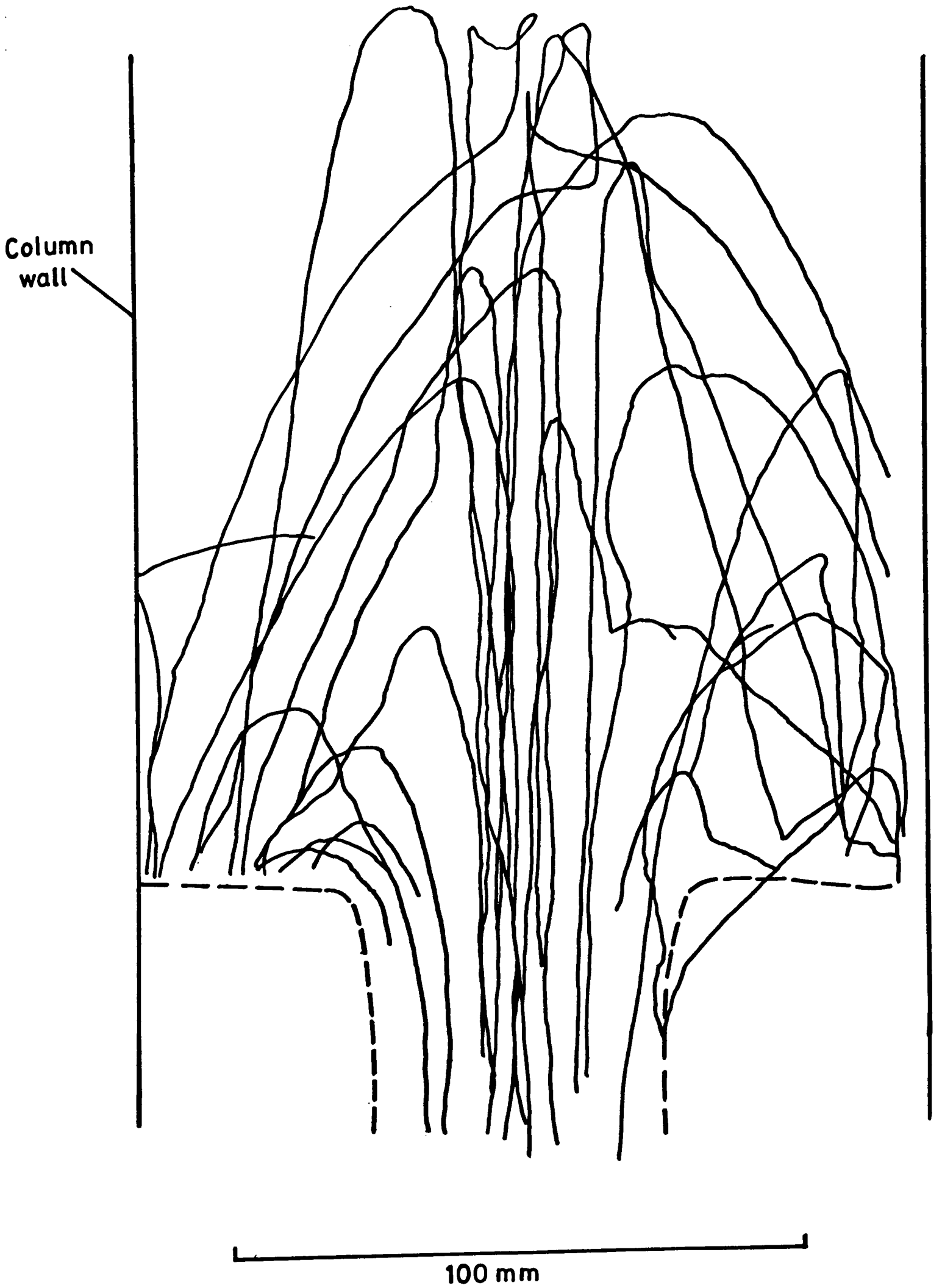


Figure 6.4 d (ii) : Brown mustard trajectories in an over-developed fountain.

Wheat and brown mustard seed mixture (z_a = 0.9)

Experimental conditions in Table 6.4 a : Run C.

fountain. While tracing a trajectory, errors may be introduced if the fountain changes position. Consideration of the above times shows this movement to be small, but to minimise any errors, particle trajectories were only traced when the spout and fountain were vertical. In Figures 6.4b, c and d, trajectories of brown mustard seeds appear predominant in the central core of the spout and fountain. This is not because a higher proportion of mustard seed is present, but is due to clearer visibility of seeds in this region.

Differences between the trajectories of wheat and mustard seeds are not immediately apparent. However, if the radial landing position of a particle r_l is plotted against its radial position in the spout at surface level r_t, a comparison is possible [McNab (1977 b)]. These results for the deep bed are shown in Figures 6.4e and f for the partial and full fountains respectively. The experimental conditions are given in Table 6.4a. Trajectories on the left side of the column are distinguished from those on the right since the centre of the spout was found to lie a few millimetres to the left of the centre of the column, as was also reported by McNab (1977 c).

There is a large scatter of data. This can in part be attributed to wavering of the fountain and spout for the full fountain. However, for the partial fountain (Figure 6.4e) little wavering occurred and scatter remains considerable. Consistent data can only be expected if time-averaged values of r_t and r_l are used since particle collisions will cause fluctuations in the absolute values. McNab's data shows little scatter (Figure 6.2a) but he does not describe the method used to measure each value of r_t and r_l and the accuracy of this data is therefore unknown.

A least squares fit to the data was computed; its parameters are given in Table 6.4b. The experimental conditions for all runs

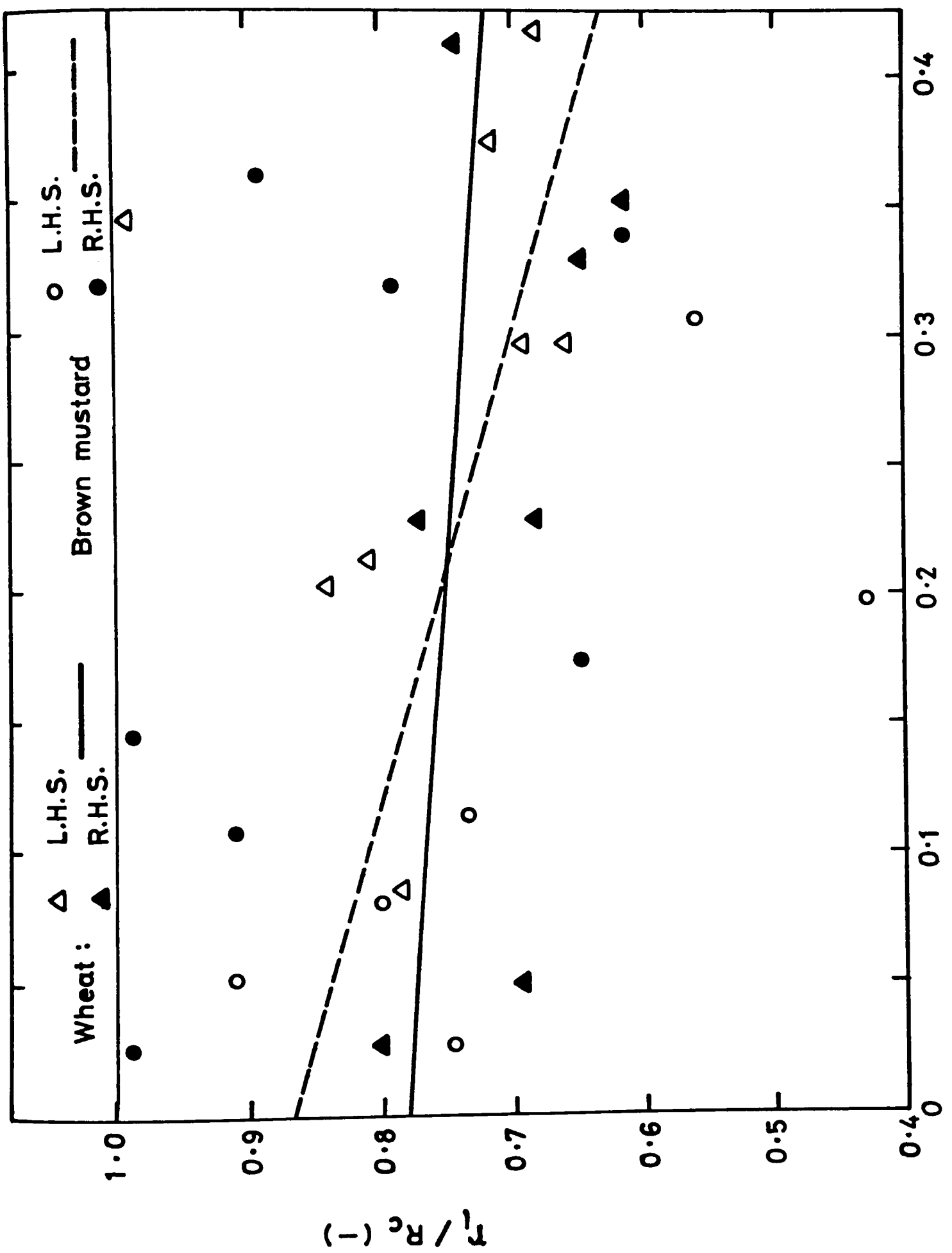


Figure 6.4 e : Radial position on landing, r_1/R_c vs. Radial position at top of spout, r_t/R_c

Partial fountain
Experimental conditions in Table 6.4 a : Run A.

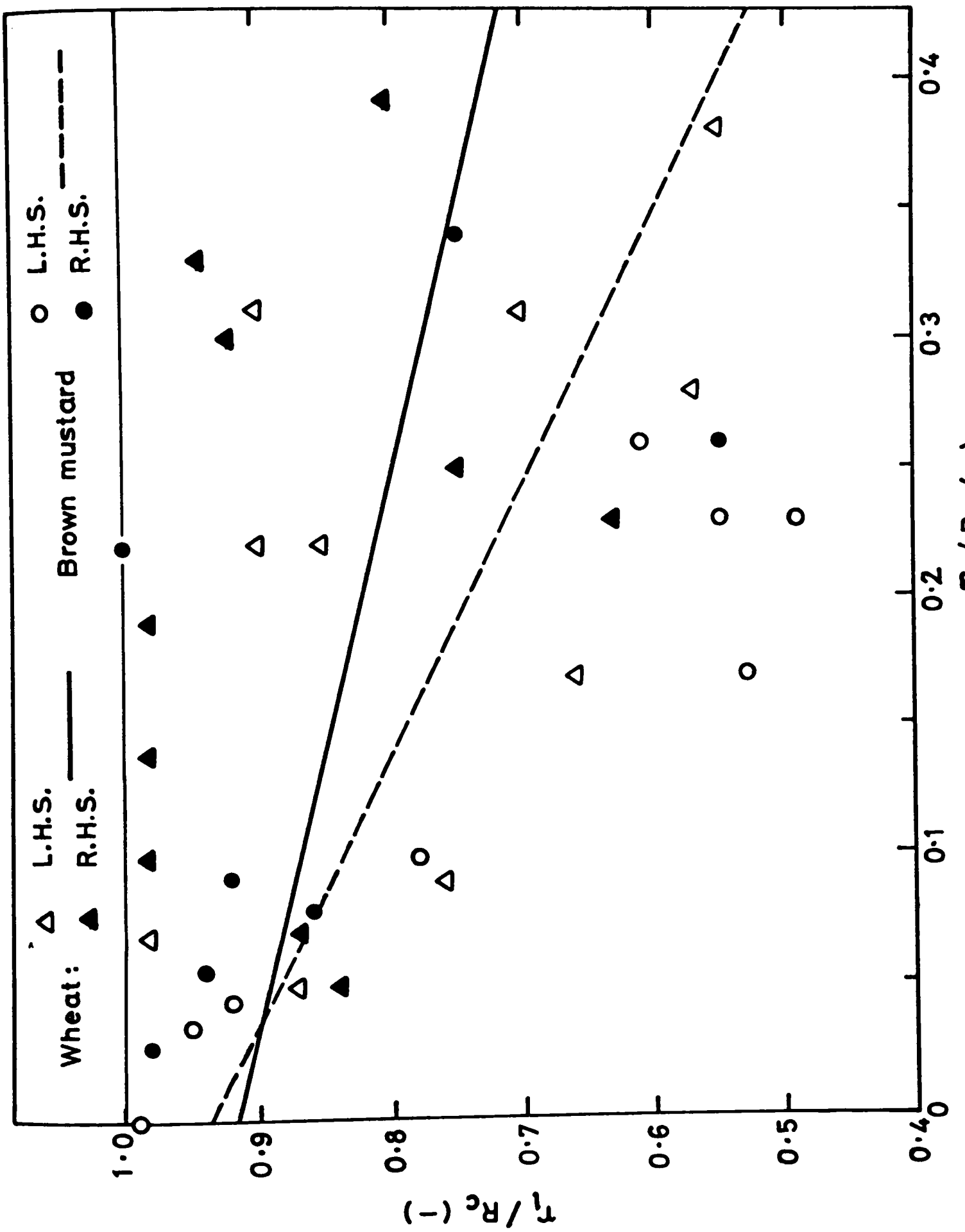


Figure 6.4 f : Radial position on landing r_1/R_c vs. Radial position at top of spout, r_t/R_c

Full fountain
Experimental conditions in Table 6.4 a : Run B.

Run	z_a (-)	H (mm)	m ($g\ s^{-1}$)	H_f (mm)	N_f (-)	Film Speed ($fr\ s^{-1}$)
A	0.9	665	0	40	0.47	800
B	0.9	665	0	85	1.00	800
C	0.9	665	0	130	1.53	800
D	0.9	245	0	80	0.84	1600
E	0.9	245	0	180	1.89	1600
F	0.9	245	0	260	2.74	2000

Table 6.4a Experimental conditions for runs where cine film of the spout, fountain and annulus was taken.

Run	Fountain Shape	Particle	a	s.e. (a)	b	s.e. (b)
A	P	W	0.78	0.06	-0.15	0.21
"	"	M	0.87	0.08	-0.55	0.39
B	F	W	0.92	0.05	-0.48	0.23
"	"	M	0.93	0.06	-0.94	0.29

Tabel 6.4b : Parameters for least squares curve fit to fountain data of the form : $r_l = a + b\, r_t$

Key : P - partial
F - full
O - over-developed
W - wheat
M - brown mustard

where high speed cine film was taken are given in Table 6.4a. For partial and full fountains, the gradient of the straight line fit is less for wheat than for mustard, indicating a tendency for wheat particles to migrate to the outer part of the fountain. The tendency cannot be declared significant, however, because of the large standard errors in the gradients of the straight line fits.

In overdeveloped fountains, the movement of brown mustard seeds is chaotic and collisions with the vessel wall and with other particles often occur. To a lesser extent, inter-particle collisions occur in partial and full fountains. Collisions between mustard seeds and wheat particles can result in large changes in speed and direction of the mustard seed; the resulting disturbance to the trajectories of wheat particles is usually slight. Often, mustard seeds make more than one collision during their flight in the fountain. Some examples of inter-particle collisions are shown in Figure 6.4g. The proportion of particles undergoing such collisions can not be evaluated from the film, however, and doubt is cast on the usefulness of trajectory theory to predict particle movement in the fountain, especially when it is overdeveloped.

Some brown mustard seeds were seen to bounce on impact with the free surface. The direction of movement after impact was always outwards, either through the air or along the bed surface. Some such particle paths were traced out and can be seen in Figures 6.4b(ii), c(ii) and d(ii). The extent of this outward migration is not evaluated, but may result in a higher concentration of mustard seeds in the outer upper annulus.

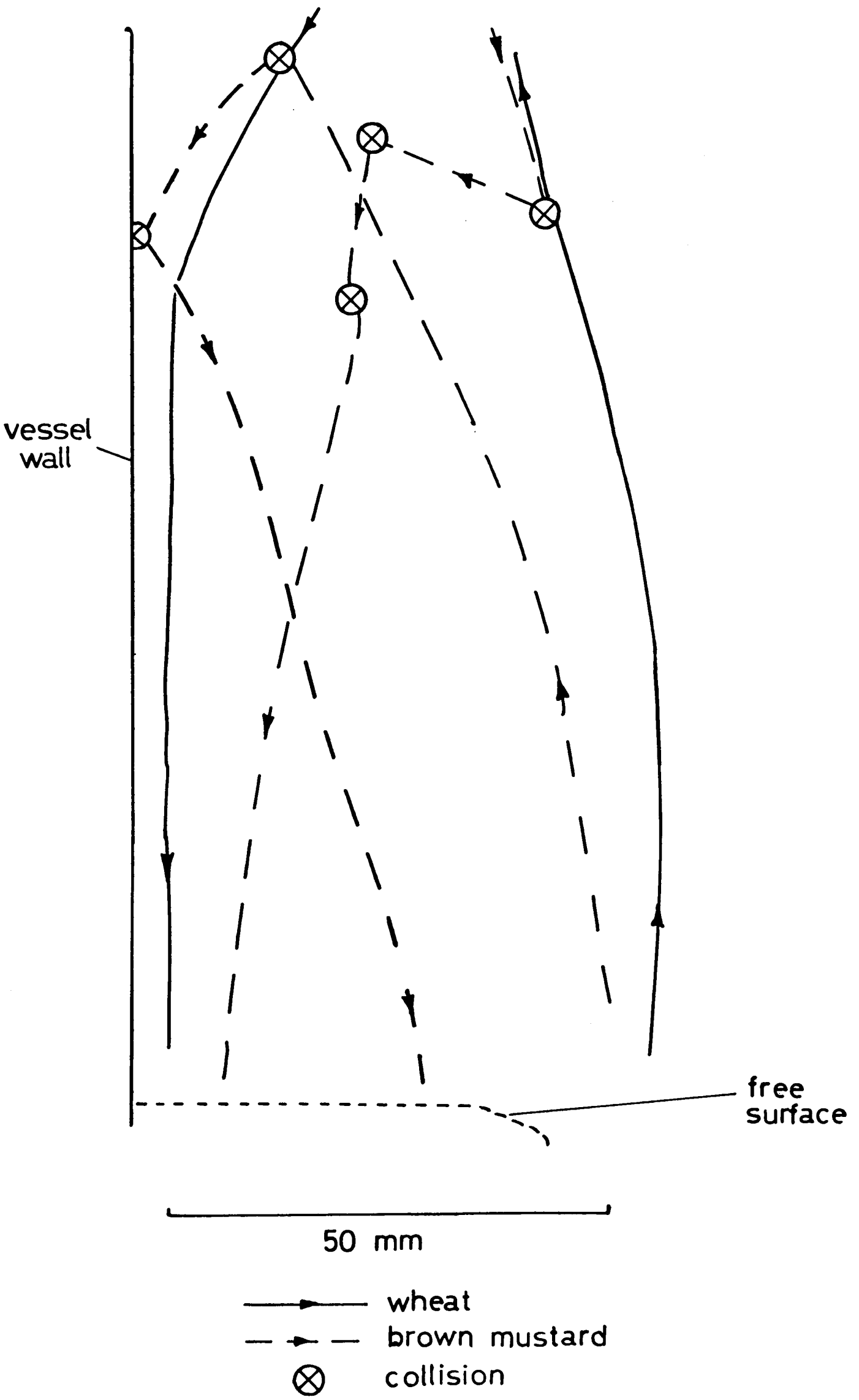


Figure 6.4 g (i) : Inter-particle collisions in an over-developed fountain.

Left side of fountain
Experimental conditions in Table 6.4 a : Run C

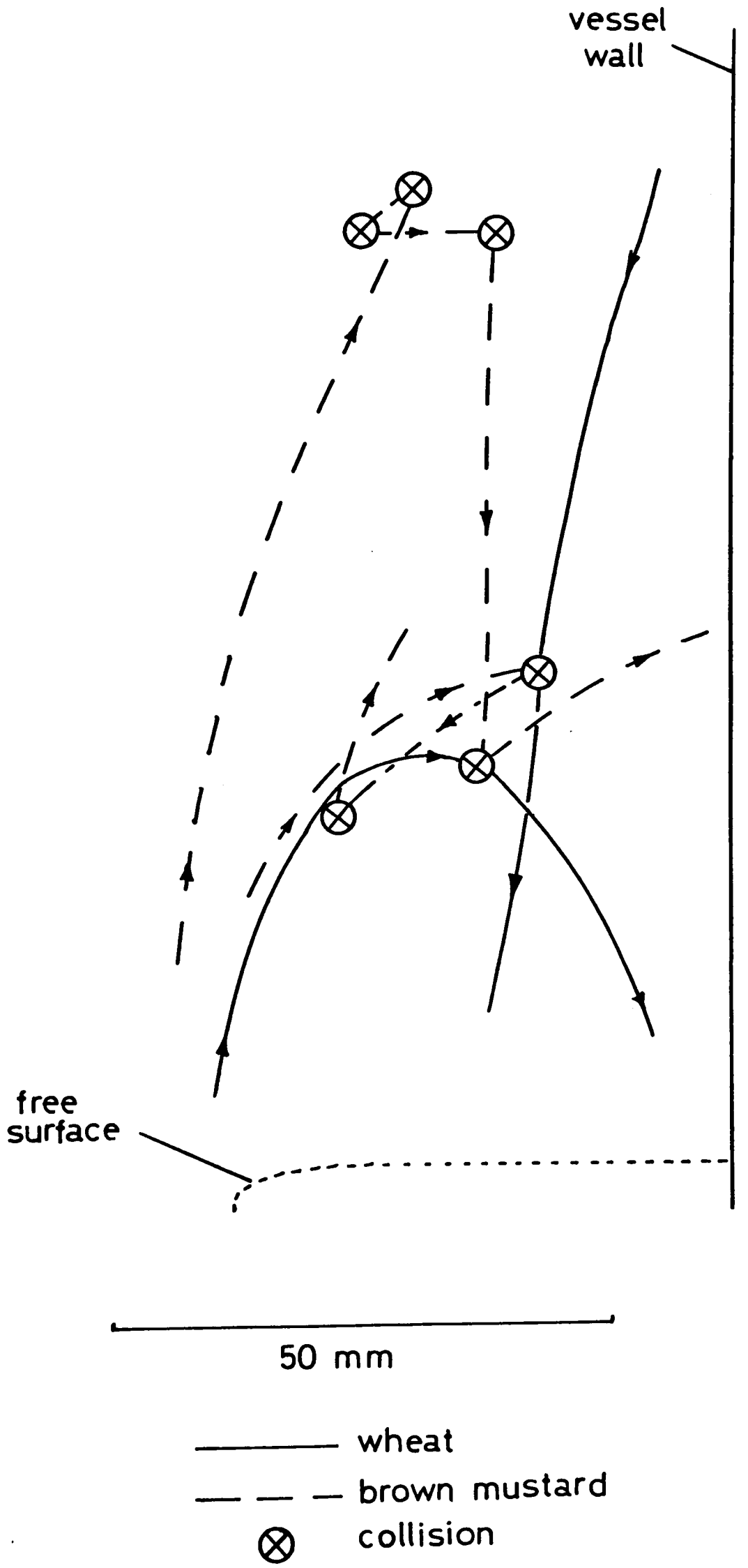


Figure 6.4 g (ii) : Inter-particle collisions in an over-developed fountain.

Right side of fountain
Experimental conditions in Table 6.4 a : Run C

6.5 The Spout

Film was taken at speeds between 800 and 2000 fr s^{-1} of the fountain and upper parts of the annulus and spout in the half-bed. This was used to estimate the radial mean spout voidage and to measure the vertical component of particle velocity in the spout.

To measure particle velocities, a grid was laid over the projection as shown in Figure 6.5a. The grid was positioned at a depth d from the free surface since the spout diverged above this depth. Values of d and spout radius r_s for each run are given in Table 6.5a. The film was projected in reverse at 2 x magnification using the Lafayette analyzer. For a particle passing through a point A, B ... F, the subsequent number of film frames n_f taken to reach the horizontal plane XX was counted. The vertical component of particle velocity, v_s is given by:

$$v_s = 0.025 \times \frac{800}{n_f} \quad ms^{-1} \qquad (6.5)$$

for a film speed of 800 fr s^{-1}. Where the particles were distinguishable, the velocities of each component were measured but only where the spout, if wavering, was in a vertical position. Radial components of particle velocity were too small to be measured accurately by this method. In some experiments, the average position of the spout centre was found to be a few millimetres to the left of the column centre probably because of slight asymmetry in the geometry of the gas inlet or column. As a result, point F in the grid was at the edge of the spout and measurement of particle velocities at this position was not possible for these runs.

Figure 6.5b shows the radial profile of particle velocity for run B, a full fountain in a bed of depth 665 mm. Limits of 95% confidence are shown. Figure 6.5c shows the profiles for run A, a partial fountain and run C, an overdeveloped fountain in the

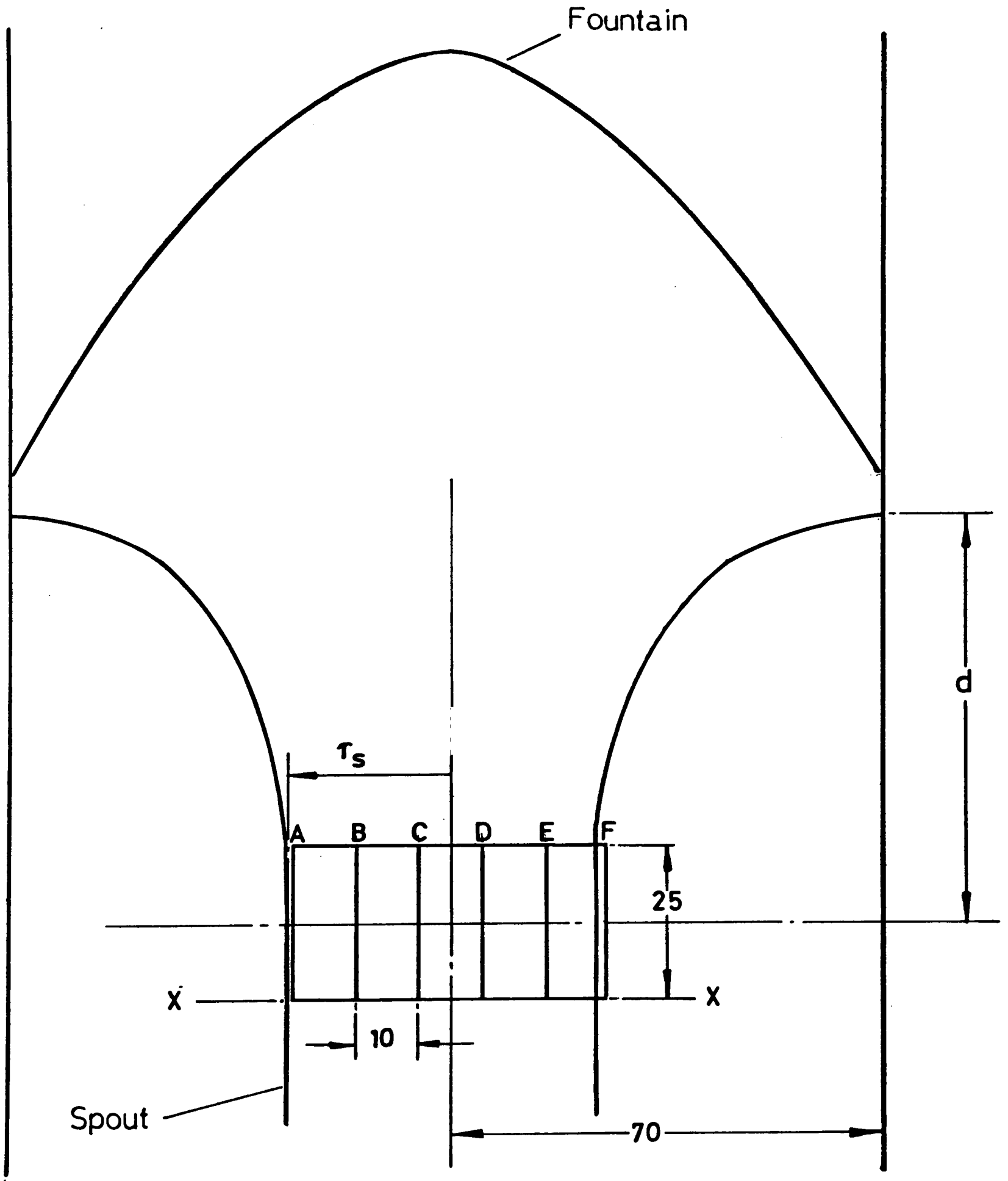


Figure 6.5 a : Grid used for measurement of particle velocities in the spout.

All dimensions in mm
Values of r_s and d given in Table 6.5 a for all runs.

Run	d (mm)	r_s (mm)
A	60	30
B	20	25
C	25	25
D	40	18
E	37	19
F	40	19

Table 6.5a : Depth d of the centre of the measuring grid below the free surface and radius of the spout at this level r_s.

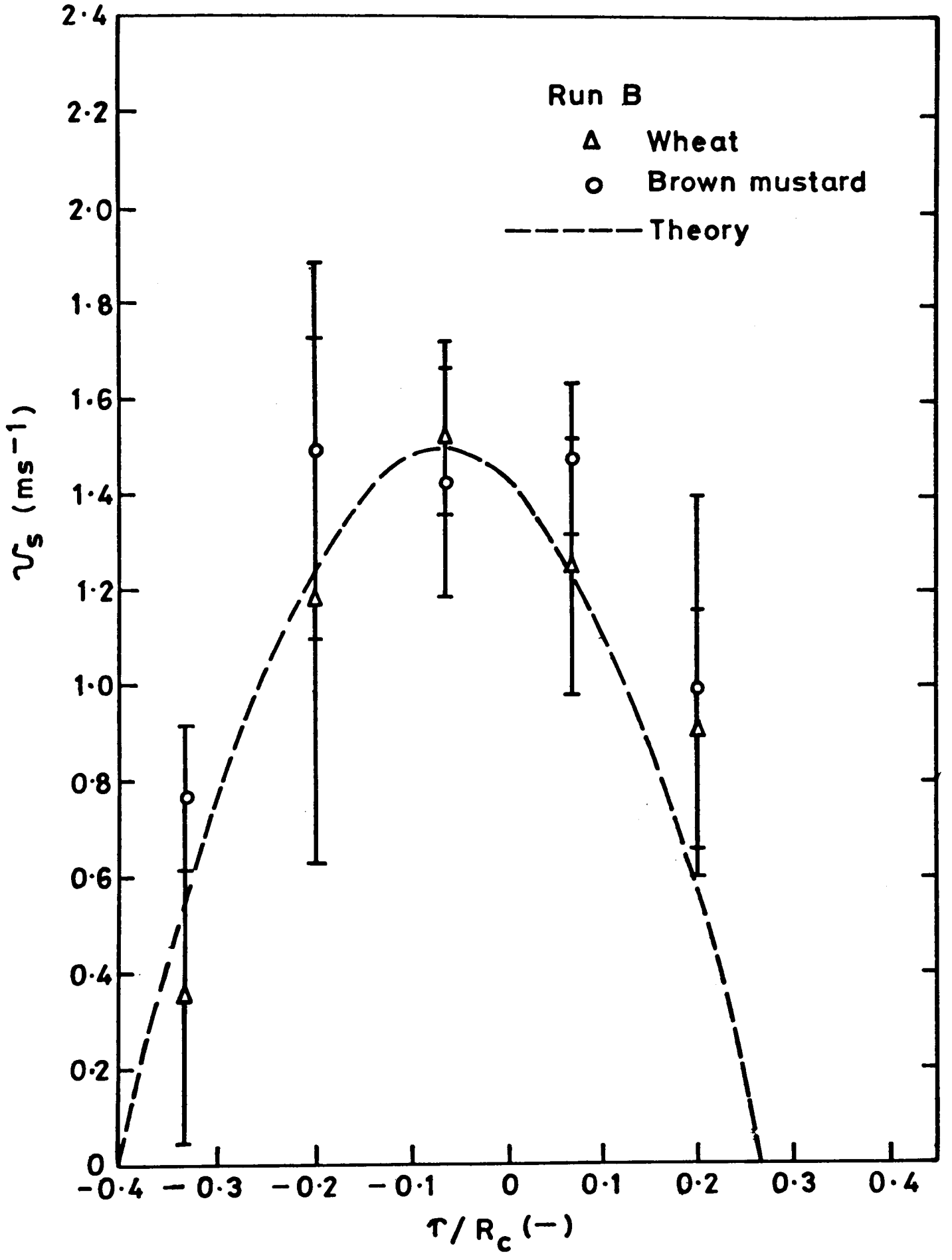


Figure 6.5 b : Vertical component of particle velocity in the spout, v_s vs. Radial position in the spout r/R_c.

Full fountain
Limits of 95% confidence are shown.

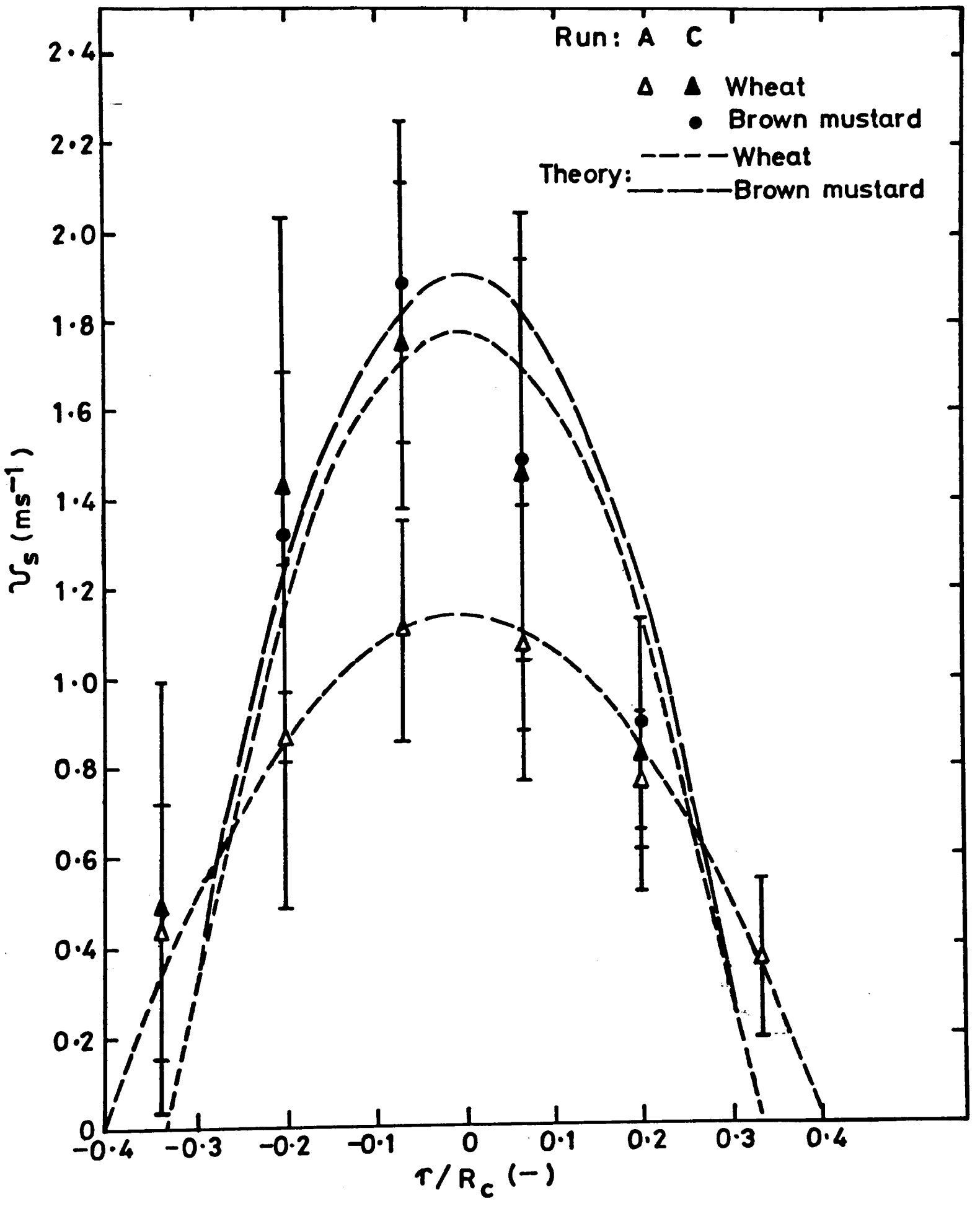


Figure 6.5 c : Vertical component of particle velocity in the spout, v_s vs. Radial position in the spout r/R_c.

Partial fountain : Run A.
Over-developed fountain : Run C.
Limits of 95% confidence are shown.

bed. For run A, mustard particles were not distinguishable by eye from wheat seeds and velocities of wheat particles only are shown. Using equations (5.1) and (5.2), a t-test was performed at each radial position to assess the significance of the difference between velocities of mustard and wheat seeds. The results are shown in Table 6.5b, where t is calculated from equation (5.1) and t_p is the t value at 95% probability, obtained from mathematical tables. At each radial position, the difference in velocities is significant at the 95% level of confidence if t is greater than t_p. Velocities of wheat particles are significantly lower than those of mustard seed at three out of five positions in run B and at two out of five positions in run C; they are never significantly greater.

Also shown on Figures 6.5b and c are theoretical, parabolic velocity profiles. These were calculated according to equation (6.4) with n = 2 and using experimental points to estimate $v_{s_{max}}$, the vertical particle velocity at the column axis. The spout radius r_s was measured from the film and values are given in Table 6.5a. The best fit to the experimental data is found for run A, the partial fountain. The fit is less good for runs B and C, where greater errors in velocity measurements can be expected due to the wavering spout. Mathur and Epstein (1974) found a parabolic profile gave the best fit to experimental data from several independent sources. However, Lim and Mathur (1978) obtained better fits with values of n between 1.3 and 2.2, so the fit to data of runs A and C may also be improved by appropriate adjustment of the index n.

Wheat and mustard seed particle velocities were also measured in the annulus. Film from each run was projected onto a grid and the number of frames for particles to travel between two horizontal

Run	r	Wheat			Brown Mustard			t	t_p
	(mm)	$\bar{v}_s$ (mms^{-1})	σ (mms^{-1})	n (-)	$\bar{v}_s$ (mms^{-1})	σ (mms^{-1})	n (-)		
B	-25	0.35	0.18	3	0.77	0.08	4	3.22	2.57
"	-15	1.18	0.27	16	1.49	0.20	10	3.13	2.06
"	-5	1.52	0.09	10	1.43	0.12	11	1.92	2.09
"	5	1.25	0.14	8	1.48	0.08	8	4.04	2.14
"	15	0.91	0.13	7	1.0	0.2	9	2.04	2.14
C	-15	1.43	0.30	6	1.33	0.18	7	0.74	2.20
"	-5	1.75	0.18	9	1.89	0.18	7	2.65	2.14
"	5	1.46	0.29	14	1.49	0.23	7	0.24	2.09
"	15	0.83	0.16	6	0.45	0.12	7	2.39	2.20

Table 6.5b Measured particle velocities in the spout

lines 10 mm apart was counted. The grid was centred at the same depth as that used for measuring particle velocities in the spout and velocities were measured at eight radial positions, A - H in Figure 6.5d. At each position, a downward moving particle will also move inwards because of entrainment of particles by the spout. Velocities measured in the annulus by this method are thus the vertical components of the particle velocities. The radial average spout voidage can be estimated from a solids flow rate balance across a horizontal plane YY in the bed. For this, the annulus was divided into four zones as defined in Figure 6.5e. As an example, the vertical volumetric flow rate of the solids and voids in zone II is given by:

$$Q_{II} = \frac{\pi}{2} (r_2^2 - r_1^2) \; v_{a_{II}} \qquad (6.6)$$

where $v_{a_{II}}$ is the average vertical velocity of solids in this zone. This velocity is taken to be the average of the two velocities in this zone measured at the flat face. However, Q may be in error for several reasons:

(i) if the centre of the spout does not coincide with the centre of the column, the average of velocities measured at points D and E will not be a good estimate of the average velocity in zone I,

(ii) as the solids are moving radially inwards across the horizontal plane YY (Figure 6.5d), the measured velocity of a particle which crosses say, point C, is really an average velocity over the radial distance Δr and not an exact value for point C and

(iii) particle velocities measured at the flat face may not be equal to particle velocities at the same radius elsewhere in the annulus, due to wall effects.

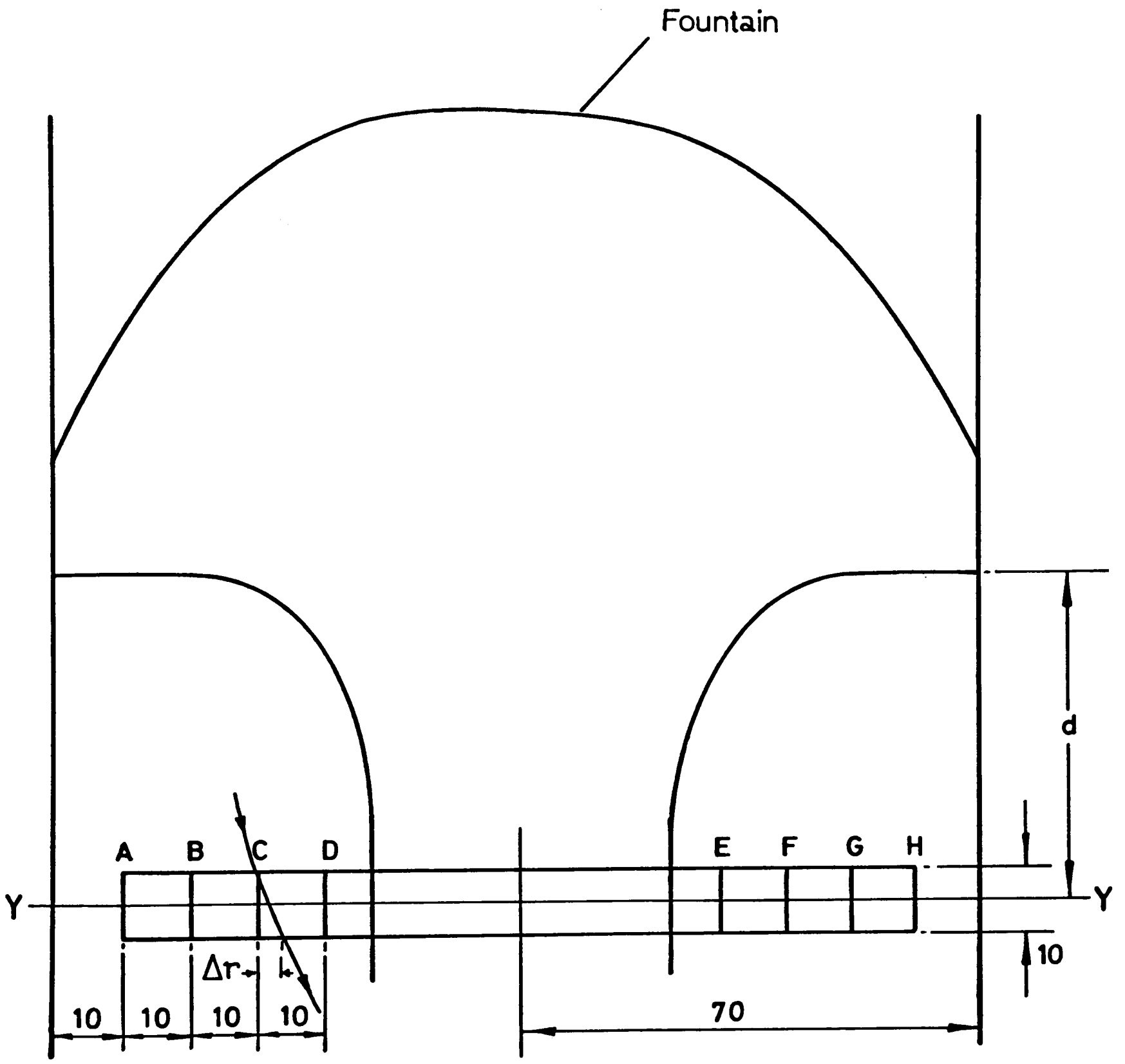


Figure 6.5 d : Grid used for measurement of particle velocities in the annulus.

All dimensions in mm
Values of d given in Table 6.5 a for all runs.

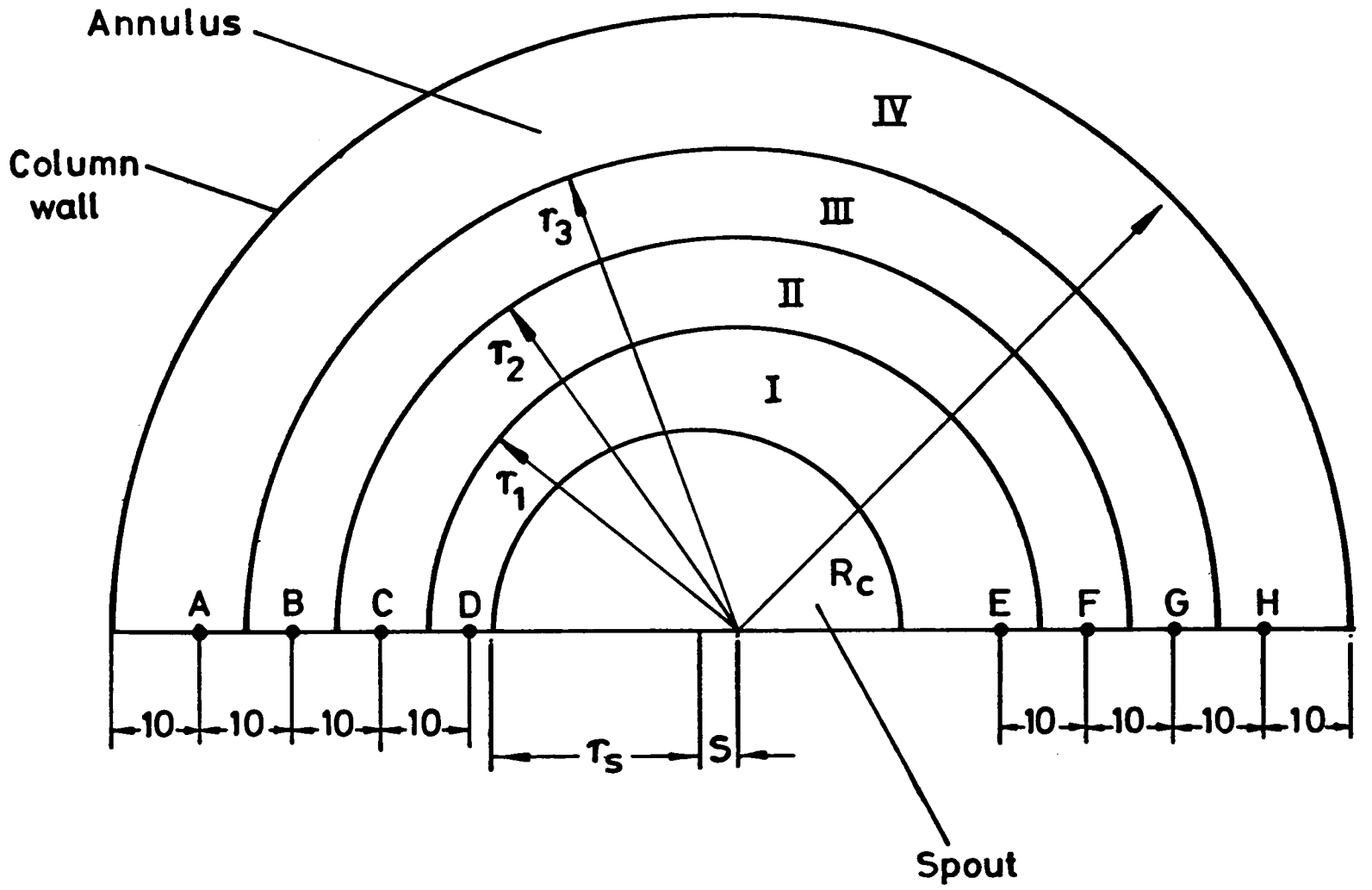


Figure 6.5 e : Zones I to IV for calculation of solids flow rate in the annulus.

All dimensions in mm.

r_1 = 35 mm
r_2 = 45 mm
r_3 = 55 mm
R_c = 70 mm

r_s = spout radius - values given in Table 6.5 c.

s = offset of spout centre from column centre

If equation (6.6) is taken as correct, then the mass flow rate of solids is given by:

$$W_{II} = \frac{\pi}{2} (r_2^2 - r_1^2) v_{a_{II}} \rho_b \qquad (6.7)$$

where ρ_b is the average bulk density of solids in zone II. The summation of the mass flow rate of solids in each zone yields the total solids flow rate in the annulus across the section YY. This total mass flow rate must equal that of solids in the spout at the same level and thus yields the radial average spout voidage. Details of this calculation are given in Appendix E and the cal lated spout void fractions and solids flow rates are given in Table 6.5c.

At a bed depth of 665 mm the radial average spout voidage lies between 0.59 and 0.69, depending on the value of N_f. These values are 7-20% lower than those calculated by Mathur and Gishler (1955) for a bed of the same diameter and a depth of 640 mm. They used wheat seeds as the spouting material and calculated the spout voidage by a mass balance of solid flow rates in the spout and annulus, although they do not give details of the calculation; the bulk density or void faction of material in the annulus is required for the calculation and they may have selected a different value to that used in the present study. This would account for the difference in calculated void fractions.

At a bed depth of 245 mm, the spout void fraction increases from 0.75 for the partial fountain to 0.84 for an overdeveloped fountain. Again, these values are lower than those obtained by Mathur and Gishler, by up to 25%.

Since Mathur and Gishler used a bed filled entirely with wheat and in the present study a mixture of wheat and brown mustard was used, a true comparison of results is not possible. The lower

$^{-1}$)	$v_{a_{II}}$ (mm s^{-1})	$v_{a_{III}}$ (mm s^{-1})	$v_{a_{IV}}$ (mm s^{-1})	W_a (kg s^{-1})	d (mm)	r_s (mm)	$v_{s_{max}}$ (m s^{-1})	ρ_s (kg m^{-3})	ϵ_s (-)
	79	77	71	0.71	60	30	1.13	1400	0.68
	95	75	87	0.84	20	25	1.50	1400	0.59
	94	89	68	0.75	25	25	1.77	1400	0.69
	28	28	27	0.28	40	18	1.60	1400	0.75
	32	32	33	0.34	37	19	2.41	1400	0.82
	39	35	35	0.38	40	19	3.03	1400	0.84

Measured velocities in the annulus and calculated average spout voidages.
Other experimental conditions for these runs are given in Table 6.4a.

voidages measured here may be a result of the presence of mustard seeds in small quantities but, without further investigations, the reasons for this difference cannot be confirmed.

6.6 Submerged Outlet

If in a continuously operated spouted bed the solids mass flow rate m is sufficiently great, the outlet orifice will become submerged. For a few operating conditions, this mode of operation was reported in Chapter 4, section 4.6 where a bed of mixture C (weak in brown mustard) was studied; as m was increased to a value where the outlet was submerged by a constant 40 mm, the mean residence time ratio t_o also increased. An explanation for this behaviour was sought and an experimental investigation is reported here.

In a bed with a submerged outlet, a failure zone is present in the annulus adjacent to the outlet where particles leaving the bed separate from those remaining, as shown in Figure 6.6a. In this zone of undetermined extent, element A say, undergoes shear strain as it moves towards the outlet. If the particles in element A are distributed in size, inter-particle percolation may occur. This process is defined [Scott and Bridgwater (1975)] as the drainage of one component, usually the smaller one, through another in highly strained failure zones. It has been studied, in the absence of any gas flow, by Bridgwater, Cooke and Scott (see Chapter 2). In the failure zone near the submerged outlet of a spouted bed, this process would promote longer residence times for smaller components of a mixture since these would drain out of the failure zone and remain in the bed longer. However, the reverse effect, an increase in t_o, was observed experimentally and could be a result of percolation due to gas flow occurring in this zone. The pressure of interstitial gas, being greater than atmospheric pressure, gives

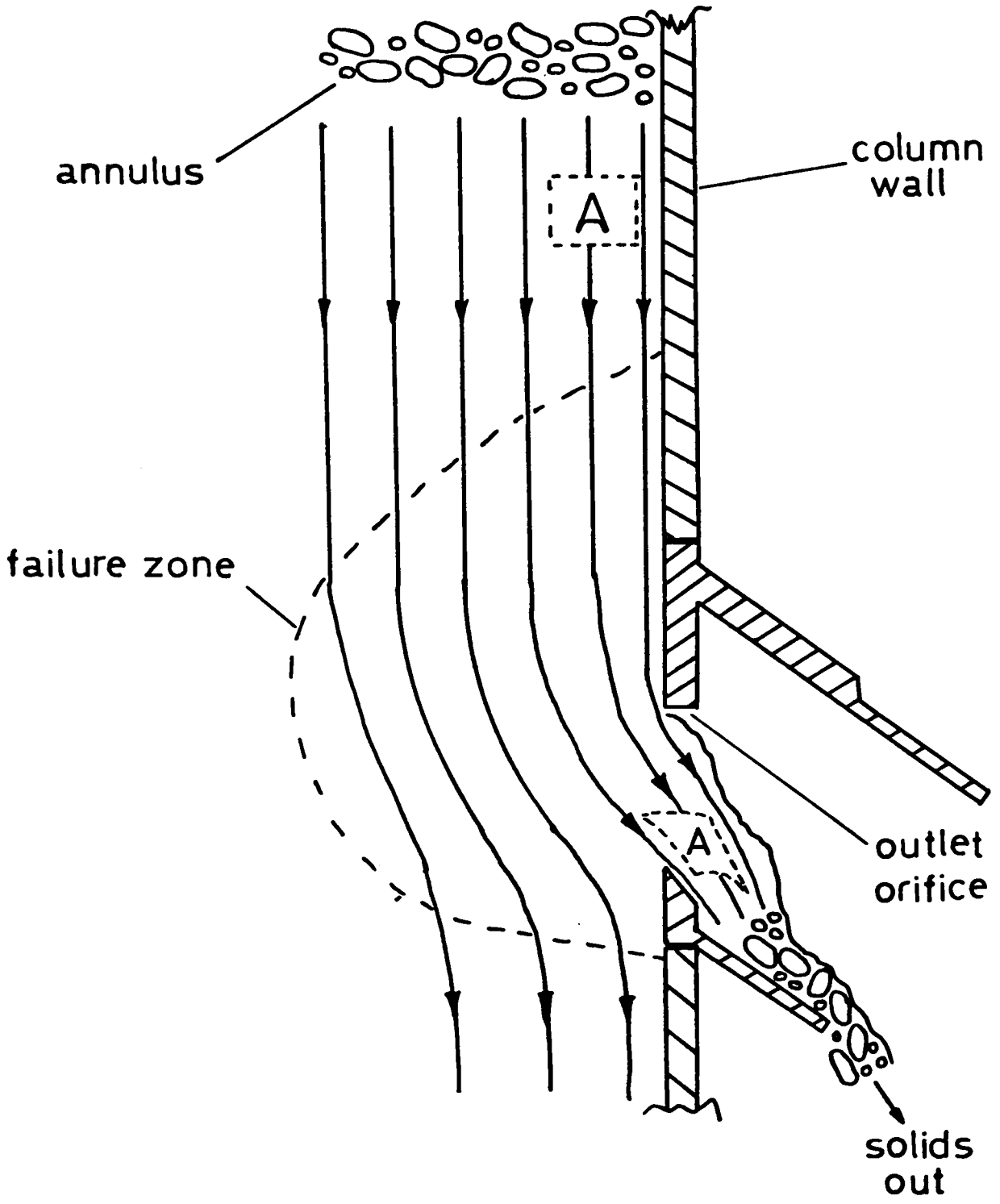


Figure 6.6 a : Flow pattern of solids in the region of a submerged outlet.

rise to a radial pressure gradient towards the orifice and the smaller size fractions in a mixture, preferentially influenced by the resulting gas flow, could then move towards the outlet by percolation. Segregation by this mechanism could cause an increase in t_o.

Mixture C, lean in brown mustard seed, was used in an experimental study. A perspex column of 80 mm i.d. and 2 m in length was suspended vertically and fitted with an outlet hole of 26 mm diameter, as in Figure 6.6b. A base plate was attached, (Figure 6.6c) having four holes of diameters 18.5, 19, 20 and 24 mm to allow release of solids at different rates. The column was filled by pouring material into the open top through a static mixer. The mixer was constructed from five mesh grids of hole size 9 x 9 mm, layered horizontally, 50 mm apart in a cylinder of 80 mm i.d. as shown in Figure 6.6d. This type of mixer has been shown [Cooke and Bridgwater (1977)] to give an even distribution of material over its outlet area. The experimental procedure was as follows. Using the static mixer the column was completely filled with material of mixture C ($z_a = 0.90$). A plug at the side outlet and selected plugs in the base plate were then removed simultaneously; material was collected from both outlets until the free surface level was within 50 mm of the side outlet when both outlets were resealed. Collected material was sieved and the components weighed to yield values of solids mass flow rates at the side outlet W_s, solids mass flow rate in the column above the outlet W_c and the mass proportion of wheat in each stream, y_s and x_c. A segregation factor s_o, defined by

$$s_o = \frac{x_c - y_s}{1 - x_c} \qquad (6.8)$$

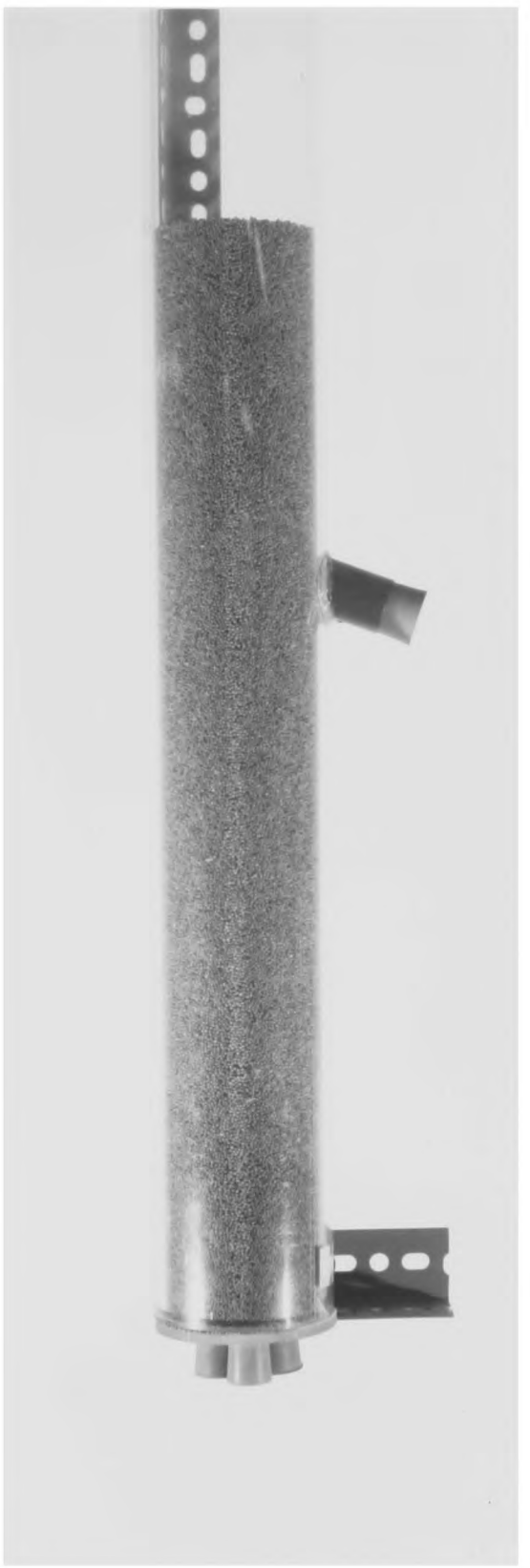


Figure 6.6b : The 80 mm i.d. column used for the investigation of segregation at a submerged outlet

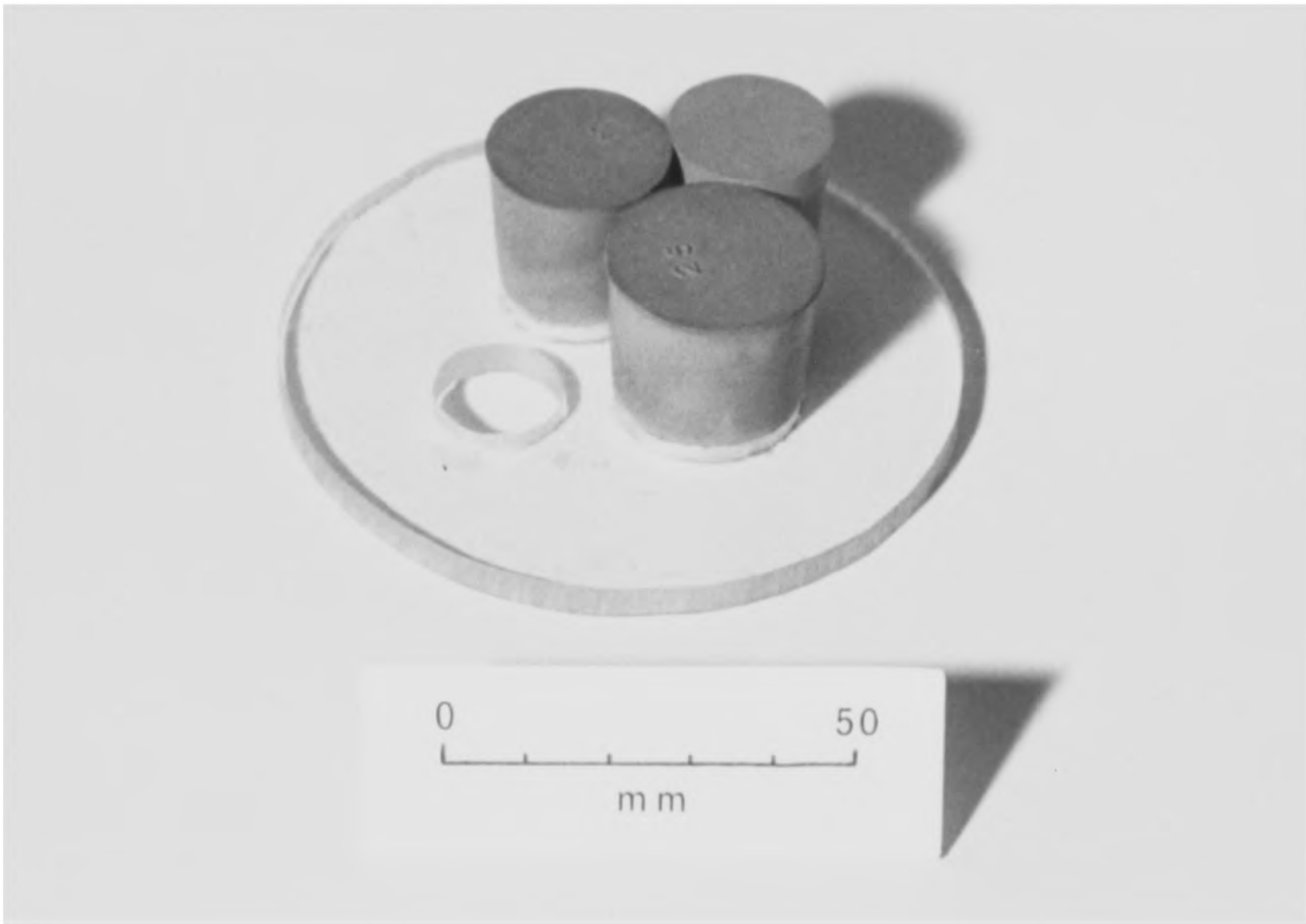


Figure 6.6c : Base plate for the column in Figure 6.6b

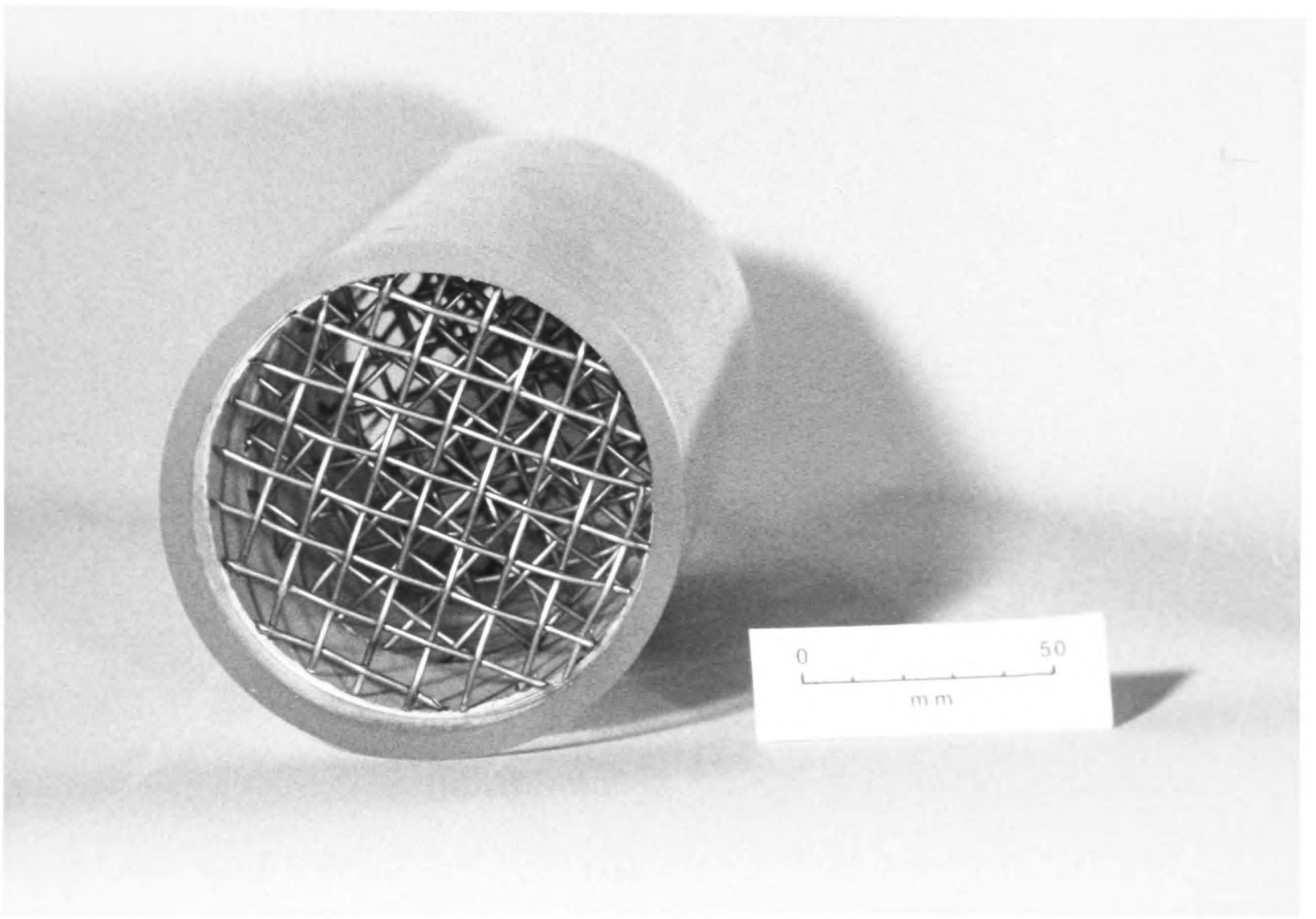


Figure 6.6d : The static mixer

was calculated for each run. s_o is the fractional increase in the proportion of brown mustard leaving the side outlet; a negative value of s_o indicates a lower mass fraction of brown mustard at the side outlet than in the column. For a wide range of solids flow rates, s_o is plotted in Figure 6.6e against a discharge ratio, D where

$$D = \frac{W_s}{W_c} \tag{6.9}$$

When the base plate is sealed, and material only allowed to flow out of the side outlet, D = 1.0. As larger holes in the base plate are successively opened, W_c increases and D approaches zero. It was not possible to perform any runs with D in the range 0.62 to 0.99 since this would require a hole diameter less than 18.5 mm in the base plate; such a hole was used but continuous solids flow was not then possible. All runs are detailed in Table 6.6a.

At a discharge ratio of 1.0, the reduction in the proportion of mustard seed at outlet is 1½%, probably largely due to percolation of mustard seeds into the stagnant region of the column below the outlet.

At a discharge ratio of 0.62, the reduction in the proportion of mustard seed at the side outlet is 25%, which decreases to about 10% as D is reduced to 0.15. This shortage is also likely to be due to percolation of material through the active zone, the extent of which decreases as D is reduced.

As D is reduced further, from 0.13 to 0.03, the outlet mixture changes from one weaker in mustard than the material in the upper column, to a mixture richer in mustard seed by up to 30%. At low

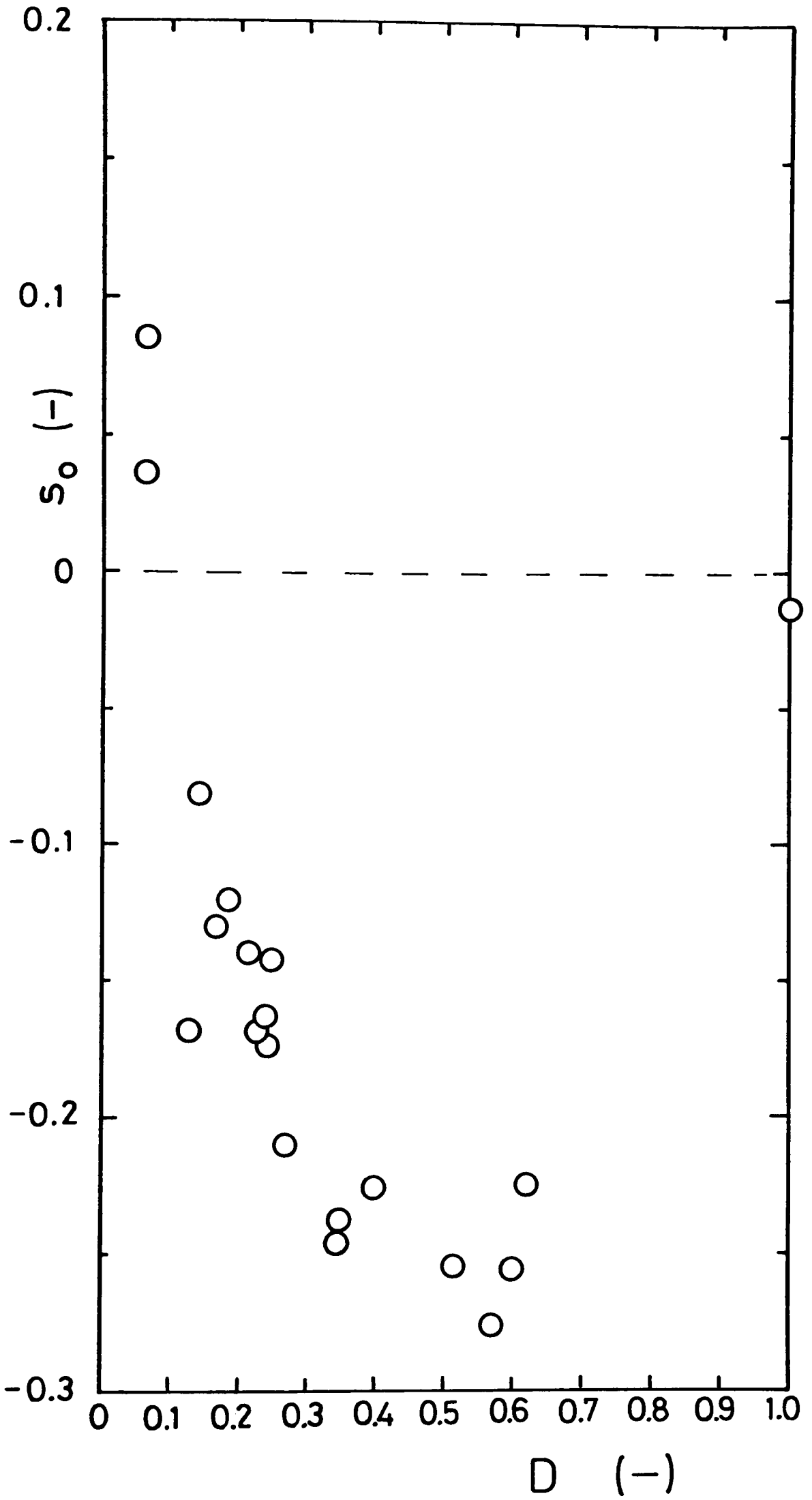


Figure 6.6 e : Segregation factor at a submerged outlet, s_o vs. Discharge ratio, D.

Column diameter = 80 mm
Side outlet diameter = 26 mm
Mixture of wheat and brown mustard (z_a = 0.9).

Run	d_b (mm)	W_s ($g\ s^{-1}$)	W_c ($g\ s^{-1}$)	y_s (-)	x_c (-)	D (-)	s_o (-)
06	†	30	30	0.087	0.088	1.0	-0.015
07	20, 24	25	102	0.076	0.089	0.25	-0.143
08	20, 24	25	104	0.073	0.089	0.24	-0.176
09	24	24	91	0.071	0.089	0.27	-0.211
010	20	23	60	0.069	0.090	0.39	-0.227
011	17	26	42	0.070	0.090	0.62	-0.225
012	20, 24	25	103	0.075	0.090	0.24	-0.164
013	*	25	418	0.093	0.090	0.06	+0.037
014	24	20	90	0.074	0.089	0.23	-0.169
015	24	9	69	0.079	0.095	0.13	-0.168
016	*	17	658	0.128	0.097	0.03	+0.321
017	17	15	27	0.068	0.095	0.58	-0.277
018	20	16	48	0.070	0.093	0.34	-0.247
019	20, 24	16	99	0.079	0.091	0.16	-0.131
020	24	17	78	0.077	0.895	0.21	-0.141
021	20	18	51	0.070	0.092	0.35	-0.238
022	17	22	37	0.069	0.092	0.60	-0.256
023	19	22	43	0.068	0.091	0.51	-0.255
024	18.5, 20, 24	21	115	0.077	0.088	0.18	-0.121
025	*	22	155	0.083	0.090	0.14	-0.082
026	*	20	317	0.099	0.091	0.06	+0.085

Table 6.6a Details of runs to investigate segregation at a submerged outlet

d_b Diameters of holes in the base which were open

† No solid flow through base plate

* Base plate partly removed to allow very large flow rates in column

values of D, the majority of down-flowing material leaves the column by the holes in the base. An explanation for this reverse of behaviour is given in Figure 6.6f. When particles are packed into any vessel, the local void fraction is found to increase sharply near the vessel wall [Haughey and Beveridge (1969)]. If a mixture of large and small particles is present, the smaller particles will preferentially fill these voids resulting in a local increase in the concentration of this component next to the vessel wall. As shown in Figure 6.6f, at low discharge ratios a high proportion of material is drawn off from this region of the downward moving packed bed. Therefore when D is reduced sufficiently, in this case to below 0.1, the concentration of mustard seed in the part of the bed adjacent to the wall may override any segregation due to percolation, and this will determine s_o. The results obtained using this column can only be used to predict mean residence times of particles in a spouted bed with a submerged outlet if the corresponding discharge ratio is known. In the spouted bed, the larger column diameter and presence of a spout makes discharge ratios difficult to apply. Consider instead the hopper in Figure 6.6f(i). The solids flow rates in the column and at outlet are given by

$$\left.\begin{aligned} W_c &= \frac{1}{4}\pi D_c^{\,2} v_c \rho_b \\ W_s &= \frac{1}{4}\pi d_s^{\,2} v_s \rho_b \end{aligned}\right\} \qquad (6.10)$$

where ρ_b is the average bulk density of solids at the point under consideration. Hence, by equation(6.9),

$$D = \frac{v_s}{v_c}\left(\frac{d_s}{D_c}\right)^2 \qquad (6.11)$$

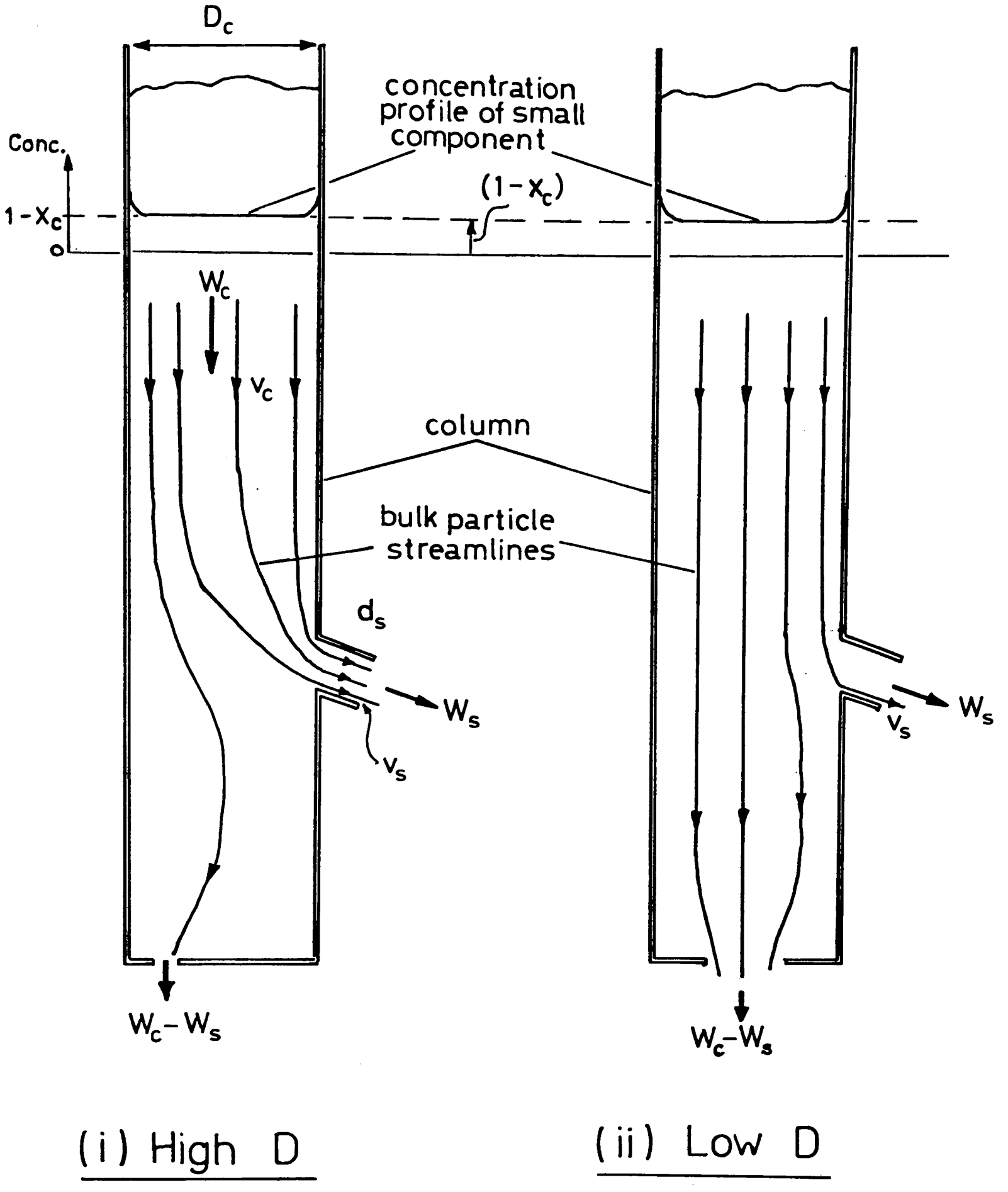


Figure 6.6 f : Flow pattern of solids into a submerged outlet for high and low values of discharge ratio D (= W_s/W_c).

if the velocity profiles in the column and across the outlet are uniform and the bulk densities of material at each point are equal. For a spouted bed with a submerged outlet, a discharge ratio may be calculated using Equation (6.11) if estimates for v_s and v_c are obtained. The value of v_c may be estimated from particle velocities measured at the wall, listed in Table 5.2. The particle velocity in the column is found to be in the range 50 - 75 mm s^{-1}. Also, the outlet became submerged at solids mass flow rates W_s between 0.5 and 0.6 kg min^{-1}, which corresponds to average outlet velocities v_s of 34 - 43 mm s^{-1} by Equation (6.10), if a bulk density of 840 kg m^{-3} is assumed for material leaving the bed. Then, by Equation (6.11) and given the values of v_s and v_c, the range of discharge ratios expected at the submerged outlet of the spouted bed is 0.05 to 0.09.

In the 80 mm column, at such low discharge ratios a mixture richer in mustard seed is dis charged. If this is also the case in the spouted bed, an increase in t_o may be expected when the outlet becomes submerged using mixture C as the results in Figure 4.5h showed. No account has been taken of the direction and magnitude of gas flow at outlet which would be towards the lower pressure at outlet and exert a greater effect on the smaller sized components. Any segregation by this mechanism would also increase t_o.

In Chapter 4, the dependence of the mean residence time ratio t_o on the solids feed rate m was studied for two feed compositions of mixture A and mixture C. For mixture C, a sharp increase in t_o was observed as m increased sufficiently to submerge the solids outlet. For mixture A, no similar increase in t_o was observed. The radial variation in concentration of small particles in a packed bed, as depicted in Figure 6.6f, will be large for mixture C and

small for mixture A. Thus, this variation is responsible, at least in part, for the sharp increase in t_o observed for a submerged outlet with mixtue C.

6.7 Summary

Segregation of particles on the free surface of a spouted bed in the region of the outlet may be an important factor controlling particle mean residence times. A method of studying this segregation has been developed. The materials used were wheat and mustard seeds and special tracer particles for each component were prepared. Tracers were dropped to a point on the free surface and for each component the probability of immediate discharge from the bed was measured. A parameter P_o, defined as the ratio of the exit probability of wheat to that of mustard was calculated for each condition. Provided P_o is related to the degree of segregation in the outlet region, a correlation between P_o and t_o can be used to assess the importance of free surface segregation.

If free surface segregation is an important factor, then the following would be expected: (i) $P_o > 1$ for $t_o < 1$ and (ii) increasing values of P_o for those conditions giving decreasing values of t_o. The former was observed for mixtures B and C and the latter for mixtures A and B. This suggests that free surface segregation influences the mean residence times of components in all three mixtures.

Drahun (1979) studied free surface segregation although no air flow was present. The results of the present study can only be partially explained by Drahun's findings. Fundamental studies of free surface segregation in the presence of an upward air flow are required to clarify the mechanisms operating on the free surface of a spouted bed.

Bouncing of wheat particles on impact with the free surface was not observed. Bouncing of mustard seeds was sometimes observed; this was always outward from the centre of the bed and occurred at all fountain heights. This movement results in an increase in the concentration of the smaller component of the mixture near the wall of a spouted bed. If the solids are discharged from this region the mean residence time of the smaller particles may be reduced. For mixture C, t_o was greater than unity for all fountain heights and bouncing of the smaller component may be a contributing factor.

Alternatively, segregation occurring in the spout or fountain could be an important factor controlling mean residence times. Particle movement in the spout and fountain was investigated using high speed cinephotography. This allowed measurement of particle velocities at the top of the annulus and spout and tracing of particle trajectories in the fountain. The impact of particles on the free surface was also observed. Film was only taken of mixture C since when mixture B or A was spouted, the high proportion of mustard seeds at the front face obscured the view of wheat seeds.

The film of particles in the spout enabled velocities to be measured by counting frames. This was only possible in the deepest bed when particle velocities in the spout were lowest. The resolution of particles could be improved by the use of more sophisticated filming equipment which would enable velocities in shallower beds to be measured. For the conditions studied, velocities of the larger particles in the spout were in some cases significantly less than those of small particles at the same radii; they were never significantly greater.

The observed velocity profiles in the spout were compared to parabolic profiles. Little significant deviation from this profile was found, although the centre was sometimes displaced radially due to

eccentricity of the spout.

Any difference of particle velocities in the spout may result in higher trajectories in the fountain for the faster component. Trajectories were studied for partial, full and over-developed fountains. The radial landing position of each particle was plotted against its radial position at the top of the spout. A straight line was fitted to the points for each component. No significant difference in the gradients and intercepts was found. Hence there is no evidence for particle segregation in the fountain. However, these results are restricted to mixture C.

It has been suggested in the literature that the motion of particles in the fountain may be treated as that of simple projectiles. This is an over-simplification since the motion of smaller particles was sometimes observed to be chaotic due to the high frequency of collisions.

A mass balance between solids moving upwards in the spout and downwards in the annulus gave an estimate of the voidage at the top of the spout. The spout voidages were found to be 7-25% lower than those observed by Mathur and Gishler (1955) in beds of 100% wheat. This could be due to the filling of voids between wheat seeds by the smaller mustard seeds in the congested spout.

A limited study of segregation at a submerged discharge point was performed. In Chapter 4, an increase in t_o was observed when the solids flow rate of mixture C was increased sufficiently to submerge the outlet. The results of this study show that in the absence of any air flow, using mixture C, two segregation mechanisms operate near the outlet: (i) segregation by percolation of the smaller component away from the failure zone at the outlet and (ii)

segregation of particles near to the wall due to uneven packing since a higher proportion of the smaller component is present in the few particle layers adjacent to the wall. For the conditions of discharge at the submerged outlet in Chapter 4, material is drawn from the outer few mm of the annulus. This results in preferential extraction of the smaller component supporting the observed increase in t_o.

CHAPTER 7

Conclusion

The mixing of particulate material in a spouted bed with continuous throughput of solids has been investigated for a range of conditions. Parameters varied were gas flow rate, bed depth, mass flow rate of solids and the proportion of large and small particles in the feedstock. A novel design of base cone for the spouted bed was developed which enabled different bed depths to be studied while retaining only two openings for solids inflow and outflow. The use of two pressurised sealing tubes around the edge of the base cone effected an airtight seal between the cone and the column wall at any selected height.

Stimulus-response techniques are often used to study the mixing behaviour in a system with continuous material throughput. In a particulate system, this requires the use of tracer particles with identical mechanical properties to those of the bulk material. Methods used by previous workers had various drawbacks. Some used coloured tracers involving tedious analysis of samples and others used radioactive tracers. The latter requires elaborate safety precautions and both were regarded as unacceptable for the present study.

A method of magnetically tagging the particles was developed which involved a negligible change in particle size and a mass increase of less than 5%. Separation of tracers from bulk material can be effected easily using magnets. This technique has the benefits of easy analysis of tracer concentrations in the samples of the discharged material and simple regeneration of all solids passed through the bed; it has potential for

further applications in the field of particle processing.

Using the magnetic tagging method, beds with a mono-sized material feed were studied. The mixing was found to be nearly perfect. This is in good agreement with the results of previous workers and establishes the suitability of the technique. It was then extended to beds with a binary-sized material feed. Using tracers of each particle size the self-mixing of each component was found to be nearly perfect. However, the components did not have equal mean residence times and this was the subject of further studies.

For a range of bed depths and gas velocities three mixtures of wheat and brown mustard seeds were studied: (i) a mass proportion of wheat in the feed, z_a, of 0.13, (ii) $z_a = 0.55$ and (iii) $z_a = 0.90$. To assess the difference in mean residence times the mean residence time ratio t_o (wheat/mustard) was defined, and calculated for each bed condition.

The bed variables which affect mean residence times for a given mixture are fountain shape, bed depth and mass flow rate of solids. It was thought that the distribution of material on the free surface and the extent of the fountain were more important in determining t_o than a measurement of absolute gas velocities. Therefore, the dimensionless ratio N_f was introduced as a parameter dependent on gas flow rate. It is defined as the ratio of the fountain height to that fountain height at which the falling material just covers the free surface. In all experiments, this parameter was used to gauge the air flow rate.

For all mixtures studied, t_o was found to increase with increasing bed depth. Generally, t_o increased with increasing N_f, except for some bed depths of a mixture rich in coarse particles when the dependence was not marked. The range of t_o was 0.62 to 1.66 over all conditions. t_o was only less than unity for mixtures with $z_a = 0.13$ at low values of N_f.

Two consequences of these findings are: (i) if large particles need to be retained preferentially, then for a 150 mm i.d. bed this can best be achieved with a deep bed and a large gas flow rate, and (ii) if small particles need to be retained, a shallow bed and small gas flow rate are preferable.

The difference in mean residence times of the large and small components must be a result of particle segregation. Four regions in the bed were studied to find evidence of this segregation: the annulus, the top of the spout, the fountain and the free surface, especially in the region of the solids outlet. Segregation was observed in all areas except the fountain, where it was not possible to examine a sufficient number of trajectories to make reliable deductions, due mainly to the chaotic motion of particles in this region.

To study segregation in the annulus, a second particle tagging technique and an electromagnetic detection system were developed to allow automatic measurement of particle cycle times. The high sensitivity of this system permitted detection of tracer particles many times smaller than those used by previous workers measuring cycle times. The tracer particles used in this study were almost identical to the bulk and this detection method should be applicable to tuture studies of particle movement in industrial processing equipment.

The apparatus was used to measure circulation times in beds with either large or small particles as the bulk material. Segregation in the bed as a whole was not sufficient to be detected by a measurement of cycle times, except in one case. For small particles as the bulk in a deep bed (H = 585 mm), a large tracer particle was found to execute very short cycles almost as often as cycles of equal duration to those of bulk particles. This was accounted for by free surface segregation.

Robinson and Waldie (1978) proposed that after executing one short cycle, a particle was then more likely to execute a second short cycle. This hypothesis was tested by measurement of sequences of cycle times. It was found that except for the isolated case mentioned above the length of a cycle is not dependent on the length of the previous cycle. This supports the evidence which showed the self-mixing of each component to be nearly perfect.

Using a mixture rich in the coarse component, photographic evidence suggests that there is no significant difference in the trajectories of the components in the fountain. Velocities of the larger particles in the spout were sometimes significantly less than those of the smaller particles at the same radius but were never significantly greater.

Segregation observed in the spout, fountain and annulus as a whole is not sufficient to explain the large differences in mean residence times. Hence, major segregation must occur on the free surface or in the outlet region. In a mixture rich in the coarse component, the small particles often bounced outwards on impact with the free surface. By this mechanism, the smaller component may accumulate at the perimeter of the free surface, a contributing factor to the shorter mean residence times for this component. Also, the portion of free surface deformed in the outlet region was studied for evidence of segregation. A correlation between the degree of segregation and the mean residence time ratio t_o confirmed that segregation in this region is important at all mixture strengths. Fundamental studies of the segregation mechanisms on slopes of material with an upward air flow are required to provide a fuller explanation of these results.

However, the segregation observed in the outlet region is not restricted to the free surface. The few particle layers at the top of the annulus and next to the column wall in this region are important in

determining the mixture strength selected by the outlet. Measurement of particle velocities adjacent to the column wall at the top of the annulus showed segregation to be significant. Except for a mixture rich in small particles, the smaller particles had lower downward velocities resulting in a concentration above average for this component at the top of the annulus. This segregation became more pronounced in deeper beds and is also a major factor contributing to the difference in mean residence times. If in larger beds, the ratio of outlet size to particle size also increases, the effect of this segregation on mean residence times will become less.

Knowledge of particle movement within mixtures continuously distributed in size and with a distribution in density would be desirable but for reasons of availability, the particles studied were restricted mainly to wheat seeds and mustard seeds: particles with a large size difference but of similar densities. The study was also restricted to one bed diameter and a gas inlet diameter suitable for spouting any mixture used. Experiments on larger beds are important and desirable, especially when the bed is operated with a partial fountain for reasons of economy. Under these conditions, free surface segregation may become the dominant factor controlling mean residence times. None the less, the significant areas where segregation can occur and the effects of this on the mixing and movement of solids within a spouted bed have been identified.

Appendix A: Mixing in continuous flow systems

The residence time distribution (RTD) of material flowing steadily through a vessel can be determined experimentally by a stimulus - response technique. The stimulus is usually either a pulse of labelled material injected at inlet or a sudden change of feed from, say, red to white material. The response at outlet is measured as the concentration C(t) of labelled material in a sample when the tracer is injected as a pulse or as the fraction F(t) of labelled material when injected as a continuous stream. The relationship between the RTD, C and F will now be shown [Danckwerts (1952)].

a) Response to a step-change

The specific case of a perfectly mixed vessel will be considered first, followed by a general analysis for any vessel.

(i) Perfectly mixed vessel

For a sudden change in feed from white to red in a perfectly mixed vessel of hold-up mass H_p and flow rate m, a mass balance at time t for the red material over time dt gives:

Entered	$m\ dt$
Left	$F(t)\ m\ dt$
Accumulation	$H_p\ dF(t)$

Then

$$m\ dt - F(t)\ m\ dt = H_p\ dF(t)$$

or

$$\frac{m}{H_p}\ dt = \frac{dF(t)}{1-F(t)}$$

Integrating: $\frac{mt}{H_p} = -\ln (1 - F(t))$

Now the initial condition is $F(t) = 0$ at $t = 0$

and so $F(t) = 1 - \exp (-\frac{mt}{H_p})$

or $\underline{F(\theta) = 1 - \exp (-\theta)}$ (A.1)

where θ is dimensionless time given by t/τ where $\tau = \frac{H_p}{m}$

(ii) Any vessel

Those elements of material in the vessel which have been in it for a time t are said to have an "age" t. The fraction of material in the system having ages between t and (t + dt) is I(t) dt and the fraction of the material leaving the system having ages between t and (t + dt) is E(t), where I and E are called the internal and exit age-distribution functions respectively. E is commonly termed the residence time distribution. The relationship between E, I and F can be shown by imagining the ingoing stream, as before, to change from white to red at time $t = 0$.

After time t the balance for red material is

Entered $= mt$

In the system $= H_p \int_0^t I(t')\, dt'$

Left system $= m \int_{t''=0}^{t} \int_{t'=0}^{t''} E(t')\, dt'\, dt''$

the latter following since the rate at which red material flows out at any time t" after the change of colour is

$m \int_0^{t''} E(t')\, dt'$

Then

$$\frac{mt}{H_p} = \int_0^t I(t')\, dt' + \frac{m}{H_p} \int_{t''=0}^{t} \int_{t'=0}^{t''} E(t')\, dt'\, dt'' \quad (A.2)$$

and the total fraction F(t) of red material in the outflow at any time t is

$$F(t) = \int_0^t E(t')\, dt' \qquad (A.3)$$

If equation (A.2) is differentiated with respect to t then

$$1 - \int_0^t E(t')\, dt' = \frac{H_p}{m} I(t)$$

hence from equation (A.3)

$$1 - F(t) = \frac{H_p}{m} I(t) = \tau I(t) \qquad (A.4)$$

or

$$\underline{1 - F(\theta) = I(\theta)} \qquad (A.4a)$$

Also

$$\frac{d}{dt} F(t) = E(t)$$

or

$$\underline{\frac{d}{d\theta} F(\theta) = E(\theta)} \qquad (A.5)$$

b) Response to a pulse

For the injection of a pulse of tracer of mass Q it can be shown by similar methods to those used above, that,

$$C(t) = \frac{Q}{m} \frac{d}{dt} \left\{F(t)\right\} = \frac{Q}{m} E(t) \qquad (A.6)$$

If tracer concentration is normalised by dividing C(t) by the concentration in the vessel initially, $\frac{Q}{H_p}$, then

$$C_0(\theta) = \frac{C(\theta)}{Q/H_p} = \frac{d}{d\theta} (F(\theta)) = E(\theta) \qquad (A.7)$$

where $C_0(\theta)$ denotes the normalised concentration and $\theta = t/\tau$.
For a perfectly mixed vessel, $F(\theta)$ is given by equation (A.1), therefore,

$$C_0(\theta) = E(\theta) = \exp(-\theta) \qquad (A.8)$$

In some cases during the present work, the cumulative discharge D has been used as the time dependent variable. If a substitution of $t = \frac{D}{m}$ is made in equation A.6, then

$$C(D) = \frac{Q}{m} E(D) \qquad (A.9)$$

since m is constant.
Equation A.8 then becomes

$$C_0(D) = \exp(-D/H_p) \qquad (A.10)$$

where H_p is the hold-up mass in the vessel.

Appendix B : Particle Properties

Bulk Particles

	Shape	Mean Diameter (mm)	Lower Sieve Cut (mm)	Upper Sieve Cut (mm)	ρ_b (kgm^{-3})	ρ_s kgm^{-3})
Wheat	Ovoid	6.0x3.2	2.8	4.0	830	1260
Brown Mustard	Sphere	1.6	1.18	2.0	680	1120
White Mustard	Sphere	2.1	1.7	2.36	710	1160
Molecular Sieve Beads*	Sphere	3.8	2.8	5.0	740	1210

Tracer Particles

Wheat	Ovoid	6.0x3.2	2.8	4.0		1420
Brown Mustard	Sphere	1.6	1.18	2.0		1170

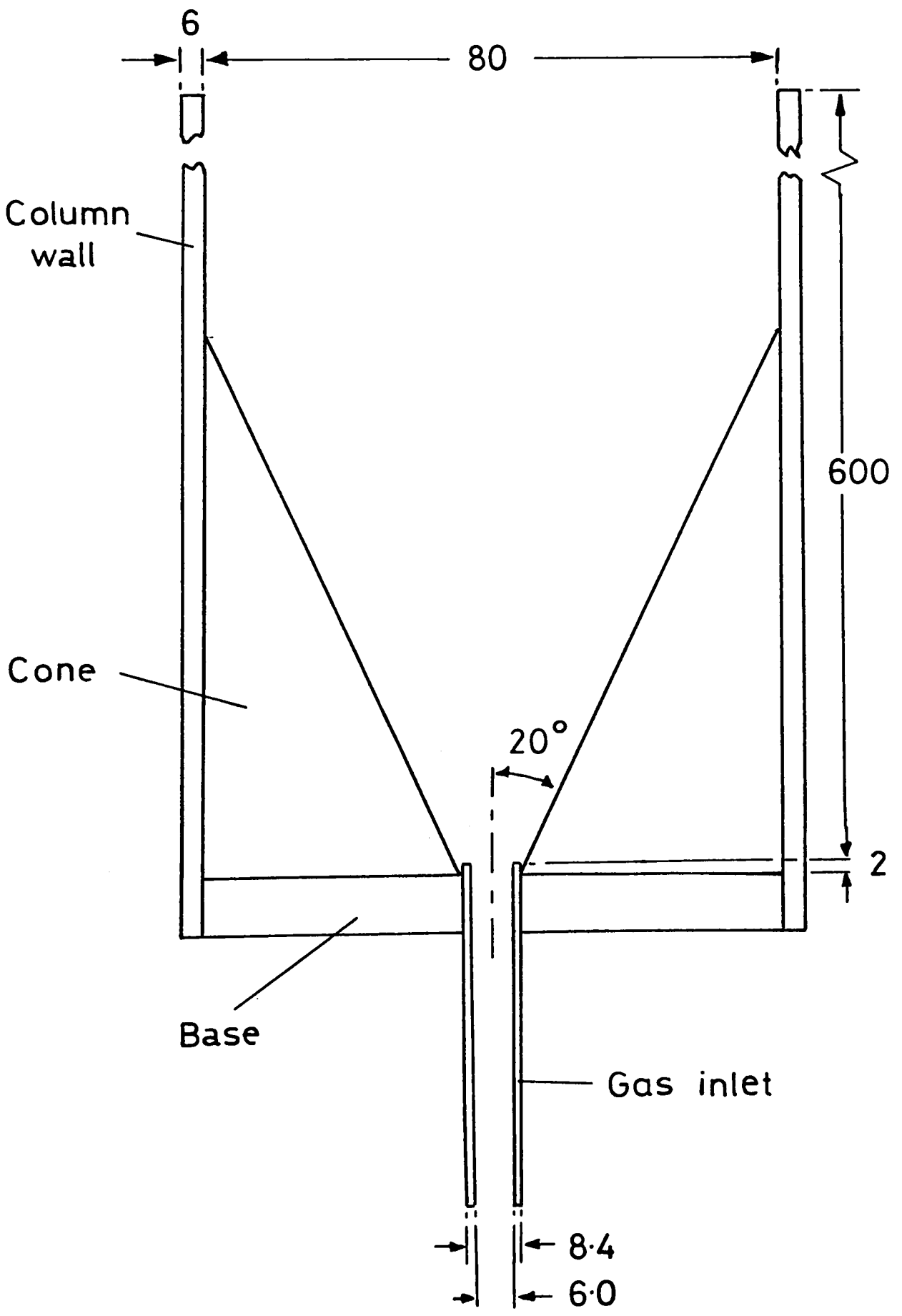
*Manufactured by Grace Davison Chemical ; Grade 513

Appendix C : Details of the 80 mm i.d. half-section bed

Materials of construction

Column : Perspex
Cone : Perspex
Base : Perspex
Gas inlet : Duraluminium

All dimensions in mm.



Appendix D: Calculation of the standard deviation of the ratio of two variable quantities.

If a number of measured quantities have means v_1, v_2 .....v_n with standard deviations σ_1 , σ_2 .....σ_n, respectively and each quantity is normally distributed, then the standard deviation of any function of v_1, v_2 .....v_n, namely $f(v_1, v_2 ....., v_n)$, is σ where

$$\sigma^2 = \left(\frac{\partial f}{\partial v_1}\right)^2 \sigma_1{}^2 + \left(\frac{\partial f}{\partial v_2}\right)^2 \sigma_2{}^2 + ... + \left(\frac{\partial f}{\partial v_n}\right)^2 \sigma_n{}^2 \qquad (D.1)$$

Therefore if: $$v = \frac{\bar{v}_x}{\bar{v}_y} = f(\bar{v}_x , \bar{v}_y) \qquad (D.2)$$

$$\sigma_v^2 = \frac{\sigma_x^2}{\bar{v}_y^2} + \frac{\bar{v}_x^2 \sigma_y^2}{\bar{v}_y^4} \qquad (D.3)$$

$$\text{or} \quad \sigma_v = \frac{1}{\bar{v}_y}\left[\sigma_x^2 + \left(\frac{\bar{v}_x}{\bar{v}_y}\right)^2 \sigma_y^2\right]^{\frac{1}{2}} \qquad (D.4)$$

[Topping (1972)]

Appendix E : Estimation of void fraction in the spout

Across any horizontal section through a spouted bed, if the feed and the overflow are above the point under consideration, the downward mass flow rate of solids in the annulus must be equal to the upward mass flow rate of solids in the spout. If the velocity profiles of material in the annulus and spout are specified and the bulk density of material in the annulus is known, then the average bulk density of solids in the spout can be calculated from a mass balance. The average void fraction in the spout may then be calculated.

The mass flow rate of solids in the annulus at a given section W_a is given by

$$W_a = \sum_{i=I,IV} W_i \qquad (E.1)$$

where W_i is the mass flow rate of solids in zone i, as defined in Figure 6.5e. Each W_i has been shown (in Section 6.5, Equation(6.7)) to be of the form

$$W_i = \frac{\pi}{2} (r_2^2 - r_1^2) v_{a_i} \rho_{ba}$$

where ρ_{ba} is the average bulk density of the mixture in the annulus. For any material, the relationship between bulk density ρ_b, mean solid density ρ_s and the void fraction is

$$\epsilon = 1 - \frac{\rho_b}{\rho_s} \qquad (E.2)$$

if the mass of interstitial gas is negligible. Since two components are present in this case, the mean true solid density of the mixed material will be used; it can be shown to be given by:

$$\rho_s = \left[\frac{1 - z_a}{\rho_{sb}} + \frac{z_a}{\rho_{sa}} \right]^{-1} \qquad (E.3)$$

where z_a is the mass proportion of component A in the mixture and ρ_{sa} and ρ_{sb} are the solid densities of components A and B respectively. Then from Equation (E.2), the bulk density of solids in the annulus is given by

$$\rho_{ba} = (1 - \epsilon) \left[\frac{1 - z_a}{\rho_{sb}} + \frac{z_a}{\rho_{sa}} \right]^{-1} \qquad (E.4)$$

Since the solids in the annulus are essentially in the loose packed condition [Epstein (1968)] the void fraction will be taken to be 0.44 [Haughey and Beveridge (1969)] for all calculations.

For a spout of semicircular cross-section, the volumetric bulk flow rate of solids in the spout is given by

$$Q_s = \int_{r=0}^{s} v_s \, \pi \, r \, dr \qquad (E.5)$$

where v_s is the vertical component of particle velocity in the spout at a radius r.

In section 6.4, the profile of particle velocity in the spout was not found to be exactly parabolic, but to simplify the analysis a profile defined by equation (6.4) with n = 2 will be used, i.e.

$$\frac{v_s}{v_{s_{max}}} = 1 - \left(\frac{r}{r_s} \right)^2$$

Hence, for a half-bed

$$Q_s = \int_{r=0}^{r_s} v_{s_{max}} \pi \left(r - \frac{r^3}{r_s^2} \right) dr$$

which on integration gives

$$Q_s = \frac{\pi}{2} r_s^2 v_{s_{max}} \tag{E.6}$$

and may be evaluated from measured values of r_s and $v_{s_{max}}$. The mass flow rate of solid material in the spout is given by

$$W_s = Q_s \rho_{bs} \tag{E.7}$$

where ρ_{bs}, the radial average bulk density of solid material in the spout, is unknown. Since, from continuity $W_s = W_a$, ρ_{bs} is given by

$$\rho_{bs} = \frac{2 W_a}{\pi r_s^2 v_{s_{max}}} \tag{E.8}$$

So, by Equation (E.2), the radial average void fraction of material in the spout is

$$\epsilon_s = 1 - \frac{2 W_a}{\pi r_s^2 v_{s_{max}} \cdot \rho_s} \tag{E.9}$$

where W_a and ρ_s are given by Equations (E.1) and (E.3) respectively.

NOMENCLATURE

English Letters

a	constant in Equation (4.5)	[-]
b	constant in Equation (4.5)	[-]
$C_0(D)$	normalised tracer concentration at vessel outlet after a discharge of solids of mass D	[-]
$C_0(\theta)$	normalised tracer concentration at vessel outlet at dimensionless time θ	[-]
D	cumulative mass of material discharged from the bed	[M]
D	discharge ratio (= W_s / W_c)	[-]
D_c	diameter of column	[L]
D_t	depth over which particles were timed	[L]
d	depth of measurement grid below the free surface (Figure 6.5 a)	[L]
d_s	diameter of side outlet	[L]
E (θ)	exit age distribution function (or RTD) of solids in the vessel at dimensionless time θ	[-]
e	constant (= 2.718 28)	[-]
F(t)	fraction of tracer particles in the material leaving the vessel at time t	[-]
g	acceleration due to gravity (= 9.81 ms^{-2})	[LT^{-2}]
H	depth of material in the bed when spouting (defined in Figure 3.5 a)	[L]
H_f	height of the fountain in the spouted bed	[L]
H_{fo}	height of the fountain when just covering the top free surface (defined in Figure 4.6 c)	[L]
H_k	hold-back (defined by Equation (4.1))	[-]
H_m	maximum spoutable bed depth	[L]
H_p	hold-up mass of solids in the vessel	[M]
H_s	height of free surface above centre of submerged solids outlet	[L]
H_t	height above gas inlet at which D_t is centred	[L]
h	height of material in the inlet hopper	[L]

$I(\theta)$	internal age distribution function of solids in the vessel	[-]
i	zone number in the annulus	[-]
j	integer	[-]
K_s	coefficient of skewness	[-]
k	integer	[-]
l	number of ratios used to calculate a mean particle velocity ratio	[-]
l_o	overhang distance of tracer feed pipe	[L]
$M_a(t)$	hold-up mass of the larger component at time t	[M]
M_{ao}	mass of the larger component leaving the bed in time Δt	[M]
$M_b(t)$	hold-up mass of the smaller component at time t	[M]
M_{bo}	mass of the smaller component leaving the bed in time Δt	[M]
M_i	total mass of solids entering the bed in time Δt	[M]
m	mass flow rate of solids into the vessel	$[MT^{-1}]$
m	fitted constant in Equation (6.2)	[-]
N	number of particle drops used to calculate P_m	[-]
$N(t)$	number of cycles of lengths between t and $t + \Delta t$ executed by a particle during time T	[-]
N_f	fountain shape number ($= H_f / H_{fo}$)	[-]
N_s	spouting number ($= U / U_{ms}$)	[-]
N_1	Number of particle drops used to calculate P_1	[-]
N_2	Number of particle drops used to calculate P_2	[-]
n	parameter in Equation (6.4)	[-]
n_e	rate at which particles of a given size fraction leave the bed	$[T^{-1}]$
n_f	number of frames of film	[-]
$n_i(x,y)$	number flux of particles of a given size fraction impacting the free surface at point (x,y)	$[L^{-2}T^{-1}]$
n_1	number of velocity ratios in group 1	[-]
n_2	number of velocity ratios in group 2	[-]

$P(x,y)$	probability of a particle leaving the bed soon after landing at the point (x,y) on the free surface	[-]
P_m	exit probability measured by experiment	[-]
P_o	exit probability ratio (= P_1/P_2)	[-]
P_1	probability of exit for tracer particles of species 1 (the larger size)	[-]
P_2	probability of exit for tracer particles of species 2 (the smaller size)	[-]
p	absolute pressure at the upstream venturi pressure tapping (mm Hg)	[L]
Q	mass of tracer injected at the solids inlet	[M]
Q_i	downward volumetric flow rate of solids in zone i of the annulus	$[L^3T^{-1}]$
Q_s	volumetric flow rate of solids in the spout	$[L^3T^{-1}]$
R_c	radius of column	[L]
r	radial distance	[L]
r_1	radial position of a particle upon landing on the free surface	[L]
r_s	radius of the spout	[L]
r_t	radial position of a particle at the top of the spout	[L]
r_1, r_2, r_3	radial positions of zones in the annulus	[L]
s	distance from the centre of the spout to the centre of the column	[L]
s	parameter defined by Equation (5.2)	[-]
s_o	segregation factor (= $(x_c - y_s)/(1 - x_c)$)	[-]
s_1	standard deviation of the group 1 ratios of mean particle velocity	[-]
s_2	standard deviation of the group 2 ratios of mean particle velocity	[-]
T	operating time	[T]
T_a	absolute gas temperature at the upstream venturi tapping	[Θ]
t	time	[T]
t	Student's t-statistic	[-]
$\bar{t}$	mean particle cycle time of the NCD	[T]

t_m	median particle cycle time of the NCD	[T]
t_m^*	median cycle time of the SNCD	[T]
t_{max}	cycle time of particle taking longest possible path in the vessel	[T]
t_o	mean residence time ratio (= τ_a/τ_b)	[-]
t_p	t-value at the 95% probability level	[-]
t_v	time taken for a particle at the wall to travel from the free surface to the top of the base cone	[T]
U	superficial velocity of gas in the bed	$[LT^{-1}]$
U_{ms}	minimum superficial gas velocity required to spout the bed	$[LT^{-1}]$
V	volume of the vessel	$[L^3]$
v	ratio of mean particle velocities measured at the wall (= v_a/v_b)	[-]
v_a	mean downward velocity of a wheat particle at the vessel wall	$[LT^{-1}]$
v_{ai}	average downward vertical velocity of solids in zone i of the annulus	$[LT^{-1}]$
v_b	mean downward velocity of a brown mustard particle at the vessel wall	$[LT^{-1}]$
v_c	downward vertical velocity of solids in the column above the submerged column side outlet	$[LT^{-1}]$
v_o	vertical component of particle velocity in the spout at a radius r at the free surface level	$[LT^{-1}]$
$v_{o_{max}}$	vertical component of particle velocity at the centre-line of the spout at the free surface level	$[LT^{-1}]$
v_s	vertical component of particle velocity in the spout at radis r	$[LT^{-1}]$
$\bar{v}_s$	average velocity of solids leaving the submerged side outlet	$[LT^{-1}]$
$v_{s_{max}}$	vertical component of particle velocity at the centre-line of the spout	$[LT^{-1}]$
$\bar{v}_x$	variable quantity in Appendix D	[-]
$\bar{v}_y$	variable quantity in Appendix D	[-]
v_1	a velocity ratio from group 1	[-]
$\bar{v}_1$	average of the group 1 ratios of mean particle velocity	[-]

v_2	a velocity ratio from group 2	[-]
$\bar{v}_2$	average of the group 2 ratios of mean particle velocity	[-]
W	mass flow rate of gas into the bed	$[MT^{-1}]$
W_a	downward mass flow rate of solids in the annulus	$[MT^{-1}]$
W_c	downward mass flow rate of solids in the column above the submerged outlet	$[MT^{-1}]$
W_i	downward mass flow rate of solids in zone i	$[MT^{-1}]$
W_s	mass flow rate of solids through the submerged column outlet	$[MT^{-1}]$
x	coordinate	[L]
$x_a(t)$	mass proportion of the larger component in the bed at time t	[-]
$x_b(t)$	mass proportion of the smaller component in the bed at time t	[-]
x_c	mass proportion of the larger component in the column above the submerged outlet	[-]
y	coordinate	[L]
y_s	mass proportion of the larger component in solids leaving the submerged outlet	[-]
z_a	mass proportion of the larger component in the solids feed	[-]

Greek Letters

Δr	difference in radial distance	[L]
Δp	difference in pressure between upstream and downstream venturi tappings (mm Hg)	[L]
Δt	time interval	[T]
ϵ	void fraction	[-]
ϵ_s	radial mean void fraction in the spout	[-]
θ	dimensionless time ($= t/\tau$)	[-]
ρ_A	bulk density of component A (the larger)	$[ML^{-3}]$
ρ_B	bulk density of component B (the smaller)	$[ML^{-3}]$
ρ_b	bulk density of material	$[ML^{-3}]$
ρ_{ba}	average bulk density of material in the annulus at a given horizontal section	$[ML^{-3}]$

ρ_{bs}	radial mean bulk density of solids in the spout	$[ML^{-3}]$
ρ_g	gas density	$[ML^{-3}]$
ρ_s	true solid particle density	$[ML^{-3}]$
ρ_{sa}	true solid particle density of component A (the larger)	$[ML^{-3}]$
ρ_{sb}	true solid particle density of component B (the smaller)	$[ML^{-3}]$
σ	standard deviation	[-]
σ	(Chapter 5) standard deviation of the mean cycle time t	[T]
σ_v	standard deviation of the velocity ratio v	[-]
σ_{vl}	standard deviation of the k^{th} velocity ratio in group 1	[-]
σ_x	standard deviation of variable (Appendix D)	[-]
σ_y	standard deviation of variable (Appendix D)	[-]
τ	mean residence time of solids in the vessel	[T]
τ_a	mean residence time of the larger component in the bed	[T]
τ_b	mean residence time of the smaller component in the bed	[T]

Abbreviations

NCD	number of cycles distribution
RTD	residence time distribution
SNCD	subsequent number of cycles distribution

REFERENCES

BARTON, R.K., RIGBY, G.R. and RATCLIFFE, J.S. (1968)
"The use of a spouted bed for the low temperature carbonisation of coal."
Instn. Eng. Aust. Mech. Chem. Eng. Tr. MC4, 105, 1968

BECKER, H.A. and SALLANS, H.R. (1960)
"Drying wheat in a spouted bed."
Chem. Eng. Sci. 13, 97, 1960

BERQUIN, Y.F. (1964)
"Improvements in the granulating and drying of fluid materials such as aqueous solutions, pastes and slurries"
British Patent No. 962265, 1964

BOWLING, K. McG. and WATTS, A. (1961)
"Determination of particle residence time in a fluidized bed: theoretical and practical aspects."
Aus. J. App. Sci. 12, 413, 1961

BRIDGWATER, J. (1975)
"The influence of fluid flow on slope stability."
Powder Technology 11, 199, 1975

BRIDGWATER, J., COOKE, M.H. and SCOTT, A.M. (1978)
"Inter-particle percolation: equipment development and mean percolation velocities."
Trans. I. Chem. Eng. 56, 157, 1978

BROWN, R.L. (1939)
"The fundamental principles of segregation"
J. Inst. Fuel 13. 15, 1939

CAMPBELL, A.P. and BRIDGWATER, J. (1973)

"The mixing of dry solids by percolation."

Trans. I. Chem. Eng. 51, 72, 1973

COOK, H.H. and BRIDGWATER, J. (1978)

"Segregation in spouted beds."

Can. J. Chem. Eng. 56, 636, 1978

COOKE, M.H. and BRIDGWATER, J. (1977)

"A distribution index and its application to static powder mixers."

2nd European Conf. on Powder Mixing, 30 March - 1 April, 1977,

Cambridge, England, Paper D3.

COOKE, M.H. and BRIDGWATER, J. (1979)

"Inter-particle percolation: a statistical mechanical interpretation."

Ind. Eng. Chem. Fund. 18, 25, 1979

CRAVEN, P. (1970)

"The effect of gas maldistribution on catalyst performance"

Brit. Chem. Eng. 15, 918, 1970

DRAHUN, J.A. (1979)

"The Segregation of Powders."

D. Phil. Thesis, University of Oxford

DANCKWERTS, P.V. (1953)

"Continuous flow systems."

Chem. Eng. Sci. 2, 1, 1953

EPSTEIN, N. (1968)

"Void fraction variation in the spouted bed annulus"

Ind. Eng. Chem. Proc. Des. Dev. 7, 157, 1968

EPSTEIN, N. and MATHUR, K.B. (1971)

"Heat and mass transfer in spouted beds - a review."

Can. J. Chem. Eng. 49, 467, 1971

FOO, W.S. (1978)

"Powder mixing in failure zones."

M.Sc. Thesis, University of Oxford

GEIGY, J.R. (1970)

"Scientific Tables"

Edited by K. Diem and C. Lentner.

J.R. Geigy, S.A., Basle, Switzerland.

GRACE. J.R. and MATHUR, K.B. (1978)

"Height and structure of the fountain region above spouted beds."

Can. J. Chem. Eng. 56, 533, 1978

HAUGHEY, D.P. and BEVERIDGE, G.S.G. (1969)

"Structural properties of packed beds - a review"

Can. J. Chem. Eng. 47, 130, 1969

HULL, R.L. and ROSENBERG, A.E. von (1960)

"Radiochemical tracing of fluid catalyst flow."

Ind. Eng. Chem. 52, 989, 1960

JENIKE, A.W. (1960)

"A preliminary study of segregation."

Bull. Univ. Utah 51, Paper No. 24, 1960

KUGO, M., WATANABE, N., UEMAKI, O. and SHIBATA, T. (1965)

"Drying of wheat by a spouted bed."

Bull. Hokkaido Univ., Sapporo, Japan 39, 95, 1965

LEFROY, G.A. and DAVIDSON, J.F. (1969)

"The mechanics of spouted beds."

Trans. Instn. Chem. Eng. 47, T120, 1969

LIM, C.J. and MATHUR, K.B. (1978)

"Modelling of particle movement in spouted beds."

Fluidization, Collected Papers, Cambridge University Press.

McNAB, G.S. (1977)

"Mechanics of spouted beds."

D.Phil. Thesis, University of Oxford

McNAB, G.S. (1977 a)

"Mechanics of spouted beds."

D.Phil. Thesis, University of Oxford, Page 188.

McNAB, G.S. (1977 b)

"Mechanics of spouted beds."

D.Phil. Thesis, University of Oxford, Fig. 7.25.

McNAB, G.S. (1977 c)

"Mechanics of spouted beds."

D.Phil. Thesis, University of Oxford, Page 188.

McNAB, G.S. and BRIDGWATER, J. (1979)

"Solids mixing and segregation in spouted beds."

3rd European Conf. on Mixing, 4-6 April, 1979, York, England,

Paper B1.

MADONNA, L.A. (1968)

"Void fraction variation in the spouted bed annulus."

Ind. Eng. Chem. Proc. Des. Dev. 7, 158, 1968

MANN, U. and CROSBY, E.J. (1975)

"Cycle time distribution measurements in spouted beds."

Can. J. Chem. Eng. 53, 579, 1975

MATHUR, K.B. and EPSTEIN, N. (1974)

"Spouted Beds."

Academic Press, Page 72

MATHUR, K.B. and EPSTEIN, N. (1974,I)

"Developments in spouted bed technology."

Can. J. Chem. Eng. 52, 129, 1974

MATHUR, K.B. and GISHLER, P.E. (1955)

"A technique for contacting gases with coarse solid particles."

A.I. Ch. E. J. 1, 157, 1955

PALLAI, E. and NEMETH, J. (1971)

"Measurement and regulation of particle residence time in spouted bed dryers."

3rd Int. Conf. Drying, Budapest, September 1971, Paper No. D.7. 1971

PALLAI, I. and NEMETH, J. (1972)

"Residence time distribution in spouted beds."

4th Int. Congr. Chem. Eng. (CHISA), Prague, September 1972, Paper C3 11.

PICCININI, N., BERNHARD, A., CAMPAGNA, P. and VALLANA, F. (1977)

"Segregation phenomenon in spouted beds."

Can. J. Chem. Eng. 55, 122, 1977

PICCININI, N., BERNHARD, A., CAMPAGNA, P. and VALLANA, F. (1977 a)

"Segregation phenomenon in spouted beds."

Can. J. Chem. Eng. 55, 122, 1977, Fig. 3

PICCININI, N. (in press)

"Particle segregation in continuously operated spouted beds."

REYNOLDS, O. (1885)

"On the dilatancy of media composed of rigid particles in contact."

Phil. Mag. 20, 469, 1885

ROBINSON, T. and WALDIE, B. (1978)

"Particle cycle times in a spouted bed of polydisperse particles."

Can. J. Chem. Eng. 56, 632, 1978

ROSCOE, K.H. (1967)

"Shear strength of soil other than clay." Panel discussion.

Proc. Geotech. Conf. Oslo 2, 188, 1967

SCOTT, A.M. (1974)

"Inter-particle percolation."

D.Phil. Thesis, University of Oxford

SCOTT, A.M. and BRIDGWATER, J. (1975)

"Interparticle percolation: a fundamental solids mixing mechanism."

Ind. Eng. Chem. Fund. 14, 22 1975

SHINOHARA, K., HAYASHI, K. and TANAKA, T. (1973)

"Residence time distribution of particles within pneumatic escalator."

J. Chem. Eng. Jap. 6, 447, 1973

SINGER, E., TODD, D.B. and GUINN, V.P. (1957)

"Catalyst mixing patterns in commercial catalytic cracking units."

Ind. Eng. Chem. 49, 11, 1957

STEPHENS, D.J. and BRIDGWATER, J. (1978)

"The mixing and segregation of cohesionless particulate materials",

parts I and II.

Powder Technology 21, 17, 1978

SUTHERLAND, K.S. (1961)

"Solids mixing studies in gas fluidized beds. Part 1 : A preliminary comparison of tapered and non-tapered beds."

Trans. Instn. Chem. Eng. 39, 188, 1961

TAILBY, S.R. and COCQUEREL, M.A.T. (1961)

"Some studies of solids mixing in fluidized beds."

Trans. I. Chem. Eng. 39, 195, 1961

THORLEY, B., SAUNBY, J.B., MATHUR, K.B. and OSBERG, G.L. (1959)

"An analysis of air and solid flow in a spouted wheat bed."

Can. J. Chem. Eng. 37, 184, 1959

TOPPING, J. (1972)

"Errors of observation and their treatment."

Halstead Press, John Wiley & Sons Inc., New York

van VELZEN, D., FLAMM, H.J., LANGENKAMP, H. and CASILE, A. (1974)

"Motion of solids in spouted beds."

Can. J. Chem. Eng. 52, 156, 1974

WILLEMSE, Th.W. (1961)

"De fysica van het mengen van droge korrelvormige stoffen."

Chemisch Weekblad 57, 377, 1961

WILLIAMS, J.C. (1963)

"The segregation of powders and granular materials."

J. Fuel Soc. Univ. Sheffield 14, 29, 1963